Spatiotemporal building stock modeling for residential decarbonization in the Netherlands

Yang, X.

Spatiotemporal building stock modeling for residential decarbonization in the Netherlands

Xining Yang

杨希宁

Spatiotemporal building stock modeling for residential decarbonization in the Netherlands

PhD Thesis at Leiden University, The Netherlands

The research described in this thesis was conducted at the Institute of Environmental Sciences (CML), Leiden University, the Netherlands.

ISBN: 9789051912777

Cover: Xining Yang

Layout: Xining Yang

Printing: GVO printers & designers - www.proefschriften.nl

Spatiotemporal building stock modeling for residential decarbonization in the Netherlands

Proefschrift

ter verkrijging van

de graad van doctor aan de Universiteit Leiden,

op gezag van rector magnificus prof.dr.ir. H. Bijl,

volgens besluit van het college voor promoties

te verdedigen op dinsdag 28 juni 2022

klokke 10.00 uur

door

Xining Yang

geboren te Baoding, Hebei province, China

in 1991

Promotor:

Prof. dr. A. Tukker

Co-promotores:

Dr. B. Steubing
Dr. M. Hu

Promotiecommissie:

Prof. dr. H.X. Lin
Prof. dr. E. van der Voet
Prof. dr. S. Pauliuk (University of Freiburg, Germany)
Dr. T. Fishman
Dr. D. Peck (Technische Universiteit Delft)

Table of Contents

Chapter 1 General introduction

1.1 Background

Buildings provide people with comfortable shelter for daily activities, such as sleeping, working, and relaxing [1–3], while they are characterized as highly intensive in the use of resources and energy and the generation of residues [4]. Currently, the building sector accounts for around 35% of global energy consumption and nearly 55% of global electricity is consumed by building operations [5]. Building operation and construction represent 38% of global greenhouse gas (GHG) emissions, mainly due to the combustion of fossil fuels (natural gas, oil, and solid fuels) for onsite space heating and cooking and offsite heat (e.g. district heating networks) and electricity generation [1,5]. 40-50% of globally extracted resources are used for constructing buildings and infrastructures [5–7]. In the European Union (EU), construction and demolition waste (CDW) accounts for 25-30% of the total generated waste, by weight [5,8]. The building sector thus has to play a significant role in ambitions concerning climate change mitigation [9,10].

Policies have been developed, from the EU to the national level, to accelerate the decarbonization of the EU building stock [11]. However, large-scale construction of new buildings and renovation of existing buildings with more complex technical systems will continue in the next decades [12], mainly driven by ongoing population increase, urbanization, and continuous increases in living standards, such as floor space per capita [13] and higher thermal comfort requirements for space heating and cooling [3,14,15]. This trend will inevitably pose great challenges for reducing the demand for primary materials and energy and the generation of CDW [16], which further emphasizes the urgency of reducing/decarbonizing the materials and energy consumed in the building sector to realize the circular economy, energy-neutral and climate-neutral targets [17–19].

1.2 GHG emissions in buildings

The GHG emissions of buildings are mainly composed of embodied and operational emissions [1,20]. Embodied emissions are primarily related to building material (component) manufacturing, transportation, installation, and end-of-lifespan treatment during construction, renovation, maintenance, and demolition processes [1,11,20,21]. The consumption of cement, concrete, bricks, and steel during initial construction accounts for the most embodied GHG emissions [1]. Operational emissions are from energy use, including the direct emissions from fossil fuel combustion for space heating, hot water, and cooking, and the indirect emissions from heat (heat networks) and public grid electricity generated by fossil fuels [22].

The amounts of life-cycle GHG emissions and the respective share of embodied and operational emissions are determined by many factors, such as the local climate, construction techniques, energy performance standards, and energy supply systems

[20]. The embodied GHG emissions from construction range from 250 to 400 kg CO_2-eq/m^2 [23], which occur in the relatively short construction phase (typically around one year) [20]. Renovation and maintenance during the operation phase can also lead to embodied emissions, but these emissions are less than 50% of the GHG emissions released during initial construction [1]. In contrast, the operational emissions per year range from 30 to 50 kg CO_2-eq/m^2 [23]. Since buildings are long-lifetime products [24] over the lifetime of the building, operational GHG emissions are more important than the embodied emissions related to construction. The proportion of operational GHG emissions can be changed by energy-efficiency renovations during the operation phase [25].

In addition to the building itself, the lifestyle of occupants can also greatly affect the living space per capita and energy demand per floor area. Greening lifestyles (e.g. shorter showers, more people living together in one house, and living in smaller houses) due to people's increased awareness of environmental protection can also be regarded as an important decarbonization strategy [26–28].

1.3 Towards climate-neutral building stock

According to the literature [1,28–31], decarbonization of the built environment can be pursued via three approaches: realizing a material transition, realizing an energy transition, and pursuing green lifestyles.

1.3.1 Material transition

Given the major contribution of building material production to embodied GHG emissions [32], it is critical to reduce the primary material extraction and decarbonize the building materials, i.e. material efficiency improvement and the substitution of carbon-intensive materials with low-carbon materials [33,34].

Material efficiency

Previous literature [3,34,35] suggests that strategies for material efficiency improvement mainly include:

(1) **Lifetime extension**. Increasing the lifetime of a building or component can reduce the life-cycle material demand [36]. New building construction will require large amounts of materials, especially for the foundation, structure, and walls, which consume the most carbon-intensive materials such as concrete, cement, bricks, and steel. Therefore, extending the lifetime of existing buildings by deep renovation rather than demolition and reconstruction can not only reduce the generation of CDW but also reduce new material demand. Demolition can be an option only when the building can hardly meet current function demand or its structure is seriously defective (e.g. foundation settlement), which makes the renovation too expensive or almost technically impossible. As for new buildings, advanced urban planning and better building design (increased durability of components) can greatly reduce the construction of short-lifetime buildings. This is an important lesson learned from China where the building lifetimes are very short [37,38] and large-scale demolition

and construction activities generate very high CDW amounts leading to unnecessarily high consumption of primary raw materials [39,40].

(2) **Material recovery**. This mainly encompasses reuse and recycling [41]. Some components can be directly reused for new construction or renovation [4], such as the components made of wood and steel. Some materials, such as metals, plastics, wood, and concrete, can be recycled and used to produce secondary materials. Concrete can be crushed into aggregate for new concrete manufacturing [42] although additional cement, sand, and water are required [43]. In practice, CDW is commonly used as road foundation or backfilling [43], which represents a form of downcycling and should be transformed into high-level recycling [44]. In addition, future building construction should develop towards manufacturing off-site prefabricated modular components [45] that are easy to disassemble [46,47] which will increase the closed-loop use of materials [5]. Standardized component libraries can be built and thus enhance component universality between different buildings, which can effectively reduce CDW generation and crushing works.

(3) **Lightweight design**. The structures account for a significant proportion of material consumption. Reducing the weight of structures without loss of mechanical properties and specific functionality should therefore be pursued [3,5]. Some components (e.g. non-load-bearing walls) can be constructed with lightweight materials. Innovative technologies for low-density material production can be of great benefit in the future [48] and are highly advocated as these materials have advantages of seismic resistance, fewer environmental impacts, and shorter construction time [49]. In addition, the building type choice can also affect the component weight, especially for high-rise buildings, which tend to use large amounts of concrete and steel for foundations, pillars, and beams.

Low-carbon materials

Raw material extraction and building material production cause a great impact in terms of biodiversity loss and carbon emissions [5,50]. It is therefore important to substitute carbon-intensive materials (e.g. metals, concrete, and masonry) with bio-based materials, such as wood [3,51]. Some bio-based materials can sequester CO_2 emissions during growing and can act as carbon storage [3,5,50]. Wood can be used in different parts of the buildings, such as structures, window frames, walls, and roofs. Bio-based materials can also become a good choice for insulating building envelopes [52]. Bio-based materials (e.g. bamboo or timber) have been the main building materials in human history but, with the fast population increase and urbanization in the process of the industrial revolution, other materials that can be produced on a large scale and have better properties began to be used in buildings in the past two to five hundred years. Given that the supply of bio-materials is limited due to the slow growth of forestry, using materials from fast-growing bio-based plants (e.g. bamboo, straw, hemp, and flax) can be a sound option as they can store carbon in less than 10 years and more easily keep pace with the material demand [53].

In addition to material substitution, decarbonizing the material production is also critical because wood can hardly meet the material demand in most countries [54], such as the Netherlands and China. Further, harvesting trees from unmanaged forests will harm the ecosystem [53]. The GHG emissions of building material production (e.g. metals and cement) are mainly related to the energy supply from fossil fuel combustion [39]. Therefore, increasing the energy efficiency during material production, developing low-carbon processes particularly cement and steel production [55,56], and enhancing the share of renewable energy in upstream energy systems can greatly reduce material-related GHG emissions [50].

1.3.2 Energy transition

The energy transition is regarded as an important measure in reducing GHG emissions in the building sector. The main reason is that energy-related GHG emissions related to the operational energy use of buildings account for the largest share of life-cycle emissions [1].

Building energy efficiency improvement

Realizing climate change targets will be extremely challenging and expensive if the energy demand is not significantly reduced [57,58] because a substantial increase would be required in renewable energy infrastructure construction and carbon dioxide removal (CDR) technology adoption [58]. The GHG emissions during building operations mainly involve fossil fuel combustion for space heating, hot water, and cooking, and electricity consumption for cooling, lighting, and appliances [11]. In many EU countries, space heating is the dominant form of energy use (mainly in the form of natural gas), corresponding with about 66% of total household energy consumption [23], but this share can be larger in Northern Europe [1]. Considering that most EU countries' building stocks are rather aged and most existing buildings will continue to exist in the next decades [15], renovating existing buildings is regarded as an important strategy to reduce operational energy consumption [1,11,59]. This mainly encompasses insulating the building envelopes and replacing current heating systems with more efficient ones. In addition to heating systems, ventilation systems with heat recovery are also important to reduce heat losses. Smart ventilation systems are recommended as they can maintain a comfortable home in terms of both temperature and fresh air control [60]. Moreover, more energy-efficient appliances can also contribute to reducing household electricity consumption.

As regards the construction of new buildings, it is important to ensure that these are energy efficient. Many EU member states have made national plans to encourage the construction of "nearly Zero-Energy Buildings" (nZEB) [61,62], which are defined by the Energy Performance of Buildings Directive (EPBD) as "a building that has a very high energy performance, as determined in accordance with Annex I, and states that the nearly zero amount of primary energy required should be covered to a very significant extent by energy from renewable sources, including those produced on-site or nearby". According to EPBD [61], after 31 December 2018 buildings occupied and owned by public authorities must reach the nZEB energy standard and from 2021 all the new buildings have to be nZEBs.

Renewable energy supply

Increasing the renewable energy share in electricity generation can reduce the carbon emissions of many types of electricity uses, such as lighting, appliances, and electric cooking [63,64]. It can also contribute to the decarbonization of space heating and cooling systems. Phasing out the onsite fossil fuel use of buildings mainly involves installing new heating systems (e.g. heat pumps, heat networks, and green gas boilers) that do not directly combust fossil fuels [60]. Replacing water heaters based on electricity and fossil fuels with solar water heaters can greatly reduce GHG emissions as hot water is provided with energy from the sun. Besides, increasing the installation of electric cooking systems (e.g. induction cooking) instead of natural gas cookers is also an option to reduce natural gas use.

Rather than consuming energy, buildings can also produce energy onsite by installing solar panels [29,65]. In recent decades, solar panel technologies have become mature and their price and installation cost has dropped significantly [66]. Solar panels can be installed on the roofs of existing buildings and are commonly installed on new buildings heated with heat pumps [67], especially on the roofs of nZEBs [68]. The solar panel system can convert energy from the sun into electricity and is regarded as an important option for renewable electricity generation [66]. Compared with a conventional pattern where power plants are far from buildings, meeting electricity demand with locally generated electricity from rooftop PV (photovoltaics) has the advantage of saving the cost of electricity transmission and distribution infrastructure and reducing electricity losses in transmission processes [69]. A report [70] estimated that there are 892 km^2 of roof surfaces suitable for solar PV installation in the Netherlands, which can potentially meet half of the national electricity demand and greatly reduce the fossil fuel combustion for electricity generation. Given that the electricity generation of solar panels is limited by the weather and sun, the supply peaks are usually not in line with the demand peaks [71]. Therefore, the combination of solar panels with energy storage technologies (e.g. lithium-ion batteries) can balance the different peaks of demand and supply [66]. When the electricity generated from solar panels exceeds buildings' demand and can supply surplus electricity to the public grid, such buildings or neighborhoods are named positive energy buildings (PEBs) or positive energy neighborhoods (PENs) [1,72].

1.3.3 Green lifestyles

In addition to technical measures, the GHG emissions of building stock can also be reduced by changing occupants' lifestyles [57,73]. Reducing the demand for floor area per capita (more intensive use of buildings [3]) can directly reduce the consumption of both materials and energy. Along with economic development and urbanization, house prices are increasing, which leads to decreasing family size (partly due to a lower marriage rate and birth rate than before) and the demand by individuals for increasing living space [3]. Policymakers and urban planners can mitigate this trend by constructing more multi-family houses rather than single-family houses. The size of single-family houses can also be reduced by constructing smaller buildings. Further, the greener lifestyles of building occupants can also lead to a reduction in the demand for energy and water, such as lowering room temperature and reducing shower time. Imposing taxes on fossil fuels and increasing the cost of energy can also contribute to the decrease in energy consumption [74].

1.4 Methods for analyzing building stock

The tools for analyzing building stocks include building stock models, which are usually based on material flow analysis (MFA), and life cycle assessment (LCA) [29]. In this thesis, the development of building stocks is calculated by combining an Urban mining model that analyses how much materials are stocked at a point in time in the built environment, with a Dynamic building stock model based on MFA that calculates material inflows and outflows per unit of time, and as a result, development of the building stock. We further use a Building stock energy model to analyze the energy requirements of the building stock, while we use LCA to assess the life cycle impacts of material and energy flows. These methods and their applications are introduced below.

1.4.1 Urban mining model

Urban mining models quantify how many, where and what kinds of materials are stocked in the current buildings and infrastructures [75,76]. They are mostly used to assess the potential of current anthropogenic material stock to provide secondary material to meet future material demand, such as concrete, bricks, wood, steel, and copper [76,77]. The amounts of building materials are usually estimated by multiplying the floor area of different types of buildings with the corresponding material intensities (kg/m^2) [78,79]. Many of these models apply GIS (geographical information system) data of buildings and infrastructures to estimate the floor area stock or the length of roads. For example, Mastrucci and colleagues [80] developed a bottom-up material stock model based on GIS and combined it with LCA to assess the end-of-lifespan scenarios of demolition wastes in a city in Luxembourg. Arora and colleagues [77] proposed a model framework for investigating the urban mining, recovery, and reuse potential of building materials on a city scale and demonstrated the framework in the public building stock of Singapore. Guo and colleagues [81] conducted a case study for Beijing, China, which quantifies the material stock in different kinds of roads. Arbabi and colleagues [82] presented a framework that can estimate the material stock at the building component level based on a mobile-sensing approach. Peled and Fishman [83] used nightlight radiance values as a proxy for built-up volume and linked it with the material stock distribution of Europe based on regression analysis. It is worth mentioning that Heeren and Fishman [84] created a comprehensive and harmonized material intensity database differentiated by climate and socioeconomic indicators by extracting data from 33 worldwide studies, which greatly helps data provided for use in urban stock models. Based on an extensive survey (813 sample buildings), Yang and colleagues [85] created the material intensity data of buildings differentiated by structure, function, construction period, and provinces in China. These datasets can increase granularity and consider the heterogeneity of buildings, which benefits model accuracy [10]. Nasir and colleagues [75] and Fu and colleagues [86] have provided an overview and comparison of approaches to urban mining models.

1.4.2 Building stock energy model

The end-use energy can be grouped into space heating, space cooling, domestic hot water, appliances, and lighting [87,88]. The end-use energy types can be very different, depending largely on the climatic and socioeconomic conditions [89]. For example, most residential buildings in the Netherlands do not have air conditioning systems for space cooling (moderately warm summers) while air conditioning systems are installed in most buildings in southern China (hot summers).

Building stock energy models (or urban building energy models) estimate the energy demand on a large scale to support decision-making in energy performance improvement and climate change mitigation [90]. This mainly involves assessing and comparing the energy-saving effects of different renovation measures, especially for reducing the space heating demand. Modeling the building stock energy demand is hindered by a lack of data on so many heterogeneous buildings on an urban or national scale, such as building geometries, physical properties, and occupant behavior.

Swan and Ugursal [87] classified building stock energy models into two categories: top-down models and bottom-up models. Top-down methods usually link aggregated energy consumption data from statistics with socioeconomic variables such as population, economic indicators, fuel prices, and income [91]. This kind of model mostly conducts a retrospective analysis of the relationship between sectoral energy consumption and macroeconomy [87] and estimates the potential change in energy demand and GHG emissions under certain policy scenarios in the future [92]. The technical details and end energy uses are usually omitted. In contrast, bottom-up approaches consider the end-use energy consumption intensities (kWh/m^{2}a) of archetypical buildings that are usually differentiated by construction periods and building types [93,94]. The energy demand of representative buildings is mostly aggregated to the building stock based on the distribution proportion of building archetypes [95].

Abbasabadi and Ashayeri [96] further classified bottom-up models into data-driven (statistical) and simulation (engineering-based) approaches. Data-driven models typically use statistical and artificial intelligence techniques (e.g. machine learning) to identify the mathematical relationship between energy use and the characteristics of end-users, such as urban attributes, occupant features, and building properties, while this method regards the building stock as a “black box” and relies on large-scale historical end-user datasets that are usually unavailable and need to be collected from questionnaires [96]. Engineering-based approaches use the physical properties of buildings, climate data, and occupant data to model the balance of heat transfer according to thermodynamic equations [97]. While it is almost impossible to collect so much detailed information on individual buildings, Buffat and colleagues [98] simulated the building stock heat demand building by building based on building energy modeling standards (engineering-based model) and comprehensive use of various GIS datasets in Switzerland such as building footprints and high-resolution climate data. There have already been several review articles [91,96,97,99–107] on building stock energy models.

1.4.3 Dynamic building stock model

Müller [108] developed a dynamic MFA model to determine the future product demand based on lifetimes, per capita demand, and population (stock driven). The model was applied to model the building stock development of the Netherlands and the corresponding concrete inflows, outflows, and stocks. After this, the model was widely used to model the production routes and embodied emissions of building and construction materials in general. Bergsdal and colleagues [109] employed MFA to model concrete and wood usage in residential buildings from 1900 to 2100. Material intensities differentiated by building type and vintage cohorts are multiplied with floor areas to quantify the material composition of the building stock. Hu and colleagues analyzed [110] the urban and rural floor area demand and predicted the oscillation of new construction and demolition activities in China. Hu and colleagues [111] applied MFA to estimate the amounts of CDW generation in Beijing. They found that the CDW generation will unavoidably rise and the lifetime of buildings is a key factor affecting future CDW figures. Using a cohort-based and stock-driven dynamic model developed by Deetman and colleagues [37], Zhong and colleagues [34] explored the material-related emissions for residential and commercial buildings in the world and compared the decarbonization potential of different material efficiency strategies. Heeren and Hellweg [112] applied a three-dimensional and geo-referenced building dataset to characterize the building geometries and combined this with detailed building inventory data to track future material flows and stocks in the Swiss residential building sector. They found that material outflows would be almost equal to material inflows in 2055, meaning that for the Swiss case CDW recycling has great potential to meet future material demand for construction activities, i.e. closing building material cycles. Wiedenhofer and colleagues [113] used an inflow-driven dynamic stock-flow model to analyze 14 kinds of materials in the building sector around the world and found that the rising levels of stocks in the future will lead to more waste outflows and higher material demand for maintenance, renovation, and replacement. Further information can be found in several review articles [24,114–118], which provide a comprehensive overview and comparison of modeling techniques in MFA.

Apart from material aspects, some models include the energy demand and environmental impacts in dynamic building stock analyses [79,90,119]. Heeren and colleagues [95] developed a lifecycle-based building stock framework (LC-Build) that classified the building stock according to construction periods, building types, and technical systems (e.g. heating and ventilation systems) and can assess the effect of climate change mitigation strategies on material flows, energy demand, and environmental impact. McKenna and colleagues [120] modeled the likely house stock development in Germany and modeled the energy performance change with the consideration of floor area demand, demolition and renovation rates. Roca-Puigròs and colleagues [28] developed a dynamic stock-driven model to quantify the future energy consumption and GHG emissions under different technology and lifestyle combinations in Switzerland. Recently, some researchers integrated building stock models with system dynamics models [121–123], agent-based models [124,125], and machine learning [126,127]. For instance, Nägeli and colleagues [128] employed an agent-based building stock model to explore the potential effects of different policies aimed at realizing national GHG emission reduction targets in Switzerland. There have already been some review articles [29,129,130] that classify the different building stock models and compare their modeling approaches.

1.4.4 Life cycle assessment

LCA is a method that accounts for the potential environmental impact of products and services during their life cycle [131,132]. It can help designers and policymakers to make decisions at the early stage of products, services, and policy strategy making [1,20]. ISO 14041 divides LCA into four steps: goal and scope definition, inventory analysis, environmental impact assessment, and interpretation [133]. When LCA is applied to individual buildings, it covers the product stage (raw material supply, transport, manufacturing), process stage (transport and construction), use stage (use, maintenance, repair, replacement, refurbishment, operational energy use, and operational water use) and end-of-life stage (deconstruction, transport, waste processing, disposal) [134]. The commonly used life cycle inventory databases are, e.g., ecoinvent, Gabi, ELCD, and CLCD [135–138]. The most commonly used LCA software include SimaPro, Gabi, OpenLCA, brightway [139], and the Activity Browser [140–142]. In the past decade, the ever-wider application of building information modeling (BIM) systems proved to be supportive to provide Life Cycle Inventory (LCI) data for buildings concerning detailed material and energy consumption data during building construction and operation [20,143–146].

The review by Mastrucci and colleagues [129] shows that LCA application in building stock models mainly involves: 1) assessing the performance of current building stock to inform current issues; 2) exploring the improving potential of certain measures (e.g. renovation) in comparison with the current state; 3) the environmental target realization potential during building stock evolvement. The production-construction and use stages are included in most studies while the end-of-life stage is usually omitted [29,129]. Instead of quantifying the annual environmental impact of individual buildings one by one, current building stock models usually regard the building stock as a “virtual product” providing humans with comfortable living spaces (meeting floor area demand) over a specific time frame. The material flows and energy consumption information from building stock models are typically aggregated, after which LCA is used to calculate the life cycle emissions and impacts related to these material and energy flows. Results are usually reported as annual environmental impacts or accumulated impacts in the considered time frame. For example, Göswein and colleagues [31] translated material and energy needs into an emission inventory reflecting GHG emission coefficients. Heeren and colleagues [95] used the emission factors extracted from the ecoinvent database in their dynamic building stock model to calculate both direct and indirect GHG emissions (upstream processes).

1.5 Building stock modeling in the Netherlands

Several studies have developed building stock models in the Netherlands. The building stock model developed by Müller [108] is the earliest one, which presented the basic modeling principles and applied the model to analyze concrete flows and stock. Based on the material intensity data [147] collected from demolition companies in the Netherlands, Verhagen and colleagues [44] modeled the building stock dynamics based on government plans and compared the amounts of recycled materials from demolition wastes with the material demand for construction. Zhang and colleagues [148] extended the ODYM (Open Dynamic Material Systems Model [149]) by including a renovation function and explored the potential of new technology for manufacturing prefabricated concrete elements (PCEs) from recycled CDW. Zhang and colleagues [43] further conducted a static MFA to analyze the contribution of different end-of-life scenarios to circular construction.

In addition to material usage, some other studies focused on saving energy and reducing environmental impact. Verhagen and colleagues [74] characterized the building stock with GIS data and compared the environmental and financial impact of alternative sustainable heating options to natural gas boilers. Yücel [150] presented a dynamic simulation model to analyze the importance and inertia of the existing Dutch residential stock for the energy transition. Mastrucci and colleagues [151] linked measured natural gas and electricity consumption with several variables (e.g. building type, construction year, and floor area) through multiple linear regression, and assessed the energy-saving potential of typical renovation measures in Rotterdam. Wang and colleagues [152] presented a data-driven residential heating demand model based on GIS data and Bayesian calibration and applied the model in Amsterdam. Filippidou and colleagues [153] estimated the renovation rate between 2010 and 2014 based on the SHAERE (Sociale Huursector Audit en Evaluatie van Resultaten Energiebesparing), involving 856,252 Dutch residential buildings. Liu and colleagues [154] conducted a case study for the city of Utrecht to assess the current and future energy system in 2050 under different sustainable heating scenarios.

1.6 Research gaps

Despite the progress in data application and modeling techniques, there are several limitations:

(1) **The potential development of the Dutch residential building stock in space and time**. Against the background of energy transition and climate change mitigation, the Dutch building stock composition will see substantial change due to demolishing old energy-inefficient buildings, constructing energy-efficient buildings, and upgrading the energy performance of existing buildings. To develop optimal decarbonization strategies, it is important to track this dynamic process and understand how many and which buildings will be involved with what kinds of solutions. However, previous dynamic building stock models mostly disaggregated the building stock based on statistical floor area. While the Netherlands has high-resolution GIS data of buildings that contains georeferenced information, geometries, construction year, and function, the potential of this data has not been fully explored in dynamic building stock modeling to simulate the spatiotemporal development pattern of building stock yet.

(2) **Energy-saving potential and energy supply**. Reducing energy demand and greening the energy mix is critical for the decarbonization of the residential sector. It is necessary to assess the energy-saving potential of different measures (e.g. envelope insulation and heating system replacement) and explore the potential change in energy supply structure in the building sector, particularly with the consideration of wide installation of rooftop PV. The macro policy targets (e.g. climate change mitigation) and corresponding strategies have to be realized by implementing specific measures (e.g. envelope insulation and technical system replacement or installation) that influence the material and energy use of individual buildings. However, existing dynamic building stock models are mostly top-down and usually estimate energy consumption by multiplying floor area with energy intensities of a limited number of archetype (or sample) buildings, which is too rough to capture the complex and gradual development of individual buildings in terms of material composition, technical system parameters, energy performance and environmental impact under different technical combination scenarios.

(3) **Linking material outflows with material inflows in space and time**. Previous urban mining models mainly analyze the spatial distribution of retrospective material flows and current material stock and have not yet adequately depicted the spatial distribution of future material flows, while the spatial distribution of material flows will significantly influence the cost and GHG emissions of transportation processes. In addition, the models focusing on future perspectives usually estimate the potential of CDW recycling to meet future material demand by directly comparing material inflows with material outflows. However, the amount of CDW that is recycled and comes back to the building stock is not only limited by the composition of the collected CDW but also by secondary material production practices and future building types, and associated material demand.

(4) **Overall decarbonization potential of combined strategies**. Previous studies mostly focused on either material or energy aspects separately, whereas material-related strategies (e.g. circular economy) and energy-related strategies (e.g. heat transition) are intertwined with each other and deployed together in reality. For

example, the large-scale energy-efficiency renovation of existing building stock will require large amounts of building materials, particularly insulation materials. In addition, replacing old energy-inefficient buildings with energy-efficient buildings will lead to large amounts of CDW generation and material consumption. Moreover, the lifestyle of occupants has not been well considered although it can significantly influence resource and energy consumption. It is, therefore, necessary to consider different factors together to help policymakers understand what the overall decarbonization potential of the building stock is and which strategies should be given priority.

1.7 Aims and research questions

The government of the Netherlands has established ambitious targets related to the circular economy [155], energy transition [156], and climate change mitigation [157]. This research aims to provide policymakers with the knowledge related to building stock decarbonization and support them in making reasonable climate change mitigation strategies. It involves tracking the building stock development and accounting for the associated material flows, energy demand, and environmental impacts under different scenarios. The overarching research question is:

What is the potential to reduce energy demand, close material loops, and decarbonize in the residential building sector of the Netherlands?

To answer the overall research question, the following sub-questions are developed:

(1) *How will the residential building stock develop in the Netherlands?* (Chapter 3, 4, and 5)

(2) *How much can energy demand be reduced and what is the potential of rooftop PV to meet local electricity demand?* (Chapter 2, 3, and 5)

(3) *How much primary material consumption in the Dutch residential building sector can be potentially reduced by urban mining?* (Chapter 4 and 5)

(4) *To what extent can residential GHG emissions be reduced under different decarbonization strategies and scenarios?* (Chapter 3, 4, and 5)

1.8 Thesis outline

The thesis consists of six chapters (see **Figure 1.1**).

Chapter 1 introduces the characteristics and existing challenges of the building sector in terms of material use, CDW generation, energy consumption, and GHG emissions. It reviews the main policy strategies and technical measures to reduce the GHG emissions of the building stock. An overview of relevant methods for analyzing building stock is provided, including urban mining, LCA, and building stock models. Finally, the research gaps, aims, research questions, and outlines of the thesis are presented.

Chapter 2 presents an engineering-based, bottom-up building stock energy model that can estimate the current energy demand and assess the energy-saving potential of certain energy efficiency measures. An approach to derive building information (e.g. geometries and physical properties) from GIS data and building archetypes is proposed. The model accuracy is spatially validated against statistical energy consumption. The marginal accuracy improvement due to including more parameters is explored.

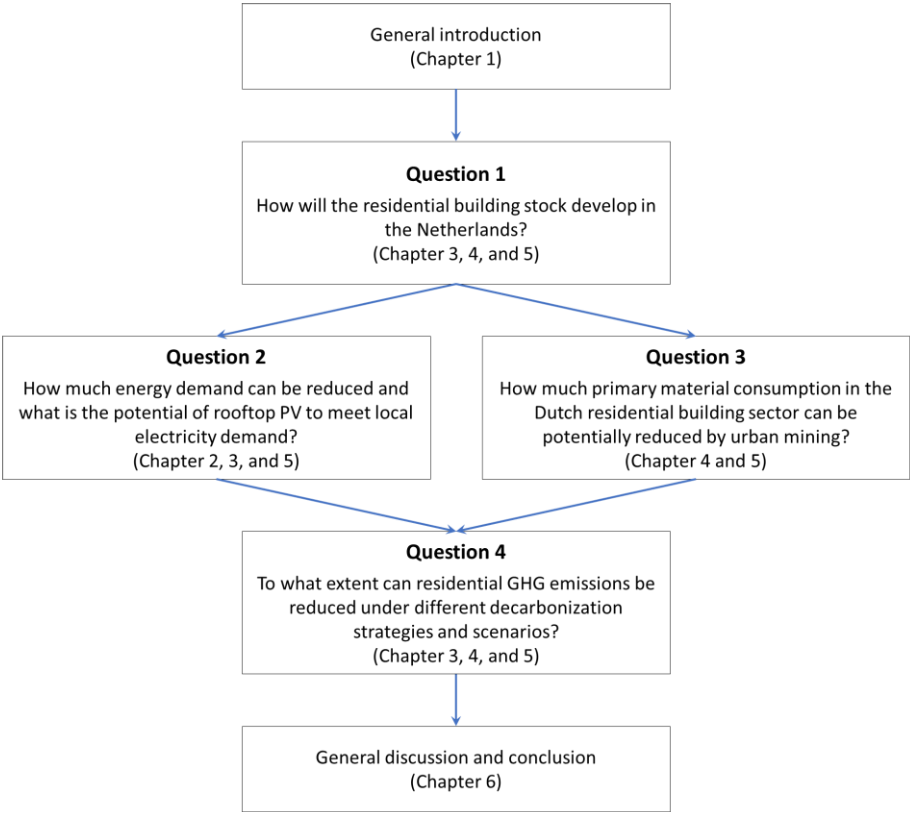

Figure 1.1 Outline of the thesis.

Chapter 3 develops a bottom-up dynamic building stock model that tracks the change in floor area composition, material stocks and flows, energy demand and supply, and GHG emissions under energy transition scenarios in the Netherlands. The overall energy and GHG emission reduction potential are analyzed. The effects of different measures on GHG emissions from space heating are compared. The potential of rooftop PV systems to meet the electricity demand for appliances and lighting is investigated.

Chapter 4 estimates the urban mining potential to substitute primary materials and reduce GHG emissions. It is based on the model from chapter 3, while it adds a module linking material inflows with material outflows. The spatial distribution of material stocks and material flows in different cities are mapped. The spatiotemporal mismatch between material demand and secondary material supply is analyzed. The decarbonization effects of urban mining and renewable electricity transition are accounted for.

Chapter 5 presents a bottom-up dynamic building stock with both spatial and temporal dimensions to assess the decarbonization potential of different strategies, mainly including material transition, energy transition, and green lifestyle. Renovation is driven by building component lifetimes instead of exogenously defined renovation rates. The maximum decarbonization potential of implementing all kinds of strategies is estimated. The effects of different decarbonization strategies are compared.

Chapter 6 answers the research questions, discusses the findings, and provides implications for making policies. The limitations of the thesis and recommendations for future research are given.

Chapter 2 A combined GIS-archetype approach to model residential space heating energy: A case study for the Netherlands including validation[1]

Abstract

High spatial resolution is critical for a building stock energy model to identify spatial hotspots and provide targeted recommendations for reducing regional energy consumption. However, input uncertainties due to lacking high-resolution spatial data (e.g. building information and occupant behavior) can cause great discrepancies between modeled and actual energy consumption. We present a modeling framework that can act as a blueprint model for most European countries based on geo-referenced data, building archetypes, and public algorithms. Further sophistication is added in a step-wise approach, including the shift from average to hourly weather data, refurbishment, and occupants' heating schedules. The model is demonstrated for the city of Leiden, the Netherlands, and the simulated results are spatially validated against the measured natural gas consumption reported at the postcode level. Results show that when these factors are considered, the model can provide a good estimate of the energy consumption at the city scale (overestimated by 6%). At the postcode level, nearly 83% of the absolute differences between modeled and measured natural gas consumption are within one standard deviation (± 25 kWh/m^{2}a, about 30% of the mean measured natural gas consumption). Further research and data would be required to provide reliable results at the level of individual buildings, e.g. information on refurbishment and occupant behavior. The model is well suited to identify spatial hotspots of residential energy consumption and could thus provide a practical basis (e.g. maps) for targeted measures to mitigate climate change.

Keywords: building stock, space heating, spatially explicit model, Geographic Information System (GIS), the Netherlands

2.1 Introduction

The building sector is important for climate change mitigation [32], as it is responsible for approximately 40% of final energy consumption and 36% of the greenhouse gas (GHG) emissions in the European Union (EU) [158]. Spatially-explicit building stock energy models can be used to identify energy consumption hotspots, assess the energy-saving potential of various technologies, such as envelope insulation, efficient HVAC (heating, ventilation, and air conditioning) system, or optimize the integration of renewables [159], such as solar photovoltaic

[1] Published as: Yang, X., Hu, M., Zhang, C., Steubing, B. A combined GIS-archetype approach to model residential space heating energy: A case study for the Netherlands including validation. Applied Energy 280, 115953 (2020).

systems (PVS), and thus support the building, neighborhood, or city-level decision making [98].

Many building stock energy models have been developed, which can be divided into top-down and bottom-up models [87]. The top-down models regard the building stock as a black box and estimate energy consumption by investigating the correlations between aggregated energy consumption and socioeconomic or sociotechnical drivers from a historical perspective, usually based on statistical data [160]. Due to lacking details of individual buildings, such models cannot capture the characteristics of the energy consumption of specific neighborhoods [161], especially those caused by discontinuous changes in techno-economic conditions, such as the wide application of new insulation materials, high-efficiency HVAC systems, and sustainable energy sources [162].

In contrast, bottom-up models use a hierarchy of disaggregated components as input data and account for the regional or national energy consumption by summation of the energy consumption of individual buildings or building groups [129]. Swan et al. [87] further classify the bottom-up models into statistical and engineering-based methods (also known as physical models or white box models [160]). The former performs statistical analysis (mostly regression techniques) on historical data and establishes the relationships between end uses and energy consumption [163] while the latter considers the building elements and HVAC of sample buildings representative of the building stock and simulates the energy demand with the balance of heat transfer following thermodynamic principles [164]. Kavgic et al. [162] add the hybrid models that estimate the energy consumption mainly influenced by occupant behavior, such as domestic hot water (DHW), cooking, lighting, and appliances with statistical methods while calculating the energy consumption for space heating and cooling with engineering-based methods due to a lack of historic data and the application of new technologies.

According to the difference of aggregation process, Mastrucci et al. [129] divide the engineering-based bottom-up model into the archetype approach and building-by-building approach. The archetype approach employs a subset of archetype or sample buildings to represent a specific building cohort that has similar properties (e.g. building type and age) and extrapolate them to total energy consumption (typically urban, regional, or national building stock) by factoring the results in proportion (by number or floor area per building type or age group) [95]. This method has been widely adopted by many studies [165]. However, the limited coverage and representativeness of archetypes for heterogeneous building stock may greatly influence the reliability of results for both individual buildings and the whole building stock [166]. Distinct from the archetype approach, the building-by-building method simulates building energy consumption one by one and then sums up the energy consumptions of individual buildings to the whole stock level. While this approach in principle can assess the different combinations of refurbishment measures applied to single buildings, expanding energy simulation tools from a single building to urban or national stock level makes data collection more challenging [103].

The input data for engineering-based building stock energy models mainly includes building geometries, physical properties (e.g. thermal transmittance, solar energy transmittance, and air exchange by infiltration), HVAC systems, occupant behavior (e.g. hours of occupancy, number of occupants, internal room temperature, internal heat gains and air exchange by use), and external weather conditions [167]. In the past decades, the method of Geographic Information System (GIS) has significantly increased the availability of large-scale geo-referenced building information, especially the building geometries, which makes such models more sophisticated and spatially explicit [129]. GIS is mostly applied in result visualization or estimating the floor areas [98]. Only a few studies [98] use GIS data to quantify the areas of envelope elements and then simulate the energy consumption building by building. The main barrier is that the non-geometric building information such as properties, HVAC, and occupant characteristics [168], is typically not available at the city scale [98]. Therefore, archetypes complemented by assumptions are usually used to fill in the data gaps [169]. Besides, refurbishment records for existing buildings (i.e. the type and extent of insulation added or the upgrade of HVAC systems) are difficult to obtain and only a few studies [98] that consider these. Therefore, simplified energy models are often used [162], while both model simplification and input data uncertainty may lead to notable discrepancies between simulated and measured energy consumptions, known as the "energy-performance gap" [170].

The review above demonstrates that lacking the data at the individual building level is the main barrier for building stock models. Different models are developed for different countries or regions, depending on data availability and research purposes. Engineering-based bottom-up models can track the energy-efficiency measures while they differ significantly in the complexity of input data and energy simulation algorithms or tools. The previous models based on the building-by-building approach require particularly large amounts of detailed data that are only available for certain countries [98]. In addition, the energy simulation methods are usually national standards or expensive software [171], some of which are incapable of processing largescale building stock. Therefore, these models have limited applicability in other countries, and typically lack the high spatial resolution of energy consumption. There is a demand for a harmonized model that estimates the energy consumption of largescale building stock (city or national scale) with a high-level spatial resolution and can act as a benchmark method for policy makers and planners to effectively quantify the energy efficiency of the current building stock, identify energy consumption hotspots, and evaluate the energy-saving effects of measures or technologies aimed at mitigating climate change in the building sector. Recently, GIS data of building footprints, archetype buildings (notably the residential archetype buildings for 21 EU countries in TABULA [68]), and other data, such as high-resolution weather data, have become available for many countries, which provides the possibility of developing such a model framework for a larger number of countries.

The goal of this paper is to develop a transferable framework for modeling residential space heating energy consumption based on GIS data and archetypes. The model maps the typical geometry parameters, physical properties, and HVAC of archetypes to individual buildings in GIS data according to age and type, and then simulates the energy consumption building by building. As in most countries, GIS data of buildings does not hold building types or simply differentiates between single-family houses and multi-family houses, we present an approach to identify them based on building size and morphology. A stepwise approach is presented to construct the model and thereby include key factors such as spatial building properties, building system, as well as temporally resolved weather data, refurbishment, and occupant schedules. The model is applied in Leiden, a city in the Netherlands and spatially validated against the measured energy consumption.

2.2 Materials and methods

2.2.1 Model overview

Table 2.1 Steps and factors increasing sophistication for the energy consumption for space heating.

Step	Main factors for energy consumption	Model implementation	Data type	Calculation method
S1	Basic input data	Derived from BAG [172] and TABULA [68]	Spatial and archetypal	Seasonal
S2	+ hourly weather data	Temperature and global solar radiation from KNMI [173]	Temporal and spatial	Hourly
S3	+ refurbishment	Random allocation by refurbishment rate [174]	Statistical	Hourly
S4	+ occupant schedule	Assumption: 18:00-08:00 (+1 day)	Temporal	Hourly

In order to develop a building stock energy model and simultaneously investigate the effects of various factors on the modeled energy consumption for space heating, we stepwise simulate the energy consumption with increasing model sophistication. Step 1 (S1) uses the seasonal heat demand calculation method while S2-4 employ the hourly calculation approach (see section **2.2.3**). All steps use the same basic input data, including geometry, physical property, supply system, and occupant-behavior data other than occupant schedule. S1 uses seasonal average weather data, while hourly weather data is introduced in S2, refurbishment in S3, and occupant schedule in S4, as shown in **Table 2.1**.

Three principal data sources are used in this study:

(1) The GIS dataset from the Basic Registration of Addresses and Buildings (BAG) contains all official addresses and basic building information of the Netherlands [172]. The main information included in this dataset is the georeferenced building footprint as a polygon, function, year of construction, building height, and registered addresses per building.

(2) The TABULA database (Typology Approach for Building Stock Energy Assessment) contains residential building typologies for 21 European countries including the Netherlands [68]. It distinguishes six construction periods, i.e. before 1965, 1965-1974, 1975-1991, 1992-2005, 2006-2014 and after 2014, and five types of residential buildings, namely single-family house, mid-terraced house, end-terrace house, apartment building, and multi-family house (see **Table S7.1.1** in Appendix), and provides archetypical information on their surface areas, the thermal properties of envelope components, and supply systems.

(3) Weather data is from the Royal Dutch Meteorological Institute (KNMI) [173].

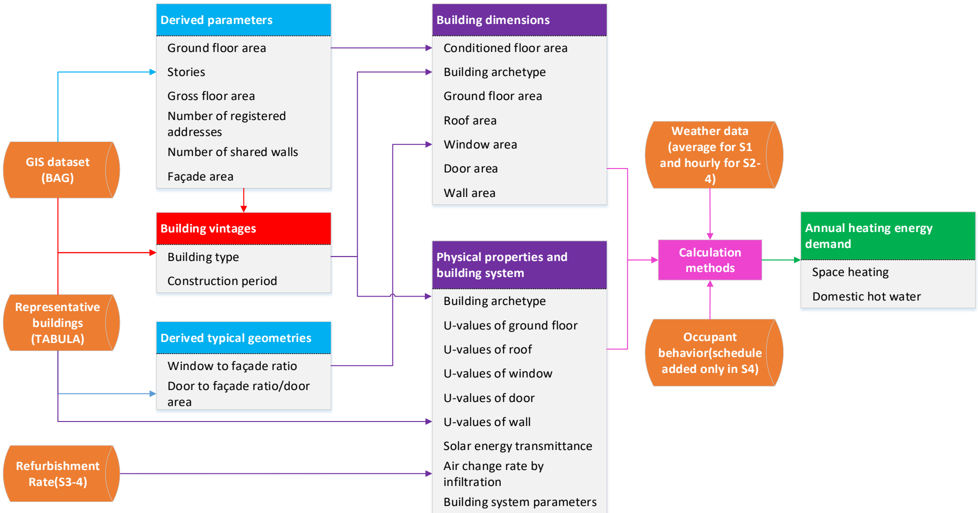

Figure 2.1 Schematic overview of the relationships between different databases. The orange denotes data sources. The blue denotes the derived basic building parameters from BAG and TABULA. The red denotes the identified construction period and building type of each building. The purple denotes the derived input data for heating energy models. The pink denotes the calculation methods. The green denotes the outputs of different models. The colors of connection arrows are in line with the latter databases.

These data sources are combined in the four models as shown in **Figure 2.1.** In order to characterize BAG buildings with TABULA archetypes, we first identify the types of BAG buildings, and then automatically map the parameters (typical geometries, physical properties, and supply system parameters) of archetypes to BAG buildings based on construction periods and building types. The following five criteria are employed to differentiate the types of BAG buildings: the number of shared walls, the number of registered addresses, building footprint area, gross floor area, and the number of stories (see details in **Table S7.1.2** in Appendix). These extracted parameters, together with the weather data, refurbishment statistics, and occupant-behavior data, constitute the input data for S1-4.

2.2.2 Input data

2.2.2.1 Building information

As proposed by Heeren and Hellweg [112], we use several strategies to correct and complete faulty and missing data. The implausible building heights (smaller than 2 meters) are automatically replaced by the heights of the nearest buildings with the "spatial join" tool of ArcGIS 10.6.1. Because floor heights vary significantly in reality and many buildings may have slanted roofs, the average floor height is assumed as 3 meters [175]. The stories of buildings are estimated as follows:

$$stories = round(height \div 3m) \qquad (1)$$

The gross floor area (A_{gross}) is calculated by multiplying the building footprint area ($A_{footprint}$) with the stories:

$$A_{gross} = A_{footprint} \times stories \qquad (2)$$

The number and area of shared walls between adjoined buildings are critical for both identifying the building type and calculating the areas of façade components exposed to the outdoor air. ArcGIS 10.6.1 is employed to generate the shared line of two adjoined building footprints. The height of a shared wall is determined by the lower height of two adjoined buildings. It is formulated in eq 3:

$$A_{shared\_wall} = \sum_{i=1}^{n} length_{shared\_line_i} \times min\,(height_{building_0}, height_{building_i}) \qquad (3)$$

where A_{shared_wall} is the area of shared walls of a given building. n is the number of walls that $building_0$ shares with its adjacent buildings. $length_{shared\_line_i}$ is the length of the shared wall between $building_0$ and its adjoined $building_i$.

BAG does not hold the types (flat or slanted) and inclination angle of roofs. According to the research by Froemelt and Hellweg [167], roof inclination has a very limited effect on overall energy consumption for space heating, so we do not consider the roof types and each building is simplified as a cube.

The area of roof and ground floor is assumed to be equal to the building footprint area. The façade consists of window, door, and external wall (exposed to the outdoor air). Its area is calculated by multiplying the perimeter of each building footprint with the corresponding building height and subtracting the areas of shared walls:

$$A_{facade} = perimeter_{footprint} \times height - A_{shared\_wall} \qquad (4)$$

In order to estimate the areas of windows, the window-to-façade ratio ($fraction_{window}$, see **Table S7.1.5** in Appendix) are derived from the envelope component areas of representative buildings in TABULA. Then the window area is calculated by multiplying the façade area with the window-to-façade ratio:

$$A_{window} = A_{facade} \times fraction_{window} \qquad (5)$$

As the difference between the door areas of the single-family house and the terraced house is typically very small, the door areas of these buildings are obtained from the representative buildings in TABULA (A_{TABULA_door}, see **Table S7.1.5** in Appendix). The door areas of multi-family houses and apartment buildings are calculated by multiplying the façade area with the door-to-façade ratio ($fraction_{door}$, see **Table S7.1.5** in Appendix):

$$A_{door} = \begin{cases} A_{TABULA\_door} & for\ single-family\ house\ or\ terraced\ house \\ A_{facade} \times fraction_{door} & else \end{cases} \qquad (6)$$

The area of the external wall is calculated by subtracting the window area and door area from the façade area:

$$A_{external\_wall} = A_{facade} - A_{window} - A_{door} \qquad (7)$$

According to the TABULA calculation method, the conditioned floor area (A_{con}) is determined by the internal dimensions [176]. In this study, the thickness of the external wall is assumed as 0.25 meters [177], [178] and the conditioned floor area is estimated by correcting the gross floor area:

$$A_{con} = A_{gross} - perimeter_{footprint} \times 0.25m \times stories \qquad (8)$$

Based on the building classification and age determined above, the U-values (thermal transmittance coefficient) of envelope components, g-values (solar energy transmittance values) of windows, air change rate by infiltration, and supply system parameters from the archetypes in TABULA are allocated to BAG buildings.

2.2.2.2 Weather data

KNMI includes 50 weather stations distributed in the territory of the Netherlands and records the weather data per station per hour [173]. The typical heating season in the Netherlands is from October 1st to April 30th (212 days) [170]. S1 uses the average hourly outdoor temperature and global solar radiation, while S2-4 use the hourly weather data.

2.2.2.3 Refurbishment

TABULA includes refurbishment standards for representative buildings, including U-values of roof, window, wall, and ground floor, and the g-values of windows. The U-values distinguish conventional refurbishment, i.e. to the current standard, and advanced refurbishment, i.e. to the nearly zero-energy level [68]. However, BAG does not hold the information on what refurbishment measures have been exactly implemented for which buildings. We allocate the refurbishment of archetypes to BAG buildings based on refurbishment rates. As the latest cumulative refurbishment rates for envelope components are only available for 2012 [174], we linearly extrapolate the annual refurbishment rates of 2013-2015 based on the average annual refurbishment rates of 2006-2012. Therefore, the cumulative refurbishment rates ($R_{component}$) of ground floors, external walls, roofs and windows are 63%, 77%, 81%, and 88%, respectively.

According to Milieu Centraal [179], the buildings constructed after 2000 are already well insulated and this is also shown by their U-values in the TABULA database [68]. In addition, these recently constructed buildings are unlikely to have undergone significant thermal refurbishment. Therefore, we assume that only buildings constructed before 2000 might have been refurbished. The number of refurbished buildings for each type of envelope component ($N_{component}$) is determined as follows:

$$N_{component} = N_{building} \times R_{component} \qquad (9)$$

Where $N_{building}$ denotes the total number of buildings; $R_{component}$ is the cumulative refurbishment rate for a specific type of envelope component.

As the refurbishment rates are not differentiated by the construction period and building type, we randomly choose $N_{component}$ BAG buildings constructed before 2000 and assume that the components of these buildings have experienced conventional refurbishment. Then the U-values of their envelope components are updated.

2.2.2.4 Occupant behavior

According to TABULA, the internal room temperature, air change rate related to the utilization of the building, and the internal heat gains from human metabolism and appliances, are 20 °C (T_{int}) and 0.4 1/h ($n_{ve,use}$) and 3 W/m^2 (q_{int}), respectively [68]. The above values are the same for S1-4 while the occupant schedule is only considered in S4. The average time that occupants stay at home differs across studies (e.g. 12 [180] or 16 [181] hours per day). Occupants are assumed present at home from 7:00 pm to 7:00 am (+1 day, 12 hours) [180], and the heating supply systems are assumed to only operate during this period.

2.2.3 Calculation of energy consumption

While the purpose of the study is to develop models for simulating the energy consumption for space heating, the validation data, apart from the energy consumption for space heating, also includes the energy for DHW. In order to ensure comparability, we thus additionally simulate the energy consumption for DHW generation. The energy demand for space heating and DHW is calculated based on EN ISO 13790 [180] and the TABULA method [176]. S1 is a seasonal model (seasonal calculation timesteps), while S2-4 are hourly models. Then the energy demand is converted into energy consumption based on the TABULA supply system simulation method [176]. The detailed calculation process can be found in section **7.1.4** and the simulation is performed with Python.

2.2.4 Case study

The residential building stock of Leiden, a city in the Netherlands is selected as a case study to demonstrate the developed model. Leiden is a typical Dutch city that has various kinds of residential buildings (29030 in total based on BAG). Its residential building stock characters can be found in **Table S7.1.3** and **Table S7.1.4** in Appendix. Almost half of the buildings are built before 1964 while the 1975-1991 period seems a high tide of construction. Terraced houses account for approximately 52% of the total conditioned floor area in Leiden. As there is no weather station in Leiden, we use the weather data (2016) of Voorschoten, the closest weather station to Leiden.

2.2.5 Spatial validation

The Central Bureau of Statistics (CBS) holds the measured natural gas consumption data at the household level [182] but the data is only publicly available in an aggregated form at the postcode level. We use the natural gas consumption data in 2016 to validate the modeled natural gas consumption (aggregated to 2950 postcodes, see the distribution of buildings per postcode in **Figure S7.1.1** in Appendix). In this study, the heating value of natural gas is used to convert the unit of measured natural gas (m^3) into kWh (1kWh=3.6MJ) and its value (35.2 MJ/m^3) is from the literature [183]. The physical properties of buildings' envelope elements vary with ages, so the "age" of the postcode is regarded as the average building construction year weighted by conditioned floor area.

The measured natural gas does not distinguish between end-use energy purposes (mainly including space heating, DHW, and cooking), but the proportion of cooking is quite small (on average only 3.9% [183]). Therefore, we subtract 3.9% of the measured natural gas from each postcode and thus the remaining natural gas is mainly related to space heating and DHW.

Then the modeled natural gas consumption and conditioned floor area aggregated at postcode level are spatially linked to the measured natural gas consumption based on postcodes (see **Figure 2.2**). The overlap ratio, defined as the ratio of the footprint area of dissolved buildings by postcode (BAG) to the footprint area of dissolved buildings by postcode (CBS) and vice versa, is used to guarantee that the same buildings are selected for validation. Only postcode pairs whose overlap ratios are within the 90-110% interval are selected (1,241 postcodes excluded and 1709 postcodes left).

When the measured natural gas consumption is normalized by the conditioned floor area, outliers (the measured natural gas consumptions that are below 20 kWh/m^2a and above 500 kWh/m^2a [184]) are found, which is mainly caused by the following reasons:

(1) There might be some data errors caused by limited data coverage or occupants' delayed registration.

(2) While the majority of buildings use natural gas for space heating and DHW in the Netherlands, some buildings are heated by other energy sources, such as electricity, CHP (combined heat and power), and geothermal heating [170]. In the

heat transition atlas [185], we find that two CHP plants exist in Leiden and many buildings are connected with the heat distribution networks, for example, the buildings in Stevenshof (see **Figure 2.2**).

(3) An extreme case is that the building's areas are only partly used by occupants and thus the natural gas consumption per conditioned floor area is very small.

(4) Some houses might have mix-use purposes. For example, ground floors are for business while the upper floors are for the living.

Therefore, the postcodes with outliers are excluded from the comparison. Finally, 44% of postcodes and 49% of modeled buildings are left (see **Figure 2.2**).

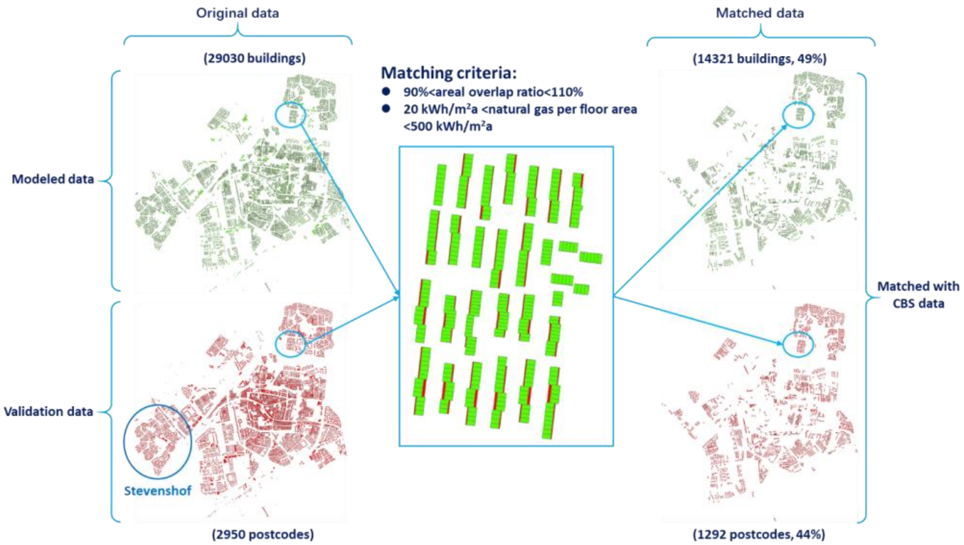

Figure 2.2 Mapping the modeled results with measured data from CBS. The green polygons are BAG buildings and the red are the CBS buildings dissolved by postcode. The natural gas consumption is expressed in kWh/m²a. In Stevenshof, the buildings are connected to district heating networks, so it is filtered.

2.3 Results

2.3.1 Cumulative results

Figure 2.3 shows the cumulative natural gas consumption for all the steps as well as validation data. S4 fits best with the measured data (overestimated by about 6% in total) and thus indicates that including all influencing factors yields the most realistic results. In contrast, S1-3 overestimate natural gas consumption. While there is hardly any difference between S1 and S2, suggesting that the additional weather model detail has little effect, the largest reduction arises from including refurbishment (S3) and then the second largest reduction from including occupant schedule (S4).

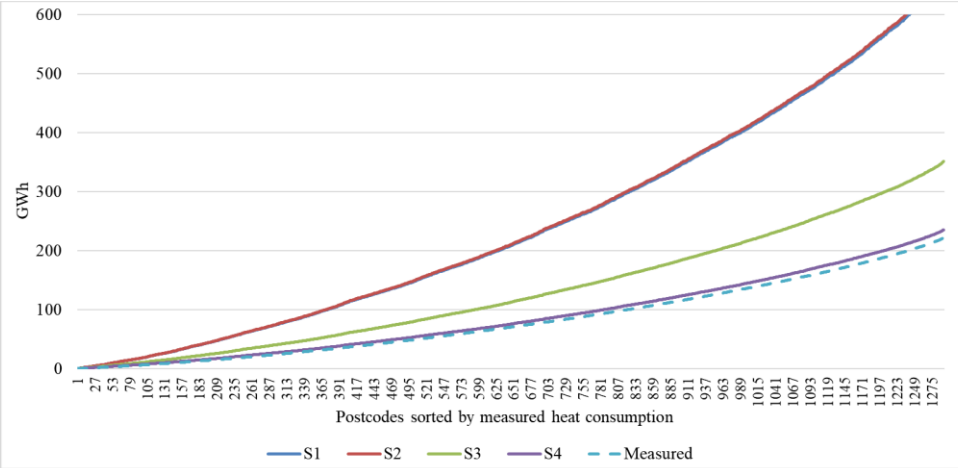

Figure 2.3 Modeled and measured natural gas consumption cumulated for all 1292 postcodes. S is the abbreviations for step (both here and below).

2.3.2 Influence of building age

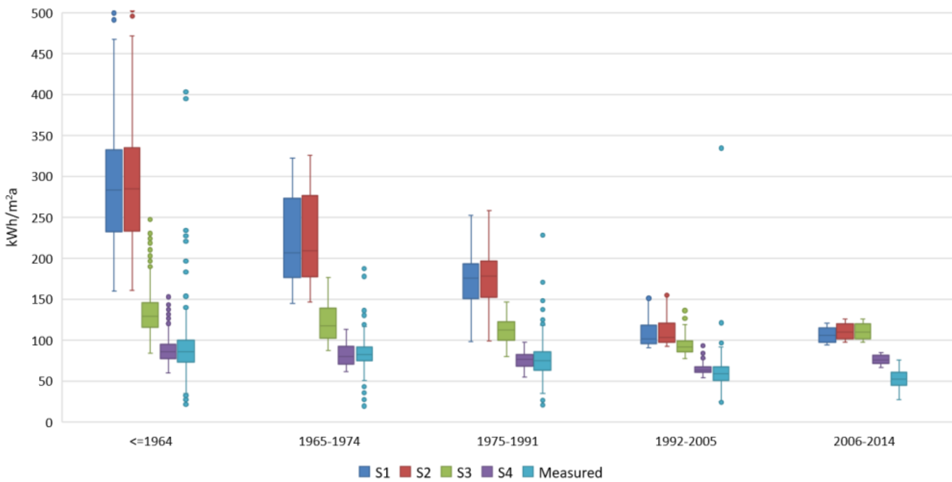

Figure 2.4 The measured and modeled annual natural gas consumption of different construction periods. The solid line in the box is the median value.

From **Figure 2.4** we can see that both the simulated and measured natural gas consumptions decrease with the increasing construction periods (except for S3-4 in the 2006-2014 period). There is no great difference between the measured natural gas consumption of different periods, but the measured natural gas consumption of the 2006-2014 period declines significantly.

The natural gas consumption modeled by S2 is only slightly larger than S1. The modeled natural gas consumption plunges after refurbishment and occupant schedules are taken into account. S4 fits best with the measured natural gas consumption, but it slightly overestimates the natural gas consumption of buildings in the 1992-2005 period and overestimates the energy consumption of buildings after 2006.

It is found that the measured natural gas consumption has a broader range than the modeled consumption. The reason is that the diversity of the real world is higher than what our models can capture. For example, the building geometries and thermal properties are derived from a limited number of representative buildings in TABULA, and occupant-related parameters are from TABULA and educated assumptions, which narrows the spectrum of modeled natural gas consumption.

2.3.3 Accuracy analysis

Figure 2.5 maps the modeled and measured natural gas consumption of each postcode. Comparing **Figure 2.5a** and **Figure 2.5b**, we can find that the natural gas consumptions are quite large for certain spatially clustered postcodes, but the extreme natural gas consumption of validation data is more obvious than that of S4. It is also found in **Figure 2.5c** that the deviations between S4 and validation data are in general very small, although the natural gas consumption modeled by S4 is not very consistent with the measured natural gas consumption for some postcodes. From **Figure 2.5d** we can see that older buildings tend to consume more natural gas, but it is not always the case.

Figure 2.6 shows the distribution of absolute deviations between S4 and validation data. The average absolute difference is -0.4 kWh/m^{2}a, which means that S4 slightly underestimates the natural gas consumption. Nearly 83% of the absolute deviations are in the $\pm\sigma$ interval while 98% are in the $\pm 2\sigma$ interval. The mean bias error (MBE) is -0.35 kWh/m^{2}a, and the coefficient of variation of root mean square error (CVRSME) is 31% [186]. Overestimations and underestimations almost symmetrically distribute on both sides of zero, which is one of the main reasons why underestimations and overestimations level off and the modeled natural gas consumption is in good agreement with the measured natural gas consumption on the Leiden building stock scale.

2.4 Discussion

2.4.1 Key factors for modeling the energy consumption for space heating

The validation reveals that S1-2 do not consider refurbishment and occupant schedule and fail in accurately simulating the natural gas consumption, while the modeled natural gas consumption becomes increasingly close to the measured natural gas consumption after refurbishment and occupant schedule are included in S3-4. Therefore, refurbishment and occupant schedule are important factors affecting the modeled natural gas consumption, which is in line with other studies [167].

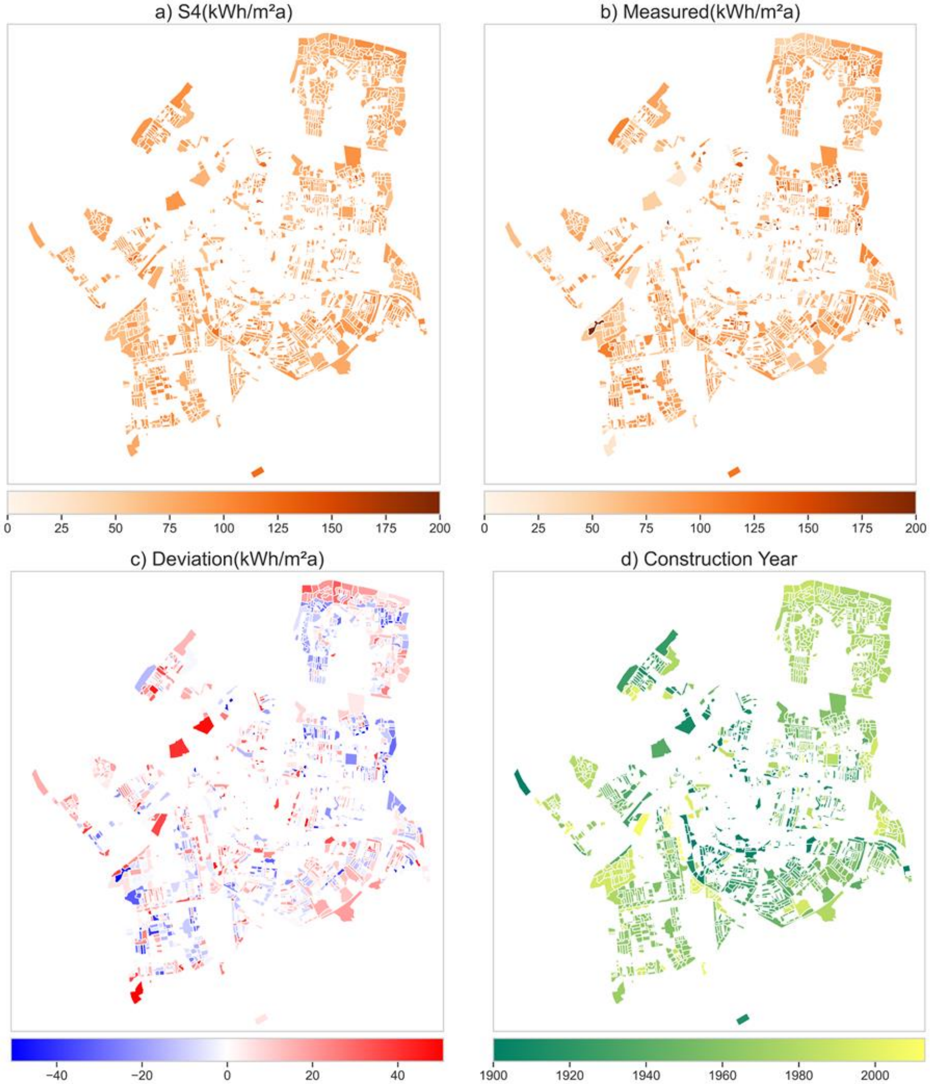

Figure 2.5 Leiden maps of modeled and measured annual natural gas consumption of 44% postcodes for space heating. Figure 2.5a shows the natural gas consumption modeled by S4. The measured natural gas consumption is shown in Figure 2.5b. The absolute deviations between S4 and the measured natural gas consumption are shown in Figure 2.5c. Figure 2.5d shows the age distribution.

In terms of the accuracy of weather data, the difference between the simple average weather data for the heating season (S1) and the hourly weather data (S2) does not make a significant difference to the modeled annual natural gas consumption (**Figure 2.4**). However, the natural gas consumptions modeled by S1-2 are obviously higher than measured natural gas consumption. One of the main reasons is that S1-2 inherently oversimplify the heating process by assuming that the buildings are heated all the time during the heating season [187]. Therefore, the seasonal heat demand model (S1) is not suitable for accurately estimating the energy reduction effect of specific energy-efficiency measures, while the hourly model (S2) can take hourly weather differences into account and has more potential for accuracy improvement by including more detailed occupant schedule (e.g. S4).

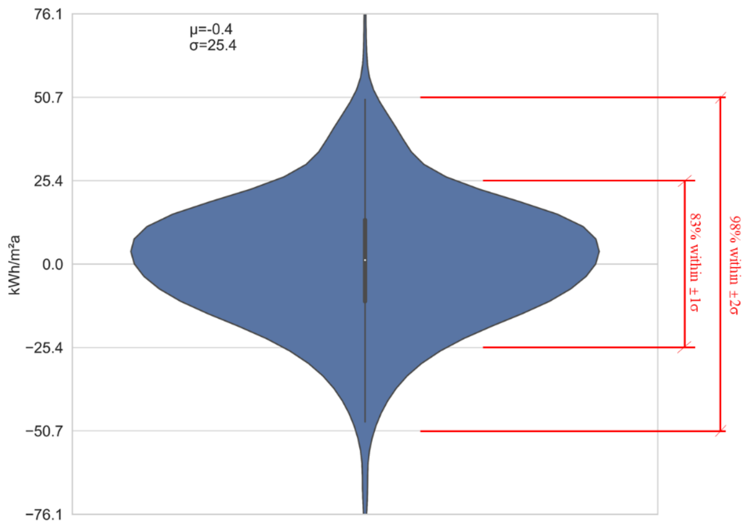

Figure 2.6 Absolute deviations between S4 and measured natural gas consumption. μ is the mean absolute deviation and σ is the standard deviation of absolute deviation.

In **Figure 2.4**, we find that including refurbishment increases more accuracy for older buildings than including occupant schedule while the opposite seems to apply for newer buildings. The reason is that newer buildings have better thermal properties and refurbishment only has a limited impact on reducing the modeled natural gas consumption, which indirectly demonstrates that refurbishing the buildings constructed before 1964 can lead to the highest natural gas reduction potential. It is also found that for S3 and S4, the modeled natural gas consumption of the 1992-2005 period is even lower than the modeled natural gas consumption after 2006. It is partially because the original thermal properties of the buildings of 1992-2005 period are only moderately worse than that of buildings after 2006, but refurbishment makes the envelope components of buildings in 1992-2005 period have even better thermal properties than the buildings after 2006 (for which no refurbishment is simulated).

S4 overestimates the natural gas consumption of almost all the buildings of the 2006-2014 period (**Figure 2.4**). One of the main reasons may be that the U-values in TABULA only meet the national minimum requirement and these values cannot represent the thermal properties of these buildings [68]. In reality, more efficient heating or ventilation systems and renewable energy sources have been applied, but S4 does not account for such increasingly applied technologies. For example, in the

Netherlands, some heat boilers using natural gas are replaced by district heating or heating pumps, and their gas stoves are replaced by electric cooking stoves [179].

Figure 2.5 suggests that the actual natural gas consumption is not only affected by the building age but also other factors such as refurbishment records and occupant schedules. Building age, as a key classification standard for TABULA archetypes applied in characterizing the Leiden residential building stock, can partially represent the energy efficiency of the current building stock, while the past refurbishment measures, in reality, have changed the energy performance of original buildings. Therefore, the refurbishment rate can be regarded as supplementary for the limited representation of TABULA archetypes.

As increasing the sophistication from S1 to S4, some assumed data are introduced (e.g. refurbishment and occupant schedule), for which no spatial information is available. While S4 is the most complete among the four steps and produces the best results at a spatially aggregated scale (neighborhood or city level), it thus comes with the trade-off of decreased spatial accuracy, at least at a single-building level (see the schematic representation in **Figure S7.1.2** and **Figure S7.1.3** in Appendix). This is a common dilemma in building stock modeling [87] and cannot be resolved unless spatially explicit data for factors such as refurbishment is available.

2.4.2 Limitations and research opportunities

The building information of TABULA archetypes is allocated to individual BAG buildings based on construction periods and the identified building types, which provides an opportunity to automatically characterize building information at large scales with limited data. However, the archetypes are unable to completely represent all the real buildings, such as geometries (e.g. window-to-façade ratio and door-to-façade ratio), physical properties, and supply systems, which is a systematical limit of the archetype-based method. In addition, sometimes the identified building types might be wrong. For example, the end-terraced houses and mid-terraced houses are assumed to respectively have one and two shared walls, but multi-family houses may also have one and two shared walls. This would cause some variations for the estimated envelope component areas (including windows, walls, and doors), while the differences between the U-values of different building types for the same period are almost negligible according to the TABULA database [68]. Moreover, the buildings are simplified as cubes, which ignore the roof types and may cause some errors for the estimation of envelope component areas.

Due to a lack of supply system information and the corresponding energy sources for individual buildings, all the buildings are assumed to use gas-fired boilers from TABULA. Although most residential buildings are heated by natural gas in the Netherlands, there are increasing exceptions. For example, some more recent houses have been installed with gas-free heating systems (e.g. heat pumps or connecting to district heating networks).

The national refurbishment rates [174] of envelope components and the usual refurbishment from the TABULA database are employed to reflect the physical properties of the current residential building stock. However, this can cause spatial uncertainty for the Leiden residential buildings stock, so more attention should be paid to reducing the uncertainties caused by unknown HVAC systems and refurbishment records (e.g. refurbishment year and insulation technologies) at postcode or even individual building level.

The presented model uses standard occupant parameters from other literature and reasonable assumptions (e.g. occupant's schedule) to fill in the data gaps and calculates the energy consumption from a demand perspective (quantify the energy required to maintain a given room temperature), while it omits the diversity of individual occupant behavior. Previous studies [51] have revealed that occupants can impose a critical impact on building energy consumption and sometimes even reach the same extent of technical interventions. For example, internal room temperature setting, ventilation (time of leaving windows and doors open), schedules, and DHW consumption highly depends on the specific occupants (e.g. living habits, number, age, income, and job) [188]. However, it is difficult to collect so much detailed occupant information on building scale especially for a city-scale energy model, and future research should pay more attention to this.

The internal room temperature of a given building varies in space and time (named as "non-uniform heating" [176]). The use status of various rooms (e.g. living rooms, bedrooms, and kitchens) can be quite different. The areas like the staircase, attics, and garages are typically unheated. Additionally, intermittent heating or reduced setting-point temperature may occur during different periods (e.g. night and weekend). However, in this study, the internal room temperature is set as a fixed value (20 °C [180]) in the whole space of buildings.

For validation, due to lacking measured energy consumption data for individual buildings, the weighted average ages rather than the pure age of individual buildings are employed to represent the construction periods of postcodes, although the buildings with the same postcode are likely to have similar ages.

2.4.3 Model applicability and transferability

Due to a lack of refurbishment records at the level of individual buildings, its accuracy for individual buildings is limited. However, the presented model qualifies to offer a good overview of the energy consumption characteristics at the neighborhood and city scales, for which validation is possible. It can also reflect the energy efficiency of buildings belonging to different age groups.

The presented model makes a compromise between sophistication and accuracy through making full use of public data sources (geometries in GIS data and TABULA archetype building information). It gathers the input data as matrices (building information) or time series (weather data and occupant behavior) and calculates energy consumption based on public energy simulation algorithm, which allows for analyzing largescale building stock (neighborhood, city, or nation) and realizing transferability to other countries.

Due to a lack of spatial data on individual buildings as well as the diverse occupant behavior, building stock energy models previously developed applied diverse input data [96]. Especially the model proposed by Buffat et al. [98] applied high-resolution spatial data available in Switzerland that is not available for many other countries. In contrast, the data required for the presented model mainly involves the GIS data (including building registration), archetype buildings, weather data, refurbishment records, and occupants, which are available and public in many countries. Below is a summary of the availability of input data:

(1) The GIS data of buildings is available in many EU members and the OpenStreetMap can be an alternative data source [98]. The availability and detail level of individual building attributes (e.g. construction year, building types, heating systems, energy sources, refurbishment records, occupant characteristics) differ significantly in each country, such as the Danish BBR [189] and the Swiss FRBD [112]. However, the building type identification method developed in this study based on building morphologies in GIS data provides opportunities for filling in these data gaps with archetypes or sample buildings.

(2) The archetype buildings are available for many countries [190] and it is also worth mentioning that the TABULA project currently contains the representative buildings of 21 European countries [68]. However, for larger countries, the archetype system might be quite complex due to various climate regions and construction technologies.

(3) The weather data is almost available for every country while its spatial and temporal resolution might be quite diverse.

(4) The detailed refurbishment records for individual buildings are very rare in most countries but can be managed by the local authorities. In some EU countries, the EPC (Energy Performance Certificate) databases contain buildings' past refurbishment or suggested energy efficiency measures as well as energy labels (A-G), actual energy use, physical properties, and HVAC systems, but the building information types in these databases differ from country to country and not every building has an energy label at present [191]. Alternatively, the refurbishment rates of building elements can be collected from the published reports (local or from other countries/regions).

(5) The occupant data (e.g. household age structure, the number of occupants, income, and education level) that is quite related to human behavior is available in some developed countries, such as the SHAERE database of the Netherlands [192] and the property register of Sweden [193], but it is usually not public and spatialized for privacy protection reasons. However, reasonable assumptions can be made to fill in the data gaps in the absence of better data (e.g. room temperature, internal heat gains, and occupant schedule).

2.5 Conclusion

This study presents a GIS-archetype-based bottom-up building stock model for energy consumption for space heating. In order to allocate the typical geometries, thermal properties, and heating systems of archetype buildings to the individual buildings, this paper develops a method to identify the types of individual buildings according to building size and the number of shared walls. Then different input data (e.g. average weather data, hourly weather data, refurbishment, and occupant behavior data) and calculation methods are gradually included to explore the key factors affecting the model accuracy. The main conclusions are:

(1) The spatial validation shows that the most sophisticated step can well reflect the energy consumption at the city scale while other steps are completely off reality. However, due to lacking heating systems, refurbishment records, and occupant behavior for individual buildings, the modeled energy consumption is moderately acceptable at the postcode level but likely inaccurate for individual buildings. This demonstrates that including more factors can increase the model accuracy at the city scale, but simultaneously increase the uncertainty for single buildings. Additionally, as more than half of the postcodes are filtered (only 44% postcodes left), the validation data of higher quality would be valuable to assess the developed model.

(2) The comparison between steps demonstrates that the seasonal model fails in accurately simulating the energy consumption for space heating. It is found that including past refurbishment in building stock energy models is necessary for achieving reliable results. Taking the assumed occupant schedule into account can narrow the gap between the modeled and measured energy consumption though the occupant behavior data in this study is quite rough.

(3) The model is valuable for city planners to understand the current energy efficiency status in space, determine the priority of implementing retrofit measures, and assess the energy-saving potentials of refurbishment technologies. Local authorities need to spatialize detailed information for individual buildings if more specific energy-efficiency suggestions are required. Furthermore, the presented model probably is transferable for other countries as long as the input data such as GIS building datasets and archetype buildings, is available.

Chapter 3 A bottom-up dynamic building stock model for residential energy transition: A case study for the Netherlands[2]

Abstract

The building sector plays a key role in energy transition and carbon reduction while capturing the dynamic characteristics (e.g. materials, energy performance, and environmental impact) of building stock is a great challenge during the gradual process. This study presents a bottom-up dynamic building stock model that links dynamic material flow analysis with building energy modeling. The environmental impact of material and energy requirements is assessed by considering future electricity mix. The model is applied to evaluate the pathways to the climate-neutral energy supply of the residential building stock in the Netherlands by 2050. Results show that space heating demand decreases by about 2/3 by 2050, while the energy for hot water increases to 92% of space heating demand. 80% of public grid electricity for appliances and lighting can be potentially substituted if rooftop photovoltaic (PV) systems are installed on 50% of renovated buildings and all the new buildings. Greenhouse gas (GHG) emissions of operational energy are reduced by approximately 60-90%, depending on the electricity mix. Annual GHG emissions from material production are not as important as those related to operational energy. Insulation materials account for a large proportion of the carbon footprint of material production. The model has a high spatial and temporal resolution and can be linked with local energy source availability (e.g. buildings or neighborhoods) to provide more accurate support for policymaking.

Keywords: dynamic building stock model, bottom-up, material flow analysis (MFA), life cycle assessment (LCA), energy transition, carbon emissions, climate change, geographic information system (GIS)

3.1 Introduction

The building sector is responsible for about 40% of the total final energy consumption and 36% of greenhouse gas (GHG) emissions in the European Union (EU) [158]. EU countries have set ambitious targets for realizing sustainable building stock, including improving envelope insulation [194], installing efficient energy systems [195], and replacing fossil fuels with renewable energy sources [74]. However, implementing these measures involves considerable construction activities (construction, renovation, and demolition), which will lead to large amounts of material consumption [20] and construction and demolition waste (CDW)

---

[2] Published as: Yang, X., Hu, M., Tukker, A., Zhang, C., Huo, T., Steubing, B. A bottom-up dynamic building stock model for residential energy transition: A case study for the Netherlands. Applied Energy 306, 118060 (2022).

[43]. It is necessary to understand the dynamics of building stock as well as the material flows and energy consumption [196], and quantitatively assess the performance (e.g. energy-saving effect, environmental impact, and cost) of various energy transformation policy strategies [24].

Dynamic building stock models (DBSMs) originate from dynamic material flow analysis (MFA) proposed by Müller [108] and account for the long-term evolution (construction, demolition, and renovation) of building stock as well as the changes of technologies [197], material flows [198], energy consumption [95], and carbon emissions [92] under different policy scenarios [125]. Many DBSMs have tried to disaggregate and characterize the building stock. For example, Sandberg et al. [199] present a segmented model that simulates the dynamics of each stock segment (defined by building type and cohort) with probability functions. Wiedenhofer et al. [200] model the nonmetallic material composition change of EU25 with typologies of buildings, roads, and railways. Heeren and Hellweg [112] develop a prospective bottom-up dynamic model that applies the GIS (geographic information system) data of buildings and the component-based inventory data of building typologies [201].

Apart from materials, some dynamic models track the evolution of energy consumption and environmental impact. Coffey et al. [202] discretize the US commercial building stock into different categories, simulate the stock growth with the rates of construction, renovation, and demolition, and estimate the energy consumption by energy-use intensity. Heeren et al. [95] propose a lifecycle-based building stock model (LC-Build) that combines construction activities and operational energy demand and includes the environmental impact from the energy supply side. Pauliuk et al. [203] combine MFA and life cycle assessment (LCA) to determine the emission reduction potential of the Norwegian dwelling stock. Vásquez et al. [204] present a dynamic Type-Cohort-Time (TCT) stock-driven model to investigate the energy reduction levels of different policy scenarios in Germany and the Czech Republic. Koezjakov et al. [205] investigate the development of the Dutch building stock and the relationship change between embodied and operational energy.

The building stock is a complex and dynamic object constituted by long-lasting buildings [24] that will be updated by different building technologies (e.g. insulation and heating systems) over time [26]. However, the following shortcomings of previous DBSMs limit their ability to track the changes of building characteristics during the gradual energy transition process:

(1) They are mostly top-down models lacking the ability to consider technical details, or bottom-up models that are disaggregated at a very limited level (typically segmenting the total floor area stock by the proportion of construction periods or building types).

(2) Material and energy (empirical or modeled) intensities [28] of representative buildings are usually employed to estimate the total material and energy stock, which omits the specific characteristics of individual buildings and cannot accurately

evaluate the energy and carbon reduction effect of energy-efficient measures.

(3) Most models have not combined materials and energy consumption together [28], while better insulation increases the relative importance of embodied environmental impact [32]. Integrated models are required to evaluate the overall impacts of both material and energy strategies on climate change target realization across different scales ranging from neighborhoods to cities, or an entire country.

This paper presents a bottom-up DBSM based on the basic principle of MFA to simulate the spatial-temporal development of the building stock, material flows, energy consumption, and environmental impact to evaluate the effects of policy strategies for the energy transition in the building sector. Individual buildings are mainly characterized by GIS data and building typologies. The space heating demand is simulated based on the model by Yang et al. [27]. The environmental impacts linked to building materials and energy supply of the energy transition are assessed by considering the likely development of future electricity production. The model is used to evaluate the Dutch national control scenario of the built environment [156] (hereafter named as national control scenario), which aims to ensure the transition towards a self-sufficient renewable energy supply, especially the electrification of the heat supply. The main research questions of the case study are:

(1) How close can the Netherlands get to the carbon-neutral residential building stock by 2050 under the national control scenario?

(2) Which are the drivers for GHG emission reductions in the building stock?

3.2 Materials and methods

3.2.1 Model overview

The model builds upon the individual buildings characterized by a series of attributes, mainly including basic building information, building geometries, envelope thermal properties, occupant behavior, ventilation systems, heating systems, rooftop photovoltaic (PV) systems, annual energy demand (space heating, domestic hot water, electricity for appliances and lighting), and materials. This study involves five types of residential buildings from TABULA [68] (single-family house, mid-terraced house, end-terraced house, apartment building, and multi-family house), which are differentiated into six construction periods (before 1964, 1965-1974, 1975–1991, 1992–2005, 2006–2014, and after 2015). The individual buildings are characterized by the method of Yang et al. [27], which assigns the attributes of archetypes to individual buildings in GIS datasets based on construction periods and building types. More details can be found in section **7.2.1**.

New construction is driven by population and lifestyle (stock-driven [26]). Mass-balance principles [108] are applied to determine the annual construction activity by considering both demolition and floor area demand. Renovation is driven by activity (renovation rate) that reflects the aggressiveness of energy transition strategies. The energy transition measures mainly include saving energy (i.e. insulation and ventilation improvement) and installing efficient heating systems that use sustainable energy sources.

In the process of building stock evolution, individual buildings can be dropped (demolition) from the building stock, added (new construction) to the stock, or updated (renovation). The relevant attributes (e.g. U-values, materials, and energy demand) of all buildings in the building stock are considered over time.

The structure of the model is shown in **Figure 3.1**. The building stock (BS) is a dynamic object, and at time t it comprises 1) new buildings that will be constructed ($BS_{new,t}$), 2) existing buildings that will not be renovated ($BS_{no\_intervention,t}$), 3) existing buildings that will be renovated ($BS_{renovation,t}$), and 4) existing buildings that will be demolished ($BS_{demolition,t}$).

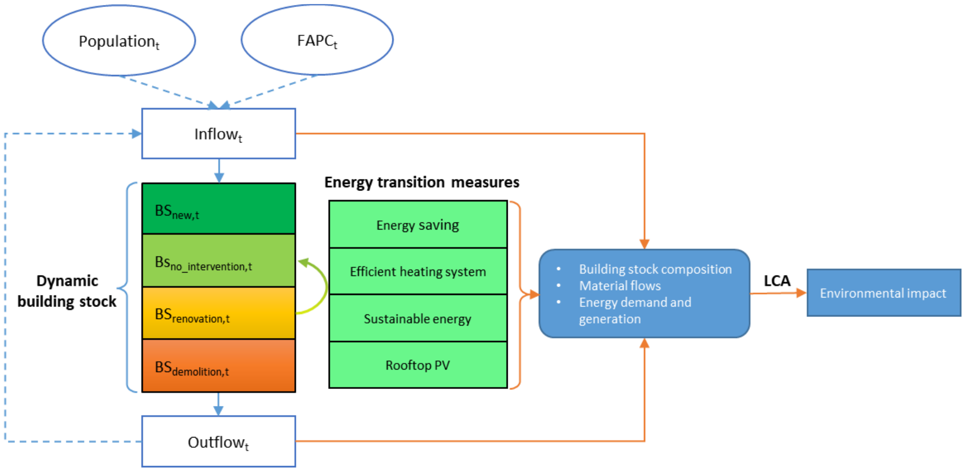

Figure 3.1 Schematic overview of the dynamic building stock model. FAPC: floor area per capita, BS: building stock, t: year, $BS_{new,t}$: newly constructed buildings, $BS_{no\_intervention,t}$: buildings that will not be technically intervened, $BS_{renovation,t}$: buildings that will be renovated, $BS_{demolition,t}$: buildings that will be demolished.

3.2.2 Construction activities

3.2.2.1 Demolition

Building lifetimes are modeled with Weibull distributions [206]. The mean historical building lifetime (130 years) of buildings in the Dutch building stock and shape parameter (k=2.95) are from Deetman et al. [37]. The scale parameter (λ) is derived based on the mean value equation of Weibull distribution:

$$\lambda = lifetime_{mean} \div \Gamma(1 + \frac{1}{k}) \qquad (1)$$

where $lifetime_{mean}$ is the mean lifetime of Dutch buildings.

There are many historical and monumental buildings in Western Europe [37]. Their ages vary significantly, so it is hard to find a reliable average lifetime for them. As their share in the whole building stock is very small (see **Figure S7.2.2** in Appendix), we assume that buildings constructed before 1900 will not be demolished but renovated in the considered time frame. An array containing random lifetime values following the Weibull distribution is generated with Python, and the bound (mean ±1.5 standard deviations [108], i.e. lower bound 58 and upper bound 202) is applied to avoid unrealistic lifetime values. The buildings are grouped by construction year, and for each group of buildings, their lifetimes are sampled from the lifetime array that filters the random values smaller than or equal to their current ages (current year minus construction year). The demolition year of each building is calculated as follows:

$$t_{dem} = t_{con} + lifetime \qquad (2)$$

where t_{dem} is the demolition year, and t_{con} is the construction year.

3.2.2.2 Construction

The annual construction floor area is calculated based on population, floor area per capita, and the demolished floor area in year t:

$$A_{new,t} = FAPC_t \times P_t - S_{t-1} + \sum_{j=1}^{N_{dem,t}} A_{t,j} \qquad (3)$$

Where $A_{new,t}$ is the new construction area in year t. $FAPC_t$ is the floor area per capita. P_t is the population. S_{t-1} is the floor area stock of the previous year. $N_{dem,t}$ is the number of demolished buildings. $A_{t,j}$ is the floor area of the demolished building j in year t.

The number for each type of building is calculated as:

$$N_{type,t} = round(A_{new,t} \times PP_{type,t} \div A_{type}) \qquad (4)$$

Where $N_{type,t}$ is the number of a building type of new buildings. $PP_{type,t}$ is the floor area proportion of a building type. A_{type} is the floor area of a TABULA archetype.

3.2.2.3 Renovation

According to the Dutch National Climate Agreement, municipalities will apply the neighborhood-oriented approach [207] to organize residents, building owners, and energy companies to collectively determine the best solution [208]. The residential buildings of the same neighborhood will be tackled together, and are likely to use the same heat source. Therefore, the existing building stock (excluding the buildings that will be demolished during the considered time frame) is grouped by neighborhood. The weighted average U-value of buildings in the same neighborhood is calculated as follows:

$$U_{neighborhood,weighted} = \frac{\sum_{1}^{N_{neighborhood}} U_{building,weighted} \times A_{building}}{\sum_{1}^{N_{neighborhood}} A_{building}} \qquad (5)$$

Where $U_{neighborhood,weighted}$ is the weighted average U-value of a neighborhood, $A_{building}$ is the floor area of a building, and $N_{neighborhood}$ is the number of buildings in a neighborhood. $U_{building,weighted}$ is the weighted average U-value of a building, which is determined as follows:

$$U_{building,weighted} = \frac{\sum_{1}^{N_{element}} U_{element} \times A_{element}}{\sum_{1}^{N_{element}} A_{element}} \qquad (6)$$

Where $U_{building,weighted}$ is the weighted average U-value of a building, $U_{element}$ is the U-value of an element, $A_{element}$ is the area of an element, and $N_{element}$ is the number of elements. In this study, the elements involve roof, external wall, window, door, and ground floor.

The neighborhoods are sorted by $U_{neighborhood,weighted}$ (descending), and then the top neighborhoods that contain $N_{ren,t}$ buildings are selected for renovation. These buildings are randomly divided into two parts. One part will be renovated with the conventional standard while the other part will be renovated with the nearly zero energy buildings (nZEB) standard. The numbers of buildings with different renovation standards are calculated as follows:

$$N_{ren\_i,t} = N_0 \times R_{ren\_i,t} \qquad (7)$$

Where N_0 is the total number of existing buildings to be renovated. $N_{ren\_i,t}$ is the number of renovated buildings for energy standard i in year t. $R_{ren\_i,t}$ is the annual renovation rate for energy standard i in the year t.

3.2.3 Materials, energy, and environmental impact

3.2.3.1 Building materials

The material amounts for a building are calculated as follows:

$$W_{mat} = A_{building} \times MI_{mat} \qquad (8)$$

Where W_{mat} is the weight of a material for a building. $A_{building}$ is the floor area of the building. MI_{mat} is the intensity of material for each building type (see **Table S7.2.7** and **Table S7.2.8** in Appendix**)**.

Glazing is renovated by replacing the existing glass with HR++ (double glazed with a coating and an insulating gas between the plates) for conventional standard and HR+++ glass (three glass plates with a coating and insulating gas) for nZEB standard [209]. The opaque elements (roof, external wall, door, and ground floor) are renovated by adding an insulation layer on top of the corresponding envelope element. The physical parameters of different renovation options for each element can be found in TABULA [210]. The details on different insulation materials can be found in **Table S7.2.9** in Appendix. The amount of insulation material for renovating an opaque element is calculated based on insulation standards and the thermal conductivity of used insulation materials [211]:

$$W_{mat,ins} = \left(\frac{1}{U_{ren,ele}} - \frac{1}{U_{exi,ele}}\right) \times k_{mat,ins} \times A_{ele} \times D_{mat,ins} \qquad (9)$$

Where $W_{mat,ins}$ is the weight of insulation material for a building. $U_{exi,ele}$ is the existing U-value of an opaque element, and $U_{ren,ele}$ is the U-value after renovation. $k_{mat,ins}$ is the thermal conductivity of insulation material.

3.2.3.2 Operational energy

The energy consumption of Dutch residential buildings is comprised mainly of space heating, domestic hot water (DHW), and electricity for appliances and lighting [183]. The space heating demand of the initial and renovated building is simulated based on Yang et al. [27]. The energy demand for DHW of existing buildings is estimated by the TABULA method [176]. For new buildings, the energy for space heating and hot water is calculated based on the energy intensities of corresponding TABULA archetypes [68]. The heat demand for space heating and DHW is converted into the final heat demand supplied by heating systems based on the TABULA method [176].

The annual electricity consumption for appliances and lighting is estimated by multiplying floor area with the sampled electricity intensities derived based on measured annual electricity consumption (CBS) and BAG (see **Figure S7.2.6** in Appendix). Due to the lack of enough energy consumption data on buildings constructed after 2015, the electricity consumption of buildings after 2015 is estimated based on the electricity consumption of buildings built in the 2006-2014 period.

The potential annual electricity generation from rooftop PV (E_{PV}) is calculated based on the following equation [212]:

$$E_{PV} = G \times \eta \times R_{performence} \times A_{roof} \times R_{reduction} \qquad (10)$$

Where G is the annual cumulative solar irradiation, which is calculated by summing up hourly values from KNMI (Royal Dutch Meteorological Institute) [173]. η is the efficiency of rooftop PV. In this study, the modern crystalline Silicon panels are applied and its efficiency is 17% [212]. $R_{performence}$ is a reduction factor that considers, e.g., sub-optimal angels and inverter losses, to better reflect the efficiency in real life, and its value is 87% in this study [212]. A_{roof} is the roof area for solar panel installation. Considering the space left for maintenance and obstacles, A_{roof} is adjusted by an additional reduction coefficient ($R_{reduction}$) and its value is 60% [213] (i.e. only 60% of the roof surface of a building can be used for rooftop PV).

3.2.3.3 Environmental impact

The GHG emissions related to materials and energy in year t ($G_{me,t}$) are calculated by multiplying GHG emission factors in year t ($F_{me,t}$) with the quantity of materials or energy in year t ($Q_{me,t}$), as follows:

$$G_{me,t} = F_{me,t} \times Q_{me,t} \qquad (11)$$

In this study, onsite construction processes are not included and only building materials are considered for the environmental impact assessment of construction activities. All materials and energies described in the previous sections are modeled using the ecoinvent database 3.6 (cut-off system model) [138] except for hybrid heat pumps and heat networks that use different energy sources. The hybrid heat pump consists of a green gas boiler and an electric heat pump. 35% of its heat is supplied by a green gas boiler (only used in cold weather) and 65% is from an electric heat pump [214]. According to the national control scenario [156], the heat in the heat network is from geothermal (70%), biogas (15%), wood chips (10%), and residual heat from waste treatment plants (5%). The GHG emission factors of hybrid heat pumps and heat networks are the weighted average GHG factors of their sub-energy technologies by proportion (see section **7.2.5**). This study selects climate change as the impact category, and then reports the results in GHG emissions measured as kg CO_2-eq (IPCC 2013 [215]).

With electric heat pumps replacing many natural gas boilers in the future, the electricity demand will increase [214], which means that the future electricity mix will highly influence the carbon emissions of the residential building stock. Therefore, the method by Beltran et al. [216] is applied to combine the ecoinvent and IMAGE 3.0 databases [217] to create future scenario databases. The IMAGE scenarios applied in this study are SSP2 (Shared Socioeconomic Pathway, Middle of the Road) [218] as the baseline scenario, and SSP2 450 representing the greener electricity mix (e.g. increasing shares of solar PV or wind offshore). We use these databases in the Activity Browser [131] LCA software to calculate the LCA results of future material production and energy consumption (for further details, please refer to Steubing and Koning [142]).

3.2.4 Case study

In the Netherlands, the majority of current residential buildings are not well insulated compared to modern building standards [157], and about 86% of houses are heated by natural gas [174]. The Dutch government wants to phase out natural gas and realize energy-neutral [219] and carbon-neutral [157] building stock by 2050. In the national control scenario [156], the target average insulation level is energy label A by 2050. 55% of existing buildings will be insulated to be suitable for electric heat pumps. 25% of buildings will be connected to heat networks (e.g. geothermal, green gas, or biomass), 20% installed with hybrid heat pumps (green gas boiler and heat pump), and 50% roof surfaces installed with solar PV. Along with this transition are large amounts of building material consumption (e.g. insulation materials) and CDW, which can significantly affect the realization of circularity of the built environment [220].

The time frame considered in this study is from 2015 to 2050. The population forecast (16.9 million in 2015 and 18.5 million in 2050) of the Netherlands [221] (see **Figure S7.2.5** in Appendix) is from the Central Bureau of Statistics (CBS), and the conditioned floor area per capita is assumed constant (83 m^2, see details in section **7.2.1**). The building materials consist of 23 most common building materials (see **Table 3.1**) in the Netherlands.

New construction is differentiated by conventional new (CNEW) buildings and nZEBs from TABULA archetypes [68], including single-family houses, mid-terraced houses, end-terrace houses, apartment buildings, and multi-family houses. According to Dutch policy [222], all the new buildings constructed after 2020 must be nZEBs. Therefore, we assume that in 2016-2020 all new buildings are CNEW, while from 2021 all new buildings are nZEBs. Both of them are installed with balanced ventilation systems. Natural gas boilers are installed on CNEW buildings to supply the heat for space heating and DHW, while nZEBs are installed with electric heat pumps for space heating, and solar water heaters for hot water. Rooftop PV is installed on all new nZEBs. The floor area proportion of each building type is assumed the same as in 2015 (see **Figure S7.2.3** in Appendix).

Table 3.1 Building material labels [211].

Label	Material name	Label	Material name
AC	Aerated concrete	PG	Primary glass
Al	Aluminum	Pl	Plywood
Ar	Argon	PUR	Polyurethane foam
Bi	Bitumen	PVC	Polyvinylchloride
Br	Brick, clay	RC	Reinforced concrete (including steel [211])
Ce	Ceramics	Sa	Sand
EPS	Expanded polystyrene	SC	Sand cement
Gr	Gravel	SW	Softwood
GY	Gypsum plaster	WF	Wood fiber
HW	Hardwood	XPS	Extruded polystyrene
MW	Mineral wool	Zn	Zinc
PC	Precast concrete	-	-

It is hard to determine the shares of different insulation levels for renovation based on the average label A in 2050 in the national control scenario [156], and the heating system choice is also related to the insulation level. For example, electric heat pumps are only applicable for very well insulated buildings as they cannot provide high enough temperature for poorly insulated houses [223]. For simplification, this study derives the shares of insulation levels based on the heating system proportions in the national control scenario [156], and defines two combinations of insulation and space heating system based on TABULA [68], which provides the renovation options (e.g. insulation levels, ventilation systems, space heating systems, and hot water systems) for buildings differentiated by types and periods:

(1) Conventional renovation. Buildings are insulated to conventional standard and heated with heat networks (district heating) or hybrid heat pumps.

(2) Advanced renovation. Buildings are insulated to nZEB standard and heated with electric heat pumps.

According to the step-by-step plan to cease residential natural gas use by Milieu

Centraal [60], we summarize the energy transition measures into 4 layers: insulation, ventilation, heating systems, and rooftop PV. All the ventilation systems of renovation and construction are balanced ventilation systems. **Table 3.2** shows the technical combinations and distributions.

Following Vásquez et al. [204], it is assumed that there will not be renovation for nZEBs in the considered time frame. CNEW buildings in 2016-2020 will not experience technical intervention in the considered time frame. The buildings that will be demolished in 2016-2050 will not be renovated while all the other existing buildings will be renovated to certain energy efficiency levels. The renovation task is evenly allocated to each year.

Table 3.2 Technical scenario parameters. In the brackets are periods or shares of technical options.

Activity	Insulation standard	Ventilation	Heat supply	Energy production
Construction	CNEW (2016-2020)	Balanced ventilation (100%)	Natural gas boiler (100%)	Rooftop PV (0%)
	nZEB (2021-2050)		Electric heat pump + solar water heater (100%)	Rooftop PV (100%)
Renovation	Conventional insulation (45%)	Balanced ventilation (100%)	1) heat networks (25%) 2) hybrid heat pump + solar water heater (20%)	Rooftop PV (50%)
	nZEB insulation (55%)		Electric heat pump + solar water heater (55%)	

3.3 Results

3.3.1 Building stock evolution

Figure 3.2a and **Figure 3.2b** show that with slower population growth in 2016–2050, the size of building stock only experiences a slight increase. For the current building stock, more than 1/3 of building stock is constructed before 1964, and even in 2050, the buildings before 1964 still have the largest share, which is followed by the buildings built in the 1975–1991 period. In 2050, most existing buildings will remain, and new buildings only occupy a small share (about 19%). The annual demolished floor area will increase and the annual constructed floor area will decrease (see **Figure 3.2c** and **Figure 3.2d**), while new construction outweighs the latter. It is also found that the demolished buildings are mainly built before 1964, and the latest period of buildings that will be demolished is 1975–1991. **Figure 3.2e** and **Figure 3.2f** show that over time the renovation share of recently built buildings is increasing (recent buildings have better insulation and will be renovated later than old buildings). There are differences (e.g. peaks) in annual renovated floor areas while the numbers of renovated buildings every year are the same, which is due to the different sizes of individual buildings. The floor area of advanced renovation is significantly larger than that of conventional renovation due to past renovation (some existing buildings have already reached the conventional insulation standard), although the difference is not large (55% advanced renovation vs. 45% conventional renovation).

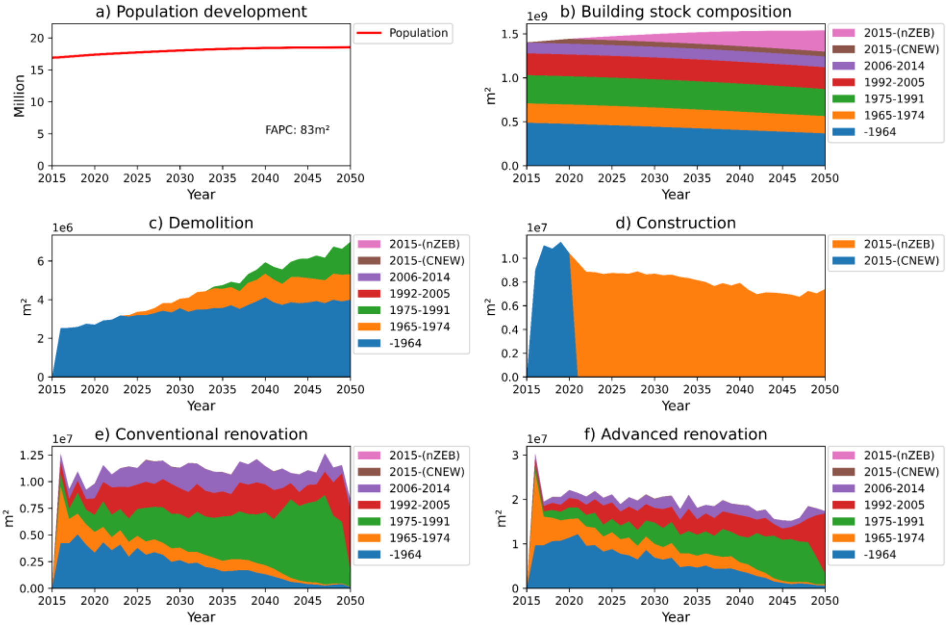

Figure 3.2 The evolution of building stock composition. “FAPC” is short for floor area per capita. The floor area here refers to the conditioned floor area. “CNEW” is short for conventional new, and “nZEB” is short for nearly Zero Energy Building.

3.3.2 Material and energy

Figure 3.3a shows that the material stock will continue to grow until 2050, albeit not to a great extent and at a slowing pace. Concrete (including prefabricated and reinforced concrete) accounts for the largest share in both material stock and flows (**Figure 3.3b** and **Figure 3.3c**), which is followed by sand. In 2050, the total material outflow is almost equal to the material inflow, which shows the potential for closing the building material loop.

From **Figure 3.3d**, we can see that due to extensive insulation and installation of balanced ventilation systems, the energy for space heating drops by nearly 2/3. Natural gas boilers are almost phased out by 2050 and the heat supply for space heating is dominated by heat networks and electric heat pumps. In contrast, the energy for hot water (**Figure 3.3e**) and the electricity for appliances and light (**Figure 3.3f**) show an opposite trend. Both their absolute amount and relative share increase. In 2050, the heat demand for hot water is almost equal to the heat demand for space heating. Solar water heater occupies the main supply for domestic hot water, which is followed by heat networks. In **Figure 3.3f**, the electricity generated by rooftop PV reaches more than 80% of the residential electricity demand in 2050, showing the great potential of rooftop PV to realize self-sufficient building stock in terms of electricity.

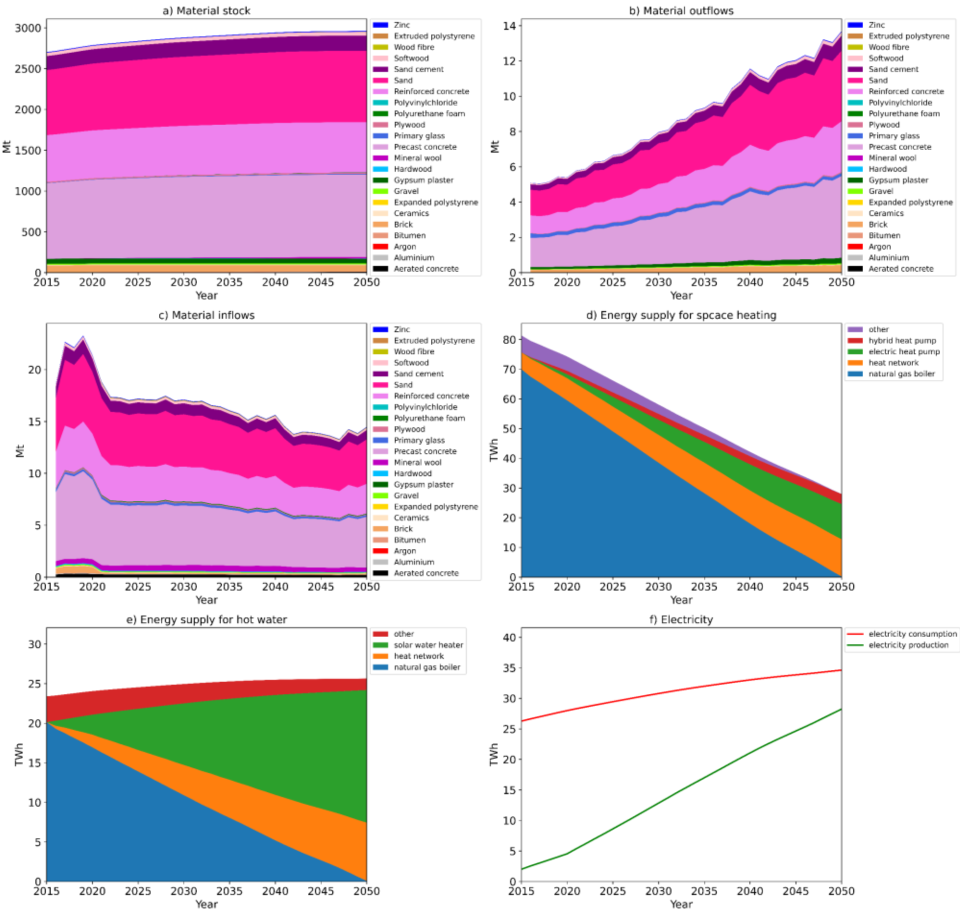

Figure 3.3 The material stock and flows, and operational energy. Steel is included in reinforced concrete [211]. The electricity consumption by heat pumps is not included in the electricity for appliances and lighting. In f), the electricity is consumed by appliances and lighting, and the electricity production is from rooftop PV.

3.3.3 GHG emissions

From **Figure 3.4a** and **Figure 3.4b**, we can find that GHG emissions are mainly from the production of mineral wool and concrete (precast and reinforced). Mineral wool dominates the total GHG emissions of materials, while its share of weight (**Figure 3.3c**) is pretty small (low density). This shows the necessity of applying more low-carbon insulation materials. In contrast, sand contributes a relatively smaller share of GHG emissions although their shares of weight are very large. The electricity under SSP2 450 is considerably less GHG intensive than SSP2, but the GHG emissions of material production only decrease slightly, showing that electricity is less important in the supply chain of most building materials.

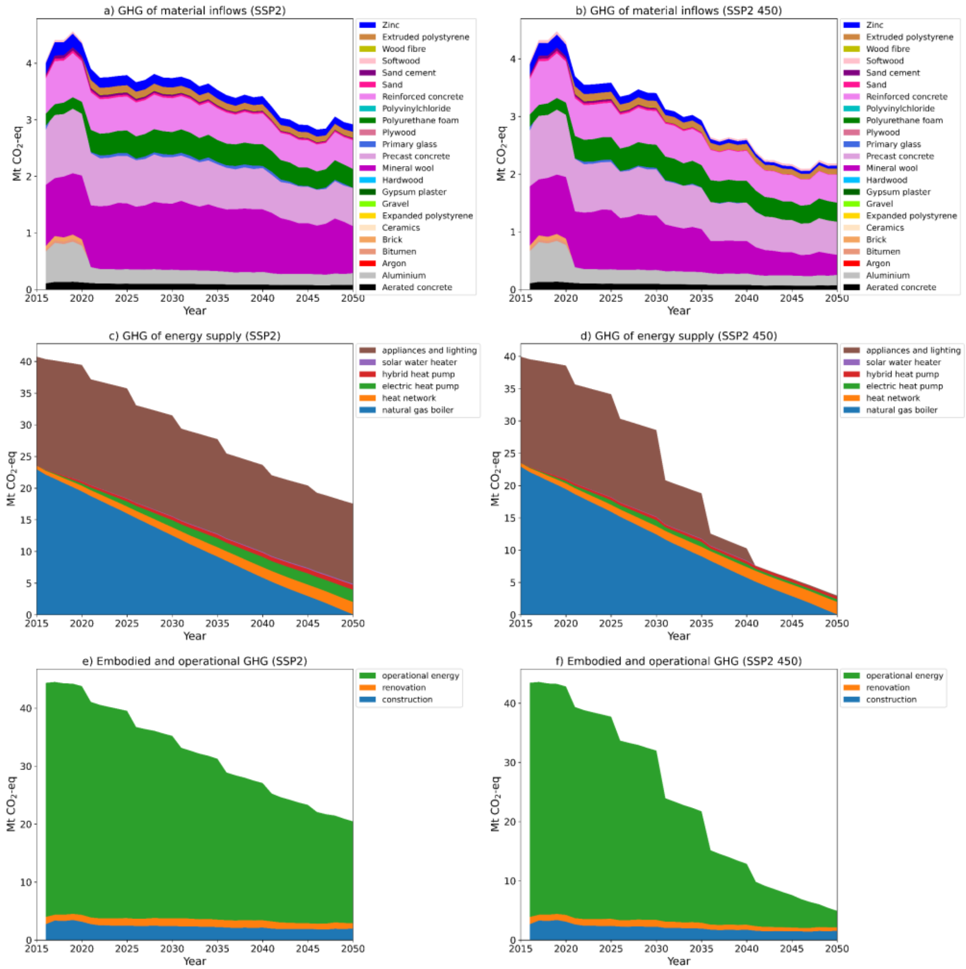

Figure 3.4 The GHG emissions of material and energy supply.

Figure 3.4c shows that the GHG emissions of operational energy supply are reduced by 57% under the SSP2 scenario. GHG emissions from heat supply (space heating and hot water) decrease by 79%. The heat supply emits about 57% of total GHG in 2015, while in 2050 the electricity for appliances and lighting contributes the most GHG emissions under the SSP2 scenario (72%). In **Figure 3.4d**, the GHG emissions of operational energy supply significantly decline (93%) under SSP2 450 scenario, and the carbon-neutral target by 2050 is almost realized in the residential building sector in terms of operational energy.

Figure 3.4e and **Figure 3.4f** show that both material production GHG and operational GHG emissions decline. The GHG emissions of material production are much smaller than operational emissions, while the share of emissions of material production increase with time, especially under the SSP2 450 scenario, meaning that GHG emissions associated with building materials will gain in relative importance in the future. The GHG emissions of renovation are much smaller than that of construction.

3.3.4 Effects of different measures

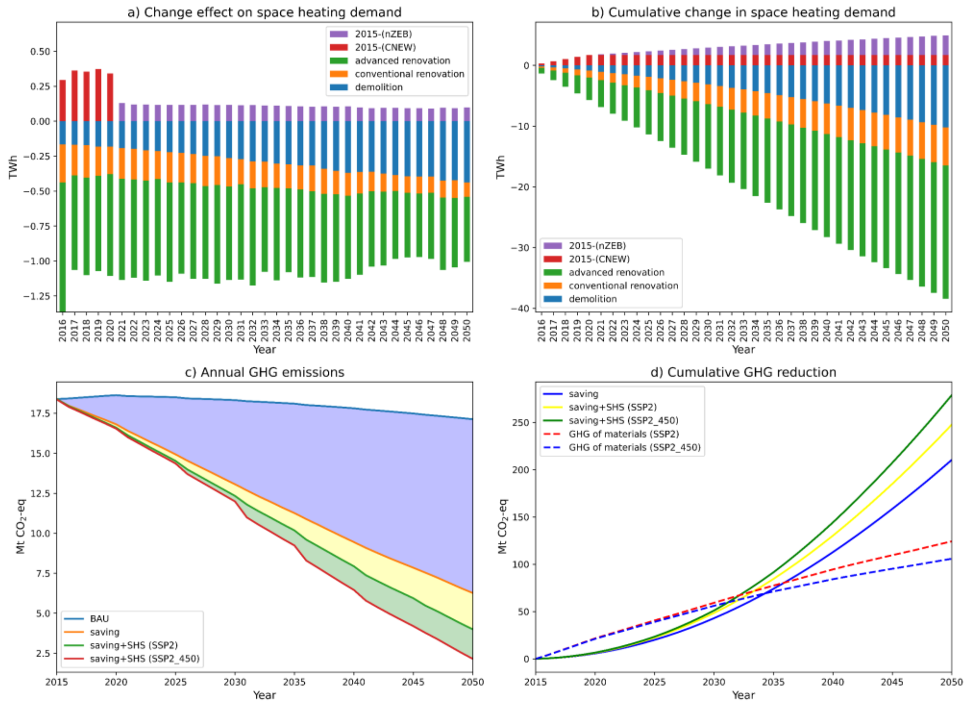

Figure 3.5 Changes in space heating and GHG emissions. Figure 3.5a shows the change effect of different construction activities on annual space demand. Figure 3.5b shows the cumulative energy reduction or increase of construction activities from 2015 to 2050. In Figure 3.5c, "BAU" (business as usual) means that neither energy-saving measures nor space heating system (SHS) replacement is implemented on existing buildings, and new buildings are heated with natural gas boilers. "saving" means that only energy-saving measures are implemented on existing buildings, while the SHSs for existing buildings remain unchanged and new buildings are heated with natural gas boilers. "saving+SHS (SSP2)" means that both energy-saving measures and SHS replacement are implemented, and the GHG emissions are calculated with the ecoinvent database SSP2. In contrast, "saving+SHS (SSP2_450)" means that the ecoinvent database SSP2_450, representing a quicker energy transition, is used for GHG emission calculation. The area in blue represents the carbon reduction by energy-saving measures "saving". The yellow area represents the carbon reduction by SHS replacement under SSP2 scenario "saving+SHS (SSP2)". The green area represents the carbon reduction by SHS replacement under SSP2 450 scenario "saving+SHS (SSP2_450)". Figure 3.5d shows the cumulative GHG savings compared to BAU. The dash lines show the cumulative GHG emissions from building material production.

Figure 3.5a shows the change in space heating demand by different construction activities. We can find that from 2021 the annual increase of heat demand drops more than 50% due to the introduction of nZEBs. The heat demand decrease by demolition and renovation is more than the increase by new construction, which makes the overall space heating demand decrease (**Figure 3.3d**). Advanced renovation reduces much more space heating demand than conventional renovation while the marginal energy-saving effect gradually declines for both conventional and advanced renovation. The space heating demand reduction effect of demolition increases with time (more buildings are demolished). From **Figure 3.5b** we can find that in 2050, the reduction of annual space heat demand is mainly due to advanced renovation and demolition.

In the "BAU" scenario of **Figure 3.5c**, the GHG emissions increase at first but gradually decline after 2020 due to the introduction of nZEBs, despite the increasing size of building stock due to population growth. In the "saving" scenario, energy-saving measures reduce GHG emissions by about 66%. Replacing natural gas boilers with other space heating systems reduces roughly another 12% of GHG emissions by 2050 for "saving+SHS (SSP2)" scenario and 22% for "saving+SHS (SSP2_450)" scenario, respectively. Energy-saving measures contribute the most to total GHG reduction among different measures. In **Figure 3.5d**, we can see that the cumulative GHG reduction increases and this trend becomes faster with time. In about 2032, the cumulative GHG emissions of building material production begin to be paid off by cumulative operational GHG reduction. By 2050, the cumulative GHG reduction reaches 1.04 (saving), 1.23 (saving+SHS (SSP2)), and 1.38 (saving+SHS (SSP2_450)) times the total GHG emissions of the Netherlands in 2015 (202 Mt [224]), respectively.

3.4 Discussion

3.4.1 Target realization potential

The national control scenario evaluation shows that the annual operational GHG emissions of residential buildings are reduced by more than 90% (about 19% of Dutch total GHG emissions in 2015 [224]), which is very close to realizing climate-neutral residential building stock. However, it requires extensive insulation, heating system replacement, and sustainable energy source application. Apart from the technical aspects, the feasibility of implementing these measures in the real world is not analyzed, especially the willingness of homeowners to adopt energy efficiency measures, e.g. financial [225] and legal aspects [226]. For example, the energy efficiency of existing buildings can differ substantially, and thus implementing energy-saving measures can lead to diverse savings of energy bills. Scaling up the energy transition measures (e.g. insulation and renewable energy sources) may lead to an economy of scale, i.e. lowering the average cost and potentially also direct environmental impacts related to energy-efficiency measures and energy infrastructure [157]. The tax on fossil fuels will also increase the competence of renewable energy sources. These factors would affect the choices of house owners, which also stresses the need for flexible and innovative business modes that can accelerate the implementation of policy strategies.

3.4.2 Drivers for GHG reduction

Figure 3.5d shows that energy-saving measures contribute more GHG reduction (especially insulation) than sustainable energy supply for the national control scenario. However, both energy-saving measures and renewable energy supply technologies are important for reducing the GHG emission of the building stock, and neither of them can achieve a near carbon-neutral building stock alone. One reason is that insulation levels can seriously affect the efficiency of heat supply systems. For example, before installing electric heat pumps, buildings have to be well insulated, because heat pumps cannot provide enough heat or will be very energy inefficient in very cold weather for badly insulated buildings [227]. Buildings heated by low-temperature heat networks (50 to 55 °C) have to be well insulated although the insulation does not have to reach nZEB level [228]. Another reason is that generating enough sustainable energy to heat badly insulated buildings can be a great challenge [228]. For example, green gas from biomass cannot be a large-scale solution for the Netherlands [229]. Following the steps into natural gas-free buildings by Milieu Centraal [227], saving energy demand (through good insulation and balanced ventilation) is the first step, after which is the installation of more efficient heating systems based on renewable energy sources. However, the marginal effect of energy-saving measures decreases with time (**Figure 3.5a**). The combination of insulation standards and heating systems is also influenced by the available energy sources (e.g. heat networks). Therefore, energy-saving measures and energy supply technologies are required in conjunction. Moreover, with the increase of electricity consumed by electric heat pumps, a greener electricity mix is important for reducing residential GHG emissions.

3.4.3 Limitations and future research

Compared with previous models, the presented model builds upon individual buildings, and includes potential future developments such as the energy transition as part of the underlying LCA model, providing the possibility for comprehensively assessing the material flows and energy demand and the related environmental impact of detailed technical measures. It can be applied to assess the performance of different energy efficiency strategies at a large scale (e.g. city or country). Our research comes with several limitations that could provide future research opportunities:

(1) In this study, the energy transition solutions for neighborhoods are randomly assigned due to lacking data on energy source availability for a specific building or neighborhood. This can lead to a mismatch between energy demand and supply. For example, the heat networks can only be available for certain areas, depending on the availability of industries or geothermal. Solar water heaters and solar PV panels are limited by the amount of sunshine [230]. High-rise buildings in dense urban areas

are likely to be connected with heat networks while rural areas are suitable for electric heat pumps [157]. Municipal authorities can collect such data at the neighborhood scale to make an alternative energy source map with temporal dimension (in which year what kind of energy sources would be available for each neighborhood).

(2) Some factors will probably change in the future while they are not accounted for in the case study. The lifestyle of people [231], such as the floor area per capita [232], rebound effect (higher room setpoint temperature and longer heating time after renovation) [233], and the technologies of appliances, lighting, and energy generation, will be probably different from now. Besides, the climate will change [30] (e.g. temperature) but we use the constant climate data. Although the presented model has the availability to simulate the energy demand change due to these mentioned dynamic factors, they are not considered in this study.

(3) The developed model can, in theory, track the material flows in space and time, but we lack spatially and temporally differentiated building material inventory data. Wood construction is currently high on the political agenda in the Netherlands and the share of wood construction has recently increased [234]. Therefore, it would be interesting to explore the material composition change of future buildings and their effect on GHG emission reduction. Also, the secondary materials from CDW recycling will reduce the future raw material demand, while our model does not address this, meaning that this study might overestimate the future raw material demand. Future research can focus on sensitivity or uncertainty analysis to account for how much materials are overestimated.

(4) The presented model combines a building energy model with MFA and LCA and builds upon a series of data sources to characterize individual buildings and the future development pattern of building stock. The uncertainties of sub-models can accumulate and thus result in considerable uncertainties for the results presented in this paper. Within the context of this paper, it was not possible to quantify these uncertainties and to validate the results. However, some of the underlying models, e.g. the building energy model [27] that we built upon, have been validated with measured energy consumption data. Future research could attempt further validation [235] and should aim at further reducing model uncertainties, e.g. by collaborating with government agencies and companies to collect additional local data [236] and by developing more specific scenarios for the development of the building stock.

3.5 Conclusion

This study presents a bottom-up dynamic building stock model that can simulate the development of the building stock as well as the associated materials flows, and operational energy transition due to insulation, renewable energy sources, and rooftop PV panels. Compared with previous models, it builds upon the individual buildings characterized by GIS data, and includes potential future developments such as the energy transition as part of the underlying LCA model, providing the possibility for comprehensively assessing the energy demand and material flows and the related environmental impact of detailed technical measures at a large scale. The national control scenario evaluation shows that energy-saving measures together with greener heat sources can reduce about 2/3 of the energy and 60-90% GHG emissions for space heating, depending on the electricity mix. However, with the decrease of space heating demand, the share of energy for hot water, appliance, and lighting will increase significantly. About 80% of residential electricity for appliances and lighting can be potentially met by rooftop PVs if they are installed on the roof surfaces of about half of the building stock. The material outflows will be almost equal to the inflows in 2050, showing the potential of reducing building raw materials by recycling the material outflows. The GHG emissions of material production will be leveled off by cumulative GHG emission reduction from operational energy in 2030-2035. The model can be applied in other countries or regions if the required data is available.

Chapter 4 Urban mining potential to reduce primary material use and carbon emissions in the Dutch residential building sector[3]

Abstract

Urban mining is regarded as an important strategy to replace primary raw materials in the building sector. This study presents a bottom-up dynamic building stock model to explore the potential of urban mining to reduce primary material consumption and greenhouse gas (GHG) emissions in the residential building sector of the Netherlands. The model builds upon geo-referenced individual buildings, making it possible to analyze the spatiotemporal pattern of material supply from demolition and material demand for construction and renovation. The main results can be summarized as three points. 1) Urban mining cannot meet future material demand due to the new construction caused by population increase and its limited ability to supply the required kinds and amounts of materials. Therefore, large amounts of primary materials still have to be consumed in the future. 2) The generation of demolition wastes and the requirement for materials will be mainly concentrated in the big cities (e.g. Amsterdam, Rotterdam, and The Hague). 3) The GHG emission reduction potential of urban mining is very small and is not as large as the transition to a greener electricity mix. Recycling together with a greener electricity mix would reduce annual GHG emissions by about 40% in 2050 compared to 2020. This study provides a tool to link future material inflows and outflows in space and time. It further helps to assess the performance of strategies aimed at closing the material loops and reducing GHG emissions in the building sector.

Keywords: dynamic building stock model, material flow analysis (MFA), life cycle assessment (LCA), construction and demolition waste (CDW), urban mining, geographical information system (GIS)

4.1 Introduction

The built environment contributes to the generation of large amounts of material consumption, construction and demolition waste (CDW), and greenhouse gas (GHG) emissions [5]. In the European Union (EU), CDW makes up 25-30% of its total waste, and much of that could be recycled [8]. Urbanization and population growth are predicted to continue in the coming decades [237], intensifying material consumption and environmental challenges [238,239]. This trend is intertwined with the transition towards energy-efficient building stock (e.g. reconstruction and renovation) [112,148], which will also cause considerable material consumption and

[3] Published as: Yang, X., Hu, M., Zhang, C., Steubing, B. Urban mining potential to reduce primary material use and carbon emissions in the Dutch residential building sector. Resources, Conservation & Recycling. 180, 106215 (2022).

CDW generation, and a shift in attention towards embodied GHG emissions [32,240]. In current practices, CDW is typically used for road construction or backfilling [43,241], which are low-value applications that make further reuse impossible [44]. The transition from downcycling to high-quality CDW recycling is essential to close the building material cycles and reduce primary resource consumption and GHG emissions [242].

Urban mining is an important strategy that exploits the anthropogenic material stock in the built environment [243]. In recent years, geographical information system (GIS) datasets have been widely used to extract the information of individual buildings (e.g. geometry, year of construction, and function) [27,98]. GIS data and material intensities (kg/m^2 or kg/m^3) of buildings and infrastructures are usually applied together to determine the material stock at a high spatial resolution (map of material deposit) [244]. [245] and [246] analyzed the spatial distribution of material stock in buildings based on GIS data and material intensities of buildings differentiated by the construction period and utilization at the city scale. In addition to buildings, [247] further included the spatial distribution of materials stocked in roads and pipe networks. [80] integrated the urban mining model with life cycle assessment (LCA) to assess the environmental impact of different end-of-life scenarios.

Material flow analysis (MFA) depicts material flows and stock [108], and its principle has been applied, amongst others, in dynamic building stock models [129]. Some review articles on MFA [24,114–118] show that recent MFA studies particularly focused on bottom-up models that are more data-intensive (e.g. more detailed building archetypes) [84], often in combination with other tools, such as GIS [248], LCA [249], and system dynamic models [121,123]. The MFA model of [112] employed GIS data, building inventory data, and lifetimes of buildings and components to characterize the Swiss residential building stock, which has the potential to geographically aggregate future materials flows to different regional levels.

The linkages between material demand and secondary material supply from urban mining have not been well studied [112]. Hu and colleagues [111] have identified the building lifetime as a key variable influencing CDW generation, whereas the lifetimes of buildings are very long and vary significantly [24,238]. The amount and structure of CDW streams might not align with the material demand for new construction and renovation [247,250]. For example, modern buildings usually use some materials that do not exist in the old buildings to be demolished, such as insulation materials. Given that building materials are mostly large-volume but low-unit-value, transportation distance is an economic barrier, and supply and demand have to be close to each other, especially for the nonmetallic mineral materials (about 50-70 kilometers) [251,252]. Therefore, linking the material outflows and inflows in space and time is critical for making feasible plans in advance to realize a circular economy in the construction industry [253,254].

While the prevailing application of GIS data in recent years can provide spatial dimensions, current models mostly focus on quantifying retrospective material flows and stock in building stock [244,255]. In contrast, prospective MFA models rarely consider the spatial dimension. [251] and [44] analyzed the mismatch between material demand and supply from recycling in time while the mismatch in space was not fully considered. Besides, existing studies mainly focus on the material demand for constructing new buildings while the materials consumed during renovation processes are rarely accounted for [3]. Moreover, previous studies hypothetically conclude the urban mining potential to close material loops simply by comparing material outflows with inflows during building stock development, which omits the limitations of CDW collection practices and secondary material production technologies [44].

In the Netherlands, the construction sector accounts for 50% of raw material consumption, 40% of wastes, and approximately 35% of GHG emissions [155]. The government aims to reduce primary material consumption by 50% in 2030, realize a circular economy, and eliminate GHG emissions in the construction industry by 2050 [44,155,234]. The research questions of this study are:

(1) How will building material demand and the potential supply from CDW develop in space and time until 2050 in the Netherlands?

(2) How much primary material demand can be met by urban mining?

(3) What is the GHG emission reduction potential of urban mining?

This paper applies a bottom-up dynamic building stock model to track future material flows and stock of the Netherlands. The building stock is composed of georeferenced individual buildings, which makes it possible to analyze the spatiotemporal pattern between material demand and secondary materials recycled from demolition waste. The GHG emission reduction potential of urban mining is analyzed.

4.2 Materials and methods

4.2.1 Model overview

The conceptual outline of the model is presented in **Figure 4.1**. $\mathrm{BS}_{\mathrm{t}_\mathrm{n}}$ is the building stock at the time t_n and $\mathrm{BS}_{\mathrm{t}_{\mathrm{n}+1}}$ is the building stock at time $\mathrm{t}_{\mathrm{n}+1}$. The development of material flows and stock is associated with the building stock dynamics, such as construction, demolition, and renovation. These are driven to a large extent by factors such as population, building age, floor area per capita, and policies, e.g. for the energy transition and circular economy [29,108]. The material outflows considered in this study are from demolition and renovation, and material inflows are due to new construction and renovation. Outflows are partly going to be recycled or used for other purposes and partly landfilled because some materials will be mixed or destroyed during demolition, making their recycling very expensive or impossible [44]. The outflows without collection will become wastes and need to be processed (e.g. landfill). The material inflows contain secondary materials and primary materials. The time frame of this study is from 2020 to 2050 as the government of the Netherlands aims to be completely circular by 2050 [220].

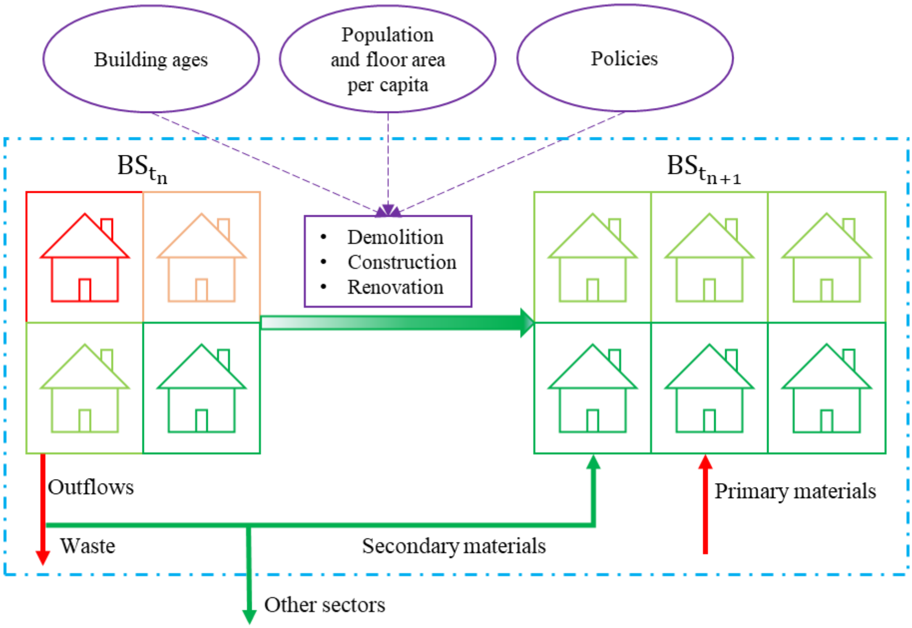

Figure 4.1 Schematic overview of the model. BS_{t_n} is short for the building stock at the time t_n and $BS_{t_{n+1}}$ is for the building stock at time t_{n+1}. The dot-and-dash line in light blue represents the system boundary. The purple color represents the factors that influence the building stock development. The red color represents the energy-inefficient buildings, waste, and the consumption of primary materials. The green color represents the energy-efficient buildings or reused materials. The efficiency of buildings in light green and orange colors is between energy-inefficient and energy-efficient buildings.

4.2.2 Material flow and stock

4.2.2.1 Building stock dynamics

The building stock dynamics are modeled based on [248], which is built upon individual buildings characterized by several attributes, mainly including building ID, construction year, building type, floor area, geometries, locations (city codes), U-values (thermal transmittances) of envelope elements (e.g. wall, roofs, and windows), and material composition. The existing buildings are characterized with basic information (e.g. footprint area and construction year) from GIS data [172] and classified based on the strategy of [27], including single-family houses, mid-terraced houses, end-terraced houses, multi-family houses, and apartment buildings. The geometries (e.g. window-to-façade ratio) and U-values of envelope elements are derived by allocating the archetype information [68] to individual buildings based on construction year and building type. As the GIS data only includes buildings built before 2015, the data gap of buildings in 2016-2020 is filled up with the stock-driven building stock model [248].

A building will be demolished after reaching its demolition year, which is determined by construction year and lifetime:

$$t_{dem} = t_{con} + t_{lifetime} \qquad (1)$$

Where t_{dem} is the demolition year, t_{con} is the construction year, and $t_{lifetime}$ is sampled based on Weibull distribution [206]. Buildings' lifetimes can vary significantly in the real world, depending on their function, ownership, and locations. In this study, lifetime differences between different building types are not considered due to a lack of data. The average lifetime is assumed as 130 years [37] and the shape parameter (k) is 2.95 [248]. Buildings constructed before 1900 are regarded as cultural heritage or protected buildings and will not be demolished in the considered time frame.

Construction activity is driven by total floor area demand as well as the demolished area at that year:

$$A_{con,t} = FAPC_t \times P_t - S_{t-1} + A_{dem,t} \qquad (2)$$

Where $A_{con,t}$ is the new construction area. $FAPC_t$ is the floor area per capita in year t and P_t is the population [221] in year t. S_{t-1} is the floor area stock of the previous year, and $A_{dem,t}$ is the demolished floor area in year t. According to the policy of the Netherlands [222], all the buildings constructed since 2021 must be nearly Zero Energy Buildings (nZEBs). The proportions of new building types are assumed the same as in 2015 [248]. The Netherlands is still under urbanization [256], so the locations (city codes) of newly constructed buildings are determined by the weight of the population per city [30]. The population map can be found in **Figure S7.3.1** in Appendix.

Renovation activity is determined by annual renovation rates derived from the national control scenario of the Netherlands [156], which is aimed at realizing a climate-neutral energy supply in the built environment. Instead of sampling individual buildings from the building stock, a neighborhood-oriented approach [157] is used to sample building groups at the neighborhood scale. The neighborhoods with high weighted average U-values will be renovated first. Insulation materials are differentiated between conventional and nZEB standards. More details can be found in [248].

4.2.2.2 Building material composition

This study involves 25 kinds of common building materials in the Netherlands (**Table 4.1**). The material composition of an individual building is determined by matching its building type with the material intensities of the corresponding archetype. The material intensities of archetypes for existing buildings are empirically sourced from demolition companies [147], and the material intensities of new buildings are from [211]. The material intensities of archetype buildings can be found in **Table S7.3.1** and **Table S7.3.2** in Appendix. The material composition of individual buildings are estimated by multiplying floor area with material intensities:

$$M_{i,j} = MI_{type,i} \times A_j \qquad (3)$$

Where $M_{i,j}$ is the mass of material i in building j. $MI_{type,i}$ is the material intensity of the corresponding building type. A_j is the floor area of building j.

Table 4.1 Material labels and names.

Label	Material name	Label	Material name
Al	Aluminum	MW	Mineral wool
Ar	Argon	Pl	Plastic
Bi	Bitumen	PUR	Polyurethane foam
CB	Clay brick	Pw	Plywood
Ce	Ceramic	RC	reinforced concrete
Co	Copper	Sa	Sand
CI	Cast iron	SC	Sand cement
Cr	Concrete	St	Steel
EPS	Expanded polystyrene	SW	Softwood
Gl	Glass	WF	Wood fiber
Gr	Gravel	XPS	Extruded polystyrene
Gy	Gypsum	Zn	Zinc
HW	Hardwood	-	-

In this study, existing glasses will be replaced by HR++ or HR+++ glass. For the roof, external wall, floor, and door, renovation is considered by adding a new insulation layer on top of the surface of each envelope element. The details on insulation materials for envelope elements can be found in **Table S7.3.3** in Appendix. The amounts of insulation materials consumed during renovation (excluding windows) are determined as follows [211]:

$$M_{i,j,e} = \left(\frac{1}{U_{insulation,j,e}} - \frac{1}{U_{exi,j,e}}\right) \times k_i \times A_{j,e} \times D_i \qquad (4)$$

Where $M_{i,j,e}$ is the mass of insulation material i required for insulating a surface element e. $A_{j,e}$ is the area of the element of building j. $U_{exi,j,e}$ is the existing U-value of the element and $U_{insulation,j,e}$ is the U-value post insulation. k_i is the thermal conductivity and D_i is the density.

4.2.2.3 Collection and recycling

The steps of processing material outflows from demolition and renovation are based on [44]. The first step is to quantify the annual material outflows and inflows, which can be calculated by grouping individual buildings by city codes and then aggregating the annual outflows and inflows of each material of individual buildings for each city. The second step is to estimate the amounts of material outflows suitable for recycling. The third step is to determine the amounts of recycled materials that can replace primary raw materials required for new construction or renovation.

The supply of collected outflows suitable for recycling is determined as follows:

$$M_{supply,i,t} = M_{outflow,i,t} \times R_{EOL_{collection},i} \qquad (5)$$

Where $M_{supply,i,t}$ is the collected material i from outflows ($M_{outflow,i,t}$) in year t. $R_{EOL_{collection},i}$ is the end-of-life (EOL) collection rate of material i (see **Table S7.3.4** in Appendix), meaning the share of material outflows collected for recycling.

The amount of waste material i in year t is calculated as follows:

$$M_{waste,i,t} = M_{outflow,i,t} \times (1 - R_{EOL_{collection},i}) \qquad (6)$$

The limited amount of recycled material used in annual construction activities is determined as follows:

$$M_{\mathrm{limit},i,t} = M_{inflow,i,t} \times R_{\mathrm{limit,i}} \qquad (7)$$

Where $M_{inflow,i,t}$ is the inflow of material i in year t. $M_{\mathrm{limit},i,t}$ is the maximum limited amount of primary material i that can be substituted by the recycled material in year t, and $R_{\mathrm{limit,i}}$ is the corresponding recycled content potential. The recycled content potential, defined as "the potential maximum fraction of secondary materials in the total input of material production", is used to estimate the maximum amounts of recycled material application in new construction and renovation [44,257]. The recycled content potential of different materials is from the literature [44] and details can be found in **Table S7.3.4** in Appendix.

To determine how many primary materials are replaced by recycled materials, the annual surplus of recycled materials ($M_{\mathrm{surplus},i,t}$) is used. It is calculated as follows:

$$M_{\mathrm{surplus},i,t} = M_{supply,i,t} - M_{\mathrm{limit},i,t} \qquad (8)$$

If $M_{\mathrm{surplus},i,t}$ is less than zero, it means that the supply of the collected material from outflows is not enough to reach the maximum recycled content potential. If $M_{\mathrm{surplus},i,t}$ is greater than zero, it means that there is residual collected material supply, which can be used for other sectors. The formula below shows the calculation of recycled materials used ($M_{\mathrm{recycled},i,t}$) in the annual residential building construction and renovation:

$$M_{\mathrm{recycled},i,t} = \begin{cases} M_{supply,i,t}, & M_{\mathrm{surplus},i,t} < 0 \\ M_{\mathrm{limit},i,t}, & M_{\mathrm{surplus},i,t} \geq 0 \end{cases} \qquad (9)$$

The annual primary material demand ($M_{\mathrm{primary},i,t}$) is calculated as follows:

$$M_{\mathrm{primary},i,t} = M_{inflow,i,t} - M_{\mathrm{recycled},i,t} \qquad (10)$$

The EOL recycling rate ($R_{recycling,i,t}$) is used to measure the proportion of the collected material that is used in construction and renovation in year t [44]. It is calculated as follows:

$$R_{\text{EOL\_}recycling,i,t} = \frac{M_{\text{recycled},i,t}}{M_{supply,i,t}} \quad (11)$$

The substitution rate ($R_{\text{substitution},i,t}$) is used to measure the proportion of the primary material that is substituted with recycled materials in year t [44]. It is calculated as follows:

$$R_{\text{substitution},i,t} = \frac{M_{\text{recycled},i,t}}{M_{inflow,i,t}} \quad (12)$$

4.2.2.4 Life cycle assessment

In this study, environmental impact is represented by GHG emissions measured as kg CO_2-eq [215]. All the GHG emissions of primary and recycled materials, treatment of wastes, and transportation are modeled with ecoinvent database 3.6 (cut-off system model) [138]. Electricity mix change will significantly influence the GHG emissions of material production [258], so the method by [216] is applied to create future background databases that represent future scenarios for electricity generation by combining ecoinvent and IMAGE database 3.0 [217]. We select two scenarios: the scenario (SSP2) based on the middle of the road following a representative concentration pathway (RCP) of 6 W/m^2 and the scenario (SSP2 450) based on a more ambitious middle of the road following RCP 4.5 (SSP2 450, greener electricity supply) [218]. The LCA software Activity Browser [131] is used to combine these datasets using the superstructure approach [142] to retrieve the GHG emission factors (see section **7.3.4**) of relevant processes.

The material-related GHG emissions are calculated as follows:

$$GHG_{i,t} = M_{i,t} \times (F_{i,t} + S_{\text{truck}} \times L_{material,\text{truck}} \times F_{\text{truck,t}} + S_{\text{ship}} \times L_{material,\text{ship}} \times F_{\text{ship,t}}) \quad (13)$$

Where $GHG_{i,t}$ is the GHG emissions of material i in year t. $M_{i,t}$ is the mass of material i. $F_{i,t}$ is the GHG emission factor of material i production or recycling. In the Netherlands, building materials are mainly transported by truck and ship. S_{truck} is the share of materials transported with trucks (72%) and S_{ship} is the share of materials transported with ships (28%) [211]. The average transportation distances are 96 km ($L_{material,\text{truck}}$) and 123 km ($L_{material,\text{ship}}$), respectively [211]. $F_{\text{truck,t}}$ is the GHG emission factor of truck and $F_{\text{ship,t}}$ is the factor for ship.

In this study, wastes are landfilled and the GHG emissions are calculated by summing up for all the waste materials as follows:

$$GHG_{landfill,t} = \sum M_{waste,i,t} \times (F_{landfill,t} + F_{\text{truck,t}} \times L_{\text{landfill,truck}}) \quad (14)$$

Where $GHG_{landfill,t}$ is the GHG emissions of waste treatment at year t. $F_{landfill,t}$ is the GHG emission factor of landfills. The average transportation distance for landfilled waste ($L_{\text{landfill,truck}}$) is 50 km [259].

4.3 Results

4.3.1 Building and material stock

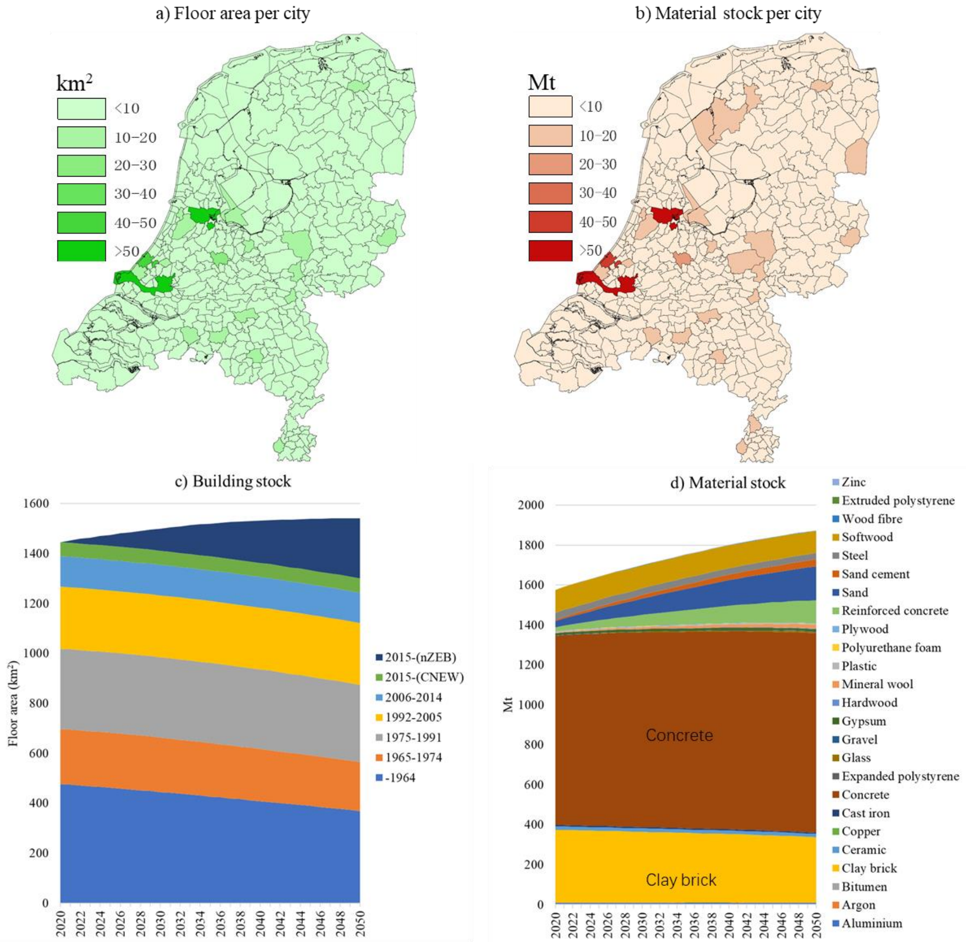

Figure 4.2 The existing building and material stock and its projected future development.

Figure 4.2a and **Figure 4.2b** show that both buildings and materials are concentrated in big cities, such as Amsterdam, Rotterdam, and The Hague. In **Figure 4.2c** and **Figure 4.2d**, both building and material stock will increase, while the increase of material stock is more obvious than that of building stock. Most existing buildings will still exist by 2050, and the buildings constructed after 2015 only occupy about 19% of the total building stock in 2050. The buildings constructed before 1964 are demolished most, but still have the largest share in 2050 (24%). Concrete (above 50%) and clay bricks (approximately 20%) dominate the material stock during the studied period.

4.3.2 Spatiotemporal material flows

Figure 4.3a shows that most of the material outflows are from Amsterdam, Rotterdam, and The Hague. From **Figure 4.3b** we can see that material outflows increase with time. Concrete (about 60%) and clay bricks (approximately 24%) occupy the largest share of material outflows. It can be found in **Figure 4.3d** that the material inflows are mainly distributed in big cities, especially in Amsterdam. **Figure 4.3e** shows that annual material inflows will decrease. The material inflows are dominated by concrete, sand, and reinforced concrete. Comparing **Figure 4.3b** with **Figure 4.3e**, we can find that the material inflows are much more than the outflows. The structure of material inflows is not in line with the structure of material outflows. For example, the share of clay bricks is very large in outflows but can almost be omitted in material inflows. **Figure 4.3c** and **Figure 4.3f** show that the spatial distribution of increased floor area is in line with the material deficit, meaning that big cities will construct more buildings and required more materials in the future. However, The Hague will not require as many new buildings and materials as Amsterdam and Rotterdam.

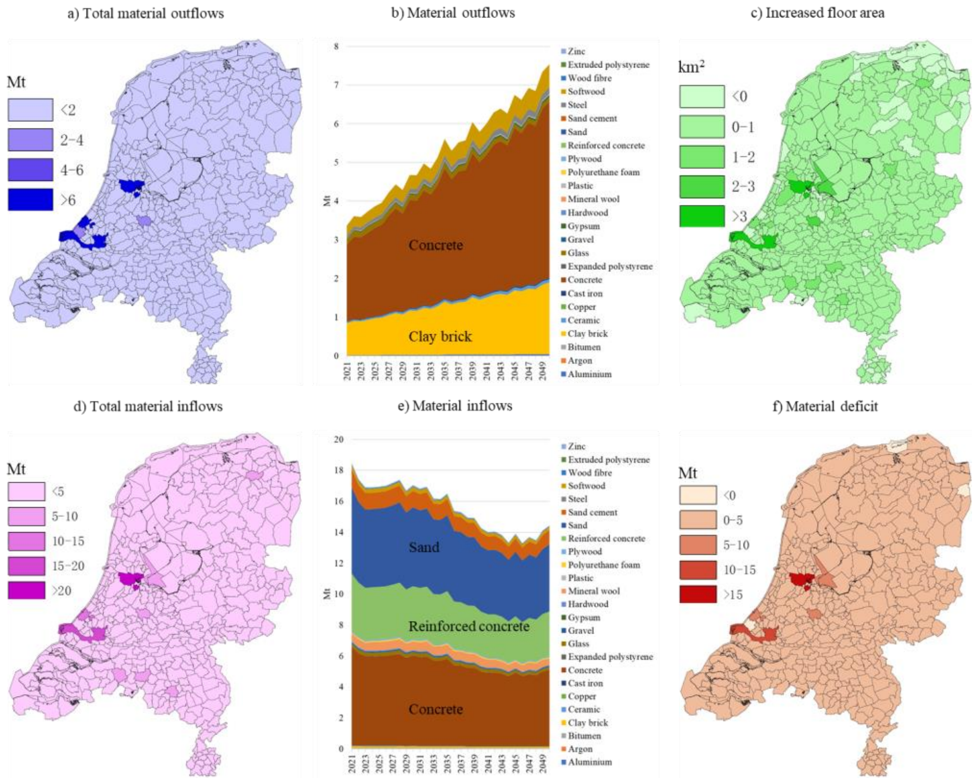

Figure 4.3 The material flows and increased floor area in space and time.

4.3.3 Substitution potential

Figure 4.4a shows that the supply of collected materials from outflows is mainly concrete and clay brick, and their amounts increase with time. In **Figure 4.4b**, the recycled material streams used in new construction and renovation mainly include concrete, wood, and glass. In 2035, the consumption of recycled materials begins to fall while the material supply from collections continues to increase, meaning that some of the recycled materials (e.g. concrete) have reached their maximum recycling potential and the residual collected materials (supply surplus) can be used in other sectors. This is also shown in **Figure 4.4c** that large amounts of the concrete surplus are generated in the 2035-2050 period. The clay brick is noteworthy as its surplus is much more than other materials. The reason is that clay brick is not intensively used in new buildings anymore. Comparing **Figure 4.3e** and **Figure 4.4d**, we can find that large amounts of primary materials (e.g. concrete and sand) will still be consumed although some material inflows are met by recycled materials.

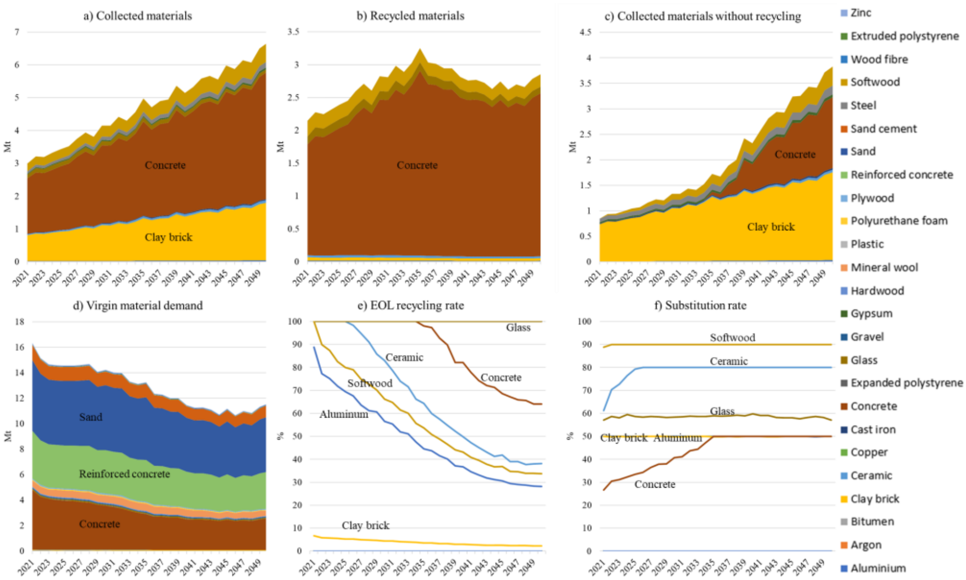

Figure 4.4 Figure 4.4a-d show the fate of demolition waste and the demand for virgin materials after considering the substitution effect of recycling. Figure 4.4e-f show the EOL recycling rates of collected material outflows and the substitution rates of secondary materials.

Figure 4.4e shows that the EOL recycling rates gradually decline for most materials. The EOL recycling rate of glass is always 100%, as the amount of recycled glass is much less than its maximum recycling content potential, and all the collected glass is consumed in new construction and renovation. This is followed by concrete, which is not enough to reach its maximum recycling content potential before 2035, while after about 2035, it begins to reach the maximum recycling content potential and the concrete surplus begins to exist. The maximum recycling content potential points of aluminum (2021), ceramic (2025), and softwood (2021) are much earlier than concrete (2035). The EOL recycle rates of other materials (e.g. clay bricks) are very low. From **Figure 4.4f** we can see that the substitution rates of many materials reach their maximum recycling potentials before 2035. The substitution rate of glass is about 59%, much lower than its maximum recycling content potential (91%), as the collected amount cannot meet the demand.

4.3.4 GHG emissions

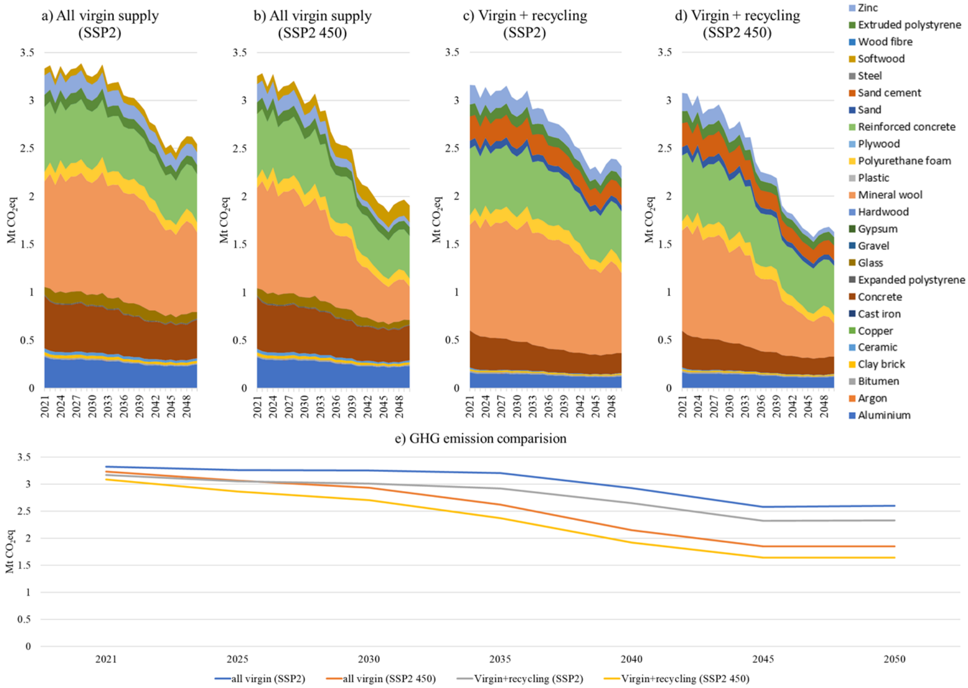

Figure 4.5 Material-related GHG emissions. In figure a-b, the substitution of recycled materials is not considered and all the materials required for construction and renovation are met by virgin materials. In figure c-d, virgin materials are partly replaced by recycled materials.

From **Figure 4.5a-d** we can find that the GHG emissions declines with time in all scenarios. Mineral wool, concrete, and reinforced concrete account for the most GHG emissions. Comparing **Figure 4.5a** with **Figure 4.5c** and **Figure 4.5b** with **Figure 4.5d**, we can find that the GHG emissions of concrete decrease due to the substitution effect of recycling. The GHG emissions of mineral wool decline significantly due to the greener electricity mix. In **Figure 4.5e**, the GHG reduction effect of a greener electricity mix is greater than substituting primary materials with recycled materials.

4.4 Discussion

This study presents a bottom-up dynamic building stock model to link future material demand and secondary material supply from urban mining. The potential of urban mining to reduce primary material use and GHG emissions in the Dutch residential building sector is investigated with the consideration of spatiotemporal dimensions. The mismatch between supply and demand is analyzed to find out what kind of materials have the biggest surplus or deficit. Compared with previous studies, the presented model focuses on future material composition evolvement of the building stock and builds upon individual buildings with georeferenced information, which enables the spatialization of material stock and flows. In addition, the material inflows and outflows during energy-efficiency renovation processes are accounted for at the building component level. Moreover, instead of directly comparing material outflows with inflows [112,248], our model not only considers the amounts of collected materials during demolition but also accounts for the amounts of recycled material used in annual construction activities. It can help local governments better manage CDW and understand the potential contribution of urban mining to realize circular economy and climate change targets.

4.4.1 Potential for substituting primary materials

The results above demonstrate that the material demand for new construction and renovation outweighs the supply of secondary materials because the increased population leads to more material demand for constructing new buildings. It might be challenging to achieve the Dutch target of reducing primary material consumption by 50% (2030) and 100% (2050) in the residential building sector through urban mining [234]. In previous studies [112,248], the material outflows are projected to nearly reach the amounts of annual material inflow by about 2050, indicating the big potential of recycling CDW to meet material demand for construction and renovation activities. Differently, the present study shows that the potential of urban mining to meet material demand is very limited as our model considers the recycling practices (i.e. CDW collection rates and recycled content potential).

This study uses fixed EOL collection rates and recycled content potential that is limited by current practice and legislation [44], while the technically recycling rates of some mineral materials can be very high and even reach 100%, such as concrete [5]. The recycled content potential might increase due to future technology and legislation change [260], so the substitution potential of urban mining might be underestimated in this study. Besides, intersectoral strategies could be made to reuse the residential material outflow surplus in another sector where it is in shortage, or vice versa [251], which also influences the substitution potential of urban mining in the residential building sector.

The economic perspective of building material recycling should also be paid enough attention to. In our research, materials are individually collected from CDW, which is a time-consuming and labor-intensive process [44], and might be economically challenging for developed countries where the labor cost for deconstruction is very high [240,261]. It is essential to change the legislation that currently limits the proportion of secondary materials in material inflows and promote the innovation of the circular business model for better managing the building material supply chain [1,44,262–264].

4.4.2 Potential for GHG emission reduction

The GHG emission reduction effect of urban mining is not as important as that of greening the electricity for material production. When a greener electricity mix is combined with a decrease of material inflows, and an increase of material outflows, the annual GHG emissions will decrease fastest, albeit only by about 40% in 2050 compared with 2020 (**Figure 4.5e**). Large amounts of concrete are still required in the future, and they contribute to a great share of GHG emissions. Thus, increasing the recycled content potential of concrete is critical for GHG emission reduction (see **Figure S7.3.2** in Appendix). Mineral wool is a widely used insulation material while reducing its application and finding alternative materials with low GHG emissions (e.g. bio-based materials) are essential [5]. In this study, the fixed recycled content potential is used but might increase in the future, so the GHG emission reduction potential of urban mining might be underestimated.

4.4.3 The mismatch between demand and supply

There is a structural contradiction between material supply and demand. On the one hand, the collected materials from waste streams do not contain some of the materials required for new construction and renovation, such as insulation materials. On the other hand, some of the collected materials from CDW will not be required too much anymore for new construction, such as clay bricks. Therefore, the choice of building materials in new construction can affect the EOL recycling rate of some materials.

The spatial mismatch between demand and supply is not obvious in this study because material deficit exists for most cities. The population will probably concentrate in metropolitan areas due to urbanization and the shrinkage of some small cities. Thus, different cities might be confronted with different situations in terms of secondary material surplus and deficit. Several neighboring municipalities can jointly plan demolition and new construction to reduce or avoid the mismatch in space and time.

The temporal mismatch between demand and supply could be resolved by better planning demolition and construction in advance to increase the overall EOL recycling rates. At the early stage, most of the recycled materials can enter the material inflows for new construction and renovation (material deficit). Nevertheless, as with the increase of demolition and the decrease of new construction, some materials gradually reach their maximum recycle content potential (material surplus).

4.4.4 Limitations and research opportunities

Some important limitations are associated with our study and can be further improved by future studies:

(1) Future demolition and construction activities could be better investigated. This study determines the future building demolition based on sampled lifetimes, and estimates new building construction based on population and floor area per capita, while it can be very far from reality, especially for mid-term prediction (from 2020 to 2050 in this study). The household size and living space per person [232] also vary significantly between different cities (see **Figure S7.3.1** in Appendix) and may change over time due to many factors (e.g. gross domestic product and immigration) [30]. Our model weights the new construction area based on the population of each city, but the population increase and migration between cities may significantly influence the spatial distribution of new construction [20,265]. Future researchers can collaborate with the governments to gain knowledge on future urban planning and socioeconomic development forecast.

(2) The future building types and technologies should be explored. The material structure of outflows and inflows are highly related to the types of buildings to demolish or construct [5,266]. As with the population increase in big cities and the scarcity of land, more high-rise apartment buildings with intensive reinforced concrete use would be built than single-family houses and terraced houses. Despite the limited GHG emission reduction potential of recycling, bio-based materials (e.g. wood) can be an alternative construction product to concrete and steel, because some bio-materials can sequester carbon emissions and act as carbon storage [5,35].

(3) The onsite material collection of demolition waste and the production of secondary materials need to be studied. The recycling of mineral materials is particularly complex [41]. Concrete, for example, is a mix of many primary materials, such as cement, sand, aggregates, and water. However, our model just assumed that the concrete from CDW is directly to substitute the primary concrete (actually similar to reuse) has not fully considered the details of production processes (e.g. crushing collected concrete into reusable aggregates). In this study, steel is collected from the outflows but its use in reinforced concrete production is not reflected. Therefore, an intermediate material classification system is required to link the material outflows and new material production [267]. Besides, future researchers can focus on the LCA of secondary material production to investigate the more accurate GHG emission reduction potential of urban mining [262].

4.5 Conclusion

This study presents a bottom-up dynamic building stock model that tracks the building stock development as well as the material stock and flows. The primary material substitution and GHG emission reduction potential of urban mining are explored by linking material demand and the material supply recycled from demolition waste.

The results demonstrate that urban mining can only replace a small share of primary material consumption mainly because the increasing population will require more new buildings. A great structural mismatch exists between recycled materials and the materials required for new buildings since some collected materials from CDW will not be used too much in new construction and renovation. In contrast, there will be large amounts of concrete outflow and inflow, showing the great recycling potential of concrete. The GHG emission reduction potential of urban mining is very limited and not as large as the transition to a greener electricity mix. Mineral wool only accounts for a very small share in terms of weight but will contribute to a great proportion of GHG emissions. Therefore, low-carbon insulation materials are required to replace it, such as bio-based insulation materials.

The model can depict the mismatch between material inflows and outflows in space and time, which provides the opportunity to better plan demolition and construction for high-quality CDW management. Future studies could focus on cross-region materials flows. For example, the recycled material outflows of shrinking cities might be used in emerging cities next to them. Neighboring cities can make recycling strategies together to improve CDW management. In addition, future research can combine residential buildings, utility buildings, and infrastructures that consume similar materials. This would better depict the overall material flows between different sectors, and thus make more systematical policy strategies for CDW management, especially for saving the cost of voluminous mineral material storage and logistics. Moreover, given that new construction requires large amounts of materials, extending the lifetime of existing buildings by extensive renovation rather than demolition and reconstruction can greatly reduce both CDW generation and primary material consumption.

Chapter 5 Key strategies for decarbonizing the residential building stock: Results from a spatiotemporal model for the Netherlands[4]

Abstract

Decarbonizing the building stock plays an important role in realizing climate change mitigation targets. To compare the decarbonization potential of different strategies, this study presents a spatiotemporal bottom-up dynamic building stock model that integrates material flow analysis, building energy modeling, and life cycle assessment. It can simulate future building stock evolution at the component level and track the associated material flows, energy demand and generation, and GHG emissions with the consideration of both endogenous factors (e.g. building energy efficiency upgrade) and exogenous factors (e.g. policies, occupant behavior, and climate scenarios). The model is applied in the residential building stock of Leiden, a municipality in the Netherlands. Results show that annual GHG emissions are reduced by about 40% under the reference scenario while annual GHG emissions can be reduced by about 90% under the ambitious scenario where all the decarbonization strategies are simultaneously implemented. Natural-gas-free heat transition and renewable electricity supply are the most effective strategies, respectively reducing the annual GHG emissions in 2050 by an additional 21% and 19% more than the reference scenario. Rooftop PV, green lifestyle, and wood construction have similar decarbonization potential (about 10%). Surplus electricity can be generated if rooftop PV systems are installed as much as possible. The decarbonization potential of demolition waste recycling is much smaller than other strategies. The model can support policymakers in assessing the decarbonization potential of different policy scenarios and prioritizing decarbonization strategies in advance.

Keywords: climate change, energy transition, circular economy, building stock model, material flow analysis, life cycle assessment

5.1 Introduction

The building sector accounts for 30% of global final energy consumption [268] and nearly 50% of all resource extraction [5]. It also generates large amounts of construction and demolition waste (CDW), equivalent to nearly 40% of annual extracted building materials [5]. The construction and operation phases contribute to 37% of greenhouse gas (GHG) emissions around the world [268], mainly from fossil fuel combustion for heat and carbon-intensive electricity consumption for appliances,

---

[4] Published as: Yang, X., Hu, M., Zhang, C., Steubing, B. Key strategies for decarbonizing the residential building stock: Results from a spatiotemporal model for Leiden, the Netherlands. Resources, Conservation & Recycling. 184, 106388 (2022).

lighting, and material production [5,269]. Ongoing urbanization and population growth [270] further emphasize the urgency of drastically decarbonizing the building sector to achieve the Paris Agreement goals [271].

GHG emission sources highlight the main decarbonization strategies in the built environment [5]. Demand-side strategies mainly include increasing material sufficiency (avoiding material demand and delivering human wellbeing within the biophysical limits of the planet) [272,273] and operational energy efficiency [11]. Supply-side strategies involve the transition towards renewable energy supply and low-carbon material production (e.g. bio-based materials) [1]. These strategies are coupled with each other during the development of the building stock [28]. For example, the reconstruction and renovation wave [274] would trigger considerable material flows and the deployment of high-quality CDW recycling [28]. Besides technical strategies, lifestyle change (e.g. floor area per capita and room temperature) [27,28] influences the demand for materials and energy, and thus affects climate change target realization [73].

Diverse models have been developed for evaluating the decarbonization strategies of building stock [29,129], mainly including building energy modeling (BEM) [27,107], material flow analysis (MFA) [24,114], and life cycle assessment (LCA) [20,134]. Dynamic building stock models further integrate these three tools to consider the overall material flows, energy demand, and environmental impact [95,248]. Despite advances in modeling techniques, existing researches have the following limitations:

(1) There is a lack of comprehensive consideration of deploying different decarbonization strategies together. For example, circular economy and energy transition are usually considered separately although they are both essential strategies deployed simultaneously in construction practices [275]. Besides, exogenous factors (e.g. technologies, policies, occupant, and climate) are usually assumed constant [5,28,276] and the interaction between them is typically neglected [3].

(2) Previous dynamic building stock models are mostly top-down models that depict the long-term trend of large-scale building stock (e.g. national or global) [29] and estimate material and energy quantities with intensities and floor area [28], limiting the evaluation of transformation strategies due to overlooking building heterogeneity [10]. To support governments in tackling local climate change issues, they have to shift towards the spatiotemporal bottom-up models that include more buildings and building technology details [248].

(3) The decarbonization opportunity of materials (e.g. CDW recycling, low-carbon production, and bio-based materials) is usually ignored [34], particularly for the materials consumed during renovation [5,28], while embodied emissions gain more importance as a result of building energy efficiency upgrade [24,277].

(4) Existing studies typically consider renovation with exogenously defined annual renovation rates based on recent trends or policy targets [26,125]. Nevertheless, the

payback time of renovation is very long due to high investment and relatively low energy bill savings [59], making it usually occur during the "natural" aging process for component replacement, maintenance, or upgrading [199,278].

This study presents a spatiotemporal bottom-up dynamic building stock model that can track material flows, energy demand and generation, and environmental impact with the consideration of different decarbonization strategies. The building stock is composed of individual buildings characterized by a series of attributes that are updated every year due to the replacement of building components and the change in exogenous factors. The model is applied in the residential building stock of the Dutch city of Leiden to answer the following research question:

To what extent can primary materials, energy, and GHG emissions be reduced under different decarbonization strategies, namely a material transition, an energy transition, and a greener lifestyle?

5.2 Materials and methods

5.2.1 Model overview

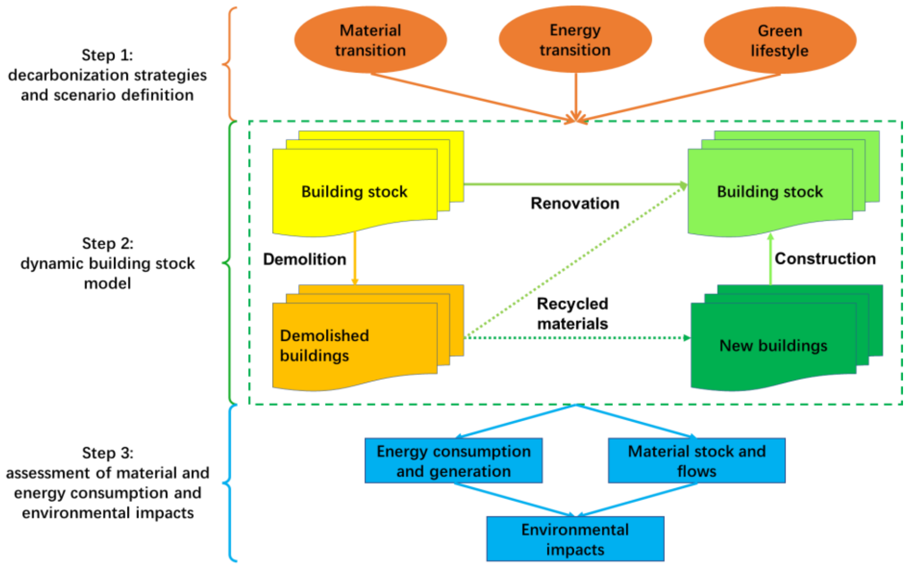

Figure 5.1 The model overview.

The modeling approach is shown in **Figure 5.1**. It encompasses three parts with temporal dimensions: decarbonization strategies and scenario definition, dynamic building stock model, and assessment of material and energy consumption and environmental impacts. Decarbonization strategies mainly consist of material transition (e.g. circular economy and bio-based construction), energy transition (e.g. energy efficiency improvement and renewable energy supply), and green lifestyle (e.g. less floor area per capita). Scenarios are differentiated by the combination of decarbonization strategies. We analyze the potential building stock development under different decarbonization strategies or scenarios that affect building stock size and composition, material flows, energy demand and generation, and the related environmental impact. The recycled materials from CDW are reused in annual construction activities. The environmental impact of material flows and energy consumption and generation during building stock development are further calculated by LCA.

The building stock is composed of individual buildings from geographic information system (GIS) data [172]. The building typologies from TABULA [68] are employed to classify buildings (see **Table S7.4.1** in Appendix) and derive building information (e.g. geometries, and physical properties) based on [27]. Buildings are characterized with several kinds of attributes, mainly including basic building information (e.g. construction year and floor area), location, components, material composition, annual energy demand and generation, and environmental impact (see more in **Table S7.4.2** in Appendix).

5.2.2 Decarbonization strategies and scenario definition

The Dutch government wants to reach carbon-neutrality [157] and full circularity [155] by 2050, including the building sector. Most existing residential buildings in the Netherlands have relatively low thermal insulation standards [208] and almost 90% of them rely on natural gas for space heating and hot water [214], suggesting its untapped decarbonization potential. Leiden, a medium-sized city in the Netherlands, has various types of residential buildings (29,030 in total), including both historical buildings and new buildings [44]. The municipality of Leiden hopes to realize a natural-gas-free heat supply [229] and a circular economy [279] in the building sector. Here we use the residential building stock of Leiden as a representative case study. The timeframe of this study is from 2015 to 2050.

Based on literature [1,28–31] and relevant Dutch policies [11,74,157,220], this study involves several main decarbonization strategies and defines two scenarios, i.e. reference scenario and ambitious scenario (see **Table 5.1**). The reference scenario follows a conservative development pattern. In the ambitious scenario, all the strategies are simultaneously adopted to investigate the maximum decarbonization potential of the residential building stock. Given the importance of prioritizing optional strategies for policymakers and other stakeholders [1], the decarbonization potential of each strategy is investigated by independently deploying them in addition to the reference scenario.

5.2.3 Dynamic building stock model

5.2.3.1 Demolition

The buildings constructed before 1920 are regarded as historical buildings [229], which will not be demolished in our model. The demolition year of individual buildings is estimated as follows:

$$t_{dem} = t_{con} + t_{lifetime,building} \qquad (1)$$

Where t_{dem} is the demolition year, t_{con} is the construction year, and $t_{lifetime,building}$ is the randomly assigned lifetime following the Weibull distribution [125] based on [248].

Table 5.1 Description of strategies and scenarios.

Decarbonization strategies		Reference scenario	Ambitious scenario
D1. Material recycling	Materials recycled from CDW are applied to substitute the primary raw materials for construction activities [280].	Current recycling practices in the Netherlands [44].	CDW is completely recycled for construction and renovation [155,234].
D2. Wood construction	Wood buildings [281] are introduced to represent the use of bio-based materials in new construction [3,5].	The share of wood buildings in annual construction is 20% [282].	The share of wood buildings in annual construction will linearly increase from 20% to 80% by 2050 [282].
D3. Heat transition	Natural gas boilers are replaced by electric heat pumps or heat networks and envelope elements are additionally insulated to improve energy performance standards [229,248].	Current heat sources (see **Table S7.4.8** in Appendix).	The share of neighborhoods implementing a natural-gas-free plan will linearly increase to 100% by 2050 [156,229].
D4. Renewable electricity	The share of renewable electricity in the public electricity grid is increased [216,248].	Conservative development of public electricity grid.	Greener public electricity grid.
D5. Rooftop PV	Solar PV systems are installed on roofs to substitute the public grid electricity consumption (towards positive energy buildings or neighborhoods) [1,156].	The share of roofs with solar panels linearly increases from 4.4% [70] to 30% [156] by 2050.	The share of roofs with solar panels linearly increases from 4.4% [70] to 100% [156] by 2050.
D6. Green lifestyle	The floor area per capita and room temperature gradually decrease due to the increase of environmental protection awareness and the reduction of vacancy rates [28,34].	Floor area per capita remains unchanged (62 m^2 per person in 2015) [172,283]. The room temperature is set as 20 °C [27].	Floor area per capita linearly decreases by 15% in 2050 compared with 2015 [28]. The share of buildings heated at 18 °C in conditioned areas linearly increases to 100% by 2050 [28].

5.2.3.2 Construction

Annual constructed floor area is driven by future population (see **Table S7.4.7** in Appendix), floor area per capita, and demolition [108]. New buildings are represented by TABULA archetypes [68]. According to Dutch policy [222], all the new buildings built from 1 January 2021 have to meet the nZEB (nearly Zero Energy Building) standard. The annual constructed floor area of a type of building ($A_{con,type,t}$) is estimated as follows:

$$A_{con,type,t} = (FAPC_t \times P_t - S_{t-1} + A_{dem,t}) \times PP_{building\_type} \qquad (2)$$

Where $FAPC_t$ is the floor area per capita in year t. P_t is the population in year t. S_{t-1} is the floor area stock of the previous year. $A_{dem,t}$ is the total demolished floor area in year t. $PP_{building\_type}$ is the proportion of a type of building. This study uses the building type proportions in 2015 [27] to segment the annual constructed floor area.

5.2.3.3 Renovation

This study models renovation at the building component level, mainly including envelope elements (roof, window, external wall, door, and ground floor), ventilation systems, space heating systems, domestic hot water systems, and rooftop PV systems. The renovation will occur after a component retires. As the ages of existing components are usually unknown, we estimate the retirement time of existing components as follows:

$$t_{retirement,existing} = t_{con} + \left\lfloor \frac{t_{start} - t_{con}}{t_{lifetime,component}} \right\rfloor \times t_{lifetime,component} + t_{lifetime,component}$$
(3)

Where $t_{retirement,existing}$ is the retirement year of an existing building component. t_{start} is the start year of the considered timeframe (i.e. 2015). $t_{lifetime,component}$ is the lifetime of the component (see section **7.4.4**).

The retirement year of a newly installed component is calculated as follows:

$$t_{retirement,new} = t_{current} + t_{lifetime,component} \qquad (4)$$

Where $t_{retirement,new}$ is the retirement year of a new building component. $t_{current}$ is the current year.

Buildings in the same neighborhood tend to have similar characteristics (e.g. construction years, building technologies, and heat sources) and can be upgraded with similar solutions [229]. In the Netherlands, municipalities are required to make a heat transition plan based on the neighborhood-oriented approach [207,248,284], which determines when and which neighborhoods will be tackled with what kinds of solutions, i.e. the dynamic heat transition map (see **Figure S7.4.1** in Appendix).

The heating system choice sets of individual buildings are linked to the corresponding neighborhood and updated every year. The alternative space heating systems in each neighborhood are from the heat vision of Leiden [229]. Insulation levels can greatly affect the efficiency of space heating systems [227,248]. For example, buildings installed with electric heat pumps and low-temperature heat networks have to be well insulated. This study considers two renovation combinations: conventional renovation and nZEB renovation [68]. The details of insulation standards and technical systems can be found in section **7.4.4**.

5.2.4 Analysis of material and energy flows and related environmental impacts

5.2.4.1 Material flows

This study involves 25 kinds of common building materials in the Netherlands (see **Table S7.4.4** in Appendix). The initial material stock of individual buildings is determined by multiplying material intensities (see **Table S7.4.5** and **Table S7.4.6** in Appendix) with the floor area. The material flows during renovation are accounted for based on [248]. The material composition of individual buildings is recorded every year (see **Table S7.4.3** in Appendix) and will be updated during envelope renovation. Individual buildings' material stock and flows are aggregated to the building stock level. The supply of secondary materials from CDW is calculated based on [280].

5.2.4.2 Energy demand and generation

The energy consumption of Dutch residential buildings mainly includes space heating, domestic hot water, and electricity for appliances and lighting [183,248]. The annual energy demand for space heating and domestic hot water is calculated based on [27]. The annual electricity demand for appliances and lighting is calculated by multiplying floor area with measured electricity consumption intensities [248]. For buildings installed with rooftop PV, the annual generated electricity is calculated based on [248]. Considering the effect of future weather change on space heating demand and electricity generation from rooftop PV [12,285,286], the climate scenario from KNMI [287] is used to represent the future weather change in the Netherlands. The temperature will linearly increase by 0.035 °C every year and the solar radiation will increase by 0.04% every year, from 2015 to 2050. Individual buildings' annual energy demand and generation are accordingly updated every year.

5.2.4.3 Life cycle assessment

Climate change is selected as the environmental impact category and measured as kg CO2-eq [215]. The current and future environmental impact for all materials and energy services is modeled based on future scenario background life cycle inventory databases as described by [216]. These databases are constructed from a combination of data from the IMAGE model [218] and the ecoinvent database (cut-off system model) [138]. Here, we have updated these databases to version 3.6 of ecoinvent and calculated climate change impacts using the superstructure approach [142] as implemented in the LCA software Activity Browser [131]. This data represents two scenarios: the SSP2-base (Shared Socio-economic Pathway) scenario, which represents the middle of the road following a representative concentration pathway (RCP) of 6 W/m^2, and the SSP2-2.6 scenario, which represents a more ambitious middle of the road scenario, characterized by a greener energy mix and limiting global warming to just below 2 degrees by 2100 [288]. SSP2-base corresponds to the reference scenario and SSP2-2.6 corresponds to the ambitious scenario (**Table 5.1**). Annual GHG emissions are calculated by multiplying the amounts of materials and energy with the related GHG emission factors (see section **7.4.5**). Details on quantifying the GHG emissions related to material transportation and end-of-life treatment can be found in [280].

5.3 Results

5.3.1 Building stock

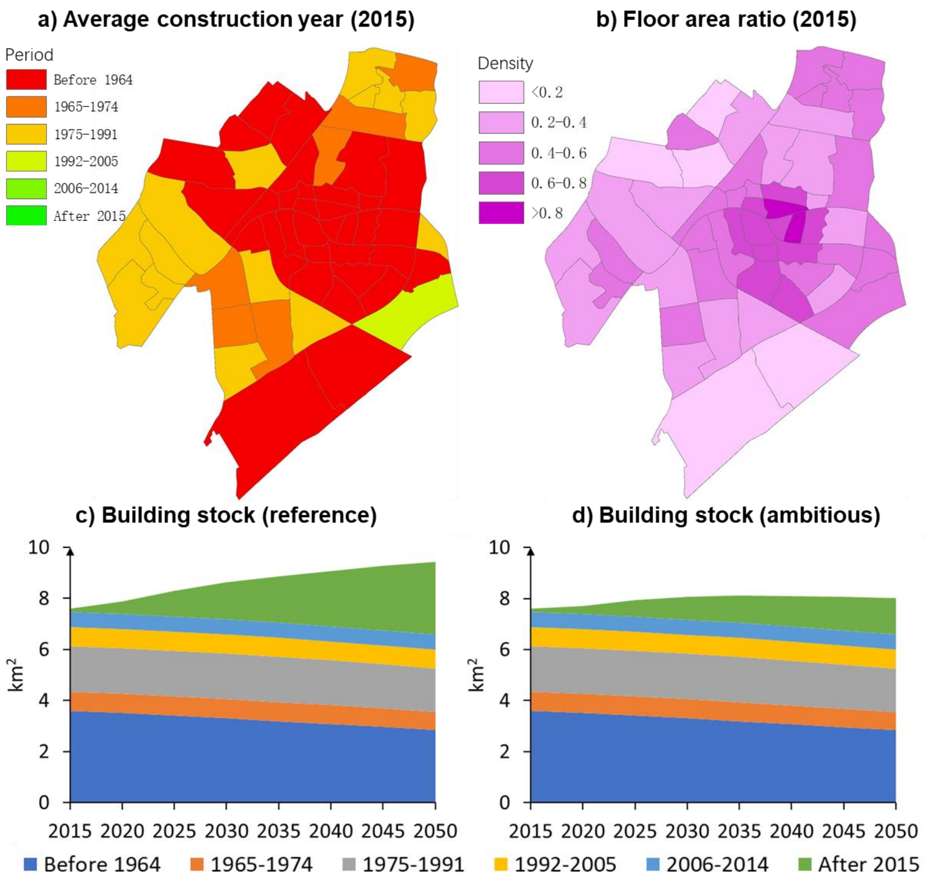

Figure 5.2 Current building stock and its future development. In Figure 5.2a, the average construction year is weighted by floor area to represent the age of building stock in each neighborhood. In Figure 5.2b, the floor area ratio[289] is calculated by dividing the total floor area per neighborhood by the neighborhood's land area. Figure 5.2c-d show the evolvement of building stock composition (total floor area of each construction period).

Figure 5.2a shows that the building stock of Leiden is very old, with nearly 50% of neighborhoods older than 1964, while there is only one neighborhood where the buildings' average construction year is after 1992. The city center (inside the moat) is the oldest and densest area (**Figure 5.2b**). In **Figure 5.2c** and d, the buildings constructed before 1964 occupy a large share (above 30%), suggesting the necessity and potential of decarbonizing the existing building stock. In the reference scenario, the building stock sees a continuous increase of 24% by 2050, making new buildings account for 30% of the total building stock. In the ambitious scenario, the building stock size increases at the start and reaches its peak at 8.1 km^2 in 2035 but begins to drop until 2050, with only 6% more than in 2015. In 2050, the proportion of new buildings is only 18%, much smaller than the reference scenario.

5.3.2 Material demand and supply

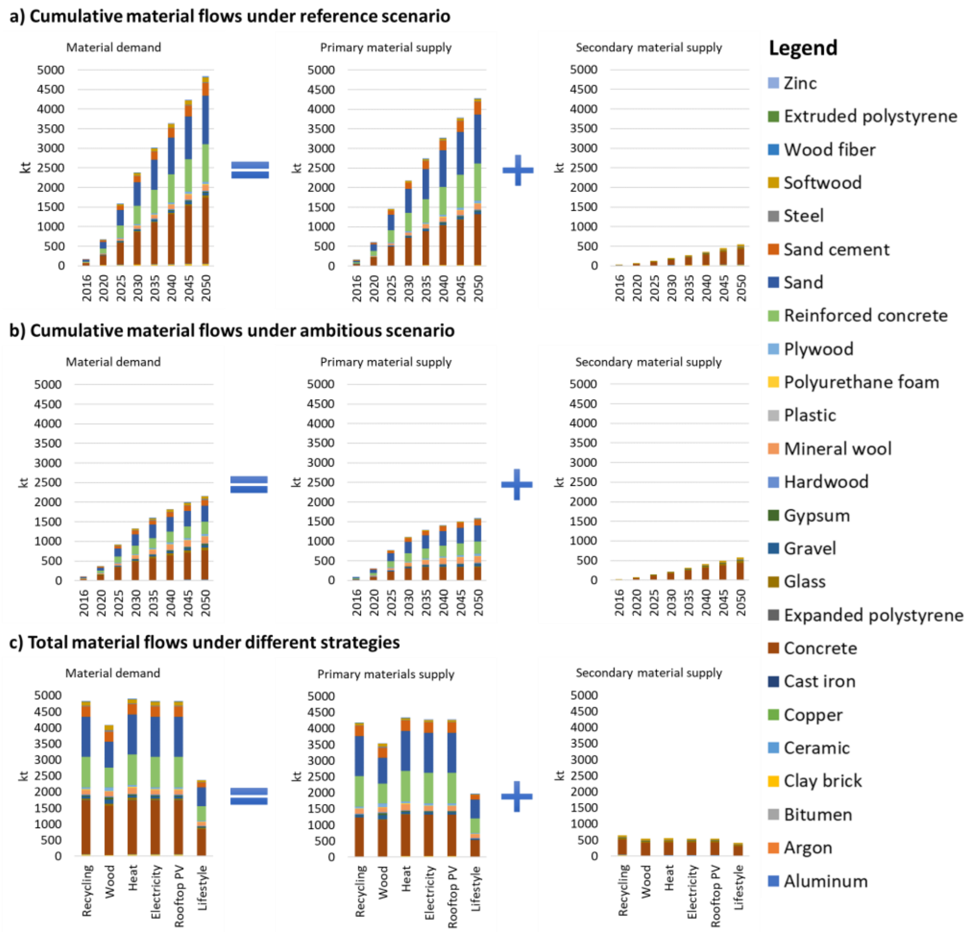

Figure 5.3 Cumulative material demand and supply. The material demand is supplied by primary and secondary materials. The amounts of materials in Figure 5.3c are the sums of material flows in the 2016-2050 period.

In **Figure 5.3**, the material demand is mainly composed of concrete and sand, regardless of scenarios and strategies. Compared with the reference scenario (**Figure 5.3a**), the total material demand (2016-2050) declines by about 55% in 2050 for the ambitious scenario (**Figure 5.3b**) and 51% for the green lifestyle (**Figure 5.3c**). The wood construction strategy reduces material demand by 15% due to the use of low-density wood materials and less concrete. Heat transition strategy slightly increases material demand as a result of more insulation material use.

Considerable primary materials are still required because the secondary materials supplied from CDW can only provide very limited amounts and kinds of materials (mainly concrete). Even though the recycling strategy is fully implemented, only about 13% of material demand can be met by secondary materials. The green lifestyle strategy reduces the new construction and thus consumes much fewer materials, around 17% of which can be supplied from secondary materials. In the ambitious scenario, around 27% of material demand is met by recycling and more than half of consumed concrete is secondary.

5.3.3 Energy demand and generation

Figure 5.4a shows that in 2015, the energy intensities of about half of the neighborhoods are more than 120 kWh/m^2a and the energy intensities of three neighborhoods are even higher than 160 kWh/m^2a. In the reference scenario, the energy intensities of most neighborhoods (77%) are below 80 kWh/m^2a in 2050. In the ambitious scenario, the energy intensities decrease dramatically in 2050 when the energy intensities of all the neighborhoods are lower than 80 kWh/m^2a.

The annual energy demand decreases by 27% in the reference scenario (**Figure 5.4b**) and 53% in the ambitious scenarios (**Figure 5.4c**), particularly for space heating demand, which is reduced by 49% in the reference scenario and 80% in the ambitious scenario. This leads to a lower proportion of space heating energy in annual energy demand, dropping from 72% in 2015 to 50% (reference scenario) and 30% (ambitious scenario) in 2050. In contrast, the shares of electricity and hot water energy experience a great increase. The proportion of electricity grows from 15% to 28% (reference scenario) and 39% (ambitious scenario). The share of hot water energy rises from 14% to 23% (reference scenario) and 31% (ambitious scenario).

Comparing different strategies (**Figure 5.4d**), we can find that heat transition has a greater effect on reducing annual space heating demand than green lifestyle, but the effect of a green lifestyle is bigger than heat transition at the early stage. In **Figure 5.4e**, rooftop PV systems can only meet about 46% of annual electricity demand in 2050 in the reference scenario. When rooftop PV systems are installed as much as possible, the building stock not only becomes self-sufficient in electricity but also has an electricity surplus (36% with 62 GWh in the ambitious scenario).

5.3.4 GHG emissions

Figure 5.5a shows that in 2015, the GHG intensities of most neighborhoods are above 30 kg CO_2-eq/m^2a and in some neighborhoods, the intensities are even more than 40 kg CO_2-eq/m^{2}a. Only three neighborhoods' intensities are below 20 kg CO_2-eq/m^{2}a. The city center is a carbon-intensive area where the GHG intensities are mostly above 40 kg CO_2-eq/m^{2}a. In 2050 of the reference scenario, the GHG intensities of most neighborhoods are below 20 kg CO_2-eq/m^{2}a while the intensities of 36% of neighborhoods are still between 20-30 kg CO_2-eq/m^{2}a. In the ambitious scenario, the GHG intensities are significantly reduced in 2050 when the GHG intensities of most neighborhoods are below 10 kg CO_2-eq/m^{2}a except for one neighborhood with intensities between 10-20 kg CO_2-eq/m^{2}a.

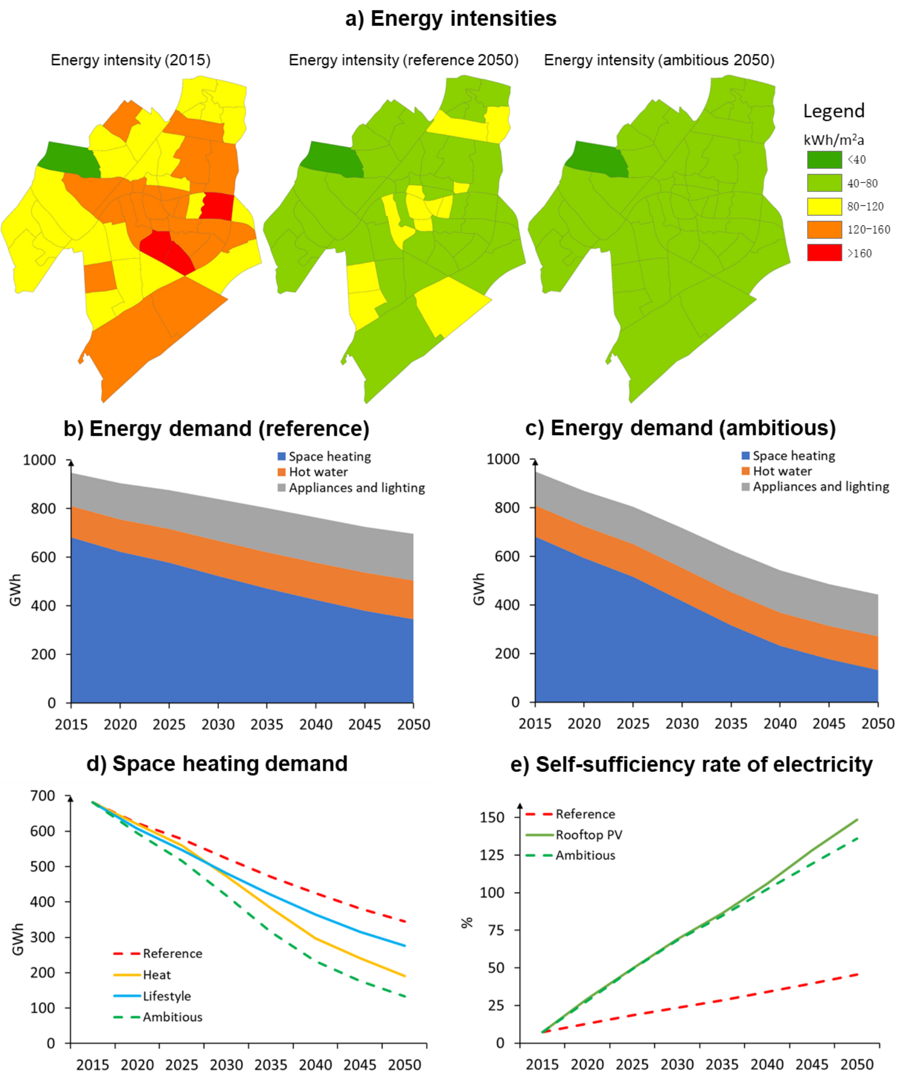

Figure 5.4 Energy demand and the electricity generated from rooftop PV.

Comparing **Figure 5.5b** with c, we can find that annual GHG emissions decrease by 40% (reference scenario) and 88% (ambitious scenario) by 2050, meaning that the carbon-neutral building stock target is nearly reached if all decarbonization strategies are deployed together. The GHG emissions of space heating occupy the largest share in all scenarios and periods, ranging from 47-75%. The share of GHG emissions from electricity generation is stable in the reference scenario (25-30%) but in the ambitious scenario, it ranges from 12% to 29%. In the ambitious scenario, the GHG emissions of hot water decline to nearly zero due to the extensive adoption of solar water heaters. Material-related emissions only account for a small share of annual GHG emissions (below 20%).

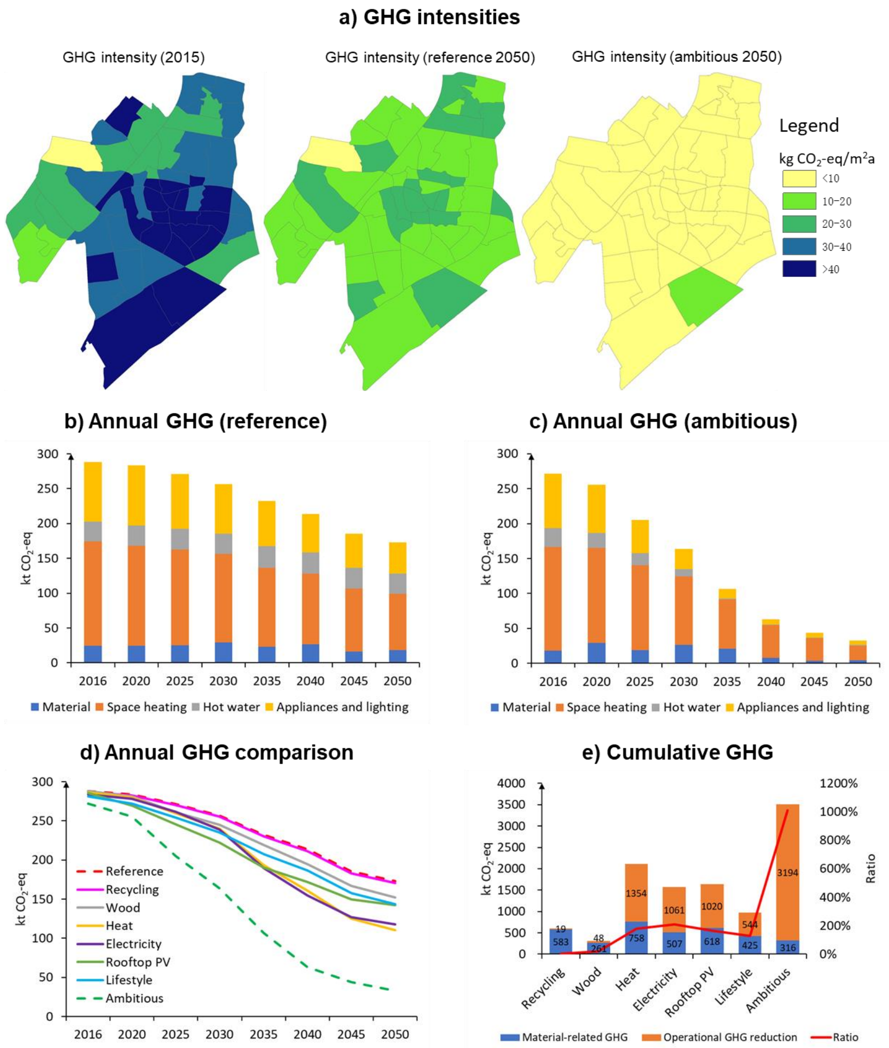

Figure 5.5 GHG emissions. Figure 5.5a and b show the annual operational GHG intensities. The percentages in Figure 5.5e are the ratios of cumulative operational GHG reduction potential in comparison with the reference scenario to cumulative material-related GHG.

Figure 5.5d shows that the heat transition strategy has the largest impact on annual GHG reduction (21% more than the reference scenario), which is closely followed by the renewable electricity strategy (19%). Rooftop PV strategy, green lifestyle strategy, and wood construction have similar decarbonization potential (about 10%). The effect of fully implementing the recycling strategy is almost negligible. **Figure 5.5e** suggests that the ambitious scenario realizes the most cumulative operational GHG reduction with the least material-related GHG emissions, which is followed by heat transition, renewable electricity, and rooftop PV.

5.4 Discussion

This study presents a spatiotemporal bottom-up building stock model to evaluate the GHG emission reduction potential of the building stock. The model builds upon individual buildings from GIS data characterized by a series of parameters (including technical details) and tracks the development of individual buildings at the component level. Future material flows, energy demand and generation, and GHG emissions are accounted for every year building by building with the consideration of both endogenous factors (e.g. building component replacement or upgrade) and exogenous factors (e.g. material and energy policies, population and occupant lifestyle, and climate change scenarios). The model can prioritize decarbonization strategies by comparing the effects of different policy strategies on the overall decarbonization potential of building stock. The employment of local and high-resolution data further strengthens its reliability and capability to support decision-makers in making neighborhood or city-specific strategies for climate change mitigation.

5.4.1 Overall decarbonization potential

Our study shows that the carbon-neutral building stock goal cannot be achieved in the reference scenario (conservative development pattern) where only around 40% of the annual GHG emissions are reduced in comparison with 2015. This demonstrates that simply upgrading building energy efficiency by envelope insulation is not enough for realizing the carbon-neutral target and replacing natural gas with renewable heat sources is also necessary. When all the decarbonization strategies are simultaneously deployed to their furthest potential, annual GHG emissions can be reduced by nearly 90%, meaning that there is still some distance to the carbon-neutral building stock. It is worth noting that these strategies involve greening the energy system and thus a wider effort than just within the building sector is required. Although the introduction of wood construction and renewable electricity generation can have positive climate effects, e.g. from temporary carbon storage [290], their absolute values are small in our study compared to other emissions.

5.4.2 The key role of energy transition

Heat transition contributes the most to reducing energy demand and GHG emissions.

Even in the reference scenario where the energy efficiency of buildings follows a natural improvement pattern, the annual energy demand and GHG emissions of space heating both decline by about 50%. A sensitivity analysis is conducted to evaluate how faster heat transition [291] influences future GHG emissions (see **Figure S7.4.2** in Appendix). It shows that early deployment of the natural-gas-free plan can gain more GHG reduction, which is in line with the finding of [291]. This highlights the need for taking action earlier to realize "no regrets" renovation [157,292–294]. The heat transition is followed by the strategy of greening the public electricity grid, which reduces annual emissions by 59%. Its distinctive feature is that it can reduce both embodied and operational GHG emissions [34,258], so it plays a key role in decarbonizing the building stock, which is also confirmed by some other studies [31,248,295,296]. Large-scale installation of rooftop PV systems has great potential for mitigating the dependence on public grid electricity and decarbonizing the building stock, which is also confirmed by some previous studies [66,70,248,297]. The green lifestyle strategy has a similar decarbonization effect to the wide installation of rooftop PV systems. Its role lies in reducing future demand for materials and energy while great uncertainties exist.

5.4.3 Limited effect of material-related strategies

The material recycling strategy has a very limited potential for reducing and decarbonizing materials. Wood construction has the potential for reducing annual GHG emissions, yet a sustainable supply of sufficient quantities may be the bottleneck [282]. In this study, material-related strategies have a much smaller effect on decarbonization than energy-related strategies during the considered time frame. The reason is that embodied GHG emissions make up only a small proportion of annual GHG emissions (**Figure 5.5**), which is also demonstrated by [248,296]. It is commonly believed that the relative share of embodied GHG emissions will increase in the future [32,248], which is also shown in **Figure 5.5c**. However, this share is also determined by what kinds of strategies are implemented to what extent. For example, greening the energy systems (e.g. renewable public electricity grid and rooftop PV installation) can significantly reduce operational emissions while the decarbonization potential of building materials is relatively smaller [248]. Wood construction can greatly reduce material-related emissions and thus makes the share of embodied emissions remain very small (**Figure 5.5d**). Some other studies [34,35] find that the lifetime extension of buildings and components is very effective in reducing GHG emissions. We plan to explore this by including the lifetime extension strategy in our model in future research.

5.4.4 Relationships between decarbonization strategies

It is worth noting that the decarbonization strategies may sometimes have co-benefits and adverse side effects on each other [34,298]. For example, implementing heat transition and wood construction strategies will require some new materials (e.g. insulation materials and wood) that CDW recycling cannot supply, which lowers the recycling rate and decarbonization potential. On the contrary, a renewable electricity mix can further enhance the effect of heat transition by decarbonizing the electricity consumed by widely installed heat pumps. In the ambitious scenario, the electricity generated from rooftop PV in 2050 can provide about 46% of the total electricity consumption of Leiden in 2015 (1821 TJ [299]). It has an electricity surplus (31%) for appliances, lighting, and electric heat pumps under the assumption that the heat pump's coefficient of performance (COP) is 3.5 [74]. However, there will also be a trade-off between the GHG emission factors of rooftop PV electricity and public grid electricity for the SSP2-2.6 scenario in about 2040 (see **Table S7.4.23** in Appendix). Therefore, the aggregated GHG reductions of each strategy are not equivalent to the reduced GHG emissions in the ambitious scenario where all strategies are simultaneously implemented. Besides, this study compares the decarbonization potentials of different strategies but it doesn't mean that the strategies with limited decarbonization potentials are unimportant. Instead, different policies are made to resolve different issues. The material recycling strategy, for example, can to some extent reduce the extraction of primary materials from nature and the generation of CDW and related environmental effects, yet its overall GHG reduction potential is rather small.

5.4.5 Model applicability and implications

The spatiotemporal model integrates MFA, BEM, and LCA, enabling it to comprehensively simulate the impacts of multiple aspects (e.g. policies, technologies, occupants, and nature) on the future development of floor area stock, technology distribution, material flows and stock, energy demand and generation, and GHG emissions. It can help policymakers prioritize the strategies for decarbonizing building stock by evaluating their performance in advance with the consideration of detailed technical practices. In theory, the model can be applied on larger scales (e.g. countries or regions) and in other countries as long as the required data is available. However, the space cooling demand model could also be included in future research as in some regions air conditioning systems are widely installed. The comparison between different strategies shows the descending order of their priority in terms of decarbonization potential for residential building stock in Leiden: heat transition, greener electricity mix, rooftop PV, green lifestyle, wood construction, and material recycling. The results might apply to some other Dutch cities because most residential buildings in the Netherlands are heated by natural gas boilers. However, the effects or order of decarbonization strategies might be very different considering the area-specific climate, building stock composition, energy supply systems, and socio-economic circumstances, as a recent study [296] shows.

5.4.6 Limitations and future research

Some potential limitations are associated with our study:

(1) The study mainly considers the effect of policy strategies from a technical perspective (e.g. lifetime-driven building component renovation) while in reality,

socioeconomic factors can greatly affect the implementation of strategies. For example, the residents might be reluctant to renovate the building to a higher efficiency level and transit to low-temperature heating systems, because investments may not pay off quickly enough [248,300–302]. The financial initiatives from the government and the legislation for building technologies can also affect the pace of implementing strategies. Future research should investigate transformation patterns that are affordable and beneficial for everyone with the consideration of potential governments actions [157].

(2) Our model only considers the energy-efficiency renovation while in practice, it often happens in combination with non-energy renovations [303]. Thus, it is important to consider them together as non-energy renovation requires large amounts of building materials.

(3) This study has not considered the increasing efficiency of appliances and lighting [156] as well as the rapid growth in the use of appliances in buildings, so the future electricity demand from appliances, combining projected use and efficiency, is subject to high uncertainty. It would be interesting to investigate future electricity demand as well as its decarbonization potential.

(4) Dynamic carbon accounting and the effect of carbon storage, as well as the wood availability and potential supply, are not included in this study, which could be explored in the future.

5.5 Conclusion

In this study, we present a bottom-up dynamic building stock model that builds upon individual buildings from GIS datasets and integrates MFA, BEM, and LCA. It is capable of tracking the building stock development and the associated material flows, energy demand and generation, and the corresponding environmental impact in space and time. Both building energy upgrade and exogenous factors (e.g. policies and occupant behavior) are considered to assess the potential effects of different policy strategies on the realization of future building stock decarbonization goals. The model is applied in a Dutch city to explore the overall decarbonization potential of the residential building stock and compare the decarbonization effects of different policy strategies.

Results show that the annual GHG emissions can be reduced by above 90% if all strategies are effectively deployed together. Energy transition plays the most critical role. Heat transition and greening the public electricity grid have similar decarbonization potential, while this is beyond the building sector itself. Wide installation of rooftop PV systems can generate surplus electricity for residential electricity consumption. Material-related strategies contribute less to GHG emission reduction than energy-related strategies due to the small share of embodied emissions in annual total GHG emissions. The decarbonization potential of CDW recycling is almost negligible as it can only provide limited amounts and kinds of materials to substitute the primary materials. Increasing the construction of wood buildings can reduce much more GHG emissions than CDW recycling.

The study demonstrates that the residential building stock has great decarbonization potential whereas different kinds of strategies need to be effectively implemented simultaneously. Reducing energy demand through wide renovations cannot lead to climate-neutral building stock. It should be accompanied by increasing the share of renewable energy in the energy mix. Future research should focus more on the socioeconomic aspects to promote the early and effective implementation of decarbonization strategies because faster energy transition can reduce more GHG emissions.

Chapter 6 General discussion

The thesis aims to help policymakers understand how building stock in the Netherlands can be decarbonized and supports them in formulating relevant climate change mitigation strategies also for the residential building sector in the Netherlands. The research gaps, research questions, and corresponding answers covered by this study are shown in **Table 6.1**. To answer the research questions, I develop a series of bottom-up building stock models to characterize the current building stock, track building stock evolution, analyze materials flows, simulate energy demand, and account for environmental impacts. The models can be applied to support policymakers in making policies related to developing a circular economy, reducing energy demand, phasing out fossil fuels, and mitigating climate change. In the remainder of this chapter, I will summarize and discuss my main findings and provide some implications for policymakers. Finally, this chapter analyzes the uncertainties and limitations of my models and provides some suggestions for further improving bottom-up building stock modeling.

Table 6.1 Research gaps, research questions, and corresponding answers of this thesis.

Research gaps	Research questions	Answers
The potential development of the Dutch residential building stock in space and time	How will the residential building stock develop in the Netherlands? (**Chapter 3, 4, and 5**)	· Improved insight into building stock composition · Insight into material flows related to demolition and new construction · Insight into the spatial distribution of stocks and flows over time
Energy-saving potential and energy supply	How much can energy demand be reduced and what is the potential of rooftop PV to meet local electricity demand? (**Chapter 2, 3, and 5**)	· Developing an engineering-based building stock energy model for assessing energy-saving potential · Insight into future energy demand · Analyzing energy-saving effects of different measures · Exploring the electricity generation potential of rooftop PV
Linking material outflows with inflows in space and time	How much primary material consumption in the Dutch residential building sector can be potentially reduced by urban mining? (**Chapter 4 and 5**)	· Insight into the spatiotemporal distribution of material flows and stock · Analyzing the mismatch between material demand and secondary material supply
Overall decarbonization potential of combined strategies	To what extent can residential GHG emissions be reduced under different decarbonization strategies and scenarios? (**Chapter 3, 4, and 5**)	· Estimating the overall decarbonization potential · Comparison between the decarbonization potential of different strategies · Discussion on the relationships between strategies

6.1 Answers to research questions

Question 1: *How will the residential building stock develop in the Netherlands?*

Chapter 3 shows that the buildings constructed before 1964 will still form the largest share of the Dutch building stock during the considered time frame (from 2015 to 2050). The annual demolished floor area will increase as an increasing number of buildings will reach the end of their lifespan. The demolished buildings are mostly constructed before 1964. The annual newly constructed floor area will become less with time as a result of a slower population increase. The floor area of newly constructed buildings (defined as buildings constructed after 2015) will account for about 20% in 2050. Most existing buildings will remain in use until 2050 or later, meaning that improving the existing buildings is the most important task for realizing energy neutrality and climate change targets.

Chapter 5 conducts a case study for Leiden. The reference scenario uses a fixed floor area per capita value while the ambitious scenario assumes that the floor area per capita will linearly decrease by 15% from 2015 to 2050. Results show that with this ambitious scenario, the total floor area will increase before 2035 and then begin to shrink, but the total floor area in 2050 is still more than in 2015 (increased by 6%). This makes the share of new buildings in the ambitious scenario (18%) smaller than that of the reference scenario (30%) in 2050.

Question 2: *How much can energy demand be reduced and what is the potential of rooftop PV to meet local electricity demand?*

To assess the energy-saving potential of energy efficiency measures, Chapter 2 develops an engineering-based space heating demand model based on EN ISO 13790 [180]. The GIS data and building archetypes in the Netherlands are used to derive individual buildings' information, such as component geometries and physical properties. The spatial validation shows that the model can well estimate the space heating demand of the residential building stock of the Dutch city of Leiden. It can provide acceptable results at the postcode scale (containing 9 buildings on average). However, there may be considerable uncertainties regarding individual buildings as the model builds upon information derived from GIS and archetypes rather than real detailed information on individual buildings, such as insulation level, heating systems, and occupant behavior. Validation for individual buildings was not conducted because the measured energy consumption is reported at the postcode level. A stepwise approach that increases the sophistication of the space heating model by gradually including more parameters shows that past renovation and occupant behavior can greatly affect the model accuracy, and thus contribute most to the reliability of model results. In contrast, increasing the temporal resolution of weather data (from seasonal to hourly) leads to a limited accuracy increase. Future research should thus mainly focus on collecting the data on past renovation records and occupant characteristics to further improve the model accuracy.

The space heating demand model in Chapter 2 is integrated into the bottom-up dynamic building stock model in Chapter 3 to estimate the energy-saving potential under the national control scenario of energy transition in the Netherlands. Results show that extensively renovating existing buildings, constructing high-energy performance buildings (nZEBs), and demolishing old energy-inefficient buildings can reduce annual space heating-related energy demand by more than 60%. In the assessed scenarios, energy-efficiency renovation contributes more to annual space heating demand reduction than demolishing old buildings, especially if it is possible to renovate buildings to the nZEB standard. As buildings with worse thermal properties are assumed to be renovated first, the marginal reduction of demand for space heating decreases with time. Constructing nZEBs instead of conventional new buildings avoids any increase in space heating demand.

The space heating demand model in Chapter 2 is also applied in the spatiotemporal building stock model in Chapter 5. Unlike the case in the dynamic building stock model in Chapter 3 where renovation is driven by exogenously defined annual renovation rates, in Chapter 5, the renovation is assumed to occur when a building component (e.g. windows) reaches retirement time. The model is used in the case study for Leiden. Results show that annual energy demand will decline by 50% by 2050 if the heat transition and green lifestyle strategy are deployed together. The reduction is mainly from lowering space heating demand due to extensive energy-efficiency renovation and lower room temperature.

Chapter 3 and Chapter 5 both show that in contrast to the development trend of space heating demand, the energy demand for domestic hot water, appliances, and lighting will experience a slight increase because these energy consumptions are driven by occupants, new construction, and installation of technical systems rather than the thermal properties of building envelopes. However, extensive installation of rooftop PV systems can greatly mitigate the dependence on public grid electricity and even generate surplus electricity. Chapter 3 shows that 80% of electricity demand can be potentially met by 2050 if 50% of building roofs are fitted with rooftop PV systems in the Netherlands. Chapter 5 shows that installing as many rooftop PV systems as possible would meet local residential electricity demand and generate 36% of surplus electricity.

Question 3: *How much primary material consumption in the Dutch residential building sector can be potentially reduced by urban mining?*

Chapter 4 shows that both material outflows and inflows of the Dutch building sector will, as expected, concentrate in big cities (e.g. Amsterdam and Rotterdam). Due to the expansion of the housing stock, material inflows outweigh material outflows. Urban mining can only supply limited amounts of specific types of building materials for annual new construction and renovation activities, meaning that additional consumption of primary raw materials is still required, such as concrete and sand. Even so, we show in Chapter 5 that the CDW reuse potential in terms of closing building material loops is much smaller than is usually suggested [112,248]. The reason is that most current studies simply check whether CDW is recycled. In the Netherlands the recycling rates of CDW are high, typically over 95% [304].

However, most of these materials are downcycled as filler or road foundation. Much more complex collection, sorting, and upgrading techniques are needed to use CDW again as primary building materials that meet the applicable legal quality standards.

The potential to meet future material demand is also determined by what kinds of and how many buildings will be built in the future. Chapter 4 shows that bricks will not be required as much as before because the brick intensities of building archetypes chosen in the case study for the Netherlands are very low. Extensive renovation will consume large amounts of insulation materials while such insulation materials are hardly present in CDW created by the demolition of very old buildings. Increasing the share of wood buildings will require more wood. Again, since wood was little used in the past, CDW from the demolition of old buildings cannot meet the specific supply of wood. Chapter 5 shows that the green lifestyle strategy (e.g. more intensive occupation of buildings) will reduce the material demand for new construction.

Question 4: *To what extent can residential GHG emissions be reduced under different decarbonization strategies and scenarios?*

Chapter 3 shows that GHG emissions in the Dutch residential building stock can be significantly reduced. Under the "National Control Scenario" of the Plan "Nederland klimaatneutraal in 2050" (Netherlands climate neutral in 2050) [156], climate neutrality of the building stock will almost be achieved by 2050. Extensive renovation, together with ceasing the use of natural gas for space heating and domestic hot water generation, reduces the annual energy-related GHG emissions by nearly 60%, but the decarbonization potential can increase to nearly 90% if the share of renewable electricity supply is significantly increased. Greening the electricity mix contributes mainly to a reduction of operational energy-related GHG emissions, but also, to a lesser degree, via the decarbonization of the production of building materials.

Chapter 5 assesses the decarbonization potential of deploying several main strategies in the residential building sector of Leiden, including CDW recycling, wood construction, heat transition, renewable electricity mix, rooftop PV, and green lifestyle. Results show that the annual GHG emissions of the residential building stock can be reduced by about 90% if all decarbonization strategies are implemented simultaneously [5]. The strategies of heat transition and greening the public electricity grid have similar decarbonization potentials (about 60%). Rooftop PV, green lifestyle, and wood construction strategies respectively reduce annual GHG emissions by about 50%. Chapter 4 shows that implementing a CDW recycling

[5] Note that the overall decarbonization potential of deploying strategies together is not equivalent to the aggregation of decarbonization potential of implementing each strategy independently. The reason is that the strategies can be mutually exclusive. For example, buildings are assumed to first use the locally generated electricity from rooftop PV. In that case, greening grid electricity only partially can give additional reductions, i.e. for the fraction of electricity that is used from the grid.

strategy would contribute only to limited GHG emission reductions due to the limited substitution potential of secondary materials recycled from CDW. Greening the public electricity mix leads to more material-related GHG emission reduction than CDW recycling. Implementing these two strategies together can reduce annual material-related GHG emissions by about 40% in 2050 in comparison with 2020 (Chapter 4).

Chapters 3 and 5 show that only reducing space heating demand through energy-efficiency renovation is not enough. Replacing natural gas boilers with alternative heating systems (e.g. electric heat pumps, heat networks, green gas boilers, and solar water heaters) can additionally lead to annual space heating-related GHG emission reduction. Along with the increased installation of electric heat pumps, the total electricity demand will also grow. Therefore, increasing the share of renewable electricity generation is also critical for reducing space heating-related GHG emissions.

Chapters 3 and 5 also show that the material-related GHG emissions area is much smaller than the GHG emissions of the operational energy supply. In the 2015-2050 period, the cumulative material-related GHG emissions from renovation and construction can be paid off by cumulatively reduced energy-related GHG emissions. However, the relative share of material-related GHG emissions in annual total GHG emissions increases over time.

The relationships between different decarbonization strategies are very complex and they can have co-benefits and mutual adverse side effects [34,298]. For example, green lifestyles and energy-efficiency renovation can reduce the energy demand, but increasing the share of renewable energy can further reduce both material and energy-related GHG emissions due to less carbon-intensive upstream processes. On the contrary, a large-scale energy-efficiency renovation will consume large amounts of materials, especially carbon-intensive insulation materials (e.g. mineral wool), leading to increased material-related GHG emissions. In addition, increasing the share of wood buildings in annual new construction will require more wood materials, which might entail difficulties in closing the building material loops. While CDW recycling can only supply very limited amounts and kinds of secondary materials and thus contribute very little to GHG emission reduction, it is still an important option for CDW management and primary material substitution.

Overall research question: *What is the potential to reduce energy demand, close material loops, and decarbonize in the residential building sector of the Netherlands?*

The thesis answers this question by developing a series of bottom-up building stock models to track future building stock development and account for the associated material flows, energy demand and supply, and the related GHG emissions. Results show that the energy use of the residential building stock can be significantly reduced, depending on what kinds of measures are deployed. While gas for space heating is assumed to be largely replaced by electricity use for heat pumps, electricity consumption will only slightly increase since well-insulated buildings have a low to zero heating demand per square meter. More intensive use of buildings and lower room temperature settings for space heating can considerably reduce the demand for both space heating and electricity. Wide installation of rooftop PV is a promising option to significantly reduce the dependence on public grid electricity and potentially meet local electricity demand.

Closing material loops in the residential building sector is challenging. Urban mining can only supply limited amounts of specific primary materials needed for renovation or new buildings. The main reason is that many new buildings will have to be built due to the population increase in the Netherlands. The building types and corresponding material inventory can also influence the potential of urban mining to meet future materials demands. For example, increasing the construction of wood buildings will consume more wood-based materials, which CDW recycling cannot adequately provide. In addition, extensive renovation activities will demand more building materials, especially insulation materials that recycling CDW from demolishing old buildings cannot supply. More intensive use of buildings can greatly reduce the material demand for new construction and, thus, to some extent help close the material loops.

In sum, the residential building stock can be almost fully decarbonized by deploying various strategies together. Reducing space heating demand by renovation and building nZEB besides phasing out natural gas boilers are both key strategies for realizing the climate-neutral residential building stock in the Netherlands. Greening the public electricity grid is also very important as it can greatly reduce both embodied and operational GHG emissions. Due to the relatively small share of material-related emissions in annual total GHG emissions, material decarbonization can only make a limited contribution to reducing GHG emissions related to the residential sector. However, the share of material-related GHG emissions will increase along with the decreased share of operational emissions, which will increase the relative importance of decarbonizing building materials. For example, increasing the proportion of wood buildings can considerably reduce GHG emissions.

6.2 Methodological advances

The building stock models in this thesis build upon real data about buildings from a Dutch GIS dataset called “Basisregistratie Addressen en Gebouwen (Base registration of Addresses and Buildings; BAG)” [172]. The GIS data contains the georeferenced information, geometries, construction year, and functions of individual buildings. However, it does not contain information on thermal properties and heating systems. TABULA [68] contains such information on Dutch building archetypes that are differentiated between building types and construction periods. To fill in the data gaps of BAG, the residential buildings in BAG are grouped according to TABULA archetypes and the information of TABULA archetype buildings is then mapped to the buildings in BAG. The material intensities of Dutch archetype buildings are further included to estimate the material composition of these individual buildings. Considering the importance of renovation in residential decarbonization, an engineering-based bottom-up space heating demand model is developed to simulate the space heating demand building by building (Chapter 2). The model is validated against the measured natural gas consumption data to guarantee the model accuracy.

To track the future building stock development and account for the associated material flows, energy demand and generation, and GHG emissions, Chapter 3 develops a bottom-up dynamic building stock model that builds upon the individual parametric buildings and integrates MFA, space heating model, and LCA. Renovation is driven by exogenously defined annual renovation rates. Chapter 4 further develops the model by linking material inflows and outflows with the consideration of recycling practices. Considering that the payback time of renovation investment is long and renovation likely occurs as a result of the natural aging process of building components, different from the dynamic model in Chapter 3, renovation is driven by the building component lifetimes in Chapter 5. Following the neighborhood-oriented approach, heat system choice sets of individual buildings are linked to the heat source availability per neighborhood.

Compared with previous building stock models, the models in this thesis build upon individual buildings with detailed information. They can capture the change in material composition, technical system parameters, energy performance, and GHG emissions of individual buildings under different technical combination scenarios and outside weather conditions. Macro policy strategies can be translated into specific technical measures for individual buildings. In addition, each building contains georeferenced information, making my models able to depict the spatiotemporal material and energy flows along with the construction, renovation, and demolition of individual buildings. It can comprehensively assess the decarbonization effects of combined policy strategies, such as material transition, energy transition, and green lifestyle. However, the models mainly focus on technical aspects. Future research can include socioeconomic aspects by integrating other related analyzing methods, such as Life cycle costing (LCC) [305] and agent-based modeling [125].

6.3 Model applicability and transferability

The models in the present thesis can support policymaking in terms of the circular economy, energy transition, and carbon reduction in the residential building sector. The modeling approach can also be applied to analyze the non-residential building stock and infrastructure stock as long as the required data is available. The GIS data of non-residential buildings are available in the Netherlands, but the archetypes of non-residential buildings with detailed attributes are, as far as I know, unavailable. The main reason is that non-residential buildings are too diverse, depending on their functions, such as office buildings, hospitals, train stations, airports, and plants. Their energy consumption patterns and material composition are too complicated and time-consuming for data collection.

The proposed building stock models can theoretically be applied in other countries if the required data is accessible. The GIS data of individual buildings are available in many countries, such as Switzerland [98], China [306], the United States [307,308], Portugal [31], Luxembourg [309], Belgium [310], Ireland [311], and Austria [312], while the amounts of building attributes (e.g. construction year and function) are different. The building archetypes are available in many countries, especially for the building material inventory. It is worth mentioning that Heeren and Fishman constructed a material intensity database of different countries from published papers [84]. In China, governments of different provinces publish the building construction inventory for the required materials, energy, and construction machinery [20]. As for the energy modeling, TABULA is notable as it contains thermal properties, technical systems, and energy intensities of building archetypes of many EU countries [313]. The model of this thesis has not yet included the module for space cooling energy demand calculation, so this module should be added if the models are applied in the countries where air conditioning systems are widely installed.

6.4 Policy implications

Most existing buildings will still be in use until 2050 and beyond. Measures for saving energy are the most direct ways to reduce annual GHG emissions, mainly through energy-efficiency renovation and conscious energy-saving behaviors of occupants. Buildings are long-lasting products and the renovation or replacement cycles of building components ranges from 15 to 40 years [74,278]. To avoid arriving at a lock-in [292,314] situation where further energy-efficiency renovation and heating systems replacement are too late and uneconomical, measures related to the heat transition (energy-efficiency renovation and phasing out natural gas boilers) should be implemented in each neighborhood before 2030 (Chapter 5). Financial tools (e.g. low-interest loans, grants, and incentives) and innovative business models should be developed to encourage the residents or landlords to renovate their houses (increasing annual renovation rates) because the renovation investment is relatively high in comparison with the saved energy bills [12,315,316]. For example, the buildings in the same neighborhoods are likely to have similar technical characteristics and can be renovated together to reach an economy of scale (neighborhood-oriented approach [207]).

Extensive renovation for building energy efficiency improvement (renovation wave [29]) will consume large amounts of carbon-intensive insulation materials (e.g. mineral and fossil-derived materials [317]) that CDW recycling cannot provide. Therefore, the use of alternative insulation materials with low embodied carbon emissions is recommended to reduce annual embodied GHG emissions [1,318].

Rooftop PV can be a good option to substitute public grid electricity as it can potentially produce enough electricity to meet the electricity demand for appliances and lighting. However, the electricity generated by rooftop PV is intermittent and inherently affected by weather conditions, which implies that peak electricity production (e.g. daytime) is not in line with the peak electricity consumption (e.g.

evening) [319]. Energy storage technologies (e.g. batteries [13] and hydrogen vector energy [320]) could be applied to balance the mismatch between local demand and supply [230,321], but have in themselves implications for the demand for materials and embodied GHG emissions.

Residents are the users of buildings, so their daily activities can drive future material consumption and energy consumption. However, the implementation of a green lifestyle strategy can in reality be challenging because occupant behavior and preferences are affected by many complicated factors, such as affluence levels, house prices, and land use planning, and are not susceptible to rapid and direct change. Increasing the price of energy, particularly increasing the carbon tax on fossil fuels, could probably reduce energy consumption [74]. Poor families might be more sensitive to this policy, and such a policy could also widen the living standard gap between the poor and rich. In addition, the government could also limit the construction of new buildings to slow the growth of floor area per capita, thus reducing the consumption of materials and energy. Moreover, helping people to gain knowledge and awareness of saving energy through education and media, particularly for children, should be a long-term strategy.

The above policy strategies may not in themselves be sufficient to ensure that the residential building stock reaches the climate-neutral target. In that case, other technologies, such as CCS (carbon capture and storage) [88,322] and green hydrogen (e.g. used for space heating) [196], would be required to reach the climate-neutral target in the residential building sector.

6.5 Limitations and future perspectives

The research in this thesis has some limitations, such as:

(1) Representativeness of archetype buildings. Although this research has tried to apply as much data as possible, the current building stock remains a “black box”. The uncertainties come mainly from the systematic drawbacks of the archetype-based derivation and aggregation approach. The building footprints and registered building information (e.g. construction year and function) from BAG/GIS data are relatively accurate to derive building geometries. However, some of the existing buildings have already undergone some renovation while this is not recorded in the BAG database. Future research can focus on neighborhood or city-scale data collection on building characteristics with the help of local governments, which will improve the accuracy of modeled results.

(2) Gaps between actual and estimated reduction. Apart from the uncertainties due to the insufficient understanding of current building stock, the energy performance and occupant use patterns of post-renovated buildings are still unknown. The building energy model in this thesis uses standard values (e.g. the operation time of heating systems [168] and room temperature [323]), which can result in large gaps between the modeled and real energy and GHG emission reduction. Increased thermal comfort demand after energy efficiency renovation (“rebound effect”

[233,324–326]) is thought to be a common phenomenon that requires further attention. Future research can conduct some experimental case studies to collect some empirical data and calculate the reduced energy consumption and GHG emissions, which might provide more plausible support in policymaking.

(3) Insufficient consideration of socioeconomic aspects. The thesis mainly focuses on the technical aspects to reduce material consumption, energy demand, and GHG emissions while the socioeconomic aspects are also critical for successfully implementing the decarbonization strategies. Policymakers have to analyze the climate-neutral transformation pathways of the building stock from the perspectives of different stakeholders to overcome socio-economic barriers and to ensure potential risks are shared, such as fuel poverty and gaps between high and low-income groups. Future research can focus on developing socio-economic tools to guarantee the effective implementation of technical measures.

(4) Extending the scope to other buildings and sectors. The thesis focuses on the residential building stock while non-residential buildings also account for a large share of GHG emissions. CDW recycling is only considered for the residential building sector, while non-residential buildings and infrastructures (e.g. roads and railways) use many similar materials (e.g. concrete and steel) to residential buildings. Renewable electricity is critical for decarbonizing the building stock, but it will trigger large-scale construction of relevant infrastructures for generating renewable electricity. This thesis reveals the great potential of rooftop PV to meet local electricity demand, while its relationship to public grid electricity in terms of stable power supply to buildings remains to be studied.

(5) Future electricity demand. The energy efficiency improvement of appliances and lighting (e.g. increased inventions in LEDs [88]) is not considered in this study, so the future electricity demand and the overall decarbonization potential may be underestimated. Future studies can integrate the future residential electricity consumption estimation in dynamic building stock modeling.

Chapter 7 Appendix

7.1 Supporting information to Chapter 2

7.1.1 Building classification and identification

Table S7.1.1 Dutch building classification and naming system used in this article.

Construction period	Single-family house	Mid-terraced house	End-terraced house	Apartment building	Multi-family house
<=1964	SFH1	Mid_TH1	End_TH1	AB1	MFH1
1965-1974	SFH2	Mid_TH2	End_TH2	AB2	MFH2
1975-1991	SFH3	Mid_TH3	End_TH3	AB3	MFH3
1992-2005	SFH4	Mid_TH4	End_TH4	AB4	MFH4
2006-2014	SFH5	Mid_TH5	End_TH5	AB5	MFH5
>=2015	SFH6	Mid_TH6	End_TH6	AB6	MFH6

Table S7.1.2 Criteria for identifying the building types.

Building type	Number of shared walls	Number of registered addresses	Building footprint area	Gross floor area	Number of Stories
Single-family House	0	<=2	<250	<400	-
Mid-Terraced House	2	<=3	<200	<400	<=4
End-Terraced House	1	<=3	<200	<400	<=4
Apartment Building	0	>3	none	>1000	-
Multi-family House	else				

These criteria in **Table S7.1.2** are based on experience and field visits. The trial-and-error experience in data processing is also taken into account to determine these values. For example, some garages are merged with the main buildings in BAG and this makes the buildings have larger ground floor areas. Therefore, we set larger gross floor areas for the criteria of single-family houses and terraced houses.

Table S7.1.3 Distribution of building types and ages (the number of buildings).

Period	Single-family house	Mid-terraced house	End-terraced house	Apartment building	Multi-family house	Total
<=1964	347	9417	3185	40	3026	16015
1965-1974	18	1156	394	34	150	1752
1975-1991	54	5576	1886	72	528	8116
1992-2005	17	1050	305	65	94	1531
2006-2014	13	854	264	29	86	1246
>=2015	11	209	94	6	50	370
All periods	460	18262	6128	246	3934	29030

Table S7.1.4 Distribution of building types and ages (the conditioned area of buildings).

Period	Single-family house	Mid-terraced house	End-terraced house	Apartment building	Multi-family house	Total
<=1964	65945	1387770	523841	312404	1303743	3593702
1965-1974	3831	163253	61644	303699	211630	744057
1975-1991	12561	839554	310542	266627	351527	1780812
1992-2005	4623	177264	57180	315307	187989	742362
2006-2014	2534	150358	48808	248657	145331	595688
>=2015	1662	21026	11206	71977	17760	123631
All periods	91155	2739225	1013221	1518671	2217980	7580252

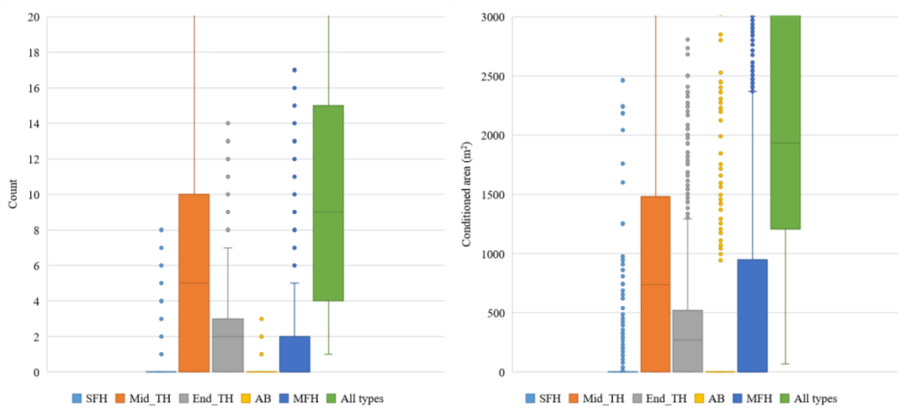

Figure S7.1.1 Distribution of dwellings per postcode. The left is for the number of dwellings per type and the right is the conditioned area of dwellings per postcode.

Not all the buildings that share walls are terraced houses. This is obvious in the city center of Leiden, where buildings are densely distributed and share walls with adjoined buildings. Therefore, in this study, the difference between the apartment building and the multi-family house is assumed that apartment buildings have larger sizes and do not share walls with other buildings. Compared with the single-family house, the multi-family house is smaller, but compared with apartment buildings, it has shared walls. In this way, all the dwellings that do not belong to the former four building types are categorized as the multi-family house.

Based on buildings' postcodes, Google Map is applied to validate the results of building category identification for some sample buildings. We find that it fitted very well in most cases.

7.1.2 Geometries of windows and doors

Table S7.1.5 Geometry information of windows and doors in TABULA.

Building type	window-to-façade ratio	door-to-façade-ratio	TABULA door area (m^2)
SFH1	0.17	-	2.90
Mid_TH1	0.30	-	2.50
End_TH1	0.19	-	2.50
AB1	0.29	0.03	-
MFH1	0.25	0.03	-
SFH2	0.23	-	1.90
Mid_TH2	0.39	-	1.60
End_TH2	0.22	-	1.60
AB2	0.43	0.04	-
MFH2	0.34	0.04	-
SFH3	0.21	-	1.90
Mid_TH3	0.32	-	1.80
End_TH3	0.18	-	1.80
AB3	0.22	0.04	-
MFH3	0.25	0.04	-
SFH4	0.21	-	4.00
Mid_TH4	0.30	-	2.30
End_TH4	0.18	-	2.30
AB4	0.32	0.04	-
MFH4	0.27	0.04	-
SFH5	0.18	-	2.40
Mid_TH5	0.39	-	2.40
End_TH5	0.21	-	2.40
AB5	0.36	0.05	-
MFH5	0.50	0.03	-
SFH6	0.18	-	2.40
Mid_TH6	0.39	-	2.40

End_TH6	0.21	-	2.40
AB6	0.35	0.05	-
MFH6	0.50	0.03	-

7.1.3 Relative deviations

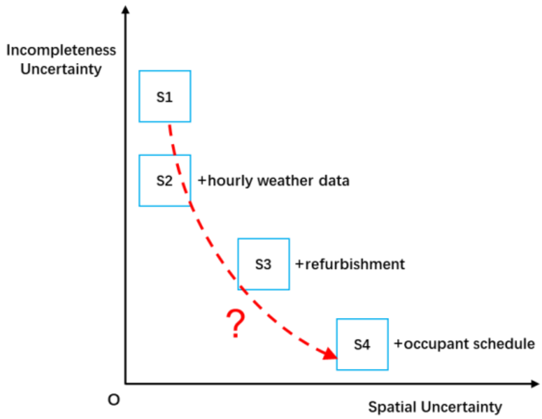

Figure S7.1.2 The evolution of models and the corresponding included factors.

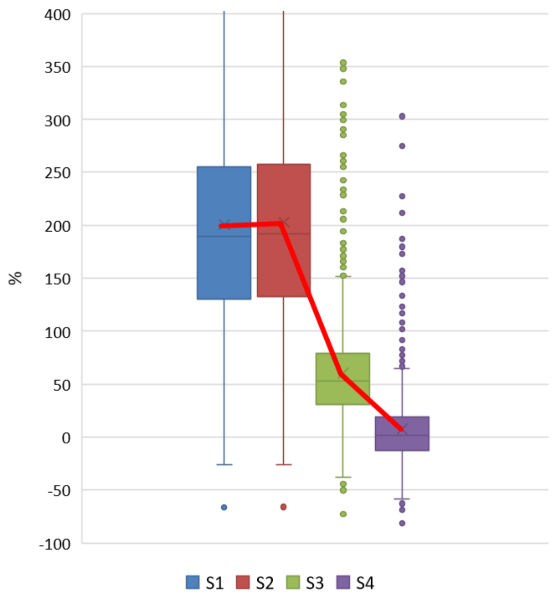

Figure S7.1.3 Relative deviations at postcode level and building stock level. The box plots show the relative deviations at the postcode level while the red line shows the relative deviations at the building stock level for Leiden.

7.1.4 Calculation method

7.1.4.1 Space heating

S1 uses the seasonal calculation method, the calculation step of which is a fixed heating season, and S2-4 use the hourly calculation method, the calculation step of which is one hour. The building energy demand for space heating (Q_{nd}) at the building level is calculated by subtracting the heat gains from heat transfer loss. Heat transfer loss is due to thermal transmission through the building envelope (Q_{tr}) and the heat flow by ventilation (Q_{ve}). The heat gains consist of the internal heat gains (Q_{int}, e.g. occupant metabolism, appliance, and lighting) and the solar radiation entering through windows (Q_{sol}). The calculation method is as follows:

$$Q_{nd} = \sum_{t=1}^{m}(Q_{tr,t} + Q_{ve,t}) - \eta_{gn}(Q_{int,t} + Q_{sol,t}) \qquad (1)$$

where nd denotes need; t denotes the time step (heating season for S1 and hour for S2-4); m denotes the total number of time steps (1 for S1, 5088 for S2-3 and 2968 for S4). η_{gn} is the dimensionless gain utilization factor for the heat gains (see section **7.1.4.3**).

The heat transfer loss by transmission through the envelope is determined as follows:

$$Q_{tr,t} = \begin{cases} \sum_{i=1}^{n} b_i A_i U_i (T_{int,t} - T_{ext,t}) & if\ T_{int,t} > T_{ext,t} \\ 0 & if\ T_{int,t} \le T_{ext,t} \end{cases} \qquad (2)$$

where A_i is the area of element i of the building envelope (roof, window, door, wall and ground floor); U_i is the thermal transmittance (U-value) of element i. T_{int} is the room temperature and T_{ext} is the temperature of the external environment. b_i is the adjustment factor, and in this study, its value for the ground floor is 0.5 while its value for other envelope elements is 1.

The heat transfer loss by ventilation is determined as follows:

$$Q_{ve,t} = \begin{cases} \rho_a c_a A_{con} * 2.5m * (n_{ve,use} + n_{ve,infiltration}) \times (T_{int,t} - T_{ext,t}) & if\ T_{int,t} > T_{ext,t} \\ 0 & if\ T_{int,t} \le T_{ext,t} \end{cases} \qquad (3)$$

where $\rho_a c_a$ is the heat capacity of air per volume and its value is 1200 $\mathrm{J/(m^3 \cdot K)}$. $2.5m$ is the ventilation reference room height from TABULA. $n_{ve,use}$ is the air change rate by use and $n_{ve,infiltration}$ is the airflow rate by infiltration.

The internal heat gains are determined as follows:

$$Q_{int,t} = t q_{int} A_{con} \qquad (4)$$

where q_{int} is the average thermal output of internal heat sources.

In this study, only the solar gain from windows is considered. As the orientation of each building is unknown, we attribute all heat gains from the solar radiation to the east and west. The solar heat gains are determined as follows:

$$Q_{sol,t} = I_{sol}(F_{east} + F_{west}) A_{window} F_{sh} (1 - F_F) F_W g_{gl} \qquad (5)$$

where I_{sol} is the global solar radiation falling onto a horizontal surface. $F_{east}(0.69)$

and F_{west} (0.68) are the factors converting the horizontal solar radiation to the windows in the east and west orientation of buildings and they are calculated based on seasonal values from TABULA. F_{sh} is the shading reduction factor for movable shading provisions and its value is 0.6. F_F is the frame fraction of the windows and its value is 0.3. F_W is the correction factor for non-scattering glazing and its value is 0.9. g_{gl} is the total solar energy transmittance.

The annual building energy need for space heating of the four models is converted to energy consumption for space heating by considering the heating system efficiency following the TABULA calculation method.[176] The annual energy consumption for space heating (q_h) is formulated in eq 6:

$$q_h = [Q_{nd}/A_{con} + q_{d.h} + q_{s,h} - \eta_{h,gn}(q_{w,h} + \eta_{ve,rec}Q_{ve})]e_{g,h}A_{con} \quad (6)$$

herein, h denotes space heating, and g denotes heat generator. $q_{d,h}$ is the effective heat loss of the space heating distribution system and $q_{s,h}$ is the effective heat loss of the space heating system storage. $q_{w,h}$ is the recoverable heat loss of the DHW system. $\eta_{ve,rec}$ is the efficiency of ventilation heat recovery. $e_{g,h}$ is the heat generation expenditure factor of the heat generator. Q_{ve} is the annual heat transfer by ventilation calculated based on the seasonal method. $\eta_{h,gn}$ is the dimensionless gain utilization factor (see section **7.1.4.3**) of ventilation heat recovery and recoverable heat loss of the DHW system.

7.1.4.2 Domestic hot water

The energy consumption for DHW (q_w) is calculated as follows:

$$q_w = (q_{nd,w} + q_{d,w} + q_{s,w})e_{g,w}A_{con} \quad (7)$$

where w denotes water. $q_{nd,w}$ is the annual energy need per conditioned floor area for DHW, $q_{d,w}$ is the heat loss of the DHW distribution system and $q_{s,w}$ is the heat loss of the DHW storage. $e_{g,w}$ is the heat generation expenditure factor of the DHW heat generator.

7.1.4.3 Gain utilization factor

In this study, the gain utilization factor (η) is used for calculating both the energy need and delivered energy for space heating. η is the function of the heat-balance ratio (γ_H). γ_H is determined as follows:

$$\gamma_H = \frac{(Q_{int,t}+Q_{sol,t})}{(Q_{tr,t}+Q_{ve,t})} \quad (8)$$

where for S1 and the calculation of delivered energy, the time step t is one season; for S2-4 the time step t is one hour.

η is calculated as follows:

$$\eta = \begin{cases} \frac{1-\gamma_H^{a_H}}{1-\gamma_H^{a_H+1}} & if\ \gamma_H > 0\ and\ \gamma_H \neq 1 \\ \frac{a_H}{a_H+1} & if\ \gamma_H = 1 \\ \frac{1}{\gamma_H} & if\ \gamma_H < 0 \end{cases} \quad (9)$$

where a_H is a dimensionless numerical parameter depending on the time constant and it is determined as follows:

$$a_H = a_{H,0} + \frac{\tau}{\tau_{H,0}} \quad (10)$$

where $a_{H,0}$ is a dimensionless reference numerical parameter and $\tau_{H,0}$ a reference time constant. Their values (from EN ISO 13790) are shown as follows:

Table S7.1.6 Values of $a_{H,0}$ and $\tau_{H,0}$.

Calculation method	$a_{H,0}$	$\tau_{H,0}$
Seasonal method of energy demand for space heating (S1)	0.8	30
Hourly method of energy demand for space heating (S2-4)	1	15
Calculation of delivered energy	0.8	30

τ is the time constant of the building and it is calculated as follows:

$$\tau = \frac{C_m A_C}{H_{tr}+H_{ve}} \quad (11)$$

where C_m is the internal heat capacity per conditioned floor area and in this study its value is 45 $\mathrm{Wh/(m^2K)}$. H_{tr} is the heat transfer coefficient by transmission and calculated as follows:

$$H_{tr} = \sum_{i=1}^{n} b_i A_i U_i \quad (12)$$

H_{ve} is the heat transfer coefficient by ventilation and calculated as follows:

$$H_{ve} = \rho_a c_a \left(q_{ve,use} + q_{ve,infiltration}\right) \quad (13)$$

7.2 Supporting information to Chapter 3

7.2.1 Building stock characterization

Figure S7.2.1 shows the process of characterizing the existing building stock. The characterization and initialization are based on the method by Yang et al. [27]. The main data sources used are:

(1) The BAG [172] dataset (GIS data) mainly contains building footprints, construction years, functions, and registered addresses, which is used to derive buildings' geometries (e.g. conditioned floor area and envelope element areas) and building types (single-family house, end-terraced house, mid-terraced house, apartment building, and multi-family house). According to BAG, the total number of residential buildings is 5,092,999 in 2015.

(2) TABULA [68] (Typology Approach for Building Stock Energy Assessment) mainly includes the archetypes of the Dutch residential buildings (differentiated by construction periods and building types), and their envelope geometries, thermal properties of different insulation standards, ventilation and heating systems. These parameters are mapped to BAG buildings according to the types and construction periods of BAG buildings.

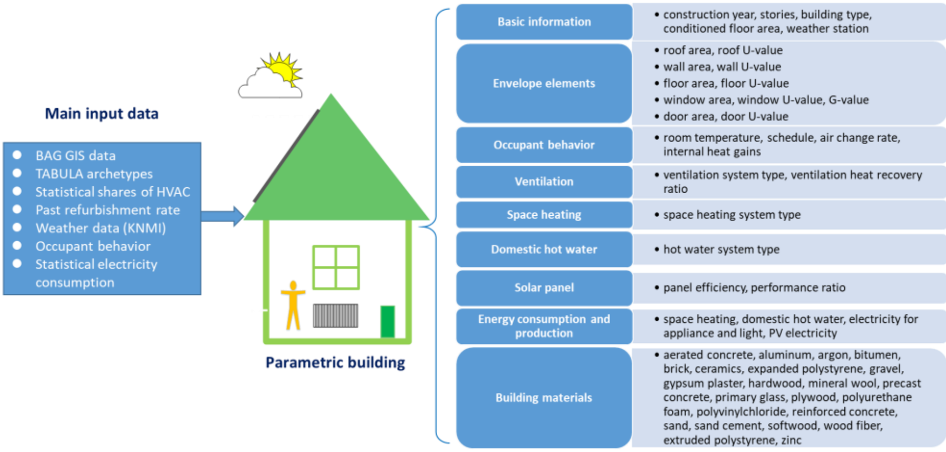

Figure S7.2.1 Building stock characterization and initialization.

(3) KNMI [173] (Royal Dutch Meteorological Institute) holds the weather records (this study uses the averaged data of 2001-2019) of different stations, which can be used to describe the outdoor environment of buildings. It also includes the longitude and latitude of each weather station, which enables the spatialization of weather records (see **Figure S7.2.4**). Individual buildings are linked to the nearest weather stations by the "Spatial Join" tool of ArcGIS 10.6. For new buildings, the weather data are mapped to new buildings by postcode to estimate the potential PV electricity generation. The postcodes of new buildings are randomly sampled from the postcodes of buildings demolished in the same year.

(4) Occupants are assumed to set the room temperature as 20 °C and heat the rooms from 7:00 pm to 7:00 am (+1 day, 12 h) [27,180].

(5) The statistical past envelope renovation rates for envelope elements (roof, external wall, window, and ground floor) [174], and the distributions of ventilation and heating systems [174] are applied to initialize the current building stock.

(6) The material intensities of different building types (see 7.2.4) are from a Dutch study [205].

(7) CBS[182] (Central Bureau of Statistics) contains the statistical electricity consumption reported at the postcode level, which is used to derive the residential electricity consumption intensities (kWh/m^2).

The past renovation rates [27] of envelope elements are applied to initialize the current physical properties. The data in **Table S7.2.2** is adapted from diffusion rates in literature [174] to initialize the space heating and hot water systems. The heat supply type "other" is used to represent the space heating and hot water systems of which we lack the details on types and shares. The diffusion rates of ventilation systems are shown in **Table S7.2.3**. The Dutch rooftop PV installation rate [70] is 4.4% in 2017 and it is used as the rate of 2015.

Table S7.2.1 Building classification and naming system.

Construction period	Single-family house	Mid-terraced house	End-terraced house	Apartment building	Multi-family house
<=1964	SFH1	Mid_TH1	End_TH1	AB1	MFH1
1965-1974	SFH2	Mid_TH2	End_TH2	AB2	MFH2
1975-1991	SFH3	Mid_TH3	End_TH3	AB3	MFH3
1992-2005	SFH4	Mid_TH4	End_TH4	AB4	MFH4
2006-2014	SFH5	Mid_TH5	End_TH5	AB5	MFH5
>=2015 (CNEW)	SFH6	Mid_TH6	End_TH6	AB6	MFH6
>=2015 (nZEB)	SFH7	Mid_TH7	End_TH7	AB7	MFH7

Table S7.2.2 The distribution of space heating systems and domestic hot water systems.

Space heating type	Domestic hot water	Proportion
Natural gas boiler	common boiler for heating and DHW	86%
Heat networks	other	7%
Other		7%

Table S7.2.3 The distribution of ventilation systems.

Ventilation type	Percentage
Natural ventilation	67%
Exhaust air ventilation	30%
Balanced ventilation	3%

In this study, the conditioned floor area [176] is used to quantify the floor area stock and flows. To validate the derived floor area based on BAG data against the statistical useful floor area, the conversion factors [327] in **Table S7.2.4** are applied. The statistical (CBS) useful floor area of the Netherlands is on average 65 m^2 per capita [232]. The derived useful floor area after conversion in this study is 69 m^2 per capita (population 16901000 in 2015). The useful floor area per capita is a bit larger than the statistical value, but they are very similar. Part of the reason for overestimation is that some building footprints include the garage or utility rooms. The distribution of construction year and building type is shown in **Figure S7.2.2** and **Figure S7.2.3**.

Table S7.2.4 Floor area conversion.

Building type	Conditioned floor area (m^2)	Conversion factor	Useful floor area (m^2)
SFH	164106085.98	0.75	123079564.49
Mid_TH	320859889.16	0.79	253479312.44
End_TH	281788682.41	0.79	222613059.10
AB	211019372.95	0.90	189917435.66
MFH	428275389.30	0.90	385447850.37
Total	1406049419.80	-	1174537222.05
Floor area per capita	83.19	-	69.49

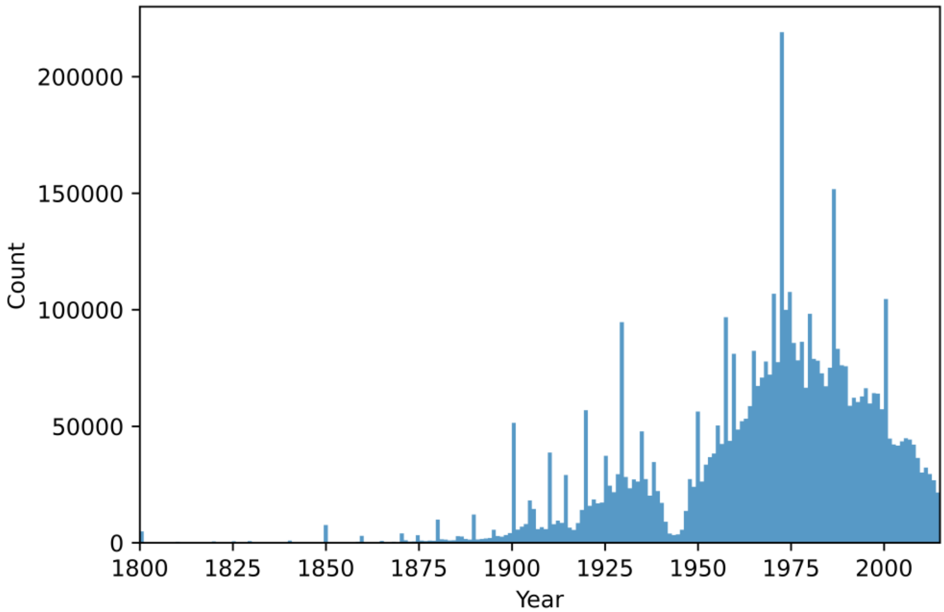

Figure S7.2.2 The distribution of construction year of Dutch residential buildings. Only the buildings built between 1800 and 2015 are shown.

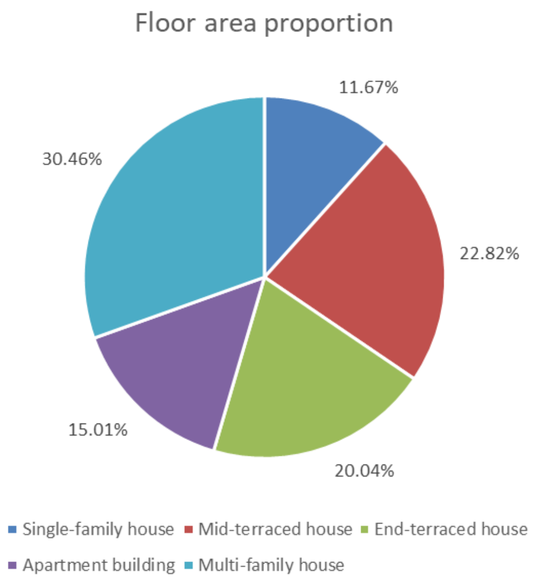

Figure S7.2.3 The proportion of building types by conditioned floor area. It is derived from BAG (GIS data of buildings) based on the method by Yang et al. [27].

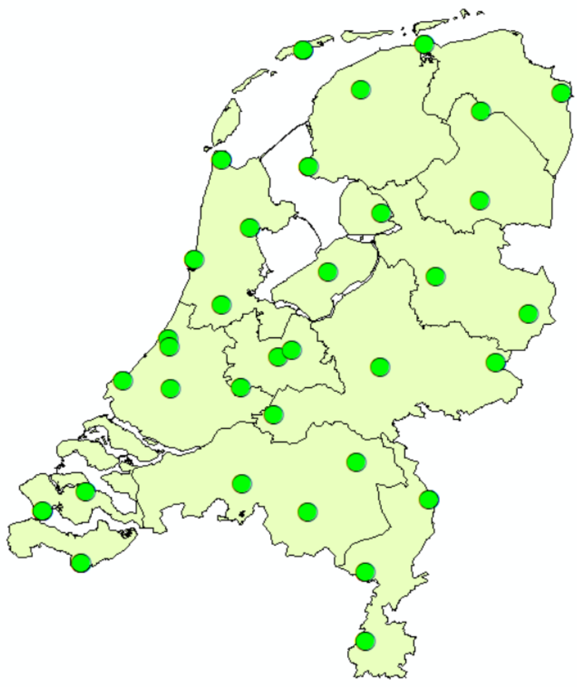

Figure S7.2.4 The map of weather stations. The green points are the weather stations included in this study.

7.2.2 Dutch population

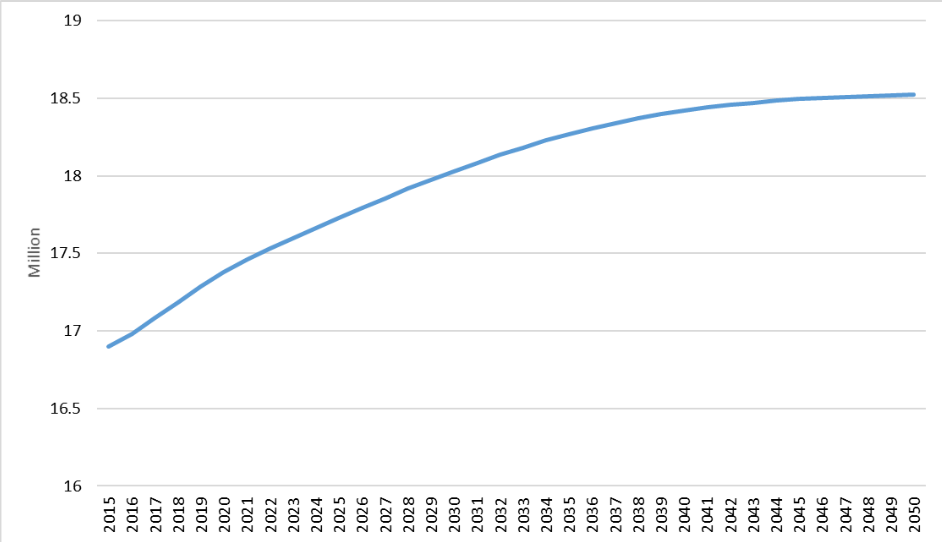

Figure S7.2.5 Population trend of the Netherlands [221].

7.2.3 Electricity intensities

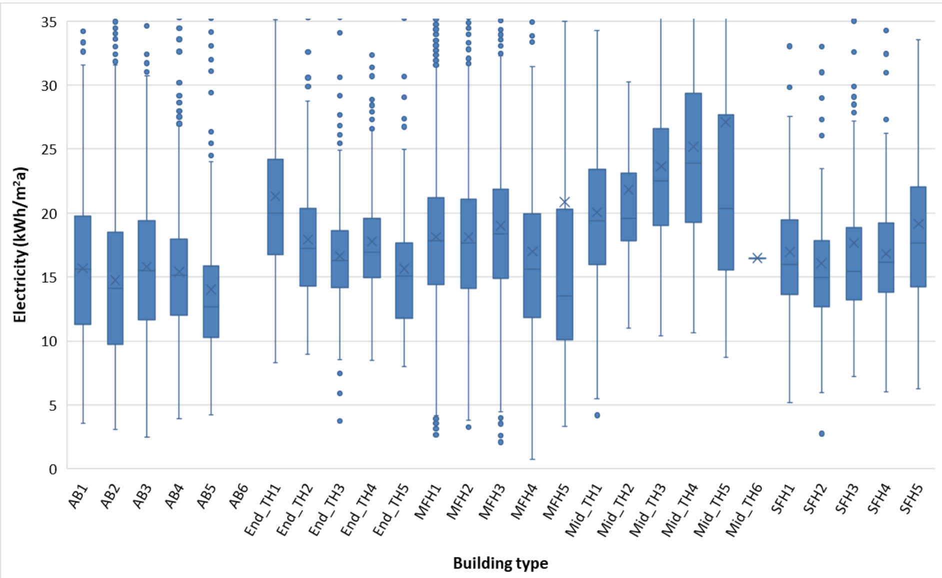

Figure S7.2.6 Distribution of electricity intensity (annual electricity consumption per conditioned floor area), derived based on the method of Yang et al. [27].

7.2.4 Building materials

Table S7.2.5 Building material densities [211].

Label	Material type	Density (kg/m^3)
AC	main material	750
Al	main material	2700
Ar	insulation material	1.66
Bi	main material	2400
Br	main material	1700
Ce	main material	2000
EPS	insulation material	27.5
Gr	main material	2240
GY	main material	1120
HW	main material	750
MW	insulation material	140
PC	main material	2200
PG	insulation material	2500
Pl	main material	540
PUR	insulation material	45
PVC	main material	1380
RC	main material	2300
Sa	main material	2240
SC	main material	2200
SW	main material	560
WF	main material	750
XPS	insulation material	37.5
Zn	main material	7000

Table S7.2.6 The matching relationship between building types of this study and literature building types [211].

Building types of this study	Literature building type
SFH1	standard single-family house
Mid_TH1	standard mid-terraced house
End_TH1	standard mid-terraced house
AB1	standard apartment
MFH1	standard apartment
SFH2	standard single-family house
Mid_TH2	standard mid-terraced house
End_TH2	standard mid-terraced house
AB2	standard apartment

MFH2	standard apartment
SFH3	standard single-family house
Mid_TH3	standard mid-terraced house
End_TH3	standard mid-terraced house
AB3	standard apartment
MFH3	standard apartment
SFH4	standard single-family house
Mid_TH4	standard mid-terraced house
End_TH4	standard mid-terraced house
AB4	standard apartment
MFH4	standard apartment
SFH5	standard single-family house
Mid_TH5	standard mid-terraced house
End_TH5	standard mid-terraced house
AB5	standard apartment
MFH5	standard apartment
SFH6	new single-family house
Mid_TH6	new mid-terraced house
End_TH6	new mid-terraced house
AB6	new apartment
MFH6	new apartment
SFH7	advanced new single-family house
Mid_TH7	advanced new mid-terraced house
End_TH7	advanced new mid-terraced house
AB7	advanced new apartment
MFH7	advanced new apartment

Table S7.2.7 Material intensities for existing residential buildings (kg/m^2) [211].

Building type	SFH1-5	Mid_TH1-5	End_TH1-5	AB1-5	MFH1-5
AC	0.00	0.00	0.00	0.00	0.00
Al	0.00	0.00	0.00	0.00	0.00
Ar	0.00	0.00	0.00	0.00	0.00
Bi	2.50	2.50	2.50	4.79	4.79
Br	96.42	48.91	48.91	55.65	55.65
Ce	5.63	5.66	5.66	4.69	4.69
EPS	0.00	0.00	0.00	0.00	0.00
Gr	6.30	6.34	6.34	12.62	12.62
GY	45.27	45.24	45.24	43.89	43.89
HW	0.00	0.00	0.00	0.00	0.00
MW	0.00	0.00	0.00	0.00	0.00

PC	844.82	725.37	725.37	550.89	550.89
PG	5.34	1.86	1.86	1.76	1.76
Pl	13.75	13.97	13.97	5.26	5.26
PUR	0.00	0.00	0.00	0.00	0.00
PVC	0.04	0.04	0.04	0.02	0.02
RC	255.76	533.10	533.10	330.88	330.88
Sa	571.90	571.95	571.95	571.68	571.68
SC	135.55	135.60	135.60	106.36	106.36
SW	53.00	52.30	52.30	1.12	1.12
WF	0.00	0.00	0.00	0.00	0.00
XPS	0.00	0.00	0.00	0.00	0.00
Zn	1.09	14.09	14.09	0.00	0.00

Table S7.2.8 Material intensities for new buildings [211].

Material labels	SFH 6	Mid_T H6	End_T H6	AB6	MF H6	SFH 7	Mid_T H7	End_T H7	AB7	MF H7
AC	30.3	30.32	30.32	24.5	24.5	30.3	30.32	30.32	24.5	24.5
Al	3.58	5.15	5.15	6.61	6.61	2.15	2.92	2.92	3.44	3.44
Ar	0.00	0.00	0.00	0.00	0.00	0.01	0.00	0.00	0.00	0.00
Bi	2.44	2.44	2.44	4.70	4.70	2.44	2.44	2.44	4.70	4.70
Br	96.4	48.94	48.94	55.4	55.4	18.3	9.29	9.29	10.4	10.4
Ce	5.66	5.59	5.59	4.70	4.70	5.66	5.59	5.59	4.70	4.70
EPS	1.12	1.12	1.12	0.12	0.12	0.62	0.62	0.62	0.16	0.16
Gr	6.34	6.41	6.41	12.5	12.5	6.34	6.41	6.41	12.5	12.5
GY	0.00	0.00	0.00	0.00	0.00	0.00	0.00	0.00	0.00	0.00
HW	8.50	7.87	7.87	7.86	7.86	8.50	7.87	7.87	7.86	7.86
MW	28.4	25.13	25.13	6.39	6.39	31.3	15.92	15.92	18.0	18.0
PC	810.	702.19	702.19	750.	750.	685.	638.85	638.85	678.	678.
PG	5.86	2.07	2.07	1.96	1.96	5.86	2.07	2.07	1.96	1.96
Pl	14.6	14.96	14.96	6.13	6.13	14.6	11.84	11.84	6.13	6.13
PUR	0.00	0.00	0.00	1.35	1.35	5.70	6.42	6.42	1.43	1.43
PVC	0.04	0.04	0.04	0.01	0.01	0.04	0.04	0.04	0.01	0.01
RC	255.	532.97	532.97	284.	284.	255.	532.97	532.97	284.	284.
Sa	571.	571.74	571.74	571.	571.	571.	587.11	587.11	571.	571.
SC	135.	135.49	135.49	105.	105.	135.	135.49	135.49	105.	105.
SW	51.4	51.39	51.39	0.00	0.00	51.4	51.39	51.39	0.00	0.00
WF	0.00	0.00	0.00	0.00	0.00	8.50	4.34	4.34	4.92	4.92
XPS	0.00	0.00	0.00	0.00	0.00	2.30	2.30	2.30	0.25	0.25
Zn	1.24	14.24	14.24	0.69	0.69	1.24	14.24	14.24	0.69	0.69

Table S7.2.9 Insulation materials. HR++ glass contains 2 plates (2×0.5cm thick) and 2 cm argon [211]. HR+++ glass is assumed to contain 3 plates (3×0.5cm thick) and 2cm argon [209,211]. The typical U-values of glasses are from TABULA and Milieu Centraal [68,209].

Insulation standards	Element	Material	Thermal conductivity (k, W/mK)	U-value	G-value [210,3	Density (kg/m³)
conventional	roof	mineral	0.037	-	-	140
	window	HR++	-	1.8	0.7	-
	wall	mineral	0.037	-	-	140
	door	-	-	-	-	-
	Ground	PUR	0.025	-	-	45
advanced	roof	PUR	0.025	-	-	45
	window	HR+++	-	1.0	0.6	-
	wall	mineral	0.037	-	-	140
	door	PUR	0.025	-	-	45
	Ground	mineral	0.037	-	-	140

7.2.5 Environmental impact factors of materials and energies

Table S7.2.10 GHG emissions factors (SSP2 [216]) of building materials from ecoinvent 3.6 (kg CO_2 eq/kg).

Materials	Product	Activity	Location	2015-2020	2021-2025	2026-2030	2031-2035	2036-2040	2041-2045	2046-2050
AC	Autoclaved aerated concrete block	market for autoclaved aerated concrete block	CH	0.43	0.43	0.42	0.41	0.41	0.40	0.40
Al	Aluminium, wrought alloy	market for aluminium, wrought alloy	GLO	11.07	10.99	10.93	10.87	10.77	10.72	10.71
Ar	Argon, liquid	market for argon, liquid	RER	2.18	1.99	1.77	1.62	1.44	1.32	1.24
Bi	Bitumen seal	market for bitumen seal	GLO	1.11	1.10	1.10	1.09	1.09	1.09	1.09
Br	Clay brick	market for clay brick	GLO	0.30	0.30	0.30	0.30	0.30	0.30	0.30

Ce	Ceramic tile	market for ceramic tile	GLO	0.73	0.71	0.70	0.69	0.69	0.69	0.69
EPS	Polystyrene foam slab, 10% recycled	polystyrene foam slab production, 10% recycled	CH	3.94	3.90	3.86	3.83	3.79	3.77	3.76
Gr	Gravel, crushed	market for gravel, crushed	CH	0.01	0.01	0.01	0.01	0.01	0.01	0.01
GY	Gypsum plasterboard	market for gypsum plasterboard	GLO	0.34	0.34	0.33	0.33	0.33	0.32	0.33
HW	Sawnwood, beam, hardwood, dried (u=10%), planed	market for sawnwood, beam, hardwood, dried (u=10%), planed	GLO	-2.14	-2.14	-2.15	-2.15	-2.15	-2.15	-2.15
MW	Glass wool mat	market for glass wool mat	GLO	2.27	2.18	2.11	2.06	2.03	2.03	2.04
PC	Concrete, sole plate and foundation	market for concrete, sole plate and foundation	CH	0.15	0.14	0.14	0.14	0.14	0.14	0.14
PG	Glazing, double, U<1.1 W/m2K	market for glazing, double, U<1.1 W/m2K	GLO	1.41	1.40	1.38	1.38	1.37	1.37	1.37
Pl	Plywood, for indoor use	market for plywood, for indoor use	RER	-3.12	-3.15	-3.19	-3.22	-3.24	-3.26	-3.27
PUR	Polyurethane, flexible foam	market for polyurethane, flexible foam	RER	5.45	5.44	5.43	5.42	5.41	5.41	5.40

PVC	Polyvinylchloride, suspension polymerised	market for polyvinylchloride, suspension polymerised	GLO	2.25	2.20	2.16	2.13	2.11	2.11	2.12
RC	Fibre-reinforced concrete	market for fibre-reinforced concrete, steel	BR	0.18	0.18	0.18	0.18	0.18	0.18	0.18
Sa	Sand	market for sand	CH	0.01	0.01	0.01	0.01	0.01	0.01	0.01
SC	Cement mortar	market for cement mortar	CH	0.24	0.24	0.23	0.23	0.23	0.22	0.22
SW	Shavings, softwood, loose, measured as dry mass	planing, board, softwood, u=10%	CH	-0.87	-0.88	-0.88	-0.88	-0.89	-0.89	-0.89
WF	Fibreboard, soft, latex bonded	market for fibreboard, soft, latex bonded	GLO	0.31	0.30	0.30	0.29	0.29	0.29	0.29
XPS	Polystyrene, extruded	market for polystyrene, extruded	GLO	9.49	9.45	9.41	9.39	9.37	9.37	9.37
Zn	Zinc	market for zinc	GLO	3.19	3.08	2.93	2.85	2.76	2.73	2.72

Table S7.2.11 GHG emissions factors (SSP2 450 [216]) of building materials from ecoinvent 3.6 (kg CO_2 eq/kg).

Materials	Product	Activity	Location	2015-2020	2021-2025	2026-2030	2031-2035	2036-2040	2041-2045	2046-2050
AC	Autoclaved aerated	market for autoclaved aerated	CH	0.43	0.42	0.41	0.38	0.36	0.36	0.36

	concrete block	concrete block								
Al	Aluminium, wrought alloy	market for aluminium, wrought alloy	GLO	11.04	10.91	10.81	10.65	10.45	10.33	10.25
Ar	Argon, liquid	market for argon, liquid	RER	2.05	1.76	1.37	0.71	0.23	0.05	0.03
Bi	Bitumen seal	market for bitumen seal	GLO	1.10	1.08	1.07	1.04	1.01	1.00	1.00
Br	Clay brick	market for clay brick	GLO	0.30	0.30	0.29	0.28	0.27	0.27	0.27
Ce	Ceramic tile	market for ceramic tile	GLO	0.70	0.67	0.63	0.57	0.51	0.49	0.48
EPS	Polystyrene foam slab, 10% recycled	polystyrene foam slab production, 10% recycled	CH	3.92	3.87	3.79	3.66	3.56	3.53	3.52
Gr	Gravel, crushed	market for gravel, crushed	CH	0.01	0.01	0.01	0.01	0.01	0.01	0.01
GY	Gypsum plasterboard	market for gypsum plasterboard	GLO	0.33	0.32	0.30	0.28	0.25	0.25	0.24
HW	Sawnwood, beam, hardwood, dried (u=10%), planed	market for sawnwood, beam, hardwood, dried (u=10%), planed	GLO	-2.14	-2.15	-2.16	-2.18	-2.19	-2.20	-2.20
MW	Glass wool mat	market for glass wool mat	GLO	2.15	1.92	1.70	1.36	1.03	0.91	0.85
PC	Concrete, sole plate and	market for concrete, sole plate	CH	0.15	0.14	0.14	0.13	0.13	0.13	0.13

	foundation	and foundation								
PG	Glazing, double, U<1.1 W/m2K	market for glazing, double, U<1.1 W/m2K	GLO	1.40	1.36	1.33	1.28	1.23	1.21	1.21
Pl	Plywood, for indoor use	market for plywood, for indoor use	RER	-3.14	-3.20	-3.26	-3.38	-3.46	-3.49	-3.50
PUR	Polyurethane, flexible foam	market for polyurethane, flexible foam	RER	5.44	5.42	5.40	5.37	5.34	5.33	5.33
PVC	Polyvinylchloride, suspension polymerised	market for polyvinylchloride, suspension polymerised	GLO	2.19	2.06	1.94	1.75	1.56	1.49	1.46
RC	Fibre-reinforced concrete	market for fibre-reinforced concrete, steel	BR	0.18	0.17	0.17	0.17	0.17	0.17	0.17
Sa	Sand	market for sand	CH	0.01	0.01	0.01	0.01	0.00	0.00	0.00
SC	Cement mortar	market for cement mortar	CH	0.24	0.23	0.23	0.21	0.20	0.20	0.20
SW	Shavings, softwood, loose, measured as dry mass	planing, board, softwood, u=10%	CH	-0.88	-0.88	-0.89	-0.90	-0.90	-0.91	-0.91
WF	Fibreboard, soft, latex bonded	market for fibreboard, soft, latex bonded	GLO	0.30	0.28	0.26	0.24	0.21	0.20	0.19

XPS	Polystyrene, extruded	market for polystyrene, extruded	GLO	9.44	9.33	9.23	9.06	8.90	8.84	8.82
Zn	Zinc	market for zinc	GLO	3.01	2.74	2.37	1.75	1.25	1.09	1.04

Table S7.2.12 GHG emissions factors (SSP2 [216]) of energy supply from ecoinvent 3.6 (kg CO_2 eq/kWh). The GHG emission factors of heat networks and hybrid heat pumps are weighted average factors of sub-energy sources [156]. Green gas is produced by drying and purifying biogas to the same quality as natural gas [329,330]. In the Netherlands, biogas will be mainly produced from animal manure (e.g. cattle and chicken) and the treatment of biowaste (e.g. fruit and vegetables) [331]. And their shares are similar (assumed as 50% for each) [331].

Energy supply	Product	Activity	Location	2015-2020	2021-2025	2026-2030	2031-2035	2036-2040	2041-2045	2046-2050
Natural gas boiler	Heat, central or small-scale, natural gas	Heat production, natural gas, at boiler condensing modulating <100kW	Europe without Switzerland	0.25	0.25	0.25	0.25	0.25	0.25	0.25
Heat network	Heat	70%: geothermal (GHG emission factor is from Verhagen et al.[74])	NL	0.09	0.09	0.09	0.09	0.09	0.09	0.09
		15%: heat and power co-generation, biogas, gas engine (biogas inputs adapted with shares of production methods of the Netherlands)	NL	0.23	0.23	0.23	0.23	0.23	0.23	0.23
		10%: heat and power co-generation, wood chips, 6667 kW,	NL	0.01	0.01	0.01	0.01	0.01	0.01	0.01

		state-of-the-art 2014								
		5%: heat, from municipal waste incineration to generic market for heat district or industrial, other than natural gas	NL	0	0	0	0	0	0	0
		Weighted average factors	-	0.10	0.10	0.10	0.10	0.10	0.10	0.10
Electric heat pump	Heat, air-water heat pump 10kW	Market for floor heating from air-water heat pump	Europe without Switzerland	0.26	0.24	0.22	0.20	0.18	0.17	0.16
Hybrid heat pump (heat pump +biogas boiler)	Heat	65%[214]: market for floor heating from air-water heat pump	Europe without Switzerland	0.26	0.24	0.22	0.20	0.18	0.17	0.16
		35%[214]: heat production from green gas boiler (adapted from natural gas boiler by replacing natural gas with green gas; 1 m³ of biogas equals to 0.63 m³ of natural gas[331])	NL	0.37	0.37	0.37	0.37	0.36	0.36	0.36
		Weighted average factors	-	0.30	0.29	0.27	0.26	0.25	0.24	0.23
Solar water heater	Heat, central or small-scale, other than natural gas	Operation, solar collector system, Cu flat plate collector, multiple dwelling, for hot water	CH	0.01	0.01	0.01	0.01	0.01	0.01	0.01

Grid electricity	Electricity, low voltage	Market for electricity, low voltage	NL	0.66	0.59	0.52	0.47	0.42	0.38	0.37
PV electricity	Electricity, low voltage	Electricity production, photovoltaic, 3kWp slanted-roof installation, multi-Si, panel, mounted	NL	0.08	0.08	0.08	0.07	0.07	0.07	0.07

Table S7.2.13 GHG emissions factors (SSP2 450 [216]) of energy supply from ecoinvent 3.6 (kg CO_2 eq/kWh). The GHG emission factors of heat networks and hybrid heat pumps are weighted average factors of sub-energy sources [156]. Green gas is produced by drying and purifying biogas to the same quality as natural gas [329,330]. In the Netherlands, biogas will be mainly produced from animal manure (e.g. cattle and chicken) and the treatment of biowaste (e.g. fruit and vegetables) [331]. And their shares are similar (assumed as 50% for each) [331].

Energy supply	Product	Activity	Location	2015-2020	2021-2025	2026-2030	2031-2035	2036-2040	2041-2045	2046-2050
Natural gas boiler	Heat, central or small-scale, natural gas	Heat production, natural gas, at boiler condensing modulating <100kW	Europe without Switzerland	0.25	0.25	0.25	0.25	0.25	0.25	0.25
Heat network	Heat	70%: geothermal (GHG emission factor is from Verhagen et al.[74])	NL	0.09	0.09	0.09	0.09	0.09	0.09	0.09
		15%: heat and power co-generation, biogas, gas engine (biogas inputs adapted with shares of production methods of the Netherlands)	NL	0.23	0.23	0.23	0.23	0.22	0.22	0.22

		10%: heat and power co-generation, wood chips, 6667 kW, state-of-the-art 2014	NL	0.01	0.01	0.01	0.01	0.01	0.01	0.01
		5%: heat, from municipal waste incineration to generic market for heat district or industrial, other than natural gas	NL	0	0	0	0	0	0	0
		Weighted average factors	-	0.10	0.10	0.10	0.10	0.10	0.10	0.10
Electric heat pump	Heat, air-water heat pump 10kW	Market for floor heating from air-water heat pump	Europe without Switzerland	0.25	0.22	0.18	0.11	0.05	0.03	0.03
Hybrid heat pump (heat pump +biogas boiler)	Heat	65%[214]: market for floor heating from air-water heat pump	Europe without Switzerland	0.25	0.22	0.18	0.11	0.05	0.03	0.03
		35%[214]: heat production from green gas boiler (adapted from natural gas boiler by replacing natural gas with green gas; 1 m³ of biogas equals to 0.63 m³ of natural gas[331])	NL	0.37	0.37	0.36	0.36	0.36	0.35	0.35
		Weighted average factors	-	0.29	0.27	0.24	0.19	0.16	0.15	0.14
Solar water heater	Heat, central or small-	Operation, solar collector system, Cu flat	CH	0.01	0.01	0.01	0.01	0.01	0.01	0.01

	scale, other than natural gas	plate collector, multiple dwelling, for hot water								
Grid electricity	Electricity, low voltage	Market for electricity, low voltage	NL	0.63	0.54	0.44	0.22	0.06	0.00	-0.01
PV electricity	Electricity, low voltage	Electricity production, photovoltaic, 3kWp slanted-roof installation, multi-Si, panel, mounted	NL	0.08	0.07	0.06	0.05	0.04	0.04	0.04

7.3 Supporting information to Chapter 4

7.3.1 Map of population per city

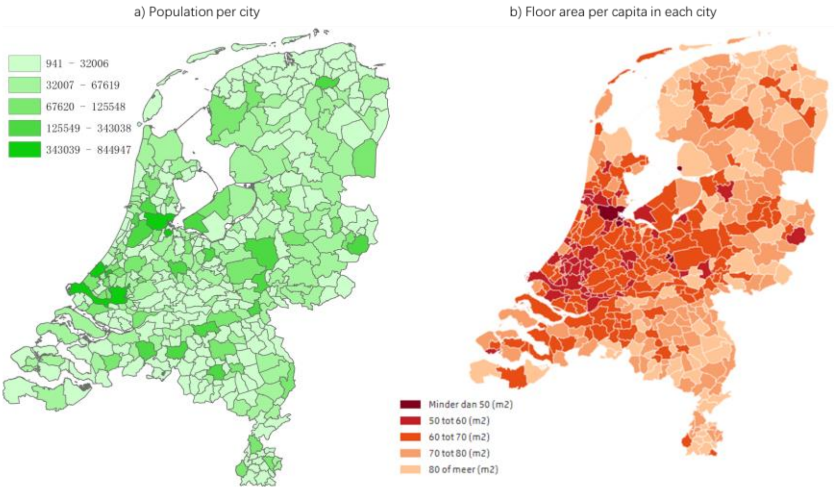

Figure S7.3.1 Population and floor area per city [232,332].

7.3.2 Material composition

Table S7.3.1 Material intensities [147] of existing buildings (kg/m^2). Apartment buildings are divided into low and high (more than 5 floors) apartment buildings [44]. SFH: single-family house. TH: terraced house. AB: apartment building.

Building type	SFH	TH	AB_low	AB_high
Al	6.05	6.05	6.05	6.05
Ar	0.00	0.00	0.00	0.00

Bi	0.00	0.00	0.00	0.00
CB	635.29	124.10	310.28	245.78
Ce	5.17	21.29	5.17	5.17
Co	0.00	0.00	0.00	0.00
CI	4.90	4.90	4.90	4.90
Cr	974.12	353.20	883.09	699.53
EPS	0.00	0.00	0.00	0.00
Gl	0.00	0.00	0.00	0.00
Gr	0.00	0.00	0.00	0.00
Gy	0.00	10.26	10.96	6.70
HW	0.00	0.00	0.00	0.00
MW	0.00	0.00	0.00	0.00
Pl	0.00	7.65	0.00	5.11
PUR	0.00	0.00	0.00	0.00
Pw	0.00	0.00	0.00	0.00
RC	0.00	0.00	0.00	0.00
Sa	0.00	0.00	0.00	0.00
SC	0.00	0.00	0.00	0.00
St	36.52	14.80	33.34	26.92
SW	246.70	69.27	49.10	61.09
WF	0.00	0.00	0.00	0.00
XPS	0.00	0.00	0.00	0.00
Zn	0.00	0.00	0.00	0.00

Table S7.3.2 Material intensities [211] of new buildings (kg/m^2). SFH: single-family house. TH: terraced house. AB: apartment building. MFH: multi-family house.

Building type	SFH 6	Mid_TH6	End_TH6	AB6	MFH6	SFH 7	Mid_TH7	End_TH7	AB7	MFH7
Al	3.58	5.15	5.15	6.61	6.61	2.15	2.92	2.92	3.44	3.44
Ar	0.00	0.00	0.00	0.00	0.00	0.01	0.00	0.00	0.00	0.00
Bi	2.44	2.44	2.44	4.70	4.70	2.44	2.44	2.44	4.70	4.70
CB	96.43	48.94	48.94	55.44	55.44	18.35	9.29	9.29	10.49	10.49
Ce	5.66	5.59	5.59	4.70	4.70	5.66	5.59	5.59	4.70	4.70
Co	0.00	0.00	0.00	0.00	0.00	0.00	0.00	0.00	0.00	0.00
CI	0.00	0.00	0.00	0.00	0.00	0.00	0.00	0.00	0.00	0.00
Cr	810.69	702.19	702.19	750.20	750.20	685.89	638.85	638.85	678.46	678.46
EPS	1.12	1.12	1.12	0.12	0.12	0.62	0.62	0.62	0.16	0.16
Gl	5.86	2.07	2.07	1.96	1.96	5.86	2.07	2.07	1.96	1.96
Gr	6.34	6.41	6.41	12.5	12.5	6.34	6.41	6.41	12.5	12.5

				0	0				0	0
Gy	0.00	0.00	0.00	0.00	0.00	0.00	0.00	0.00	0.00	0.00
HW	8.50	7.87	7.87	7.86	7.86	8.50	7.87	7.87	7.86	7.86
MW	28.47	25.13	25.13	6.39	6.39	31.38	15.92	15.92	18.03	18.03
Pl	0.04	0.04	0.04	0.01	0.01	0.04	0.04	0.04	0.01	0.01
PUR	0.00	0.00	0.00	1.35	1.35	5.70	6.42	6.42	1.43	1.43
Pw	14.60	14.96	14.96	6.13	6.13	14.60	11.84	11.84	6.13	6.13
RC	255.75	532.97	532.97	284.48	284.48	255.75	532.97	532.97	284.48	284.48
Sa	571.89	571.74	571.74	571.89	571.89	571.89	587.11	587.11	571.89	571.89
SC	135.60	135.49	135.49	105.79	105.79	135.60	135.49	135.49	105.79	105.79
St	0.00	0.00	0.00	0.00	0.00	0.00	0.00	0.00	0.00	0.00
SW	51.42	51.39	51.39	0.00	0.00	51.42	51.39	51.39	0.00	0.00
WF	0.00	0.00	0.00	0.00	0.00	8.50	4.34	4.34	4.92	4.92
XPS	0.00	0.00	0.00	0.00	0.00	2.30	2.30	2.30	0.25	0.25
Zn	1.24	14.24	14.24	0.69	0.69	1.24	14.24	14.24	0.69	0.69

Table S7.3.3 Insulation materials. HR++ glass contains 2 plates (2×0.5cm thick) and 2cm argon [211]. HR+++ glass is assumed to contain 3 plates (3×0.5cm thick) and 2cm argon [209,211]. The typical U-values of glasses are from TABULA and Milieu Centraal [68,209].

Insulation standards	Element	Material	Thermal conductivity (k, W/mK)	U-value	Density (kg/m^3)
	Roof	mineral wool	0.037	-	140
	Window	HR++ glass	-	1.8	-
conventional	Wall	mineral wool	0.037	-	140
	Door	-	-	-	-
	Ground floor	PUR	0.025	-	45
	Roof	PUR	0.025	-	45
	Glass	HR+++ glass	-	1.0	-
advanced	Wall	mineral wool	0.037	-	140
	Door	PUR	0.025	-	45
	Ground floor	mineral wool	0.037	-	140

7.3.3 Outflow collection and recycling

Table S7.3.4 EOL collection rate and recycled content potential of material outflows [44]. Considering that [44] only includes the EOL processing of 11 kinds of main materials (italicized), the EOL collection rates and recycled content potential of other materials are assumed as zero.

Material label	Material name	EOL collection rate (%)	Recycled content potential (%)
Al	*Aluminum*	*95*	*50*
Ar	Argon	0	0
Bi	*Bitumen*	*50*	*50*
CB	*Clay brick*	*95*	*50*
Ce	*Ceramic*	*95*	*80*
Co	Copper	0	0
CI	*Cast iron*	*95*	*96*
Cr	*Concrete*	*85*	*50*
EPS	Expanded polystyrene	0	0
Gl	*Glass*	*95*	*91*
Gr	Gravel	0	0
Gy	*Gypsum*	*95*	*40*
HW	*Hardwood*	*95*	*90*
MW	Mineral wool	0	0
Pl	Plastic	0	0
PUR	Polyurethane foam	0	0
Pw	Plywood	0	0
RC	reinforced concrete	0	0
Sa	Sand	0	0
SC	Sand cement	0	0
St	*Steel*	*95*	*85*
SW	*Softwood*	*95*	*90*
WF	Wood fiber	0	0
XPS	Extruded polystyrene	0	0
Zn	Zinc	0	0

7.3.4 Environmental impact factors of materials, transportation, and landfill

Table S7.3.5 GHG emissions factors (SSP2) [142,216] of building material production from ecoinvent 3.6 (kg CO_2 eq/kg) [138].

Materials	Product	Activity	Location	2015 - 2019	2020 - 2024	2025 - 2029	2030 - 2034	2035 - 2039	2040 - 2044	2045 - 2049	2050

Al	aluminium, wrought alloy	market for aluminium, wrought alloy	GLO	11.1708	11.0726	10.9905	10.9299	10.8688	10.7739	10.7226	10.7092
Ar	argon, liquid	market for argon, liquid	RoW	2.1136	2.0157	1.8903	1.7881	1.7290	1.6830	1.6788	1.6938
Bi	bitumen adhesive compound, hot	market for bitumen adhesive compound, hot	GLO	0.5125	0.5114	0.5090	0.5069	0.5056	0.5045	0.5043	0.5045
CB	clay brick	market for clay brick	GLO	0.3054	0.3041	0.3019	0.3000	0.2988	0.2979	0.2976	0.2978
Ce	ceramic tile	market for ceramic tile	GLO	0.7372	0.7252	0.7100	0.6981	0.6911	0.6857	0.6857	0.6882
Co	copper	market for copper	GLO	4.1972	4.1027	4.0054	3.9332	3.8907	3.8575	3.8601	3.8794
CI	cast iron	market for cast iron	GLO	1.7268	1.7104	1.6888	1.6710	1.6606	1.6526	1.6519	1.6547
Cr	concrete, normal	market for concrete, normal	CH	0.0737	0.0743	0.0733	0.0720	0.0711	0.0702	0.0696	0.0693
EPS	polystyrene, expandable	market for polystyrene, expandable	GLO	3.6422	3.6418	3.6412	3.6406	3.6403	3.6400	3.6400	3.6401

Gl	flat glass, coated	market for flat glass, coated	RoW	1.1517	1.1423	1.1335	1.1269	1.1234	1.1213	1.1223	1.1244
Gr	gravel, crushed	market for gravel, crushed	CH	0.0088	0.0090	0.0087	0.0083	0.0080	0.0078	0.0076	0.0075
Gy	gypsum, mineral	gypsum quarry operation	CH	0.0026	0.0027	0.0026	0.0025	0.0025	0.0024	0.0024	0.0024
HW	sawn wood, hardwood, raw	sawing, hardwood	CH	-2.1050	-2.1040	-2.1057	-2.1078	-2.1092	-2.1107	-2.1116	-2.1122
MW	glass wool mat	market for glass wool mat	GLO	2.3360	2.2667	2.1758	2.1053	2.0630	2.0302	2.0286	2.0413
Pl	extrusion, plastic pipes	market for extrusion, plastic pipes	GLO	0.3488	0.3390	0.3189	0.3009	0.2899	0.2797	0.2761	0.2761
PUR	polyurethane, flexible foam	market for polyurethane, flexible foam	RER	5.4463	5.4495	5.4394	5.4282	5.4206	5.4118	5.4061	5.4028
Pw	plywood, for indoor use	market for plywood, for indoor use	RER	-3.1333	-3.1204	-3.1531	-3.1899	-3.2151	-3.2442	-3.2631	-3.2743

RC	fibre-reinforced concrete	market for fibre-reinforced concrete, steel	BR	0.1738	0.1736	0.1736	0.1735	0.1732	0.1731	0.1733	0.1734
Sa	sand	gravel and sand quarry operation	CH	0.0037	0.0039	0.0037	0.0035	0.0033	0.0031	0.0031	0.0030
SC	cement mortar	market for cement mortar	CH	0.2401	0.2424	0.2384	0.2336	0.2304	0.2268	0.2248	0.2235
St	wire drawing, steel	market for wire drawing, steel	GLO	0.3117	0.3049	0.2992	0.2952	0.2932	0.2922	0.2933	0.2950
SW	sawn wood, softwood, raw	sawing, softwood	CH	-1.4715	-1.4705	-1.4721	-1.4741	-1.4754	-1.4768	-1.4776	-1.4781
WF	fibreboard, soft	fibreboard production, soft, from wet & dry processes	Europe without Switzerland	-0.0821	-0.0807	-0.0867	-0.0935	-0.0983	-0.1045	-0.1087	-0.1113
XPS	polystyrene, extruded	market for polystyrene, extruded	GLO	9.5244	9.4950	9.4501	9.4121	9.3897	9.3708	9.3668	9.3701

Zn	zinc	market for zinc	GLO	3.1601	3.1950	3.0817	2.9311	2.8472	2.7568	2.7267	2.7197

Table S7.3.6 GHG emissions factors (SSP2 450) [142,216] of building material production from ecoinvent 3.6 (kg CO_2 eq/kg) [138].

Materials	Product	Activity	Location	2015-2019	2020-2024	2025-2029	2030-2034	2035-2039	2040-2044	2045-2049	2050
Al	aluminium, wrought alloy	market for aluminium, wrought alloy	GLO	11.1667	11.0403	10.9137	10.8074	10.6457	10.4540	10.3293	10.2472
Ar	argon, liquid	market for argon, liquid	RoW	2.0820	1.8549	1.5417	1.2476	0.7770	0.3092	0.1337	0.0731
Bi	bitumen adhesive compound, hot	market for bitumen adhesive compound, hot	GLO	0.5119	0.5084	0.5029	0.4973	0.4885	0.4802	0.4769	0.4754
CB	clay brick	market for clay brick	GLO	0.3049	0.3014	0.2961	0.2909	0.2826	0.2747	0.2717	0.2706
Ce	ceramic tile	market for ceramic tile	GLO	0.7333	0.7047	0.6652	0.6269	0.5679	0.5106	0.4893	0.4794
Co	copper	market for copper	GLO	4.1720	3.9733	3.7175	3.4744	3.1055	2.7341	2.5898	2.5228
CI	cast iron	market for cast iron	GLO	1.7212	1.6818	1.6266	1.5741	1.4909	1.4091	1.3786	1.3668
Cr	concrete, normal	market for concrete, normal	CH	0.0734	0.0737	0.0723	0.0702	0.0666	0.0638	0.0628	0.0627
EPS	polystyrene,	market for polystyre	GLO	3.6420	3.6409	3.6392	3.6376	3.6350	3.6325	3.6316	3.6311

	expandable	ne, expandable									
Gl	flat glass, coated	market for flat glass, coated	RoW	1.1494	1.1296	1.1055	1.0838	1.0498	1.0143	1.0009	0.9956
Gr	gravel, crushed	market for gravel, crushed	CH	0.0087	0.0088	0.0084	0.0077	0.0066	0.0058	0.0055	0.0055
Gy	gypsum, mineral	gypsum quarry operation	CH	0.0026	0.0026	0.0026	0.0024	0.0022	0.0021	0.0020	0.0020
HW	sawnwood, hardwood, raw	sawing, hardwood	CH	-2.1054	-2.1050	-2.1074	-2.1108	-2.1167	-2.1213	-2.1230	-2.1232
MW	glass wool mat	market for glass wool mat	GLO	2.3139	2.1527	1.9243	1.7032	1.3646	1.0343	0.9115	0.8547
Pl	extrusion, plastic pipes	market for extrusion, plastic pipes	GLO	0.3437	0.3161	0.2702	0.2246	0.1503	0.0809	0.0549	0.0469
PUR	polyurethane, flexible foam	market for polyurethane, flexible foam	RER	5.4438	5.4419	5.4249	5.4042	5.3687	5.3417	5.3316	5.3299
Pw	plywood, for indoor use	market for plywood, for indoor use	RER	-3.1413	-3.1435	-3.1962	-3.2625	-3.3766	-3.4624	-3.4944	-3.4989
RC	fibre-reinforced concrete	market for fibre-reinforced concrete, steel	BR	0.1736	0.1723	0.1710	0.1698	0.1678	0.1660	0.1657	0.1655

Sa	sand	gravel and sand quarry operation	CH	0.0037	0.0038	0.0035	0.0032	0.0025	0.0021	0.0019	0.0019
SC	cement mortar	market for cement mortar	CH	0.2392	0.2401	0.2345	0.2266	0.2127	0.2021	0.1981	0.1977
St	wire drawing, steel	market for wire drawing, steel	GLO	0.3103	0.2963	0.2802	0.2660	0.2439	0.2202	0.2113	0.2077
SW	sawnwood, softwood, raw	sawing, softwood	CH	-1.4719	-1.4715	-1.4737	-1.4769	-1.4824	-1.4866	-1.4883	-1.4884
WF	fibreboard, soft	fibreboard production, soft, from wet & dry processes	Europe without Switzerland	-0.0837	-0.0859	-0.0968	-0.1096	-0.1319	-0.1485	-0.1544	-0.1556
XPS	polystyrene, extruded	market for polystyrene, extruded	GLO	9.5131	9.4398	9.3316	9.2277	9.0604	8.8983	8.8375	8.8170
Zn	zinc	market for zinc	GLO	3.1193	3.0114	2.7432	2.3736	1.7496	1.2504	1.0924	1.0431

Table S7.3.7 GHG emissions factors (SSP2) [142,216] of recycled building materials. The materials are from ecoinvent 3.6 (kg CO_2 eq/kg) [138]. The factors of the other recycled materials are assumed as zero.

Materials	Product	Activity	Location	2015-2019	2020-2024	2025-2029	2030-2034	2035-2039	2040-2044	2045-2049	2050
Al	aluminium scrap, post-consumer, prepared for melting	aluminium scrap, post-consumer, prepared for melting, Recycled	GLO	0.0000	0.0000	0.0000	0.0000	0.0000	0.0000	0.0000	0.0000

		Content cut-off									
Ar	-	-	-	0.0000	0.0000	0.0000	0.0000	0.0000	0.0000	0.0000	0.0000
Bi	waste bitumen sheet	market for waste bitumen sheet	CH	-2.3591	-2.3587	-2.3580	-2.3573	-2.3569	-2.3565	-2.3563	-2.3563
CB	waste brick	treatment of waste brick, recycling	CH	-0.0033	-0.0033	-0.0033	-0.0033	-0.0033	-0.0033	-0.0033	-0.0033
Ce	-	-	-	0.0000	0.0000	0.0000	0.0000	0.0000	0.0000	0.0000	0.0000
Co	-	-	-	0.0000	0.0000	0.0000	0.0000	0.0000	0.0000	0.0000	0.0000
CI	iron scrap, sorted, pressed	iron scrap, sorted, pressed, Recycled Content cut-off	GLO	0.0000	0.0000	0.0000	0.0000	0.0000	0.0000	0.0000	0.0000
Cr	waste concrete, not reinforced	treatment of waste concrete, not reinforced, recycling	Europe without Switzerland	-0.0040	-0.0040	-0.0040	-0.0040	-0.0040	-0.0040	-0.0040	-0.0040
EPS	-	-	-	0.0000	0.0000	0.0000	0.0000	0.0000	0.0000	0.0000	0.0000
Gl	glass cullet, sorted	glass cullet, sorted, Recycled Content cut-off	GLO	0.0000	0.0000	0.0000	0.0000	0.0000	0.0000	0.0000	0.0000
Gr	-	-	-	0.0000	0.0000	0.0000	0.0000	0.0000	0.0000	0.0000	0.0000

Gy	waste gypsum plasterboard	treatment of waste gypsum plasterboard, recycling	CH	-0.0033	-0.0033	-0.0033	-0.0033	-0.0033	-0.0033	-0.0033	-0.0033
HW	waste wood, post-consumer	waste wood, post-consumer, Recycled Content cut-off	GLO	0.0000	0.0000	0.0000	0.0000	0.0000	0.0000	0.0000	0.0000
MW	-	-	-	0.0000	0.0000	0.0000	0.0000	0.0000	0.0000	0.0000	0.0000
Pl	-	-	-	0.0000	0.0000	0.0000	0.0000	0.0000	0.0000	0.0000	0.0000
PUR	-	-	-	0.0000	0.0000	0.0000	0.0000	0.0000	0.0000	0.0000	0.0000
Pw	-	-	-	0.0000	0.0000	0.0000	0.0000	0.0000	0.0000	0.0000	0.0000
RC	-	-	-	0.0000	0.0000	0.0000	0.0000	0.0000	0.0000	0.0000	0.0000
Sa	-	-	-	0.0000	0.0000	0.0000	0.0000	0.0000	0.0000	0.0000	0.0000
SC	-	-	-	0.0000	0.0000	0.0000	0.0000	0.0000	0.0000	0.0000	0.0000
St	waste reinforcement steel	treatment of waste reinforcement steel, recycling	CH	-0.0574	-0.0573	-0.0572	-0.0571	-0.0571	-0.0570	-0.0570	-0.0570
SW	waste wood, post-consumer	waste wood, post-consumer, Recycled	GLO	0.0000	0.0000	0.0000	0.0000	0.0000	0.0000	0.0000	0.0000

		Content cut-off									
WF	-	-	-	0.0000	0.0000	0.0000	0.0000	0.0000	0.0000	0.0000	0.0000
XPS	-	-	-	0.0000	0.0000	0.0000	0.0000	0.0000	0.0000	0.0000	0.0000
Zn	-	-	-	0.0000	0.0000	0.0000	0.0000	0.0000	0.0000	0.0000	0.0000

Table S7.3.8 GHG emissions factors (SSP2 450) [142,216] of recycled building materials. The materials are from ecoinvent 3.6 (kg CO_2 eq/kg) [138]. The factors of the other recycled materials are assumed as zero.

Materials	Product	Activity	Location	2015-2019	2020-2024	2025-2029	2030-2034	2035-2039	2040-2044	2045-2049	2050
Al	aluminium scrap, post-consumer, prepared for melting	aluminium scrap, post-consumer, prepared for melting, Recycled Content cut-off	GLO	0.0000	0.0000	0.0000	0.0000	0.0000	0.0000	0.0000	0.0000
Ar	-	-	-	0.0000	0.0000	0.0000	0.0000	0.0000	0.0000	0.0000	0.0000
Bi	waste bitumen sheet	market for waste bitumen sheet	CH	-2.3589	-2.3579	-2.3562	-2.3544	-2.3516	-2.3490	-2.3480	-2.3477
CB	waste brick	treatment of waste brick, recycling	CH	-0.0033	-0.0033	-0.0033	-0.0033	-0.0032	-0.0032	-0.0032	-0.0032
Ce	-	-	-	0.0000	0.0000	0.0000	0.0000	0.0000	0.0000	0.0000	0.0000
Co	-	-	-	0.0000	0.0000	0.0000	0.0000	0.0000	0.0000	0.0000	0.0000

CI	iron scrap, sorted, pressed	iron scrap, sorted, pressed, Recycled Content cut-off	GLO	0.0000	0.0000	0.0000	0.0000	0.0000	0.0000	0.0000	0.0000
Cr	waste concrete, not reinforced	treatment of waste concrete, not reinforced, recycling	Europe without Switzerland	-0.0040	-0.0040	-0.0040	-0.0040	-0.0039	-0.0039	-0.0039	-0.0039
EPS	-	-	-	0.0000	0.0000	0.0000	0.0000	0.0000	0.0000	0.0000	0.0000
Gl	glass cullet, sorted	glass cullet, sorted, Recycled Content cut-off	GLO	-2.3589	-2.3579	-2.3562	-2.3544	-2.3516	-2.3490	-2.3480	-2.3477
Gr	-	-	-	0.0000	0.0000	0.0000	0.0000	0.0000	0.0000	0.0000	0.0000
Gy	waste gypsum plasterboard	treatment of waste gypsum plasterboard, recycling	CH	-0.0033	-0.0033	-0.0033	-0.0033	-0.0032	-0.0032	-0.0032	-0.0032
HW	waste wood, post-consumer	waste wood, post-consumer, Recycled Content cut-off	GLO	0.0000	0.0000	0.0000	0.0000	0.0000	0.0000	0.0000	0.0000
MW	-	-	-	0.0000	0.0000	0.0000	0.0000	0.0000	0.0000	0.0000	0.0000
Pl	-	-	-	0.0000	0.0000	0.0000	0.0000	0.0000	0.0000	0.0000	0.0000
PUR	-	-	-	0.0000	0.0000	0.0000	0.0000	0.0000	0.0000	0.0000	0.0000

Pw	-	-	-	0.0000	0.0000	0.0000	0.0000	0.0000	0.0000	0.0000	0.0000
RC	-	-	-	0.0000	0.0000	0.0000	0.0000	0.0000	0.0000	0.0000	0.0000
Sa	-	-	-	0.0000	0.0000	0.0000	0.0000	0.0000	0.0000	0.0000	0.0000
SC	-	-	-	0.0000	0.0000	0.0000	0.0000	0.0000	0.0000	0.0000	0.0000
St	waste reinforcement steel	treatment of waste reinforcement steel, recycling	CH	-0.0573	-0.0572	-0.0569	-0.0567	-0.0563	-0.0560	-0.0558	-0.0558
SW	waste wood, post-consumer	waste wood, post-consumer, Recycled Content cut-off	GLO	0.0000	0.0000	0.0000	0.0000	0.0000	0.0000	0.0000	0.0000
WF	-	-	-	0.0000	0.0000	0.0000	0.0000	0.0000	0.0000	0.0000	0.0000
XPS	-	-	-	0.0000	0.0000	0.0000	0.0000	0.0000	0.0000	0.0000	0.0000
Zn	-	-	-	0.0000	0.0000	0.0000	0.0000	0.0000	0.0000	0.0000	0.0000

Table S7.3.9 GHG emissions factors (SSP2) [142,216] of transportation from ecoinvent 3.6 (kg CO_2 eq/(kg·km)) [138].

Materials	Product	Activity	Location	2015-2019	2020-2024	2025-2029	2030-2034	2035-2039	2040-2044	2045-2049	2050
Truck transpor	transport, freight, lorry	transport, freight, lorry 16-32 metric	RER	0.0002	0.0002	0.0002	0.0002	0.0002	0.0002	0.0002	0.0002

tation (SSP2)	16-32 metric ton, EURO6	ton, EURO6									
Ship transportation (SSP2)	transport, freight, sea, container ship	market for transport, freight, sea, container ship	GLO	0.0000	0.0000	0.0000	0.0000	0.0000	0.0000	0.0000	0.0000
Truck transportation (SSP2 450)	transport, freight, lorry 16-32 metric ton, EURO6	transport, freight, lorry 16-32 metric ton, EURO6	RER	0.0002	0.0002	0.0002	0.0002	0.0002	0.0002	0.0002	0.0002
Ship transportation (SSP2 450)	transport, freight, sea, container ship	market for transport, freight, sea, container ship	GLO	0.0000	0.0000	0.0000	0.0000	0.0000	0.0000	0.0000	0.0000

Table S7.3.10 GHG emissions factors of landfill from ecoinvent 3.6 (kg CO_2 eq/kg) [138,142].

Materials	Product	Activity	Location	2015-2019	2020-2024	2025-2029	2030-2034	2035-2039	2040-2044	2045-2049	2050
Landfill (SSP2)	inert waste	treatment of inert waste, sanitary landfill	Europe without Switzerland	-0.0103	-0.0102	-0.0101	-0.0100	-0.0100	-0.0100	-0.0099	-0.0100
Landfill (SSP2 450)	inert waste	treatment of inert waste, sanitary landfill	Europe without Switzerland	-0.0103	-0.0101	-0.0098	-0.0096	-0.0092	-0.0088	-0.0087	-0.0086

7.3.5 Sensitivity analysis for concrete

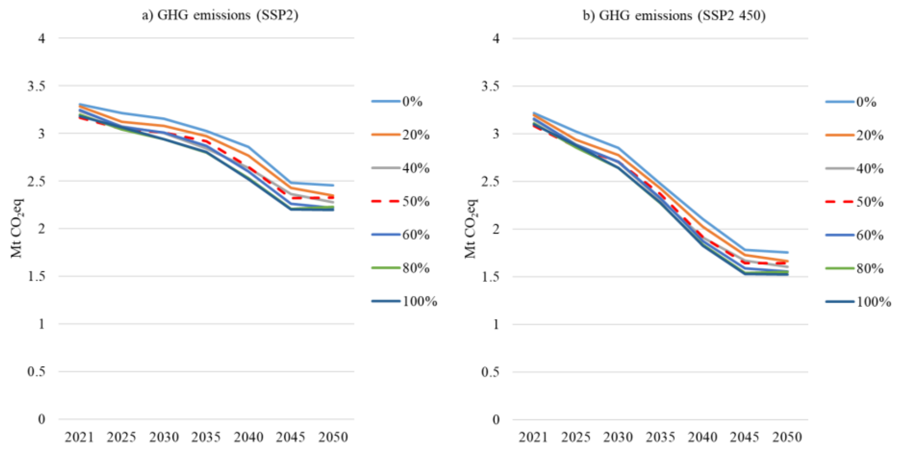

Figure S7.3.2 Sensitivity analysis for the recycled content potential of concrete. The recycled content potential for the red dash line is 50%, which is used in this study.

7.4 Supporting information to Chapter 5

7.4.1 Individual building characterization

Table S7.4.1 Building classification based on TABULA[68].

Construction period	Single-family house	Mid-terraced house	End-terraced house	Apartment building	Multi-family house	Apartment building (wood)
<=1964	SFH1	Mid_TH1	End_TH1	AB1	MFH1	-
1965-1974	SFH2	Mid_TH2	End_TH2	AB2	MFH2	-
1975-1991	SFH3	Mid_TH3	End_TH3	AB3	MFH3	-
1992-2005	SFH4	Mid_TH4	End_TH4	AB4	MFH4	-
2006-2014	SFH5	Mid_TH5	End_TH5	AB5	MFH5	-
>=2015 (conventional new)	SFH6	Mid_TH6	End_TH6	AB6	MFH6	AB6_wood
>=2015 (nZEB new)	SFH7	Mid_TH7	End_TH7	AB7	MFH7	AB7_wood

Table S7.4.2 Attributes of individual buildings.

Information type	Parameters
Basic information	ID number

	construction yeat	
	expected demolition year	
	stories	
	building type	
	conditioned floor area	
Location	postcode	
	neighborhood code	
	weather station code	
	available heat sources	
Envelope	roof	surface area
		U-value
		construction year
		retirement year
	external wall	surface area
		U-value
		construction year
		retirement year
	ground floor	surface area
		U-value
		construction year
		retirement year
	glazing	surface area
		U-value
		G-value
		construction year
		retirement year
	door	surface area
		U-value
		construction year
		retirement year
Technical system	space heating system	type
		recoverable heat loss of the heat distribution system per m²
		recoverable heat loss of the storage per m²
		annual effective heat loss of the space heating distribution system per m²
		annual effective heat loss of the heating system storage per m²
		installation year
		retirement year

	domestic hot water system	type	
		annual energy need for domestic hot water per m²	
		annual heat loss of the DHW distribution system per m²	
		annual heat loss of the DHW storage per m²	
		installation year	
		retirement year	
	ventilation system	type	
		the efficiency of ventilation heat recovery	
		installation year	
		retirement year	
	solar panel	type	
		efficiency	
		installation year	
		retirement year	
Occupant behavior	room temperature		
	time of presence		
Material composition (see **Table S7.4.3**)	material stock every year		
	material outflow every year		
	material inflow every year		
Energy	space heating		
	hot water		
	electricity for appliances and lighting		
	electricity generation		
Environmental impact	material-related emissions		
	space heating		
	hot water		
	electricity for appliances and lighting		
	electricity generation		

Table S7.4.3 The example table for recording material stock and flows.

Year	Material_1 stock	Material_2 stock	…	Material_1 outflow	Material_2 outflow	…	Material_1 inflow	Material_2 inflow	…
2015									
2016									
2017									
…									

2049									
2050									

Table S7.4.4 Building materials [280].

Label	Name	Label	Name
Al	Aluminum	MW	Mineral wool
Ar	Argon	Pl	Plastic
Bi	Bitumen	PUR	Polyurethane foam
CB	Clay brick	Pw	Plywood
Ce	Ceramic	RC	reinforced concrete
Co	Copper	Sa	Sand
CI	Cast iron	SC	Sand cement
Cr	Concrete	St	Steel
EPS	Expanded polystyrene	SW	Softwood
Gl	Glass	WF	Wood fiber
Gr	Gravel	XPS	Extruded polystyrene
Gy	Gypsum	Zn	Zinc
HW	Hardwood	-	-

Table S7.4.5 Material intensities of new buildings (kg/m^2). The material intensities of wood apartment buildings are from [211,281].

Building type	SFH6	Mid_TH6	End_TH6	AB6	MFH6	AB6_wood	SFH7	Mid_TH7	End_TH7	AB7	MFH7	AB7_wood
Al	3.58	5.15	5.15	6.61	6.61	0.10	2.15	2.92	2.92	3.44	3.44	0.10
Ar	0.00	0.00	0.00	0.00	0.00	0.00	0.01	0.00	0.00	0.00	0.00	0.00
Bi	2.44	2.44	2.44	4.70	4.70	0.00	2.44	2.44	2.44	4.70	4.70	0.00
CB	96.43	48.94	48.94	55.44	55.44	0.00	18.35	9.29	9.29	10.49	10.49	0.00
Ce	5.66	5.59	5.59	4.70	4.70	0.00	5.66	5.59	5.59	4.70	4.70	0.00
Co	0.00	0.00	0.00	0.00	0.00	0.00	0.00	0.00	0.00	0.00	0.00	0.00
CI	0.00	0.00	0.00	0.00	0.00	0.00	0.00	0.00	0.00	0.00	0.00	0.00

Cr	810.69	702.19	702.19	750.20	750.20	454.20	685.89	638.85	638.85	678.46	678.46	454.20
EPS	1.12	1.12	1.12	0.12	0.12	0.00	0.62	0.62	0.62	0.16	0.16	0.20
Gl	5.86	2.07	2.07	1.96	1.96	3.80	5.86	2.07	2.07	1.96	1.96	3.80
Gr	6.34	6.41	6.41	12.50	12.50	92.70	6.34	6.41	6.41	12.50	12.50	92.70
Gy	0.00	0.00	0.00	0.00	0.00	51.40	0.00	0.00	0.00	0.00	0.00	51.40
HW	8.50	7.87	7.87	7.86	7.86	15.70	8.50	7.87	7.87	7.86	7.86	15.70
MW	28.47	25.13	25.13	6.39	6.39	11.30	31.38	15.92	15.92	18.03	18.03	18.00
Pl	0.04	0.04	0.04	0.01	0.01	1.10	0.04	0.04	0.04	0.01	0.01	1.10
PUR	0.00	0.00	0.00	1.35	1.35	0.00	5.70	6.42	6.42	1.43	1.43	1.40
Pw	14.60	14.96	14.96	6.13	6.13	79.80	14.60	11.84	11.84	6.13	6.13	79.80
RC	255.75	532.97	532.97	284.48	284.48	0.00	255.75	532.97	532.97	284.48	284.48	0.00
Sa	571.89	571.74	571.74	571.89	571.89	0.00	571.89	587.11	587.11	571.89	571.89	0.00
SC	135.60	135.49	135.49	105.79	105.79	94.80	135.60	135.49	135.49	105.79	105.79	94.80
St	0.00	0.00	0.00	0.00	0.00	43.90	0.00	0.00	0.00	0.00	0.00	43.90
SW	51.42	51.39	51.39	0.00	0.00	73.10	51.42	51.39	51.39	0.00	0.00	73.10
WF	0.00	0.00	0.00	0.00	0.00	0.00	8.50	4.34	4.34	4.92	4.92	0.00
XPS	0.00	0.00	0.00	0.00	0.00	0.00	2.30	2.30	2.30	0.25	0.25	0.20
Zn	1.24	14.24	14.24	0.69	0.69	0.00	1.24	14.24	14.24	0.69	0.69	0.00

Table S7.4.6 Material intensities[211] of existing buildings (kg/m^2). Apartment buildings are further divided into low and high (more than 5 floors) apartment buildings [44].

Building type	SFH1-5	Mid_TH1-5	End_TH1-5	MFH1-5	AB1-5 (low)	AB1-5 (high)
Al	6.10	6.10	6.10	6.10	6.10	6.10
Ar	0.00	0.00	0.00	0.00	0.00	0.00
Bi	0.00	0.00	0.00	0.00	0.00	0.00
CB	635.30	124.10	124.10	310.30	310.30	245.80
Ce	5.20	21.30	21.30	5.20	5.20	5.20
Co	0.00	0.00	0.00	0.00	0.00	0.00
CI	4.90	4.90	4.90	4.90	4.90	4.90
Cr	974.10	353.20	353.20	883.10	883.10	699.50
EPS	0.00	0.00	0.00	0.00	0.00	0.00

Gl	0.00	0.00	0.00	0.00	0.00	0.00
Gr	0.00	0.00	0.00	0.00	0.00	0.00
Gy	0.00	10.30	10.30	11.00	11.00	6.70
HW	0.00	0.00	0.00	0.00	0.00	0.00
MW	0.00	0.00	0.00	0.00	0.00	0.00
Pl	0.00	7.70	7.70	0.00	0.00	5.10
PUR	0.00	0.00	0.00	0.00	0.00	0.00
Pw	0.00	0.00	0.00	0.00	0.00	0.00
RC	0.00	0.00	0.00	0.00	0.00	0.00
Sa	0.00	0.00	0.00	0.00	0.00	0.00
SC	0.00	0.00	0.00	0.00	0.00	0.00
St	36.50	14.80	14.80	33.30	33.30	26.90
SW	246.70	69.30	69.30	49.10	49.10	61.10
WF	0.00	0.00	0.00	0.00	0.00	0.00
XPS	0.00	0.00	0.00	0.00	0.00	0.00
Zn	0.00	0.00	0.00	0.00	0.00	0.00

7.4.2 Leiden population

Table S7.4.7 The population forecast of Leiden [283].

Year	Population	Year	Population
2015	121562	2033	140500
2016	122561	2034	141200
2017	123661	2035	141900
2018	124306	2036	142500
2019	124899	2037	143100
2020	125900	2038	143800
2021	127000	2039	144500
2022	128200	2040	145200
2023	129600	2041	145700
2024	131000	2042	146300
2025	132600	2043	146900
2026	134100	2044	147600
2027	135100	2045	148200
2028	136100	2046	148700
2029	137000	2047	149200
2030	138000	2048	149900
2031	138900	2049	150400
2032	139700	2050	151000

7.4.3 Neighborhood-oriented heat transition in Leiden

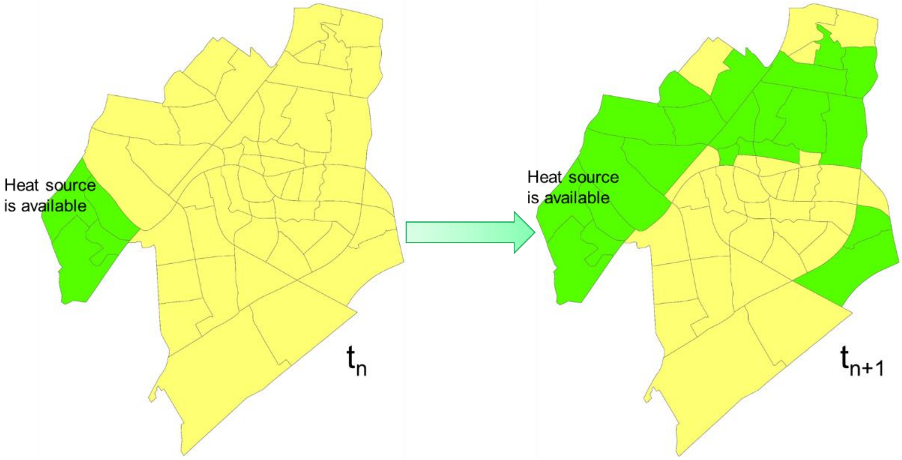

Figure S7.4.1 The schematic diagram for heat source availability per neighborhood in space and time. The neighborhoods in green are the neighborhoods where the corresponding heat source is available.

Table S7.4.8 Heat source map of Leiden [185,229]. HT is short for the high temperature.

Neighborhood code	Neighborhood name	Current heat source
BU05460000	Pieterswijk	Natural gas
BU05460001	Academiewijk	Natural gas
BU05460002	Levendaal-West	Natural gas
BU05460003	Levendaal-Oost	Natural gas
BU05460100	De Camp	Natural gas
BU05460101	Marewijk	Natural gas
BU05460102	Pancras-West	Natural gas
BU05460103	Pancras-Oost	Natural gas
BU05460104	d'Oude Morsch	Natural gas
BU05460105	Noordvest	Natural gas
BU05460106	Havenwijk-Noord	Natural gas
BU05460107	Havenwijk-Zuid	Natural gas
BU05460108	Molenbuurt	Natural gas
BU05460109	De Waard	Natural gas
BU05460200	Stationskwartier	Natural gas
BU05460300	Groenoord	Natural gas
BU05460301	Noorderkwartier	Natural gas

BU05460302	De Kooi	Natural gas
BU05460400	Meerburg	Natural gas
BU05460401	Rijndijkbuurt	Natural gas
BU05460402	Professorenwijk-Oost	Natural gas
BU05460403	Burgemeesterswijk	Natural gas
BU05460404	Professorenwijk-West	Natural gas
BU05460405	Tuinstadwijk	Natural gas
BU05460406	Cronestein	Natural gas
BU05460407	Klein Cronestein	Natural gas
BU05460408	Roomburg	Natural gas
BU05460409	Waardeiland	Natural gas
BU05460500	Vreewijk	Natural gas
BU05460501	Haagweg-Noord	Natural gas
BU05460502	Gasthuiswijk	Natural gas
BU05460503	Fortuinwijk-Noord	Natural gas
BU05460504	Boshuizen	Natural gas
BU05460505	Oostvliet	Natural gas
BU05460506	Haagweg-Zuid	Natural gas
BU05460507	Fortuinwijk-Zuid	Natural gas
BU05460600	Transvaalbuurt	Natural gas
BU05460601	Lage Mors	Natural gas
BU05460602	Hoge Mors	Natural gas
BU05460700	Pesthuiswijk	Natural gas
BU05460701	Houtkwartier	Natural gas
BU05460702	Raadsherenbuurt	Natural gas
BU05460703	Vogelwijk	Natural gas
BU05460704	Leeuwenhoek	Natural gas
BU05460800	Slaaghwijk	Natural gas
BU05460801	Zijlwijk-Zuid	Natural gas
BU05460802	Zijlwijk-Noord	Natural gas
BU05460803	Merenwijk-Centrum	Natural gas
BU05460804	Leedewijk-Zuid	Natural gas
BU05460805	Leedewijk-Noord	Natural gas

BU05460900	Schenkwijk	Heat networks (HT)
BU05460901	Kloosterhof	Heat networks (HT)
BU05460902	Dobbewijk-Noord	Heat networks (HT)
BU05460903	Dobbewijk-Zuid	Heat networks (HT)

7.4.4 Renovation options

Table S7.4.9 U-values (W/m^2 K) of different thermal standards from TABULA for buildings in the Netherlands[68].

Building type	Conventional standard					nZEN standard				
	roof	wall	floor	window	door	roof	wall	floor	window	door
SFH1	0.24	0.24	0.25	1.8	3.5	0.15	0.18	0.18	1	1.4
Mid_TH1	0.25	0.25	0.26	1.8	3.5	0.15	0.18	0.18	1	1.4
End_TH1	0.25	0.25	0.26	1.8	3.5	0.15	0.18	0.18	1	1.4
AB1	0.24	0.24	0.23	1.8	3.5	0.15	0.18	0.17	1	1.4
MFH1	0.24	0.24	0.25	1.8	3.5	0.15	0.18	0.18	1	1.4
SFH2	0.22	0.24	0.25	1.8	3.5	0.14	0.18	0.18	1	1.4
Mid_TH2	0.22	0.24	0.25	1.8	3.5	0.14	0.18	0.18	1	1.4
End_TH2	0.22	0.24	0.25	1.8	3.5	0.14	0.18	0.18	1	1.4
AB2	0.22	0.24	0.24	1.8	3.5	0.14	0.18	0.17	1	1.4
MFH2	0.22	0.24	0.25	1.8	3.5	0.14	0.18	0.18	1	1.4
SFH3	0.2	0.2	0.2	1.8	3.5	0.13	0.13	0.15	1	1.4
Mid_TH3	0.2	0.2	0.23	1.8	3.5	0.13	0.15	0.17	1	1.4
End_TH3	0.2	0.2	0.23	1.8	3.5	0.13	0.15	0.17	1	1.4
AB3	0.2	0.2	0.19	1.8	3.5	0.13	0.15	0.15	1	1.4
MFH3	0.2	0.2	0.23	1.8	3.5	0.13	0.15	0.17	1	1.4
SFH4	0.16	0.16	0.16	1.8	3.5	0.11	0.13	0.13	1	1.4
Mid_TH4	0.16	0.16	0.16	1.8	3.5	0.11	0.13	0.13	1	1.4
End_TH4	0.16	0.16	0.16	1.8	3.5	0.11	0.13	0.13	1	1.4
AB4	0.16	0.16	0.15	1.8	2	0.11	0.13	0.12	1	1.4
MFH4	0.16	0.16	0.16	1.8	3.5	0.11	0.13	0.13	1	1.4
SFH5	0.13	0.14	0.14	1.8	1.65	0.1	0.11	0.11	1	1.4
Mid_TH5	0.13	0.14	0.14	1.8	1.65	0.1	0.11	0.11	1	1.4
End_TH5	0.13	0.14	0.14	1.8	1.65	0.1	0.11	0.11	1	1.4
AB5	0.13	0.14	0.13	1.8	1.65	0.1	0.11	0.11	1	1.4
MFH5	0.13	0.14	0.14	1.8	1.65	0.1	0.11	0.11	1	1.4
SFH6	0.16	0.21	0.27	1.8	1.65	0.08	0.1	0.11	1	1.4
Mid_TH6	0.16	0.21	0.27	1.8	1.65	0.08	0.1	0.11	1	1.4

End_TH6	0.16	0.21	0.27	1.8	1.65	0.08	0.1	0.11	1	1.4
AB6	0.16	0.21	0.25	1.8	1.65	0.08	0.1	0.11	1	1.4
AB6_wood	0.16	0.21	0.25	1.8	1.65	0.08	0.1	0.11	1	1.4
MFH6	0.16	0.21	0.27	1.8	1.65	0.08	0.1	0.11	1	1.4
SFH7	0.08	0.1	0.11	1	1.4	0.08	0.1	0.11	1	1.4
Mid_TH7	0.08	0.1	0.11	1	1.4	0.08	0.1	0.11	1	1.4
End_TH7	0.08	0.1	0.11	1	1.4	0.08	0.1	0.11	1	1.4
AB7	0.08	0.1	0.11	1	1.4	0.08	0.1	0.11	1	1.4
AB7_wood	0.08	0.1	0.11	1	1.4	0.08	0.1	0.11	1	1.4
MFH7	0.08	0.1	0.11	1	1.4	0.08	0.1	0.11	1	1.4

Table S7.4.10 Insulation measures. HR++ glass contains 2 plates (2×0.5cm thick) and 2cm argon[211]. HR+++ glass is assumed to contain 3 plates (3×0.5cm thick) and 2cm argon[209,211]. The typical U-values of glasses are from TABULA and Milieu Centraal[68,209].

Insulation standards	Element	Material	Thermal conductivity (k, W/mK)	U-value	Density (kg/m^3)	Lifetime (years) [278]
conventional	Roof	mineral	0.037	-	140	30
	Window	HR++ glass	-	1.8	-	30
	Wall	mineral	0.037	-	140	40
	Door	-	-	-	-	30
	Ground	PUR	0.025	-	45	40
nZEB	Roof	PUR	0.025	-	45	30
	Glass	HR+++	-	1.0	-	30
	Wall	mineral	0.037	-	140	40
	Door	PUR	0.025	-	45	30
	Ground	mineral	0.037	-	140	40

Table S7.4.11 Ventilation systems [68].

Type	Heat recovery fraction	Electricity intensity (kWh/m^{2}a)	Lifetime (years) [333]
Natural ventilation	0	0	20
Exhaust air ventilation	0	2.4	20
Balanced ventilation	0.95	4.2	20

Table S7.4.12 Space heating system types [68,74].

Type	Lifetime (years)
Natural gas boiler	20 [334]
Heat networks (high temperature)	15 [74]

Heat networks (low temperature)	15 [74]
Electric heat pump	15 [74]

Table S7.4.13 Domestic hot water systems [68].

Type	Lifetime (years)
Natural gas boiler	20 [334]
Heat networks (high temperature)	15 [74]
Solar water heater	20 [335]
Electric water heater	15 [336]

Table S7.4.14 Solar panel [212].

Type	Panel efficiency	Performance ratio	lifetime
Modern crystalline Silicon panels	0.17	0.85	25 [337]

Table S7.4.15 Future renovation combinations [68,74,248].

<table>
<tr><th>Insulation standards</th><th>Ventilation systems</th><th>Space heating systems</th><th>Domestic hot water system</th><th>Solar panel</th></tr>
<tr><td rowspan="2">Conventional</td><td>Exhaust air ventilation</td><td>Natural gas boiler</td><td>• Solar water heater (the first choice if applicable)
• Natural gas boiler</td><td rowspan="4">Modern crystalline Silicon panels</td></tr>
<tr><td>Exhaust air ventilation</td><td>Heat networks (high temperature)</td><td>• Solar water heater (the first choice if applicable)
• Heat networks (high temperature)</td></tr>
<tr><td rowspan="2">nZEB</td><td>Balanced ventilation</td><td>Heat networks (low temperature). It is the first choice for multi-family houses and apartment buildings.</td><td>• Solar water heater (the first choice if applicable)
• Electric water heater</td></tr>
<tr><td>Balanced ventilation</td><td>Electric heat pump. It is the first choice for single-family houses and terraced houses.</td><td>• Solar water heater (the first choice if applicable)
• Electric water heater</td></tr>
</table>

7.4.5 Environmental impact factors

Table S7.4.16 GHG emissions factors (SSP2-base) [142,216] of primary material production from ecoinvent 3.6 (kg CO_2 eq/kg) [138,280].

Materials	Product	Activity	Location	2015-2019	2020-2024	2025-2029	2030-2034	2035-2039	2040-2044	2045-2049	2050
Al	aluminium, wrought alloy	market for aluminium, wrought alloy	GLO	11.1708	11.0726	10.9905	10.9299	10.8688	10.7739	10.7226	10.7092
Ar	argon, liquid	market for argon, liquid	RoW	2.1136	2.0157	1.8903	1.7881	1.7290	1.6830	1.6788	1.6938
Bi	bitumen adhesive compound, hot	market for bitumen adhesive compound, hot	GLO	0.5125	0.5114	0.5090	0.5069	0.5056	0.5045	0.5043	0.5045
CB	clay brick	market for clay brick	GLO	0.3054	0.3041	0.3019	0.3000	0.2988	0.2979	0.2976	0.2978
Ce	ceramic tile	market for ceramic tile	GLO	0.7372	0.7252	0.7100	0.6981	0.6911	0.6857	0.6857	0.6882
Co	copper	market for copper	GLO	4.1972	4.1027	4.0054	3.9332	3.8907	3.8575	3.8601	3.8794
CI	cast iron	market for cast iron	GLO	1.7268	1.7104	1.6888	1.6710	1.6606	1.6526	1.6519	1.6547
Cr	concrete, normal	market for concrete, normal	CH	0.0737	0.0743	0.0733	0.0720	0.0711	0.0702	0.0696	0.0693
EPS	polystyrene, expandable	market for polystyrene, expandable	GLO	3.6422	3.6418	3.6412	3.6406	3.6403	3.6400	3.6400	3.6401

Gl	flat glass, coated	market for flat glass, coated	RoW	1.1517	1.1423	1.1335	1.1269	1.1234	1.1213	1.1223	1.1244
Gr	gravel, crushed	market for gravel, crushed	CH	0.0088	0.0090	0.0087	0.0083	0.0080	0.0078	0.0076	0.0075
Gy	gypsum, mineral	gypsum quarry operation	CH	0.0026	0.0027	0.0026	0.0025	0.0025	0.0024	0.0024	0.0024
HW	sawnwood, hardwood, raw	sawing, hardwood	CH	-2.1050	-2.1040	-2.1057	-2.1078	-2.1092	-2.1107	-2.1116	-2.1122
MW	glass wool mat	market for glass wool mat	GLO	2.3360	2.2667	2.1758	2.1053	2.0630	2.0302	2.0286	2.0413
Pl	extrusion, plastic pipes	market for extrusion, plastic pipes	GLO	0.3488	0.3390	0.3189	0.3009	0.2899	0.2797	0.2761	0.2761
PUR	polyurethane, flexible foam	market for polyurethane, flexible foam	RER	5.4463	5.4495	5.4394	5.4282	5.4206	5.4118	5.4061	5.4028
Pw	plywood, for indoor use	market for plywood, for indoor use	RER	-3.1333	-3.1204	-3.1531	-3.1899	-3.2151	-3.2442	-3.2631	-3.2743
RC	fibre-reinforced concrete	market for fibre-reinforced concrete, steel	BR	0.1738	0.1736	0.1736	0.1735	0.1732	0.1731	0.1733	0.1734
Sa	sand	gravel and sand quarry	CH	0.0037	0.0039	0.0037	0.0035	0.0033	0.0031	0.0031	0.0030

		operation									
SC	cement mortar	market for cement mortar	CH	0.2401	0.2424	0.2384	0.2336	0.2304	0.2268	0.2248	0.2235
St	wire drawing, steel	market for wire drawing, steel	GLO	0.3117	0.3049	0.2992	0.2952	0.2932	0.2922	0.2933	0.2950
SW	sawnwood, softwood, raw	sawing, softwood	CH	-1.4715	-1.4705	-1.4721	-1.4741	-1.4754	-1.4768	-1.4776	-1.4781
WF	fibreboard, soft	fibreboard production, soft, from wet & dry processes	Europe without Switzerland	-0.0821	-0.0807	-0.0867	-0.0935	-0.0983	-0.1045	-0.1087	-0.1113
XPS	polystyrene, extruded	market for polystyrene, extruded	GLO	9.5244	9.4950	9.4501	9.4121	9.3897	9.3708	9.3668	9.3701
Zn	zinc	market for zinc	GLO	3.1601	3.1950	3.0817	2.9311	2.8472	2.7568	2.7267	2.7197

Table S7.4.17 GHG emissions factors (SSP2-2.6) [142,216] of primary material production from ecoinvent 3.6 (kg CO_2 eq/kg) [138,280].

Materials	Product	Activity	Location	2015 - 2019	2020 - 2024	2025 - 2029	2030 - 2034	2035 - 2039	2040 - 2044	2045 - 2049	2050
Al	aluminium, wrought alloy	market for aluminium, wrought alloy	GLO	11.1667	11.0403	10.9137	10.8074	10.6457	10.4540	10.3293	10.2472
Ar	argon, liquid	market for argon, liquid	RoW	2.0820	1.8549	1.5417	1.2476	0.7770	0.3092	0.1337	0.0731

Bi	bitumen adhesive compound, hot	market for bitumen adhesive compound, hot	GLO	0.5119	0.5084	0.5029	0.4973	0.4885	0.4802	0.4769	0.4754
CB	clay brick	market for clay brick	GLO	0.3049	0.3014	0.2961	0.2909	0.2826	0.2747	0.2717	0.2706
Ce	ceramic tile	market for ceramic tile	GLO	0.7333	0.7047	0.6652	0.6269	0.5679	0.5106	0.4893	0.4794
Co	copper	market for copper	GLO	4.1720	3.9733	3.7175	3.4744	3.1055	2.7341	2.5898	2.5228
CI	cast iron	market for cast iron	GLO	1.7212	1.6818	1.6266	1.5741	1.4909	1.4091	1.3786	1.3668
Cr	concrete, normal	market for concrete, normal	CH	0.0734	0.0737	0.0723	0.0702	0.0666	0.0638	0.0628	0.0627
EPS	polystyrene, expandable	market for polystyrene, expandable	GLO	3.6420	3.6409	3.6392	3.6376	3.6350	3.6325	3.6316	3.6311
Gl	flat glass, coated	market for flat glass, coated	RoW	1.1494	1.1296	1.1055	1.0838	1.0498	1.0143	1.0009	0.9956
Gr	gravel, crushed	market for gravel, crushed	CH	0.0087	0.0088	0.0084	0.0077	0.0066	0.0058	0.0055	0.0055
Gy	gypsum, mineral	gypsum quarry operation	CH	0.0026	0.0026	0.0026	0.0024	0.0022	0.0021	0.0020	0.0020
HW	sawnwood, hardwood, raw	sawing, hardwood	CH	-2.1054	-2.1050	-2.1074	-2.1108	-2.1167	-2.1213	-2.1230	-2.1232

MW	glass wool mat	market for glass wool mat	GLO	2.3139	2.1527	1.9243	1.7032	1.3646	1.0343	0.9115	0.8547
Pl	extrusion, plastic pipes	market for extrusion, plastic pipes	GLO	0.3437	0.3161	0.2702	0.2246	0.1503	0.0809	0.0549	0.0469
PUR	polyurethane, flexible foam	market for polyurethane, flexible foam	RER	5.4438	5.4419	5.4249	5.4042	5.3687	5.3417	5.3316	5.3299
Pw	plywood, for indoor use	market for plywood, for indoor use	RER	-3.1413	-3.1435	-3.1962	-3.2625	-3.3766	-3.4624	-3.4944	-3.4989
RC	fibre-reinforced concrete	market for fibre-reinforced concrete, steel	BR	0.1736	0.1723	0.1710	0.1698	0.1678	0.1660	0.1657	0.1655
Sa	sand	gravel and sand quarry operation	CH	0.0037	0.0038	0.0035	0.0032	0.0025	0.0021	0.0019	0.0019
SC	cement mortar	market for cement mortar	CH	0.2392	0.2401	0.2345	0.2266	0.2127	0.2021	0.1981	0.1977
St	wire drawing, steel	market for wire drawing, steel	GLO	0.3103	0.2963	0.2802	0.2660	0.2439	0.2202	0.2113	0.2077
SW	sawnwood, softwood, raw	sawing, softwood	CH	-1.4719	-1.4715	-1.4737	-1.4769	-1.4824	-1.4866	-1.4883	-1.4884

WF	fibreboard, soft	fibreboard production, soft, from wet & dry processes	Europe without Switzerland	-0.0837	-0.0859	-0.0968	-0.1096	-0.1319	-0.1485	-0.1544	-0.1556
XPS	polystyrene, extruded	market for polystyrene, extruded	GLO	9.5131	9.4398	9.3316	9.2277	9.0604	8.8983	8.8375	8.8170
Zn	zinc	market for zinc	GLO	3.1193	3.0114	2.7432	2.3736	1.7496	1.2504	1.0924	1.0431

Table S7.4.18 GHG emissions factors (SSP2-base) [142,216] of recycled building materials. The materials are from ecoinvent 3.6 (kg CO_2 eq/kg) [138]. The factors of the other recycled materials are assumed as zero [280].

Materials	Product	Activity	Location	2015-2019	2020-2024	2025-2029	2030-2034	2035-2039	2040-2044	2045-2049	2050
Al	aluminium scrap, post-consumer, prepared for melting	aluminium scrap, post-consumer, prepared for melting, Recycled Content cut-off	GLO	0.0000	0.0000	0.0000	0.0000	0.0000	0.0000	0.0000	0.0000
Ar	-	-	-	0.0000	0.0000	0.0000	0.0000	0.0000	0.0000	0.0000	0.0000
Bi	waste bitumen sheet	market for waste bitumen sheet	CH	-2.3591	-2.3587	-2.3580	-2.3573	-2.3569	-2.3565	-2.3563	-2.3563
CB	waste brick	treatment of waste brick, recycling	CH	-0.0033	-0.0033	-0.0033	-0.0033	-0.0033	-0.0033	-0.0033	-0.0033

Ce	-	-	-	0.0000	0.0000	0.0000	0.0000	0.0000	0.0000	0.0000	0.0000
Co	-	-	-	0.0000	0.0000	0.0000	0.0000	0.0000	0.0000	0.0000	0.0000
CI	iron scrap, sorted, pressed	iron scrap, sorted, pressed, Recycled Content cut-off	GLO	0.0000	0.0000	0.0000	0.0000	0.0000	0.0000	0.0000	0.0000
Cr	waste concrete, not reinforced	treatment of waste concrete, not reinforced, recycling	Europe without Switzerland	-0.0040	-0.0040	-0.0040	-0.0040	-0.0040	-0.0040	-0.0040	-0.0040
EPS	-	-	-	0.0000	0.0000	0.0000	0.0000	0.0000	0.0000	0.0000	0.0000
Gl	glass cullet, sorted	glass cullet, sorted, Recycled Content cut-off	GLO	0.0000	0.0000	0.0000	0.0000	0.0000	0.0000	0.0000	0.0000
Gr	-	-	-	0.0000	0.0000	0.0000	0.0000	0.0000	0.0000	0.0000	0.0000
Gy	waste gypsum plaster board	treatment of waste gypsum plaster board, recycling	CH	-0.0033	-0.0033	-0.0033	-0.0033	-0.0033	-0.0033	-0.0033	-0.0033
HW	waste wood, post-consumer	waste wood, post-consumer, Recycled Conte	GLO	0.0000	0.0000	0.0000	0.0000	0.0000	0.0000	0.0000	0.0000

		nt cut-off									
MW	-	-	-	0.0000	0.0000	0.0000	0.0000	0.0000	0.0000	0.0000	0.0000
Pl	-	-	-	0.0000	0.0000	0.0000	0.0000	0.0000	0.0000	0.0000	0.0000
PUR	-	-	-	0.0000	0.0000	0.0000	0.0000	0.0000	0.0000	0.0000	0.0000
Pw	-	-	-	0.0000	0.0000	0.0000	0.0000	0.0000	0.0000	0.0000	0.0000
RC	-	-	-	0.0000	0.0000	0.0000	0.0000	0.0000	0.0000	0.0000	0.0000
Sa	-	-	-	0.0000	0.0000	0.0000	0.0000	0.0000	0.0000	0.0000	0.0000
SC	-	-	-	0.0000	0.0000	0.0000	0.0000	0.0000	0.0000	0.0000	0.0000
St	waste reinforcement steel	treatment of waste reinforcement steel, recycling	CH	-0.0574	-0.0573	-0.0572	-0.0571	-0.0571	-0.0570	-0.0570	-0.0570
SW	waste wood, post-consumer	waste wood, post-consumer, Recycled Content cut-off	GLO	0.0000	0.0000	0.0000	0.0000	0.0000	0.0000	0.0000	0.0000
WF	-	-	-	0.0000	0.0000	0.0000	0.0000	0.0000	0.0000	0.0000	0.0000
XPS	-	-	-	0.0000	0.0000	0.0000	0.0000	0.0000	0.0000	0.0000	0.0000

Zn	-	-	-	0.0000	0.0000	0.0000	0.0000	0.0000	0.0000	0.0000	0.0000

Table S7.4.19 GHG emissions factors (SSP2-2.6) [142,216] of recycled building materials. The materials are from ecoinvent 3.6 (kg CO_2 eq/kg) [138]. The factors of the other recycled materials are assumed as zero [280].

Materials	Product	Activity	Location	2015-2019	2020-2024	2025-2029	2030-2034	2035-2039	2040-2044	2045-2049	2050
Al	aluminium scrap, post-consumer, prepared for melting	aluminium scrap, post-consumer, prepared for melting, Recycled Content cut-off	GLO	0.0000	0.0000	0.0000	0.0000	0.0000	0.0000	0.0000	0.0000
Ar	-	-	-	0.0000	0.0000	0.0000	0.0000	0.0000	0.0000	0.0000	0.0000
Bi	waste bitumen sheet	market for waste bitumen sheet	CH	-2.3589	-2.3579	-2.3562	-2.3544	-2.3516	-2.3490	-2.3480	-2.3477
CB	waste brick	treatment of waste brick, recycling	CH	-0.0033	-0.0033	-0.0033	-0.0033	-0.0032	-0.0032	-0.0032	-0.0032
Ce	-	-	-	0.0000	0.0000	0.0000	0.0000	0.0000	0.0000	0.0000	0.0000
Co	-	-	-	0.0000	0.0000	0.0000	0.0000	0.0000	0.0000	0.0000	0.0000
CI	iron scrap, sorted, pressed	iron scrap, sorted, pressed, Recycled Content cut-off	GLO	0.0000	0.0000	0.0000	0.0000	0.0000	0.0000	0.0000	0.0000

Cr	waste concrete, not reinforced	treatment of waste concrete, not reinforced, recycling	Europe without Switzerland	-0.0040	-0.0040	-0.0040	-0.0040	-0.0039	-0.0039	-0.0039	-0.0039
EPS	-	-	-	0.0000	0.0000	0.0000	0.0000	0.0000	0.0000	0.0000	0.0000
Gl	glass cullet, sorted	glass cullet, sorted, Recycled Content cut-off	GLO	-2.3589	-2.3579	-2.3562	-2.3544	-2.3516	-2.3490	-2.3480	-2.3477
Gr	-	-	-	0.0000	0.0000	0.0000	0.0000	0.0000	0.0000	0.0000	0.0000
Gy	waste gypsum plasterboard	treatment of waste gypsum plasterboard, recycling	CH	-0.0033	-0.0033	-0.0033	-0.0033	-0.0032	-0.0032	-0.0032	-0.0032
HW	waste wood, post-consumer	waste wood, post-consumer, Recycled Content cut-off	GLO	0.0000	0.0000	0.0000	0.0000	0.0000	0.0000	0.0000	0.0000
MW	-	-	-	0.0000	0.0000	0.0000	0.0000	0.0000	0.0000	0.0000	0.0000
Pl	-	-	-	0.0000	0.0000	0.0000	0.0000	0.0000	0.0000	0.0000	0.0000
PUR	-	-	-	0.0000	0.0000	0.0000	0.0000	0.0000	0.0000	0.0000	0.0000

Pw	-	-	-	0.0000	0.0000	0.0000	0.0000	0.0000	0.0000	0.0000	0.0000
RC	-	-	-	0.0000	0.0000	0.0000	0.0000	0.0000	0.0000	0.0000	0.0000
Sa	-	-	-	0.0000	0.0000	0.0000	0.0000	0.0000	0.0000	0.0000	0.0000
SC	-	-	-	0.0000	0.0000	0.0000	0.0000	0.0000	0.0000	0.0000	0.0000
St	waste reinforcement steel	treatment of waste reinforcement steel, recycling	CH	-0.0573	-0.0572	-0.0569	-0.0567	-0.0563	-0.0560	-0.0558	-0.0558
SW	waste wood, post-consumer	waste wood, post-consumer, Recycled Content cut-off	GLO	0.0000	0.0000	0.0000	0.0000	0.0000	0.0000	0.0000	0.0000
WF	-	-	-	0.0000	0.0000	0.0000	0.0000	0.0000	0.0000	0.0000	0.0000
XPS	-	-	-	0.0000	0.0000	0.0000	0.0000	0.0000	0.0000	0.0000	0.0000
Zn	-	-	-	0.0000	0.0000	0.0000	0.0000	0.0000	0.0000	0.0000	0.0000

Table S7.4.20 GHG emissions factors [142,216] of transportation from ecoinvent 3.6 (kg CO_2 eq/(kg·km)) [138,280].

Transportation methods	Product	Activity	Location	2015-2019	2020-2024	2025-2029	2030-2034	2035-2039	2040-2044	2045-2049	2050
Truck transportation	transport, freight, lorry	transport, freight, lorry 16-32 metric	RER	0.0002	0.0002	0.0002	0.0002	0.0002	0.0002	0.0002	0.0002

(SSP2-base)	16-32 metric ton, EURO6	ton, EURO6									
Ship transportation (SSP2-base)	transport, freight, sea, container ship	market for transport, freight, sea, container ship	GLO	0.0000	0.0000	0.0000	0.0000	0.0000	0.0000	0.0000	0.0000
Truck transportation (SSP2-2.6)	transport, freight, lorry 16-32 metric ton, EURO6	transport, freight, lorry 16-32 metric ton, EURO6	RER	0.0002	0.0002	0.0002	0.0002	0.0002	0.0002	0.0002	0.0002
Ship transportation (SSP2-2.6)	transport, freight, sea, container ship	market for transport, freight, sea, container ship	GLO	0.0000	0.0000	0.0000	0.0000	0.0000	0.0000	0.0000	0.0000

Table S7.4.21 GHG emissions factors of landfill from ecoinvent 3.6 (kg CO_2 eq/kg) [138,142,280].

Materials	Product	Activity	Location	2015-2019	2020-2024	2025-2029	2030-2034	2035-2039	2040-2044	2045-2049	2050
Landfill (SSP2-base)	inert waste	treatment of inert waste, sanitary landfill	Europe without Switzerland	-0.0103	-0.0102	-0.0101	-0.0100	-0.0100	-0.0100	-0.0099	-0.0100
Landfill (SSP2-2.6)	inert waste	treatment of inert waste, sanitary landfill	Europe without Switzerland	-0.0103	-0.0101	-0.0098	-0.0096	-0.0092	-0.0088	-0.0087	-0.0086

Table S7.4.22 GHG emissions factors (SSP2-base) of energy supply from ecoinvent 3.6 (kg CO_2 eq/kWh) [138,248].

Energy supply	Product	Activity	Location	2015-2020	2021-2025	2026-2030	2031-2035	2036-2040	2041-2045	2046-2050
Natural gas boiler	Heat, central or small-scale, natural gas	Heat production, natural gas, at boiler condensing modulating <100kW	Europe without Switzerland	0.25	0.25	0.25	0.25	0.25	0.25	0.25

Heat network (LT)	Heat	Geothermal (GHG emission factor is from [74])	NL	0.09	0.09	0.09	0.09	0.09	0.09	0.09
Heat network (HT)	heat, district or industrial, natural gas	heat and power co-generation, natural gas, conventional power plant, 100MW electrical	NL	0.10	0.10	0.10	0.10	0.10	0.10	0.10
Electric heat pump	Heat, air-water heat pump 10kW	Market for floor heating from air-water heat pump	Europe without Switzerland	0.26	0.24	0.22	0.20	0.18	0.17	0.16
Solar water heater	Heat, central or small-scale, other than natural gas	Operation, solar collector system, Cu flat plate collector, multiple dwelling, for hot water	CH	0.01	0.01	0.01	0.01	0.01	0.01	0.01
Grid electricity	Electricity, low voltage	Market for electricity, low voltage	NL	0.66	0.59	0.52	0.47	0.42	0.38	0.37
PV electricity	Electricity, low voltage	Electricity production, photovoltaic, 3kWp slanted-roof installation, multi-Si, panel, mounted	NL	0.08	0.08	0.08	0.07	0.07	0.07	0.07

Table S7.4.23 GHG emissions factors (SSP2-2.6) of energy supply from ecoinvent 3.6 (kg CO_2 eq/kWh) [138,248].

Energy supply	Product	Activity	Location	2015-2020	2021-2025	2026-2030	2031-2035	2036-2040	2041-2045	2046-2050
Natural gas boiler	Heat, central or small-scale, natural gas	Heat production, natural gas, at boiler condensing	Europe without Switzerland	0.25	0.25	0.25	0.25	0.25	0.25	0.25

		modulating <100kW								
Heat network (LT)	Heat	Geothermal (GHG emission factor is from [74])	NL	0.09	0.09	0.09	0.09	0.09	0.09	0.09
Heat network (HT)	heat, district or industrial, natural gas	heat and power co-generation, natural gas, conventional power plant, 100MW electrical	NL	0.10	0.10	0.10	0.10	0.09	0.09	0.09
Electric heat pump	Heat, air-water heat pump 10kW	Market for floor heating from air-water heat pump	Europe without Switzerland	0.25	0.22	0.18	0.11	0.05	0.03	0.03
Solar water heater	Heat, central or small-scale, other than natural gas	Operation, solar collector system, Cu flat plate collector, multiple dwelling, for hot water	CH	0.01	0.01	0.01	0.01	0.01	0.01	0.01
Grid electricity	Electricity, low voltage	Market for electricity, low voltage	NL	0.63	0.54	0.44	0.22	0.06	0.00	-0.01
PV electricity	Electricity, low voltage	Electricity production, photovoltaic,	NL	0.08	0.07	0.06	0.05	0.04	0.04	0.04

		3kWp slanted-roof installation, multi-Si, panel, mounted								

7.4.6 The effect of faster heat transition on GHG emissions

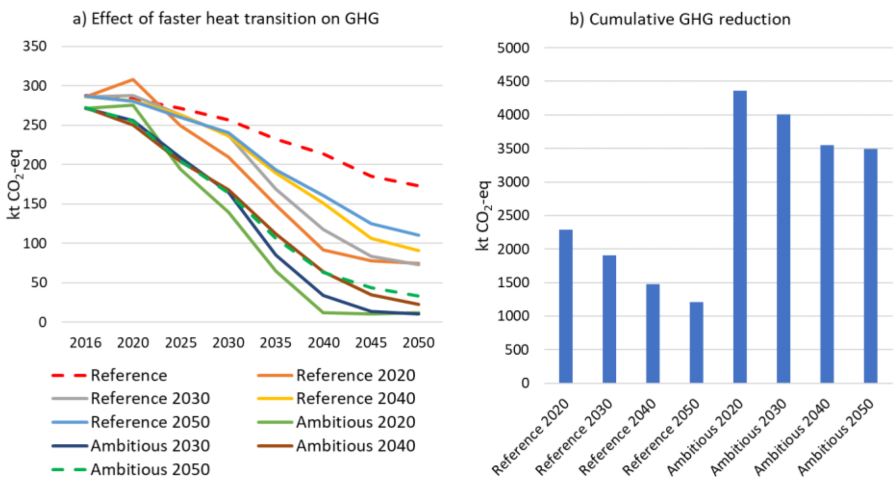

Figure S7.4.2 The effect of faster heat transition on reducing GHG emissions. The years are the earliest time when all the neighborhoods have implemented the natural-gas-free plan. It means that buildings will be installed with conventional heating systems, such as natural gas boilers if the natural-gas-free plan is not implemented. The dash lines are the default heat transition paces used in the study. The cumulative GHG emissions (2016-2050) are in comparison with the reference scenario.

References

[1] EASAC. Decarbonisation of buildings: for climate, health and jobs. 2021.

[2] Heeren N. Modelling environmental impacts of buildings – energy, material, and dynamics. ETH Zürich, 2017. doi:10.3929/ethz-a-010853498.

[3] IRP. Resource Efficiency and Climate Change: Material Efficiency Strategies for a Low-Carbon Future. 2020. doi:10.5281/zenodo.3542680.

[4] González A, Sendra C, Herena A, Rosquillas M, Vaz D. Methodology to assess the circularity in building construction and refurbishment activities. Resour Conserv Recycl Adv 2021;12:200051. doi:https://doi.org/10.1016/j.rcradv.2021.200051.

[5] United Nations Environment Programme. 2020 Global Status Report for Buildings and Construction: Towards a zero-emissions, efficient and resilient buildings and construction sector. Nairobi: 2020.

[6] Wit M de, Ramkumar JHS, Douma HFA. The Circularity Gap Report - An analysis of the circular state of the global economy. 2018.

[7] Krausmann F, Lauk C, Haas W, Wiedenhofer D. From resource extraction to outflows of wastes and emissions: The socioeconomic metabolism of the global economy, 1900–2015. Glob Environ Chang 2018;52:131–40. doi:https://doi.org/10.1016/j.gloenvcha.2018.07.003.

[8] Iyer-Raniga U, Huovila P. Global State of Play for Circular Built Environment. 2021.

[9] United Nations Environment Programme. 2021 Global Status Report for Buildings and Construction: Towards a zero-emissions, efficient and resilient buildings and construction sector. Nairobi: 2021.

[10] Mastrucci A, van Ruijven B, Byers E, Poblete-Cazenave M, Pachauri S. Global scenarios of residential heating and cooling energy demand and CO2 emissions. Clim Change 2021;168:14. doi:10.1007/s10584-021-03229-3.

[11] CE Delft. Zero carbon buildings 2050. 2020.

[12] Streicher KN, Berger M, Panos E, Narula K, Soini MC, Patel MK. Optimal building retrofit pathways considering stock dynamics and climate change impacts. Energy Policy 2021;152:112220. doi:https://doi.org/10.1016/j.enpol.2021.112220.

[13] Grubler A, Wilson C, Bento N, Boza-Kiss B, Krey V, McCollum DL, et al. A low energy demand scenario for meeting the 1.5 °C target and sustainable development goals without negative emission technologies. Nat Energy 2018;3:515–27. doi:10.1038/s41560-018-0172-6.

[14] Anu R, G. RA, J. CP, Rahul SK, Emani K. Meta-principles for developing smart, sustainable, and healthy cities. Science (80-) 2016;352:940–3. doi:10.1126/science.aaf7160.

[15] IEA (International Energy Agency). Net Zero by 2050 A Roadmap for the Global Energy Sector. 2021.

[16] Sun Z, Ma Z, Ma M, Cai W, Xiang X, Zhang S, et al. Carbon Peak and Carbon Neutrality in the Building Sector: A Bibliometric Review. Build 2022;12. doi:10.3390/buildings12020128.

[17] IRP. The Weight of Cities: Resource Requirements of Future Urbanization. 2018.

[18] Ramaswami A, Tong K, Canadell JG, Jackson RB, Stokes E (Kellie), Dhakal S, et al. Carbon analytics for net-zero emissions sustainable cities. Nat Sustain 2021;4:460–3. doi:10.1038/s41893-021-00715-5.

[19] Hamida MB, Jylhä T, Remøy H, Gruis V. Circular building adaptability and its determinants – A literature review. Int J Build Pathol Adapt 2022;ahead-of-p. doi:10.1108/IJBPA-11-2021-0150.

[20] Yang X, Hu M, Wu J, Zhao B. Building-information-modeling enabled life cycle assessment, a case study on carbon footprint accounting for a residential building in China. J Clean Prod 2018;183:729–43. doi:10.1016/j.jclepro.2018.02.070.

[21] Ibn-Mohammed T, Greenough R, Taylor S, Ozawa-Meida L, Acquaye A. Operational vs. embodied emissions in buildings—A review of current trends. Energy Build 2013;66:232–45. doi:https://doi.org/10.1016/j.enbuild.2013.07.026.

[22] Parkin A, Herrera M, Coley DA. Net-zero buildings: when carbon and energy metrics diverge. Build Cities 2020;1:86–99. doi:10.5334/bc.27.

[23] Odyssee-Mure. Energy efficiency trends in buildings in the EU. 2018.

[24] Göswein V, Dinis Silvestre J, Habert G, Freire F. Dynamic Assessment of Construction Materials in Urban Building Stocks: A Critical Review. Environ Sci Technol 2019;53:9992–10006. doi:10.1021/acs.est.9b01952.

[25] Azari R, Abbasabadi N. Embodied energy of buildings: A review of data, methods, challenges, and research trends. Energy Build 2018. doi:10.1016/j.enbuild.2018.03.003.

[26] Sandberg NH, Sartori I, Vestrum MI, Brattebø H. Using a segmented dynamic dwelling stock model for scenario analysis of future energy demand: The dwelling stock of Norway 2016–2050. Energy Build 2017;146:220–32. doi:10.1016/J.ENBUILD.2017.04.016.

[27] Yang X, Hu M, Heeren N, Zhang C, Verhagen T, Tukker A, et al. A combined GIS-archetype approach to model residential space heating energy: A case study for the Netherlands including validation. Appl Energy 2020;280:115953. doi:10.1016/j.apenergy.2020.115953.

[28] Roca-Puigròs M, Billy RG, Gerber A, Wäger P, Müller DB. Pathways toward a carbon-neutral Swiss residential building stock. Build Cities 2020;1:579–93. doi:10.5334/bc.61.

[29] Röck M, Baldereschi E, Verellen E, Passer A, Sala S, Allacker K. Environmental modelling of building stocks – An integrated review of life cycle-based assessment models to support EU policy making. Renew Sustain Energy Rev 2021;151:111550. doi:https://doi.org/10.1016/j.rser.2021.111550.

[30] Hietaharju P, Pulkkinen J, Ruusunen M, Louis J-N. A stochastic dynamic building stock model for determining long-term district heating demand under future climate change. Appl Energy 2021;295:116962. doi:https://doi.org/10.1016/j.apenergy.2021.116962.

[31] Göswein V, Silvestre JD, Monteiro C, Habert G, Freire F, Pittau F. Influence of materials choice, renovation rate, and electricity grid to achieve a Paris agreement-compatible building stock: A Portuguese case study. Build Environ 2021:107773. doi:https://doi.org/10.1016/j.buildenv.2021.107773.

[32] Röck M, Saade MRM, Balouktsi M, Rasmussen FN, Birgisdottir H, Frischknecht R, et al. Embodied GHG emissions of buildings – The hidden challenge for effective climate change mitigation. Appl Energy 2020;258:114107. doi:10.1016/J.APENERGY.2019.114107.

[33] Hertwich EG, Ali S, Ciacci L, Fishman T, Heeren N, Masanet E, et al. Material efficiency strategies to reducing greenhouse gas emissions associated with buildings, vehicles, and electronics—a review. Environ Res Lett 2019;14:043004. doi:10.1088/1748-9326/ab0fe3.

[34] Zhong X, Hu M, Deetman S, Steubing B, Lin HX, Hernandez GA, et al. Global greenhouse gas emissions from residential and commercial building materials and mitigation strategies to 2060. Nat Commun 2021;12:6126. doi:10.1038/s41467-021-26212-z.

[35] Pauliuk S, Heeren N, Berrill P, Fishman T, Nistad A, Tu Q, et al. Global scenarios of resource and emission savings from material efficiency in residential buildings and cars. Nat Commun 2021;12:5097. doi:10.1038/s41467-021-25300-4.

[36] Huang T, Shi F, Tanikawa H, Fei J, Han J. Materials demand and environmental impact of buildings construction and demolition in China based on dynamic material flow analysis. Resour Conserv Recycl 2013;72:91–101. doi:10.1016/J.RESCONREC.2012.12.013.

[37] Deetman S, Marinova S, van der Voet E, van Vuuren DP, Edelenbosch O, Heijungs R. Modelling global material stocks and flows for residential and service sector buildings towards 2050. J Clean Prod 2020;245:118658. doi:10.1016/J.JCLEPRO.2019.118658.

[38] Sorace C, Hurst W. China's Phantom Urbanisation and the Pathology of Ghost Cities. J Contemp Asia 2016;46:304–22. doi:10.1080/00472336.2015.1115532.

[39] OECD. Global Material Resources Outlook to 2060. OECD; 2019. doi:10.1787/9789264307452-en.

[40] Jiang M, Behrens P, Yang Y, Tang Z, Chen D, Yu Y, et al. Different Material Footprint Trends between China and the World in 2007-2012 Explained by Construction- and Manufacturing-associated Investment. One Earth 2022;5:109–19. doi:https://doi.org/10.1016/j.oneear.2021.12.011.

[41] Anastasiades K, Goffin J, Rinke M, Buyle M, Audenaert A, Blom J. Standardisation: An essential enabler for the circular reuse of construction components? A trajectory for a cleaner European construction industry. J Clean Prod 2021;298:126864. doi:https://doi.org/10.1016/j.jclepro.2021.126864.

[42] Kim J. Construction and demolition waste management in Korea: recycled aggregate and its application. Clean Technol Environ Policy 2021;23:2223–34. doi:10.1007/s10098-021-02177-x.

[43] Zhang C, Hu M, Yang X, Miranda-Xicotencatl B, Sprecher B, Di Maio F, et al. Upgrading construction and demolition waste management from downcycling to recycling in the Netherlands. J Clean Prod 2020;266:121718. doi:10.1016/j.jclepro.2020.121718.

[44] Verhagen TJ, Sauer ML, van der Voet E, Sprecher B. Matching Demolition and Construction Material Flows , an Urban Mining Case Study. Sustainability 2021;13. doi:10.3390/su13020653.

[45] Tavares V, Gregory J, Kirchain R, Freire F. What is the potential for prefabricated buildings to decrease costs and contribute to meeting EU environmental targets? Build Environ

2021;206:108382. doi:https://doi.org/10.1016/j.buildenv.2021.108382.

[46] O'Grady T, Minunno R, Chong H-Y, Morrison GM. Design for disassembly, deconstruction and resilience: A circular economy index for the built environment. Resour Conserv Recycl 2021;175:105847. doi:https://doi.org/10.1016/j.resconrec.2021.105847.

[47] Vandervaeren C, Galle W, Stephan A, De Temmerman N. More than the sum of its parts: Considering interdependencies in the life cycle material flow and environmental assessment of demountable buildings. Resour Conserv Recycl 2022;177:106001. doi:https://doi.org/10.1016/j.resconrec.2021.106001.

[48] Fiorito F. Trombe Walls for Lightweight Buildings in Temperate and Hot Climates. Exploring the Use of Phase-change Materials for Performances Improvement. Energy Procedia 2012;30:1110–9. doi:https://doi.org/10.1016/j.egypro.2012.11.124.

[49] Liu Z, Hou J, Meng X, Dewancker BJ. A numerical study on the effect of phase-change material (PCM) parameters on the thermal performance of lightweight building walls. Case Stud Constr Mater 2021;15:e00758. doi:https://doi.org/10.1016/j.cscm.2021.e00758.

[50] Miller SA, Habert G, Myers RJ, Harvey JT. Achieving net zero greenhouse gas emissions in the cement industry via value chain mitigation strategies. One Earth 2021;4:1398–411. doi:https://doi.org/10.1016/j.oneear.2021.09.011.

[51] Heeren N, Mutel CL, Steubing B, Ostermeyer Y, Wallbaum H, Hellweg S. Environmental Impact of Buildings—What Matters? Environ Sci Technol 2015;49:9832–41. doi:10.1021/acs.est.5b01735.

[52] Alina G, Maliki M, Alexander H, Sébastien L, Bruno S, Guillaume H. Bio-based materials as a robust and optimal solution for building renovation. CEES 2021, 2021. doi:10.3929/ethz-b-000515477.

[53] Habert G. Fast-Growing Bio-Based Materials Can Heal the World. Build Cities 2021. https://www.buildingsandcities.org/insights/commentaries/cop26-biobased-materials.html (accessed January 7, 2022).

[54] Pomponi F, Hart J, Arehart JH, D'Amico B. Buildings as a Global Carbon Sink? A Reality Check on Feasibility Limits. One Earth 2020;3:157–61. doi:https://doi.org/10.1016/j.oneear.2020.07.018.

[55] Cao Z, Myers RJ, Lupton RC, Duan H, Sacchi R, Zhou N, et al. The sponge effect and carbon emission mitigation potentials of the global cement cycle. Nat Commun 2020;11. doi:10.1038/s41467-020-17583-w.

[56] Ren L, Zhou S, Peng T, Ou X. A review of CO2 emissions reduction technologies and low-carbon development in the iron and steel industry focusing on China. Renew Sustain Energy Rev 2021;143:110846. doi:https://doi.org/10.1016/j.rser.2021.110846.

[57] Creutzig F, Niamir L, Bai X, Callaghan M, Cullen J, Díaz-José J, et al. Demand-side solutions to climate change mitigation consistent with high levels of well-being. Nat Clim Chang 2021. doi:10.1038/s41558-021-01219-y.

[58] John Barrett, Steve Pye, Sam Betts-Davies, Nick Eyre, Oliver Broad, James Price, Jonathan Norman, Jillian Anable, George Bennett, Christian Brand, Rachel Carr-Whitworth, Greg Marsden, Tadj Oreszczyn, Jannik Giesekam, Alice Garvey PR and KS. The role of energy

demand reduction in achieving net-zero in the UK. 2021.

[59] Knobloch F, Pollitt H, Chewpreecha U, Daioglou V, Mercure J-F. Simulating the deep decarbonisation of residential heating for limiting global warming to 1.5 °C. Energy Effic 2019;12:521–50. doi:10.1007/s12053-018-9710-0.

[60] Milieu Centraal. Step-by-step plan for natural gas-free living n.d. https://www.milieucentraal.nl/energie-besparen/energiezuinig-huis/wonen-zonder-aardgas/stappenplan-aardgasvrij-wonen/ (accessed October 26, 2020).

[61] EPBD. Directive 2010/31/EU of the European Parliament and of the Council of 19 May 2010 on the energy performance of buildings 2010.

[62] Ahmed A, Ge T, Peng J, Yan W-C, Tee BT, You S. Assessment of the renewable energy generation towards net-zero energy buildings: A review. Energy Build 2021:111755. doi:https://doi.org/10.1016/j.enbuild.2021.111755.

[63] Langevin J, Harris CB, Satre-Meloy A, Chandra-Putra H, Speake A, Present E, et al. US building energy efficiency and flexibility as an electric grid resource. Joule 2021;5:2102–28. doi:10.1016/j.joule.2021.06.002.

[64] Hainsch K, Löffler K, Burandt T, Auer H, Crespo del Granado P, Pisciella P, et al. Energy transition scenarios: What policies, societal attitudes, and technology developments will realize the EU Green Deal? Energy 2022;239:122067. doi:https://doi.org/10.1016/j.energy.2021.122067.

[65] Gassar AAA, Cha SH. Review of geographic information systems-based rooftop solar photovoltaic potential estimation approaches at urban scales. Appl Energy 2021;291:116817. doi:https://doi.org/10.1016/j.apenergy.2021.116817.

[66] Lu X, Chen S, Nielsen CP, Zhang C, Li J, Xu H, et al. Combined solar power and storage as cost-competitive and grid-compatible supply for China's future carbon-neutral electricity system. Proc Natl Acad Sci 2021;118:e2103471118. doi:10.1073/pnas.2103471118.

[67] Mi P, Zhang J, Han Y, Guo X. Operation performance study and prediction of photovoltaic thermal heat pump system engineering in winter. Appl Energy 2022;306:118071. doi:https://doi.org/10.1016/j.apenergy.2021.118071.

[68] TABULA. National Building Typologies 2013. http://episcope.eu/building-typology/ (accessed October 10, 2019).

[69] Grossmann WD, Grossmann I, Steininger KW. Distributed solar electricity generation across large geographic areas, Part I: A method to optimize site selection, generation and storage. Renew Sustain Energy Rev 2013;25:831–43. doi:https://doi.org/10.1016/j.rser.2012.08.018.

[70] Broersen S, Van den Berg N, Van Deutekom C, van Erk R, Hompes M, Lijding K, et al. State of the State report Solar panels could provide half of Dutch electricity demand. 2018.

[71] Eshraghi H, Rodrigo de Queiroz A, Sankarasubramanian A, DeCarolis JF. Quantification of climate-induced interannual variability in residential U.S. electricity demand. Energy 2021;236:121273. doi:https://doi.org/10.1016/j.energy.2021.121273.

[72] Magrini A, Lentini G, Cuman S, Bodrato A, Marenco L. From nearly zero energy buildings (NZEB) to positive energy buildings (PEB): The next challenge - The most recent European trends with some notes on the energy analysis of a forerunner PEB example. Dev Built

Environ 2020;3:100019. doi:https://doi.org/10.1016/j.dibe.2020.100019.

[73] Khanna TM, Baiocchi G, Callaghan M, Creutzig F, Guias H, Haddaway NR, et al. A multi-country meta-analysis on the role of behavioural change in reducing energy consumption and CO2 emissions in residential buildings. Nat Energy 2021. doi:10.1038/s41560-021-00866-x.

[74] Verhagen TJ, der Voet E, Sprecher B. Alternatives for natural-gas-based heating systems: A quantitative GIS-based analysis of climate impacts and financial feasibility. J Ind Ecol 2021:jiec.13047. doi:10.1111/jiec.13047.

[75] Nasir U, Chang R, Omrany H. Calculation Methods for Construction Material Stocks: A Systematic Review. Appl Sci 2021;11. doi:10.3390/app11146612.

[76] Blok M. Urban mining and circular construction - what, why and how it works n.d. https://www.metabolic.nl/news/urban-mining-and-circular-construction/ (accessed February 12, 2022).

[77] Arora M, Raspall F, Cheah L, Silva A. Buildings and the circular economy: Estimating urban mining, recovery and reuse potential of building components. Resour Conserv Recycl 2020;154:104581. doi:https://doi.org/10.1016/j.resconrec.2019.104581.

[78] Kloostra B, Makarchuk B, Saxe S. Bottom-up estimation of material stocks and flows in Toronto's road network. J Ind Ecol 2022;n/a. doi:https://doi.org/10.1111/jiec.13229.

[79] Soonsawad N, Martinez RM, Schandl H. Material demand, and environmental and climate implications of Australia's building stock: Current status and outlook to 2060. Resour Conserv Recycl 2022;180:106143. doi:https://doi.org/10.1016/j.resconrec.2021.106143.

[80] Mastrucci A, Marvuglia A, Popovici E, Leopold U, Benetto E. Geospatial characterization of building material stocks for the life cycle assessment of end-of-life scenarios at the urban scale. Resour Conserv Recycl 2017. doi:10.1016/j.resconrec.2016.07.003.

[81] Guo Z, Hu D, Zhang F, Huang G, Xiao Q. An integrated material metabolism model for stocks of urban road system in Beijing, China. Sci Total Environ 2014;470–471:883–94. doi:10.1016/J.SCITOTENV.2013.10.041.

[82] Arbabi H, Lanau M, Li X, Meyers G, Dai M, Mayfield M, et al. A scalable data collection, characterization, and accounting framework for urban material stocks. J Ind Ecol 2021;n/a. doi:https://doi.org/10.1111/jiec.13198.

[83] Peled Y, Fishman T. Estimation and mapping of the material stocks of buildings of Europe: a novel nighttime lights-based approach. Resour Conserv Recycl 2021;169:105509. doi:https://doi.org/10.1016/j.resconrec.2021.105509.

[84] Heeren N, Fishman T. A database seed for a community-driven material intensity research platform. Sci Data 2019;6:23. doi:10.1038/s41597-019-0021-x.

[85] Yang D, Guo J, Sun L, Shi F, Liu J, Tanikawa H. Urban buildings material intensity in China from 1949 to 2015. Resour Conserv Recycl 2020;159. doi:10.1016/j.resconrec.2020.104824.

[86] Fu C, Zhang Y, Deng T, Daigo I. The evolution of material stock research: From exploring to rising to hot studies. J Ind Ecol 2021;n/a. doi:https://doi.org/10.1111/jiec.13195.

[87] Swan LG, Ugursal VI. Modeling of end-use energy consumption in the residential sector: A review of modeling techniques. Renew Sustain Energy Rev 2009;13:1819–35. doi:10.1016/J.RSER.2008.09.033.

[88] Probst B, Touboul S, Glachant M, Dechezleprêtre A. Global trends in the invention and diffusion of climate change mitigation technologies. Nat Energy 2021;6:1077–86. doi:10.1038/s41560-021-00931-5.

[89] Duan H, Chen S, Song J. Characterizing regional building energy consumption under joint climatic and socioeconomic impacts. Energy 2022;245:123290. doi:https://doi.org/10.1016/j.energy.2022.123290.

[90] Yamaguchi Y, Kim B, Kitamura T, Akizawa K, Chen H, Shimoda Y. Building stock energy modeling considering building system composition and long-term change for climate change mitigation of commercial building stocks. Appl Energy 2022;306:117907. doi:https://doi.org/10.1016/j.apenergy.2021.117907.

[91] Wong CHH, Cai M, Ren C, Huang Y, Liao C, Yin S. Modelling building energy use at urban scale: A review on their account for the urban environment. Build Environ 2021;205:108235. doi:https://doi.org/10.1016/j.buildenv.2021.108235.

[92] Sandberg NH, Sartori I, Heidrich O, Dawson R, Dascalaki E, Dimitriou S, et al. Dynamic building stock modelling: Application to 11 European countries to support the energy efficiency and retrofit ambitions of the EU. Energy Build 2016;132:26–38. doi:10.1016/j.enbuild.2016.05.100.

[93] Hong T, Chen Y, Luo X, Luo N, Lee SH. Ten questions on urban building energy modeling. Build Environ 2020;168:106508. doi:10.1016/j.buildenv.2019.106508.

[94] Zhong X, Hu M, Deetman S, Rodrigues JFD, Lin H-X, Tukker A, et al. The evolution and future perspectives of energy intensity in the global building sector 1971-2060. J Clean Prod 2021:127098. doi:https://doi.org/10.1016/j.jclepro.2021.127098.

[95] Heeren N, Jakob M, Martius G, Gross N, Wallbaum H. A component based bottom-up building stock model for comprehensive environmental impact assessment and target control. Renew Sustain Energy Rev 2013;20:45–56. doi:https://doi.org/10.1016/j.rser.2012.11.064.

[96] Abbasabadi N, Mehdi Ashayeri JK. Urban energy use modeling methods and tools: A review and an outlook. Build Environ 2019;161:106270. doi:10.1016/J.BUILDENV.2019.106270.

[97] Wang Z, Srinivasan RS. A review of artificial intelligence based building energy use prediction: Contrasting the capabilities of single and ensemble prediction models. Renew Sustain Energy Rev 2017;75:796–808. doi:10.1016/J.RSER.2016.10.079.

[98] Buffat R, Froemelt A, Heeren N, Raubal M, Hellweg S. Big data GIS analysis for novel approaches in building stock modelling. Appl Energy 2017;208:277–90. doi:https://doi.org/10.1016/j.apenergy.2017.10.041.

[99] Johari F, Peronato G, Sadeghian P, Zhao X, Widén J. Urban building energy modeling: State of the art and future prospects. Renew Sustain Energy Rev 2020;128:109902. doi:https://doi.org/10.1016/j.rser.2020.109902.

[100] Nägeli C, Camarasa C, Delghust M, Fennell P, Hamilton I, Jakob M, et al. Best practice reporting guideline for building stock energy models. Energy Build 2022;260:111904. doi:https://doi.org/10.1016/j.enbuild.2022.111904.

[101] Ferrando M, Lavagna M, Causone F. Life cycle assessment approaches applied to energy

modelling of urban building stocks: a literature review. n.d.

[102] Malhotra A, Bischof J, Nichersu A, Häfele K-H, Exenberger J, Sood D, et al. Information modelling for urban building energy simulation—A taxonomic review. Build Environ 2021:108552. doi:https://doi.org/10.1016/j.buildenv.2021.108552.

[103] Reinhart CF, Cerezo Davila C. Urban building energy modeling – A review of a nascent field. Build Environ 2016;97:196–202. doi:https://doi.org/10.1016/j.buildenv.2015.12.001.

[104] Fennell PJ, Ruyssevelt PA, Mata É, Jakob M. A Review of the Status of Uncertainty and Sensitivity Analysis in Building-stock Energy Models. Proc. Build. Simul. 2019 16th Conf. IBPSA, 2019, p. 3353–60.

[105] Ali U, Shamsi MH, Hoare C, Mangina E, O'Donnell J. Review of urban building energy modeling (UBEM) approaches, methods and tools using qualitative and quantitative analysis. Energy Build 2021;246:111073. doi:https://doi.org/10.1016/j.enbuild.2021.111073.

[106] Langevin J, Reyna JL, Ebrahimigharehbaghi S, Sandberg N, Fennell P, Nägeli C, et al. Developing a common approach for classifying building stock energy models. Renew Sustain Energy Rev 2020;133. doi:10.1016/j.rser.2020.110276.

[107] Oraiopoulos A, Howard B. On the accuracy of Urban Building Energy Modelling. Renew Sustain Energy Rev 2022;158:111976. doi:https://doi.org/10.1016/j.rser.2021.111976.

[108] B. Müller D. Stock dynamics for forecasting material flows—Case study for housing in The Netherlands. Ecol Econ 2006;59:142–56. doi:https://doi.org/10.1016/j.ecolecon.2005.09.025.

[109] Bergsdal H, Brattebø H, Bohne RA, Müller DB. Dynamic material flow analysis for Norway's dwelling stock. Build Res Inf 2007;35:557–70. doi:10.1080/09613210701287588.

[110] Hu M, Bergsdal H, Van Der Voet E, Huppes G, Muller DB. Dynamics of urban and rural housing stocks in China. Build Res Inf 2010;38:301–17. doi:10.1080/09613211003729988.

[111] Hu M, Van Der Voet E, Huppes G. Dynamic Material Flow Analysis for Strategic Construction and Demolition Waste Management in Beijing. J Ind Ecol 2010;14:440–56. doi:10.1111/j.1530-9290.2010.00245.x.

[112] Heeren N, Hellweg S. Tracking Construction Material over Space and Time: Prospective and Geo-referenced Modeling of Building Stocks and Construction Material Flows. J Ind Ecol 2019;23:253–67. doi:10.1111/jiec.12739.

[113] Wiedenhofer D, Fishman T, Plank B, Miatto A, Lauk C, Haas W, et al. Prospects for a saturation of humanity's resource use? An analysis of material stocks and flows in nine world regions from 1900 to 2035. Glob Environ Chang 2021;71:102410. doi:https://doi.org/10.1016/j.gloenvcha.2021.102410.

[114] Lanau M, Liu G, Kral U, Wiedenhofer D, Keijzer E, Yu C, et al. Taking Stock of Built Environment Stock Studies: Progress and Prospects. Environ Sci Technol 2019;53:8499–515. doi:10.1021/acs.est.8b06652.

[115] Augiseau V, Barles S. Studying construction materials flows and stock: A review. Resour Conserv Recycl 2017;123:153–64. doi:https://doi.org/10.1016/j.resconrec.2016.09.002.

[116] Müller E, Hilty LM, Widmer R, Schluep M, Faulstich M. Modeling Metal Stocks and Flows: A Review of Dynamic Material Flow Analysis Methods. Environ Sci Technol 2014;48:2102–13. doi:10.1021/es403506a.

[117] Guo D, Huang L. The State of the Art of Material Flow Analysis Research Based on Construction and Demolition Waste Recycling and Disposal. Buildings 2019;9. doi:10.3390/buildings9100207.

[118] Allesch A, Brunner PH. Material Flow Analysis as a Decision Support Tool for Waste Management: A Literature Review. J Ind Ecol 2015;19:753–64. doi:https://doi.org/10.1111/jiec.12354.

[119] Wang D, Landolt J, Mavromatidis G, Orehounig K, Carmeliet J. CESAR: A bottom-up building stock modelling tool for Switzerland to address sustainable energy transformation strategies. Energy Build 2018;169:9–26. doi:10.1016/J.ENBUILD.2018.03.020.

[120] McKenna R, Merkel E, Fehrenbach D, Mehne S, Fichtner W. Energy efficiency in the German residential sector: A bottom-up building-stock-model-based analysis in the context of energy-political targets. Build Environ 2013;62:77–88. doi:10.1016/J.BUILDENV.2013.01.002.

[121] Yang D, Dang M, Sun L, Han F, Shi F, Zhang H, et al. A System Dynamics Model for Urban Residential Building Stock towards Sustainability: The Case of Jinan, China. Int J Environ Res Public Health 2021;18:9520. doi:10.3390/ijerph18189520.

[122] Francis A, Thomas A. A framework for dynamic life cycle sustainability assessment and policy analysis of built environment through a system dynamics approach. Sustain Cities Soc 2022;76:103521. doi:https://doi.org/10.1016/j.scs.2021.103521.

[123] Tang S, Zhang L, Hao Y, Chang Y, Liu G, Liu Q, et al. System dynamics modeling for construction material flows of urban residential building: A case study of Beijing, China. Resour Conserv Recycl 2021;168:105298. doi:https://doi.org/10.1016/j.resconrec.2020.105298.

[124] Zhao F. AGENT-BASED MODELING OF COMMERCIAL BUILDING STOCKS FOR ENERGY POLICY AND DEMAND RESPONSE ANALYSIS. 2012.

[125] Nägeli C, Jakob M, Catenazzi G, Ostermeyer Y. Towards agent-based building stock modeling: Bottom-up modeling of long-term stock dynamics affecting the energy and climate impact of building stocks. Energy Build 2020;211:109763. doi:10.1016/J.ENBUILD.2020.109763.

[126] Ebrahimi B, Rosado L, Wallbaum H. Machine learning-based stocks and flows modeling of road infrastructure. J Ind Ecol 2022;n/a. doi:https://doi.org/10.1111/jiec.13232.

[127] Mulero-Palencia S, Álvarez-Díaz S, Andrés-Chicote M. Machine Learning for the Improvement of Deep Renovation Building Projects Using As-Built BIM Models. Sustain 2021;13. doi:10.3390/su13126576.

[128] Nägeli C, Jakob M, Catenazzi G, Ostermeyer Y. Policies to decarbonize the Swiss residential building stock: An agent-based building stock modeling assessment. Energy Policy 2020;146:111814. doi:10.1016/j.enpol.2020.111814.

[129] Mastrucci A, Marvuglia A, Leopold U, Benetto E. Life Cycle Assessment of building stocks from urban to transnational scales: A review. Renew Sustain Energy Rev 2017;74:316–32. doi:https://doi.org/10.1016/j.rser.2017.02.060.

[130] Kurvinen A, Saari A, Heljo J, Nippala E. Modeling Building Stock Development.

Sustainability 2021;13. doi:10.3390/su13020723.

[131] Steubing B, De Koning D, Haas A, Mutel CL. The Activity Browser-An open source LCA software building on top of the brightway framework. Softw Impacts 2020;3:100012. doi:10.1016/j.simpa.2019.100012.

[132] Hollberg A, Kiss B, Röck M, Soust-Verdaguer B, Wiberg AH, Lasvaux S, et al. Review of visualising LCA results in the design process of buildings. Build Environ 2021;190:107530. doi:https://doi.org/10.1016/j.buildenv.2020.107530.

[133] Varun, Bhat IK, Prakash R. LCA of renewable energy for electricity generation systems—A review. Renew Sustain Energy Rev 2009;13:1067–73. doi:https://doi.org/10.1016/j.rser.2008.08.004.

[134] Helena DSG, Silvia D. Model for Life Cycle Assessment (LCA) of buildings. 2018. doi:10.2760/10016.

[135] Life Cycle Initiative. Interactive map of lca databases n.d. https://www.lifecycleinitiative.org/applying-lca/lca-databases-map/ (accessed January 11, 2022).

[136] Piacenza JR, Tumer IY, Seyedmahmoudi SH, Haapala KR, Hoyle C. Comparison of Sustainability Performance for Cross Laminated Timber and Concrete 2013. doi:10.1115/DETC2013-12267.

[137] Mao R, Bao Y, Duan H, Liu G. Global urban subway development, construction material stocks, and embodied carbon emissions. Humanit Soc Sci Commun 2021;8:83. doi:10.1057/s41599-021-00757-2.

[138] Wernet G, Bauer C, Steubing B, Reinhard J, Moreno-Ruiz E, Weidema B, et al. The ecoinvent database version 3 (part I): overview and methodology. Int J Life Cycle Assess 2016;21:1218–30. doi:10.1007/s11367-016-1087-8.

[139] Mutel C. Brightway: An open source framework for Life Cycle Assessment. J Open Source Softw 2017;2:236. doi:10.21105/joss.00236.

[140] Moschetti R, Mazzarella L, Nord N. An overall methodology to define reference values for building sustainability parameters. Energy Build 2015;88:413–27. doi:10.1016/J.ENBUILD.2014.11.071.

[141] IKE. eFootprint LCA software n.d. http://www.ike-global.com/#/ (accessed January 11, 2022).

[142] Steubing B, de Koning D. Making the use of scenarios in LCA easier: the superstructure approach. Int J Life Cycle Assess 2021. doi:10.1007/s11367-021-01974-2.

[143] Zimmermann RK, Bruhn S, Birgisdóttir H. BIM-Based Life Cycle Assessment of Buildings—An Investigation of Industry Practice and Needs. Sustain 2021;13. doi:10.3390/su13105455.

[144] Potrč Obrecht T, Röck M, Hoxha E, Passer A. BIM and LCA Integration: A Systematic Literature Review. Sustain 2020;12. doi:10.3390/su12145534.

[145] Obrecht TP, Röck M, Hoxha E, Passer A. The challenge of integrating Life Cycle Assessment in the building design process – a systematic literature review of BIM-LCA workflows. IOP Conf Ser Earth Environ Sci 2020;588:32024. doi:10.1088/1755-

1315/588/3/032024.

[146] Llatas C, Soust-Verdaguer B, Passer A. Implementing Life Cycle Sustainability Assessment during design stages in Building Information Modelling: From systematic literature review to a methodological approach. Build Environ 2020;182:107164. doi:https://doi.org/10.1016/j.buildenv.2020.107164.

[147] Sprecher B, Verhagen TJ, Sauer ML, Baars M, Heintz J, Fishman T. Material intensity database for the Dutch building stock: Towards Big Data in material stock analysis. J Ind Ecol 2021;n/a. doi:https://doi.org/10.1111/jiec.13143.

[148] Zhang C, Hu M, Sprecher B, Yang X, Zhong X, Li C, et al. Recycling potential in building energy renovation: A prospective study of the Dutch residential building stock up to 2050. J Clean Prod 2021;301:126835. doi:https://doi.org/10.1016/j.jclepro.2021.126835.

[149] Pauliuk S, Heeren N. ODYM—An open software framework for studying dynamic material systems: Principles, implementation, and data structures. J Ind Ecol 2020;24:446–58. doi:https://doi.org/10.1111/jiec.12952.

[150] Yücel G. Extent of inertia caused by the existing building stock against an energy transition in the Netherlands. Energy Build 2013;56:134–45. doi:10.1016/J.ENBUILD.2012.09.022.

[151] Mastrucci A, Baume O, Stazi F, Leopold U. Estimating energy savings for the residential building stock of an entire city: A GIS-based statistical downscaling approach applied to Rotterdam. Energy Build 2014;75:358–67. doi:10.1016/J.ENBUILD.2014.02.032.

[152] Wang CK, Tindemans S, Miller C, Agugiaro G, Stoter J. Bayesian calibration at the urban scale: a case study on a large residential heating demand application in Amsterdam. J Build Perform Simul 2020;13:347–61. doi:10.1080/19401493.2020.1729862.

[153] Filippidou F, Nieboer N, Visscher H. Are we moving fast enough? The energy renovation rate of the Dutch non-profit housing using the national energy labelling database. Energy Policy 2017;109:488–98. doi:10.1016/j.enpol.2017.07.025.

[154] Liu W, Best F, Crijns-Graus W. Exploring the pathways towards a sustainable heating system – A case study of Utrecht in the Netherlands. J Clean Prod 2021;280:125036. doi:https://doi.org/10.1016/j.jclepro.2020.125036.

[155] Government of the Netherlands. A circular economy in the Netherlands by 2050. 2016.

[156] Ouden B den, Kerkhoven J, Warnaars J, Terwel R, Coenen M, Verboon T, et al. Nederland klimaatneutraal in 2050: vier scenario's (The Netherlands will be climate neutral in 2050: four scenarios). 2020.

[157] Dutch government. National Climate Agreement - The Netherlands. 2019.

[158] European Commission. Financing the energy renovation of buildings with Cohesion Policy funding 2014. https://ec.europa.eu/regional_policy/en/information/publications/guides/2014/financing-the-energy-renovation-of-buildings-with-cohesion-policy-funding (accessed October 9, 2019).

[159] Delmastro C, Gargiulo M. Capturing the long-term interdependencies between building thermal energy supply and demand in urban planning strategies. Appl Energy 2020;268:114774. doi:https://doi.org/10.1016/j.apenergy.2020.114774.

[160] Ma W, Fang S, Liu G, Zhou R. Modeling of district load forecasting for distributed energy

system. Appl Energy 2017. doi:10.1016/j.apenergy.2017.07.009.

[161] Johansson T, Olofsson T, Mangold M. Development of an energy atlas for renovation of the multifamily building stock in Sweden. Appl Energy 2017;203:723–36. doi:https://doi.org/10.1016/j.apenergy.2017.06.027.

[162] Kavgic M, Mavrogianni A, Mumovic D, Summerfield A, Stevanovic Z, Djurovic-Petrovic M. A review of bottom-up building stock models for energy consumption in the residential sector. Build Environ 2010;45:1683–97. doi:https://doi.org/10.1016/j.buildenv.2010.01.021.

[163] Nutkiewicz A, Yang Z, Jain RK. Data-driven Urban Energy Simulation (DUE-S): A framework for integrating engineering simulation and machine learning methods in a multi-scale urban energy modeling workflow. Appl Energy 2018. doi:10.1016/j.apenergy.2018.05.023.

[164] Chen Y, Hong T, Piette MA. Automatic generation and simulation of urban building energy models based on city datasets for city-scale building retrofit analysis. Appl Energy 2017;205:323–35. doi:10.1016/J.APENERGY.2017.07.128.

[165] Mata É, Sasic Kalagasidis A, Johnsson F. Building-stock aggregation through archetype buildings: France, Germany, Spain and the UK. Build Environ 2014;81:270–82. doi:10.1016/J.BUILDENV.2014.06.013.

[166] Sokol J, Cerezo Davila C, Reinhart CF. Validation of a Bayesian-based method for defining residential archetypes in urban building energy models. Energy Build 2017;134:11–24. doi:10.1016/J.ENBUILD.2016.10.050.

[167] Froemelt A, Hellweg S. Assessing Space Heating Demand on a Regional Level: Evaluation of a Bottom-Up Model in the Scope of a Case Study. J Ind Ecol 2016;21:332–43. doi:10.1111/jiec.12438.

[168] Bianchi C, Zhang L, Goldwasser D, Parker A, Horsey H. Modeling occupancy-driven building loads for large and diversified building stocks through the use of parametric schedules. Appl Energy 2020;276:115470. doi:https://doi.org/10.1016/j.apenergy.2020.115470.

[169] Lim H, Zhai ZJ. Review on stochastic modeling methods for building stock energy prediction. Build Simul 2017;10:607–24. doi:10.1007/s12273-017-0383-y.

[170] van den Brom P, Meijer A, Visscher H. Performance gaps in energy consumption: household groups and building characteristics. Build Res Inf 2018;46:54–70. doi:10.1080/09613218.2017.1312897.

[171] Hall LMH, Buckley AR. A review of energy systems models in the UK: Prevalent usage and categorisation. Appl Energy 2016. doi:10.1016/j.apenergy.2016.02.044.

[172] BAG. Basisregistratie Adressen en Gebouwen (Basic registration Addresses and Buildings) 2018. https://www.geobasisregistraties.nl/basisregistraties/adressen-en-gebouwen (accessed October 10, 2019).

[173] KNMI (the Royal Netherlands Meteorological Institute). Weather data of the Netherlands n.d. https://www.knmi.nl/home (accessed October 8, 2019).

[174] Ministry of the Interior and Kingdom Relations. Figures about Housing and Construction 2013 (Cijfers over Wonen en Bouwen 2013). 2013.

[175] García-Pérez S, Sierra-Pérez J, Boschmonart-Rives J. Environmental assessment at the urban level combining LCA-GIS methodologies: A case study of energy retrofits in the Barcelona metropolitan area. Build Environ 2018;134:191–204. doi:10.1016/J.BUILDENV.2018.01.041.

[176] TABULA Project Team. TABULA Calculation Method – Energy Use for Heating and Domestic Hot Water. Institut Wohnen und Umwelt GmbH; 2013.

[177] Filogamo L, Peri G, Rizzo G, Giaccone A. On the classification of large residential buildings stocks by sample typologies for energy planning purposes. Appl Energy 2014;135:825–35. doi:10.1016/J.APENERGY.2014.04.002.

[178] Vasallo A, Vallejo E, Massa G, Macía A, Pablos L, Criado C, et al. The District Energy-Efficient Retrofitting of Torrelago (Laguna de Duero – Spain). IOP Conf Ser Earth Environ Sci 2019;290:012138. doi:10.1088/1755-1315/290/1/012138.

[179] Milieu Centraal. Stappenplan aardgasvrij wonen (Natural gas-free living step-by-step plan) n.d. https://www.milieucentraal.nl/energie-besparen/energiezuinig-huis/wonen-zonder-aardgas/stappenplan-aardgasvrij-wonen/ (accessed October 18, 2019).

[180] International Organization for Standardization. Energy performance of buildings — Calculation of energy use for space heating and cooling (ISO 13790:2008). Brussels: 2008.

[181] Soheil Alavirad. Robust energy-retrofit strategy for dutch archetypes： A demand reduction approach. Technische Universiteit Eindhoven, 2018.

[182] Het Centraal Bureau voor de Statistiek (CBS). Energielevering aan woningen en bedrijven naar postcode (Energy supply to homes and businesses by postcode) 2015. https://www.cbs.nl/nl-nl/maatwerk/2019/11/energielevering-aan-woningen-en-bedrijven-naar-postcode (accessed October 9, 2019).

[183] Majcen D, Itard LCM, Visscher H. Theoretical vs. actual energy consumption of labelled dwellings in the Netherlands: Discrepancies and policy implications. Energy Policy 2013;54:125–36. doi:10.1016/J.ENPOL.2012.11.008.

[184] Brøgger M, Bacher P, Madsen H, Wittchen KB. Estimating the influence of rebound effects on the energy-saving potential in building stocks. Energy Build 2018;181:62–74. doi:10.1016/j.enbuild.2018.10.006.

[185] Heat Transition Atlas (Warmte transitie atlas) n.d. http://pzh.maps.arcgis.com/apps/MapJournal/index.html?appid=4c8e61a776eb4a6e8aaec99653d22b62# (accessed October 14, 2019).

[186] Li W, Zhou Y, Cetin K, Eom J, Wang Y, Chen G, et al. Modeling urban building energy use: A review of modeling approaches and procedures. Energy 2017;141:2445–57. doi:10.1016/J.ENERGY.2017.11.071.

[187] Majcen D, Itard L, Visscher H. Actual and theoretical gas consumption in Dutch dwellings: What causes the differences? Energy Policy 2013;61:460–71. doi:10.1016/J.ENPOL.2013.06.018.

[188] D'Oca S, Hong T. Occupancy schedules learning process through a data mining framework. Energy Build 2015;88:395–408. doi:10.1016/J.ENBUILD.2014.11.065.

[189] Kragh J, Wittchen KB. Development of two Danish building typologies for residential

buildings. Energy Build 2014;68:79–86. doi:10.1016/J.ENBUILD.2013.04.028.

[190] Ballarini I, Corgnati SP, Corrado V. Use of reference buildings to assess the energy saving potentials of the residential building stock: The experience of TABULA project. Energy Policy 2014;68:273–84. doi:10.1016/J.ENPOL.2014.01.027.

[191] Magalhães SMC, Leal VMS. Characterization of thermal performance and nominal heating gap of the residential building stock using the EPBD-derived databases: The case of Portugal mainland. Energy Build 2014;70:167–79. doi:10.1016/j.enbuild.2013.11.054.

[192] van den Brom P, Hansen AR, Gram-Hanssen K, Meijer A, Visscher H. Variances in residential heating consumption – Importance of building characteristics and occupants analysed by movers and stayers. Appl Energy 2019;250:713–28. doi:10.1016/J.APENERGY.2019.05.078.

[193] Österbring M, Camarasa C, Nägeli C, Thuvander L, Wallbaum H. Prioritizing deep renovation for housing portfolios. Energy Build 2019;202:109361. doi:10.1016/J.ENBUILD.2019.109361.

[194] Rogeau A, Girard R, Abdelouadoud Y, Thorel M, Kariniotakis G. Joint optimization of building-envelope and heating-system retrofits at territory scale to enhance decision-aiding. Appl Energy 2020;264:114639. doi:https://doi.org/10.1016/j.apenergy.2020.114639.

[195] Chang M, Thellufsen JZ, Zakeri B, Pickering B, Pfenninger S, Lund H, et al. Trends in tools and approaches for modelling the energy transition. Appl Energy 2021;290:116731. doi:https://doi.org/10.1016/j.apenergy.2021.116731.

[196] Shimoda Y, Sugiyama M, Nishimoto R, Momonoki T. Evaluating decarbonization scenarios and energy management requirement for the residential sector in Japan through bottom-up simulations of energy end-use demand in 2050. Appl Energy 2021;303:117510. doi:https://doi.org/10.1016/j.apenergy.2021.117510.

[197] Bui D-K, Nguyen TN, Ghazlan A, Ngo TD. Biomimetic adaptive electrochromic windows for enhancing building energy efficiency. Appl Energy 2021;300:117341. doi:https://doi.org/10.1016/j.apenergy.2021.117341.

[198] Cao Z, Liu G, Duan H, Xi F, Liu G, Yang W. Unravelling the mystery of Chinese building lifetime: A calibration and verification based on dynamic material flow analysis. Appl Energy 2019;238:442–52. doi:10.1016/J.APENERGY.2019.01.106.

[199] Sandberg NH, Sartori I, Brattebø H. Using a dynamic segmented model to examine future renovation activities in the Norwegian dwelling stock. Energy Build 2014;82:287–95. doi:10.1016/J.ENBUILD.2014.07.005.

[200] Wiedenhofer D, Steinberger JK, Eisenmenger N, Haas W. Maintenance and Expansion: Modeling Material Stocks and Flows for Residential Buildings and Transportation Networks in the EU25. J Ind Ecol 2015;19:538–51. doi:10.1111/jiec.12216.

[201] Ostermeyer Y, Nägeli C, Heeren N, Wallbaum H. Building Inventory and Refurbishment Scenario Database Development for Switzerland. J Ind Ecol 2017;22:629–42. doi:10.1111/jiec.12616.

[202] Coffey B, Borgeson S, Selkowitz S, Apte J, Mathew P, Haves P. Towards a very low-energy building stock: Modelling the US commercial building sector to support policy and

innovation planning. Build Res Inf 2009;37:610–24. doi:10.1080/09613210903189467.

[203] Pauliuk S, Sjöstrand K, Müller DB. Transforming the Norwegian Dwelling Stock to Reach the 2 Degrees Celsius Climate Target: Combining Material Flow Analysis and Life Cycle Assessment Techniques. J Ind Ecol 2013;17:542–54. doi:10.1111/j.1530-9290.2012.00571.x.

[204] Vásquez F, Løvik AN, Sandberg NH, Müller DB. Dynamic type-cohort-time approach for the analysis of energy reductions strategies in the building stock. Energy Build 2016;111:37–55. doi:10.1016/J.ENBUILD.2015.11.018.

[205] Koezjakov A, Urge-Vorsatz D, Crijns-Graus W, van den Broek M. The relationship between operational energy demand and embodied energy in Dutch residential buildings. Energy Build 2018;165:233–45. doi:10.1016/J.ENBUILD.2018.01.036.

[206] Miatto A, Schandl H, Tanikawa H. How important are realistic building lifespan assumptions for material stock and demolition waste accounts? Resour Conserv Recycl 2017;122:143–54. doi:10.1016/j.resconrec.2017.01.015.

[207] Klimaatakkoord. Climate Agreements for Built Environment n.d. https://www.klimaatakkoord.nl/gebouwde-omgeving (accessed October 30, 2020).

[208] Visscher H. Innovations for a carbon free Dutch housing stock in 2050. IOP Conf Ser Earth Environ Sci 2019;329. doi:10.1088/1755-1315/329/1/012003.

[209] Milieu Centraal. Double glass, HR ++ glass and triple glass n.d. https://www.milieucentraal.nl/energie-besparen/energiezuinig-huis/isoleren-en-besparen/dubbel-glas-hr-glas-en-triple-glas/ (accessed October 8, 2021).

[210] TABULA Project Team. TABULA WebTool 2017. https://webtool.building-typology.eu/#bm (accessed October 8, 2021).

[211] Koezjakov A. The Effect of an Increase in Energy Efficiency on Embodied Energy use: a scenario analysis for Dutch residential buildings. Utrecht University, 2017.

[212] Gernaat DEHJ, de Boer H-S, Dammeier LC, van Vuuren DP. The role of residential rooftop photovoltaic in long-term energy and climate scenarios. Appl Energy 2020;279:115705. doi:https://doi.org/10.1016/j.apenergy.2020.115705.

[213] Bódis K, Kougias I, Jäger-Waldau A, Taylor N, Szabó S. A high-resolution geospatial assessment of the rooftop solar photovoltaic potential in the European Union. Renew Sustain Energy Rev 2019;114:109309. doi:10.1016/J.RSER.2019.109309.

[214] Ende E van den. A revolution: The Netherlands kisses gas goodbye – but will it help the climate? Energypost 2017. https://energypost.eu/a-revolution-the-netherlands-kisses-gas-goodbye-but-will-it-help-the-climate/ (accessed October 26, 2020).

[215] IPCC. IPCC, 2013: Climate Change 2013: The Physical Science Basis. Contribution of Working Group I to the Fifth Assessment Report of the Intergovernmental Panel on Climate Change. 2013.

[216] Mendoza Beltran A, Cox B, Mutel C, van Vuuren DP, Font Vivanco D, Deetman S, et al. When the Background Matters: Using Scenarios from Integrated Assessment Models in Prospective Life Cycle Assessment. J Ind Ecol 2018;24:64–79. doi:10.1111/jiec.12825.

[217] PBL. Integrated Assessment of Global Environmental Change with IMAGE 3.0 - Model description and policy applications. 2014.

[218] O'Neill BC, Kriegler E, Riahi K, Ebi KL, Hallegatte S, Carter TR, et al. A new scenario framework for climate change research: the concept of shared socioeconomic pathways. Clim Change 2014;122:387–400. doi:10.1007/s10584-013-0905-2.

[219] The Energy Agreement for sustainable growth (Energieakkoord voor duurzame groei) 2013. https://www.ser.nl/nl/thema/energie-en-duurzaamheid/energieakkoord/domeinen/01 (accessed October 26, 2020).

[220] Rijksoverheid. The Netherlands circular in 2050 (Nederland circulair in 2050) 2018. https://www.rijksoverheid.nl/onderwerpen/circulaire-economie/nederland-circulair-in-2050 (accessed February 28, 2021).

[221] CBS. Population forecast of the Netherlands 2018. https://www.cbs.nl/en-gb/news/2018/51/forecast-18-million-inhabitants-in-2029#id=undefined (accessed November 8, 2020).

[222] RVO. Energieprestatie-BENG (Energy performance-NZEB) 2021. https://www.rvo.nl/onderwerpen/duurzaam-ondernemen/gebouwen/wetten-en-regels/nieuwbouw/energieprestatie-beng (accessed July 21, 2021).

[223] Milieu Centraal. Complete heat pump n.d. https://www.milieucentraal.nl/energie-besparen/energiezuinig-huis/energiezuinig-verwarmen-en-warm-water/volledige-warmtepomp/ (accessed November 7, 2020).

[224] CBS. Emissions to air by the Dutch economy-national accounts 2020. https://opendata.cbs.nl/#/CBS/en/dataset/83300ENG/table?searchKeywords=CO2 (accessed April 13, 2021).

[225] Kong M, Hong T, Ji C, Kang H, Lee M. Development of building driven-energy payback time for energy transition of building with renewable energy systems. Appl Energy 2020;271:115162. doi:https://doi.org/10.1016/j.apenergy.2020.115162.

[226] Mata É, Wanemark J, Nik VM, Sasic Kalagasidis A. Economic feasibility of building retrofitting mitigation potentials: Climate change uncertainties for Swedish cities. Appl Energy 2019;242:1022–35. doi:10.1016/j.apenergy.2019.03.042.

[227] Milieu Centraal. Low temperature heating n.d. https://www.milieucentraal.nl/energie-besparen/energiezuinig-huis/energiezuinig-verwarmen-en-warm-water/lage-temperatuur-verwarming-ltv/ (accessed November 11, 2020).

[228] Heat network without natural gas n.d. https://www.milieucentraal.nl/energie-besparen/energiezuinig-huis/wonen-zonder-aardgas/warmtenet-verwarmen-zonder-aardgas/ (accessed November 1, 2020).

[229] Municipality of Leiden. Heat vision Leiden VERSION FOR PARTICIPATION FINAL. 2017.

[230] Wei M, Lee SH, Hong T, Conlon B, McKenzie L, Hendron B, et al. Approaches to cost-effective near-net zero energy new homes with time-of-use value of energy and battery storage. Adv Appl Energy 2021;2:100018. doi:https://doi.org/10.1016/j.adapen.2021.100018.

[231] He Z, Hong T, Chou SK. A framework for estimating the energy-saving potential of occupant behaviour improvement. Appl Energy 2021;287:116591.

doi:https://doi.org/10.1016/j.apenergy.2021.116591.

[232] CBS. Living space in the Netherlands 2018. https://www.cbs.nl/nl-nl/achtergrond/2018/22/woonoppervlakte-in-nederland (accessed November 12, 2020).

[233] Galvin R. Making the 'rebound effect' more useful for performance evaluation of thermal retrofits of existing homes: Defining the 'energy savings deficit' and the 'energy performance gap.' Energy Build 2014;69:515–24. doi:10.1016/J.ENBUILD.2013.11.004.

[234] Rijksoverheid. Construction Transition Agenda (Transitieagenda Bouw) 2018. https://www.rijksoverheid.nl/onderwerpen/circulaire-economie/documenten/rapporten/2018/01/15/bijlage-4-transitieagenda-bouw (accessed June 10, 2021).

[235] Chen Y, Deng Z, Hong T. Automatic and rapid calibration of urban building energy models by learning from energy performance database. Appl Energy 2020;277:115584. doi:https://doi.org/10.1016/j.apenergy.2020.115584.

[236] Xiao T, Xu P, He R, Sha H. Status quo and opportunities for building energy prediction in limited data Context—Overview from a competition. Appl Energy 2022;305:117829. doi:https://doi.org/10.1016/j.apenergy.2021.117829.

[237] Sun H, Kporsu AK, Taghizadeh-Hesary F, Edziah BK. Estimating environmental efficiency and convergence: 1980 to 2016. Energy 2020;208:118224. doi:https://doi.org/10.1016/j.energy.2020.118224.

[238] Stephan A, Athanassiadis A. Towards a more circular construction sector: Estimating and spatialising current and future non-structural material replacement flows to maintain urban building stocks. Resour Conserv Recycl 2018;129:248–62. doi:10.1016/J.RESCONREC.2017.09.022.

[239] Babí Almenar J, Elliot T, Rugani B, Philippe B, Navarrete Gutierrez T, Sonnemann G, et al. Nexus between nature-based solutions, ecosystem services and urban challenges. Land Use Policy 2021;100:104898. doi:https://doi.org/10.1016/j.landusepol.2020.104898.

[240] Zabek M, Hildebrand L, Brell-Cokcan S, Wirth M. Used building materials as secondary resources – Identification of valuable building material and automized deconstruction. J Facade Des Eng 2017;5:25–33. doi:10.7480/jfde.2017.2.1684.

[241] Koutamanis A, van Reijn B, van Bueren E. Urban mining and buildings: A review of possibilities and limitations. Resour Conserv Recycl 2018;138:32–9. doi:10.1016/J.RESCONREC.2018.06.024.

[242] Di Maria A, Eyckmans J, Van Acker K. Downcycling versus recycling of construction and demolition waste: Combining LCA and LCC to support sustainable policy making. Waste Manag 2018;75:3–21. doi:https://doi.org/10.1016/j.wasman.2018.01.028.

[243] Akbarieh A, Schäfer M, Waldmann D, Teferle FN. Post-Urban Mining Automation and Digitalisation for a Closed- Loop Circular Post-Urban Mining Automation and Digitalisation for a Closed- Loop Circular Construction. Proc. 38th Int. Conf. CIB W78, Luxembourg: 2021.

[244] Tanikawa H, Fishman T, Okuoka K, Sugimoto K. The Weight of Society Over Time and Space: A Comprehensive Account of the Construction Material Stock of Japan, 1945–2010.

J Ind Ecol 2015;19:778–91. doi:10.1111/jiec.12284.

[245] Kleemann F, Lederer J, Rechberger H, Fellner J. GIS-based Analysis of Vienna's Material Stock in Buildings. J Ind Ecol 2017;21:368–80. doi:10.1111/jiec.12446.

[246] Mao R, Bao Y, Huang Z, Liu Q, Liu G. High-Resolution Mapping of the Urban Built Environment Stocks in Beijing. Environ Sci Technol 2020;54:5345–55. doi:10.1021/acs.est.9b07229.

[247] Lanau M, Liu G. Developing an Urban Resource Cadaster for Circular Economy: A Case of Odense, Denmark. Environ Sci Technol 2020;54:4675–85. doi:10.1021/acs.est.9b07749.

[248] Yang X, Hu M, Tukker A, Zhang C, Huo T, Steubing B. A bottom-up dynamic building stock model for residential energy transition: A case study for the Netherlands. Appl Energy 2022;306:118060. doi:10.1016/j.apenergy.2021.118060.

[249] Meglin R, Kytzia S, Habert G. Regional circular economy of building materials: Environmental and economic assessment combining Material Flow Analysis, Input-Output Analyses, and Life Cycle Assessment. J Ind Ecol 2021;n/a. doi:https://doi.org/10.1111/jiec.13205.

[250] Tanikawa H, Hashimoto S. Urban stock over time: spatial material stock analysis using 4d-GIS. Build Res Inf 2009;37:483–502. doi:10.1080/09613210903169394.

[251] Schiller G, Gruhler K, Ortlepp R. Continuous Material Flow Analysis Approach for Bulk Nonmetallic Mineral Building Materials Applied to the German Building Sector. J Ind Ecol 2017;21:673–88. doi:10.1111/jiec.12595.

[252] Schebek L, Schnitzer B, Blesinger D, Köhn A, Miekley B, Linke HJ, et al. Material stocks of the non-residential building sector: the case of the Rhine-Main area. Resour Conserv Recycl 2017;123:24–36. doi:10.1016/J.RESCONREC.2016.06.001.

[253] Lederer J, Gassner A, Kleemann F, Fellner J. Potentials for a circular economy of mineral construction materials and demolition waste in urban areas: a case study from Vienna. Resour Conserv Recycl 2020;161. doi:10.1016/j.resconrec.2020.104942.

[254] Lismont A, Allacker K. Turning the existing building stock into a resource mine: Proposal for a new method to develop building stock models. IOP Conf Ser Earth Environ Sci 2019;323. doi:10.1088/1755-1315/323/1/012070.

[255] Bogoviku L, Waldmann D. Modelling of mineral construction and demolition waste dynamics through a combination of geospatial and image analysis. J Environ Manage 2021;282:111879. doi:https://doi.org/10.1016/j.jenvman.2020.111879.

[256] Aaron O'Neill. Netherlands: Degree of urbanization from 2009 to 2019. Statista 2019. https://www.statista.com/statistics/276724/urbanization-in-the-netherlands/ (accessed July 2, 2021).

[257] UNEP. Recycling Rates of Metals - A Status Report. A Report of the Working Group on Global Metal Flows to the International Resource Panel. 2011.

[258] Potrč Obrecht T, Jordan S, Legat A, Passer A. The role of electricity mix and production efficiency improvements on greenhouse gas (GHG) emissions of building components and future refurbishment measures. Int J Life Cycle Assess 2021;26:839–51. doi:10.1007/s11367-021-01920-2.

[259] Hart J, D'Amico B, Pomponi F. Whole-life embodied carbon in multistory buildings: Steel, concrete and timber structures. J Ind Ecol 2021;25:403–18. doi:https://doi.org/10.1111/jiec.13139.

[260] Sun H, Edziah BK, Kporsu AK, Sarkodie SA, Taghizadeh-Hesary F. Energy efficiency: The role of technological innovation and knowledge spillover. Technol Forecast Soc Change 2021;167:120659. doi:https://doi.org/10.1016/j.techfore.2021.120659.

[261] Tsydenova N, Becker T, Walther G. Optimised design of concrete recycling networks: The case of North Rhine-Westphalia. Waste Manag 2021;135:309–17. doi:https://doi.org/10.1016/j.wasman.2021.09.013.

[262] Nußholz JLK, Nygaard Rasmussen F, Milios L. Circular building materials: Carbon saving potential and the role of business model innovation and public policy. Resour Conserv Recycl 2019;141:308–16. doi:https://doi.org/10.1016/j.resconrec.2018.10.036.

[263] Vegter D, van Hillegersberg J, Olthaar M. Supply chains in circular business models: processes and performance objectives. Resour Conserv Recycl 2020;162:105046. doi:https://doi.org/10.1016/j.resconrec.2020.105046.

[264] Hart J, Adams K, Giesekam J, Tingley DD, Pomponi F. Barriers and drivers in a circular economy: the case of the built environment. Procedia CIRP 2019;80:619–24. doi:https://doi.org/10.1016/j.procir.2018.12.015.

[265] Huo T, Xu L, Feng W, Cai W, Liu B. Dynamic scenario simulations of carbon emission peak in China's city-scale urban residential building sector through 2050. Energy Policy 2021;159:112612. doi:https://doi.org/10.1016/j.enpol.2021.112612.

[266] Arceo A, Tham M, Guven G, MacLean HL, Saxe S. Capturing variability in material intensity of single-family dwellings: A case study of Toronto, Canada. Resour Conserv Recycl 2021;175:105885. doi:https://doi.org/10.1016/j.resconrec.2021.105885.

[267] Zhang C, Hu M, Di Maio F, Sprecher B, Yang X, Tukker A. An overview of the waste hierarchy framework for analyzing the circularity in construction and demolition waste management in Europe. Sci Total Environ 2022;803:149892. doi:https://doi.org/10.1016/j.scitotenv.2021.149892.

[268] IEA. Energy Technology Perspectives 2020. 2020. doi:10.1787/ab43a9a5-en.

[269] Xi F, Davis SJ, Ciais P, Crawford-Brown D, Guan D, Pade C, et al. Substantial global carbon uptake by cement carbonation. Nat Geosci 2016;9:880–3. doi:10.1038/ngeo2840.

[270] United Nations Population Division. World Urbanization Prospects 2018. 2018.

[271] GlobalABC, IEA, UNEP. GlobalABC Roadmap for Buildings and Construction 2020-2050. Glob Status Rep 2020:110. http://globalabc.org/our-work/forging-regional-pathways-global-and-regional-roadmap (accessed July 12, 2021).

[272] Saheb Y. COP26: Sufficiency should be first. Build Cities 2021.

[273] Bocken NMP, Niessen L, Short SW. The Sufficiency-Based Circular Economy—An Analysis of 150 Companies. Front Sustain 2022;3:1–18. doi:10.3389/frsus.2022.899289.

[274] European Commission. COM 662 final. A Renovation Wave for Europe - greening our buildings, creating jobs, improving lives. 2020.

[275] Kullmann F, Markewitz P, Stolten D, Robinius M. Combining the worlds of energy systems and material flow analysis: a review. Energy Sustain Soc 2021;11:13. doi:10.1186/s13705-021-00289-2.

[276] Fathi S, Srinivasan R, Fenner A, Fathi S. Machine learning applications in urban building energy performance forecasting: A systematic review. Renew Sustain Energy Rev 2020;133:110287. doi:https://doi.org/10.1016/j.rser.2020.110287.

[277] Akbarnezhad A, Xiao J. Estimation and Minimization of Embodied Carbon of Buildings: A Review. Buildings 2017;7. doi:10.3390/buildings7010005.

[278] Filippidou F. Energy performance progress of the Dutch non-profit housing stock: a longitudinal assessment. TU Delft, 2018.

[279] Municipality of Leiden. Op weg naar een circulair Leiden (Towards a circular Leiden) 2019:1–76. https://www.gagoed.nl/op-weg-naar-een-circulair-leiden/ (accessed June 20, 2021).

[280] Yang X, Hu M, Zhang C, Steubing B. Urban mining potential to reduce primary material use and carbon emissions in the Dutch residential building sector. Resour Conserv Recycl 2022;180:106215. doi:https://doi.org/10.1016/j.resconrec.2022.106215.

[281] Takano A, Hafner A, Linkosalmi L, Ott S, Hughes M, Winter S. Life cycle assessment of wood construction according to the normative standards. Eur J Wood Wood Prod 2015;73:299–312. doi:10.1007/s00107-015-0890-4.

[282] Bronsvoort E, Veldboer T, te Slaa A, Kaptein T. Bouwen aan een houten toekomst-Scenario's voor bouwen met klimaatpositieve materialen (Building a wooden future-Scenarios for building with climate-positive materials). 2020.

[283] Municipality of Leiden. 2020-2050 Bevolkingsprognose Leiden (Leiden population forecast). 2020.

[284] PAW. Transition vision heat n.d. https://aardgasvrijewijken.nl/themas/regieenorganisatie/transitievisie+warmte2/default.aspx (accessed May 1, 2021).

[285] Lombardi F, Rocco MV, Belussi L, Danza L, Magni C, Colombo E. Weather-induced variability of country-scale space heating demand under different refurbishment scenarios for residential buildings. Energy 2022;239:122152. doi:10.1016/j.energy.2021.122152.

[286] Buffat R, Heeren N, Froemelt A, Raubal M. Impact of CH2018 Climate Change Scenarios for Switzerland on today's Swiss building stock. J Phys Conf Ser 2019;1343:12004. doi:10.1088/1742-6596/1343/1/012004.

[287] Royal Netherlands Meteorological Institute. 14 climate scenarios for the Netherlands 2015. https://www.knmiprojects.nl/projects/climate-scenarios/documents/publications/2015/01/01/folder-knmi14-climate-scenarios (accessed October 26, 2021).

[288] Romainsacchi. Use examples of premise n.d. https://github.com/romainsacchi/premise/blob/master/examples/examples.ipynb (accessed December 1, 2021).

[289] Joshi KK, Kono T. Optimization of floor area ratio regulation in a growing city. Reg Sci

Urban Econ 2009;39:502–11. doi:https://doi.org/10.1016/j.regsciurbeco.2009.02.001.

[290] Guest G, Cherubini F, Strømman AH. Global Warming Potential of Carbon Dioxide Emissions from Biomass Stored in the Anthroposphere and Used for Bioenergy at End of Life. J Ind Ecol 2013;17:20–30. doi:https://doi.org/10.1111/j.1530-9290.2012.00507.x.

[291] Walter T, Mathew P. GHG policy impacts for Seattle's buildings: targets, timing, and scope. Build Cities 2021;2:283–301. doi:10.5334/bc.81.

[292] Müller A. Energy Demand Assessment for Space Conditioning and Domestic Hot Water: A Case Study for the Austrian Building Stock [Dissertation]. 2015.

[293] Reyna JL, Chester M V. The Growth of Urban Building Stock: Unintended Lock-in and Embedded Environmental Effects. J Ind Ecol 2014;19:524–37. doi:10.1111/jiec.12211.

[294] Bernstein S, Hoffmann M. Climate politics, metaphors and the fractal carbon trap. Nat Clim Chang 2019;9:919–25. doi:10.1038/s41558-019-0618-2.

[295] de Oliveira Fernandes MA, Keijzer E, van Leeuwen S, Kuindersma P, Melo L, Hinkema M, et al. Material-versus energy-related impacts: Analysing environmental trade-offs in building retrofit scenarios in the Netherlands. Energy Build 2021;231:110650. doi:https://doi.org/10.1016/j.enbuild.2020.110650.

[296] Vahidi E, Kirchain R, Burek J, Gregory J. Regional variation of greenhouse gas mitigation strategies for the United States building sector. Appl Energy 2021;302:117527. doi:https://doi.org/10.1016/j.apenergy.2021.117527.

[297] Lausselet C, Lund KM, Brattebø H. LCA and scenario analysis of a Norwegian net-zero GHG emission neighbourhood: The importance of mobility and surplus energy from PV technologies. Build Environ 2021;189:107528. doi:https://doi.org/10.1016/j.buildenv.2020.107528.

[298] Luderer G, Pehl M, Arvesen A, Gibon T, Bodirsky BL, de Boer HS, et al. Environmental co-benefits and adverse side-effects of alternative power sector decarbonization strategies. Nat Commun 2019;10:5229. doi:10.1038/s41467-019-13067-8.

[299] Rijkswaterstaat. The climate monitor n.d. https://klimaatmonitor.databank.nl/jive (accessed December 2, 2021).

[300] Streicher KN, Berger M, Chambers J, Schneider S, Patel MK. Combined geospatial and techno-economic analysis of deep building envelope retrofit. J. Phys. Conf. Ser., vol. 1343, Institute of Physics Publishing; 2019. doi:10.1088/1742-6596/1343/1/012028.

[301] Galimshina A, Moustapha M, Hollberg A, Padey P, Lasvaux S, Sudret B, et al. What is the optimal robust environmental and cost-effective solution for building renovation? Not the usual one. Energy Build 2021:111329. doi:https://doi.org/10.1016/j.enbuild.2021.111329.

[302] Zuberi MJS, Chambers J, Patel MK. Techno-economic comparison of technology options for deep decarbonization and electrification of residential heating. Energy Effic 2021;14:75. doi:10.1007/s12053-021-09984-7.

[303] Directorate-General for Energy. Comprehensive study of building energy renovation activities and the uptake of nearly zero-energy buildings in the EU. Final report. 2019. doi:10.2833/14675.

[304] RIVM. Circular economy in the Dutch construction sector - A perspective for the market and

government. 2015.

[305] Zhang C, Hu M, Laclau B, Garnesson T, Yang X, Li C, et al. Environmental life cycle costing at the early stage for supporting cost optimization of precast concrete panel for energy renovation of existing buildings. J Build Eng 2021;35:102002. doi:https://doi.org/10.1016/j.jobe.2020.102002.

[306] Wang H, Chen D, Duan H, Yin F, Niu Y. Characterizing urban building metabolism with a 4D-GIS model: A case study in China. J Clean Prod 2019;228:1446–54. doi:https://doi.org/10.1016/j.jclepro.2019.04.341.

[307] Passe U, Dorneich M, Krejci C, Koupaei DM, Marmur B, Shenk L, et al. An urban modelling framework for climate resilience in low-resource neighbourhoods. Build Cities 2020;1:453–74. doi:10.5334/bc.17.

[308] Cerezo Davila C, Reinhart CF, Bemis JL. Modeling Boston: A workflow for the efficient generation and maintenance of urban building energy models from existing geospatial datasets. Energy 2016;117:237–50. doi:10.1016/J.ENERGY.2016.10.057.

[309] Mastrucci A, Marvuglia A, Benetto E, Leopold U. A spatio-temporal life cycle assessment framework for building renovation scenarios at the urban scale. Renew Sustain Energy Rev 2020;126. doi:10.1016/j.rser.2020.109834.

[310] Verellen E, Allacker K. Inventory of the existing residential building stock for the purpose of environmental benchmarking. IOP Conf Ser Earth Environ Sci 2019;323:12029. doi:10.1088/1755-1315/323/1/012029.

[311] Ali U, Shamsi MH, Bohacek M, Purcell K, Hoare C, Mangina E, et al. A data-driven approach for multi-scale GIS-based building energy modeling for analysis, planning and support decision making. Appl Energy 2020;279:115834. doi:10.1016/j.apenergy.2020.115834.

[312] Reimer F, Kral U. The Viennese Building Stock from 1920 to 2018: a Prototype Model. Real Corp 2020, 2020. doi:10.5281/zenodo.5109660.

[313] TABULA Project Team. Typology Approach for Building Stock Energy Assessment 2017. http://episcope.eu/index.php?id=97 (accessed October 6, 2019).

[314] Cabeza LF, Ürge-Vorsatz D. The role of buildings in the energy transition in the context of the climate change challenge. Glob Transitions 2020;2:257–60. doi:https://doi.org/10.1016/j.glt.2020.11.004.

[315] Liu G, Ye K, Tan Y, Huang Z, Li X. Factors influencing homeowners' housing renovation decision-making: Towards a holistic understanding. Energy Build 2022;254:111568. doi:https://doi.org/10.1016/j.enbuild.2021.111568.

[316] Bianco V, Sonvilla PM, Gonzalez Reed P, Villoslada Prado A. Business models for supporting energy renovation in residential buildings. The case of the on-bill programs. Energy Reports 2022;8:2496–507. doi:https://doi.org/10.1016/j.egyr.2022.01.188.

[317] Rabbat C, Awad S, Villot A, Rollet D, Andrès Y. Sustainability of biomass-based insulation materials in buildings: Current status in France, end-of-life projections and energy recovery potentials. Renew Sustain Energy Rev 2022;156:111962. doi:https://doi.org/10.1016/j.rser.2021.111962.

[318] Palumbo M, Lacasta AM, Giraldo MP, Haurie L, Correal E. Bio-based insulation materials and their hygrothermal performance in a building envelope system (ETICS). Energy Build 2018;174:147–55. doi:https://doi.org/10.1016/j.enbuild.2018.06.042.

[319] He W, King M, Luo X, Dooner M, Li D, Wang J. Technologies and economics of electric energy storages in power systems: Review and perspective. Adv Appl Energy 2021;4:100060. doi:https://doi.org/10.1016/j.adapen.2021.100060.

[320] Așchilean I, Cobîrzan N, Bolboaca A, Boieru R, Felseghi R-A. Pairing solar power to sustainable energy storage solutions within a residential building: A case study. Int J Energy Res 2021;n/a. doi:https://doi.org/10.1002/er.6982.

[321] Li H, Wang Z, Hong T, Piette MA. Energy flexibility of residential buildings: A systematic review of characterization and quantification methods and applications. Adv Appl Energy 2021;3:100054. doi:https://doi.org/10.1016/j.adapen.2021.100054.

[322] Martin-Roberts E, Scott V, Flude S, Johnson G, Haszeldine RS, Gilfillan S. Carbon capture and storage at the end of a lost decade. One Earth 2021;4:1569–84. doi:10.1016/j.oneear.2021.10.002.

[323] Chatterjee S, Oreggioni G, Stavrakas V, Aryandoust A, Ürge-Vorsatz D, Staffell I, et al. Model development to match models to the user needs 2021. doi:10.5281/ZENODO.5915372.

[324] Shinde R, Peng S, Vijay S, Hellweg S, Froemelt A. Data mining for evaluating the rebounds-associated emissions due to energy-related consumer behavioural shifts in Switzerland. J Phys Conf Ser 2021;2042:12127. doi:10.1088/1742-6596/2042/1/012127.

[325] Guerra Santin O. Occupant behaviour in energy efficient dwellings: evidence of a rebound effect. J Hous Built Environ 2013;28:311–27. doi:10.1007/s10901-012-9297-2.

[326] Frithjof Laubinger. A bottom-up analysis of household energy consumption in Amsterdam Resolving policy barriers in the residential building sector. VU University Amsterdam, 2015.

[327] Morseletto P. Restorative and regenerative: Exploring the concepts in the circular economy. J Ind Ecol 2020;24:763–73. doi:https://doi.org/10.1111/jiec.12987.

[328] Green Building Store. Understanding windows: U values, Psi values and g values. Green Build Store 2018. https://www.greenbuildingstore.co.uk/understanding-windows-u-values-psi-values-g-values/ (accessed October 8, 2021).

[329] Groengas Nederland. What is green gas? n.d. https://groengas.nl/groen-gas/wat-is-groen-gas/ (accessed April 22, 2021).

[330] Energie Vergelijken. Green gas in the Netherlands n.d. https://www.energievergelijken.nl/duurzame-energie/groen-gas (accessed April 22, 2021).

[331] Green Gas Forum. Green gas roadmap. 2014.

[332] Jim van der Kooij A. Environmental impact of the materials used in the Dutch heat transition. 2018.

[333] Borg AA. The Environmental Impact of Ventilation Systems in a Norwegian Office Building from a Life Cycle Perspective. Norwegian University of Science and Technology, 2016.

[334] Fonseca JA, Nguyen T-A, Schlueter A, Marechal F. City Energy Analyst (CEA): Integrated

framework for analysis and optimization of building energy systems in neighborhoods and city districts. Energy Build 2016;113:202–26. doi:10.1016/J.ENBUILD.2015.11.055.

[335] Milieu Centraal. Solar water heater 2021. https://www.milieucentraal.nl/energie-besparen/duurzaam-warm-water/zonneboiler/ (accessed August 12, 2021).

[336] Hinckley M. What is the Life Span of a Water Heater? n.d. https://www.hunker.com/12151423/what-is-the-life-span-of-a-water-heater (accessed August 12, 2021).

[337] Milieu Centraal. How Do Solar Panels Work? n.d. https://www.milieucentraal.nl/energie-besparen/zonnepanelen/hoe-werken-zonnepanelen/ (accessed August 13, 2021).

Summary

The building sector accounts for large amounts of material consumption, demolition waste generation, fossil fuel energy consumption, and greenhouse gas emissions. Decarbonizing the building stock plays an important role in realizing the climate-neutral target for the Netherlands. Dutch residential buildings are mostly relatively old and energy-inefficient and rely heavily on natural gas for space heating and domestic hot water supply, which occupy the largest share of annual residential energy consumption. This means that decarbonization policy strategies need to understand the characteristics of the current building stock and its future evolvement patterns. Accordingly, this thesis employs multi-source data, mainly including GIS data of building footprints and the archetypes representative of Dutch residential buildings, to develop a series of bottom-up building stock models to track future material stock and flows, energy demand, electricity generation, and GHG emissions.

Chapter 2 develops a bottom-up building stock energy model based on GIS data and archetypes of residential buildings differentiated by building types and construction periods. Archetypical information on buildings, such as geometries (e.g. window to wall ratio), thermal properties of envelope elements, and parameters of technical systems, is mapped to the individual buildings from GIS data, which provides a method to characterize the residential building stock in the Netherlands. At the same time, to investigate what kinds of information contributes most to model accuracy improvement, the detailed data (e.g. hourly climate data) is added stepwise to the basic model. The model is spatially validated against the measured natural gas consumption reported at the postcode level. Results show that past renovation and occupant behavior can greatly affect the modeled space heating demand. While uncertainties exist for individual buildings due to a lack of detailed individual building information, the modeled results are acceptable at the building stock level.

Chapter 3 presents a bottom-up dynamic building stock model capable of simulating future building stock development and accounting for the associated material and energy flows, and annual GHG emissions. Contrary to previous bottom-up dynamic building stock studies, the model builds upon archetypical building types retrieved from GIS data and simulates the potential energy demand taking into account (future) energy-efficient building renovation. The model is applied to assess the effect of the "Nederland klimaatneutraal in 2050" (Netherlands climate neutral in 2050) scenario, which aims to realize renewable energy supply systems in the Netherlands. Results show that the annual GHG emissions can be reduced by nearly 90% by 2050 if existing buildings undergo a thorough renovation, phase out natural gas boilers, and use a renewable electricity mix. Rooftop PV can potentially supply 80% of the annual electricity demand for appliances and lighting if solar panels are installed on 50% of roofs. The annual material-related GHG emissions are much less than annual energy-related emissions. The cumulative material-related GHG emissions from construction and renovation activities will be counteracted by the cumulative reduced space heating-related emissions by 2035.

Chapter 4 further develops the bottom-up dynamic building stock model in Chapter 5 by linking material inflows and outflows during construction, demolition, and renovation in space and time to explore the urban mining potential to reduce primary material consumption and GHG emissions. The CDW collection rates and the recycled content potentials are used to account for the amounts of recycled CDW that are used in construction and renovation processes. Results show that most building materials and floor areas are stocked in big cities, such as Amsterdam, Rotterdam, and The Hague. These cities also dominate future material inflows and outflows, but there are fewer outflows than inflows, meaning that urban mining can only provide limited amounts and kinds of materials for construction and renovation, especially for the insulation materials that most old buildings do not contain. There is a large temporal mismatch between material demand and secondary material supply; consequently, some materials have a deficit in the early years but have a surplus in later years. The limited ability of urban mining to substitute primary materials leads to limited GHG emission reduction potential. Greening the electricity mix for material production has a much bigger effect on GHG emission reduction than urban mining.

Chapter 5 integrates the models in the previous chapters to investigate the overall GHG emission reduction potential of combined policy strategies and compare the decarbonization potential of different strategies, such as material transition (CDW recycling and wood construction), energy transition (heat transition, renewable electricity mix, and rooftop PV), and implementing green lifestyles. Results show that if all the strategies are effectively implemented together, the overall GHG emission reduction potential can be over 90%. The energy transition strategy, especially the heat transition and renewable electricity supply, plays the most important role. Rooftop PV can supply surplus electricity if as many roofs as possible are fitted with solar panels. The material transition strategy contributes much less to GHG emission reduction than the energy transition strategies. The green lifestyle strategy has a similar decarbonization potential to a wide installation of rooftop PV systems.

Together, the chapters of this thesis demonstrate the great potential for GHG emission reduction, while the decarbonization strategies should be effectively and extensively implemented. Saving space heating energy consumption is the most direct way to reduce annual GHG emissions. Considering that most existing residential buildings will still be in use in 2050, renovating them with high energy performance standards is required. Despite the great potential of renovation, it alone is not enough to realize the climate-neutral target in the residential building stock because the upstream fossil fuel-based energy systems still emit large amounts of GHG. Replacing fossil fuels with renewable energy sources is a critical path, mainly involving onsite natural gas combustion for space heating and offsite natural gas and coal combustion for electricity and heat (in heat networks) generation. Urban mining cannot contribute to as much emission reduction as energy transition strategies, but it should nonetheless still be implemented as it can reduce the primary material consumption and generation of CDW. In addition to the technical aspects considered in this thesis, it is also necessary to develop feasible policies in terms of socioeconomic aspects to guarantee the effective and quick deployment of these technical strategies.

Samenvatting

De bouwsector gebruikt enorme hoeveelheden primair materiaal, genereert een grote hoeveelheid bouw- en sloopafval, en is daarnaast verantwoordelijk voor een aanzienlijk gebruik van fossiele brandstoffen en daaraan gerelateerde uitstoot van broeikasgassen. Het koolstofvrij maken van de gebouwde omgeving speelt een belangrijke rol bij het klimaatneutraal maken van Nederland. Nederlandse huizen zijn echter relatief oud en energie-inefficiënt en zijn in hoge mate afhankelijk van aardgas voor ruimteverwarming en warmwatervoorziening. Dit vormt het grootste aandeel van het jaarlijkse energieverbruik van woningen. Om beleidsstrategieën voor het koolstofarm maken van woningen te kunnen uitstippelen, is inzicht nodig in de kenmerken van het huidige woningvoorraad en de toekomstige ontwikkeling daarin. Om dit inzicht te verkrijgen worden in dit proefschrift gegevens uit verschillende bronnen gebruikt. Het betreft voornamelijk GIS-data over de gebouwde omgeving in combinatie met archetypen die representatief zijn voor Nederlandse typen woonhuizen. Met deze data wordt een reeks bottom-up modellen ontwikkeld voor de ontwikkeling van de woningvoorraad, waarmee inzicht verkregen kan worden in de toekomstige materiaalvoorraden en -stromen, de vraag naar energie inclusief elektriciteit, en de hieraan gerelateerde broeikasgasemissies.

Hoofdstuk 2 ontwikkelt een bottom-up model van energiegebruik in de woningvoorraad in Nederland, gebaseerd op GIS data en archetypes van woongebouwen gedifferentieerd naar gebouwtype en bouwperiode. Informatie over archetypes van gebouwen, zoals de geometrie (b.v. verhouding tussen raam- en muuroppervlak), het isolerend vermogen van de buitenste gebouwschil, en gegevens over efficiëntie van technische systemen zoals het verwarmingssysteem, worden in kaart gebracht op basis van GIS data. Dit blijkt een goede een methode om de woningvoorraad in Nederland qua energiegebruik te karakteriseren. Tegelijkertijd worden, om te onderzoeken welke soort additionele informatie het meest bijdraagt aan de verbetering van de nauwkeurigheid van het model, diverse gedetailleerde gegevens (bijv. klimaatgegevens zoals buitentemperatuur per uur) stapsgewijs toegevoegd aan het basismodel. Het model wordt gevalideerd aan de hand van het gemeten aardgasverbruik dat op postcodeniveau wordt gerapporteerd. De resultaten tonen aan dat gedrag van bewoners en of er in het verleden renovatie heeft plaatsgevonden grote invloed kan hebben op de gemodelleerde vraag naar ruimteverwarming. Hoewel er onzekerheden bestaan voor individuele gebouwen door een gebrek aan gedetailleerde informatie op individueel gebouwniveau, zijn de gemodelleerde resultaten goed bruikbaar voor de Nederlandse woningvoorraad als geheel.

In hoofdstuk 3 wordt een dynamisch bottom-up model voor de woningvoorraad ontwikkeld. Hiermee kan de toekomstige ontwikkeling van de woningvoorraad worden ingeschat en kunnen de bijbehorende materiaal- en energiestromen en jaarlijkse broeikasgasemissies in kaart worden gebracht. Anders dan met eerdere dynamische bottom-up studies van de woningvoorraad, modelleert het model

archetypische woningen op basis van GIS gegevens en schat het de potentiële energievraag in, rekening houdend met (toekomstige) verbetering van de energie-efficiëntie door renovatie. Het model wordt toegepast om het effect door te rekenen van een "Nederland klimaatneutraal in 2050" scenario, dat moet leiden tot het gebruik van hernieuwbare energiebronnen in Nederland. De resultaten tonen aan dat de jaarlijkse broeikasgasemissies in 2050 met bijna 90% kunnen worden verminderd als de bestaande gebouwen worden gerenoveerd, verwarming met aardgas wordt uitgefaseerd, en er koolstofarme elektriciteit wordt gebruikt. PV op daken kan in potentie voorzien in 80% van de jaarlijkse elektriciteitsvraag voor apparaten en verlichting als op 50% van de daken zonnepanelen worden geïnstalleerd. De jaarlijkse materiaalgerelateerde broeikasgasemissies zijn veel lager dan de jaarlijkse energiegerelateerde emissies. De extra cumulatieve materiaalgerelateerde broeikasgasemissies van bouw- en renovatieactiviteiten zullen tegen 2035 worden gecompenseerd door de cumulatieve verminderde emissies gerelateerd aan ruimteverwarming.

In hoofdstuk 4 wordt het dynamische bottom-up model van de woningvoorraad in hoofdstuk 5 verder ontwikkeld door de materiaalinstroom en -uitstroom tijdens de bouw, sloop en renovatie in ruimte en tijd te koppelen om het potentieel van urban mining te onderzoeken om het verbruik van primaire materialen en de broeikasgasemissies te verminderen. Op basis van inzamelingspercentages van Bouw en Sloopafval (BSA)en het potentieel voor recycling van materialen wordt ingeschat hoeveel gerecycleerd BSA in bouw- en renovatieprocessen kan worden ingezet. De resultaten geven aan dat het gros van het vloeroppervlak en de daaraan gerelateerde 'urban mine' aan bouwmaterialen zich bevindt in grote steden, zoals Amsterdam, Rotterdam en Den Haag. Deze steden domineren ook de in- en uitstroom van toekomstig materiaal, maar de uitstroom is veel kleiner dan de instroom, wat betekent dat 'urban mining' slechts beperkte hoeveelheden en soorten materialen voor nieuwbouw en renovatie kan leveren. Dit is vooral het geval voor isolatiematerialen, die vaak afwezig zijn in oude gebouwen. Er bestaat in de tijd een groot verschil in de vraag naar materialen en het aanbod van secundaire materialen, wat betekent voor sommige materialen in de eerste jaren er een tekort aan secondair materiaal bestaat, maar in latere jaren een overschot. Omdat 'urban mining' dus maar een beperkte mogelijkheid geeft om primaire materialen te vervangen, geeft dit ook maar een beperkte mogelijkheid de broeikasgasemissies gerelateerd aan materiaalgebruik te verminderen. Het koolstofneutraal maken van de elektriciteitsvoorziening heeft voor de productie van materialen een veel groter effect op de vermindering van de broeikasgasemissies dan het optimaliseren van 'urban mining'.

Hoofdstuk 5 integreert de modellen uit de voorgaande hoofdstukken om het totale potentieel ten aanzien van reductie van broeikasgasemissies te onderzoeken, en te analyseren wat de bijdrage is van specifieke strategieën zoals het de materiaaltransitie (recycling van BSA en meer gebruik van hout in bouwconstructies), de energietransitie (warmtetransitie, gebruik van koolstofarme elektriciteit en het installeren van PV op daken), en het overgaan op een duurzame levensstijl. Uit de resultaten blijkt dat als alle strategieën in combinatie worden geïmplementeerd, een totale reductie van broeikasgassen van 90% of meer kan worden gerealiseerd. Het doorvoeren van een energietransitie speelt de belangrijkste rol, met name de warmtetransitie en het realiseren van een koolstofarme elektriciteitsvoorziening. PV op daken kan een zelfs zorgen voor een overschot aan groene elektriciteit als alle daken zoveel mogelijk worden voorzien van zonnepanelen. Een materiaaltransitie waarbij ingezet wordt op gebruik van secondair materiaal draagt veel minder bij aan de reductie van broeikasgasemissies voornoemde energietransitie. Duurzame levensstijlen kunnen vergelijkbaar bijdragen aan de reductie van emissies van broeikasgassen als een breed doorgevoerde installatie van PV-systemen op daken.

Acknowledgments

My PhD career in the CML family was really interesting, challenging, and memorable for professional and personal growth. I am excited to arrive at the stage of concluding the writing of my PhD thesis and finally to show my appreciation to all the people who have ever helped and accompanied me.

I would like to thank my daily supervisors - Bernhard Steubing and Mingming Hu, and PhD supervisor - Arnold Tukker, for all their patient guidance and kind help. Attending the Industrial Ecology course taught by Mingming Hu at Chongqing University was one of the best choices I have ever made because it developed my keen interest in Industrial Ecology. I still remember the first time I discussed my research with them online, with little confidence. Then Bernhard and Mingming sent me some papers related to building stock modeling, a topic unfamiliar to me. Under their supervision, I managed to develop a series of building stock models for the Netherlands and in the end finished four papers. They revised my terrible manuscripts carefully and provided me with many constructive comments on the color, font size, and layout of the figures, which helped to get my papers published without too many problems. Also, Arnold always sent me feedback very quickly.

I want to thank my colleague, Teun Verhagen, for his kind and practical help. It was he who shared the GIS data of Dutch building stocks and spatialized energy consumption data with me. I learned lots of basic knowledge about Dutch buildings and programming skills from him. I also benefitted a lot from our discussions on building stock modeling and finding interesting research questions. I thank Sander van Nielen and Brenda Miranda Xicotencatl for helping me in programming and looking for data. Apart from work, we have enjoyed lots of happy moments and learned about many cultural differences from our daily chats. I am also grateful for their kind support in the past years when the COVID-19 pandemic made life a bit crazy. The secretaries at CML gave a lot of timely support to my research. Here I cannot list all the colleagues who have helped me but I want to say thanks to all of them.

I also want to thank my Chinese friends. I enjoyed lots of delicious food and happy times with them during important festivals. We have traveled to many beautiful places. They have also encouraged me to be confident and not to be discouraged at times when things were a bit difficult.

I am very grateful to the China Scholarship Council (CSC) for funding me over the past four years.

Last but not least, I want to thank my family for their continuous encouragement and all kinds of support during my whole study career.

致谢所有，江湖再见。

一切过往，皆为序章。

List of publications

(1) Yang, X., Hu, M., Zhang, C., Steubing, B. A combined GIS-archetype approach to model residential space heating energy: A case study for the Netherlands including validation. Applied Energy 280, 115953 (2020).

(2) Yang, X., Hu, M., Tukker, A., Zhang, C., Huo, T., Steubing, B. A bottom-up dynamic building stock model for residential energy transition: A case study for the Netherlands. Applied Energy 306, 118060 (2022).

(3) Yang, X., Hu, M., Zhang, C., Steubing, B. Urban mining potential to reduce primary material use and carbon emissions in the Dutch residential building sector. Resources, Conservation & Recycling. 180, 106215 (2022).

(4) Yang, X., Hu, M., Zhang, C., Steubing, B. Key strategies for decarbonizing the residential building stock: Results from a spatiotemporal model for Leiden, the Netherlands. Resources, Conservation & Recycling. 184, 106388 (2022).

Curriculum Vitae

Xining Yang (杨希宁) was born on 26 September 1991, in Baoding City, Hebei Province, China. He graduated from Laiyuan County No. 1 Middle School in 2011. From 2011 to 2015, he studied at Shijiazhuang Tiedao University and obtained a BSc degree in Engineering Management. He majored in Technical Economy and Management at Chongqing University from 2015 to 2018. During this period, he was supervised by Bin Zhao and Mingming Hu and mainly engaged in combining Life Cycle Assessment with Building Information Modeling to assess the life cycle environmental impacts of buildings at the design stage.

Funded by the China Scholarship Council (CSC), he joined the Institute of Environmental Science (CML) at Leiden University as a PhD candidate in September 2018. Under the supervision of Dr Bernhard Steubing, Dr Mingming Hu, and Prof. Arnold Tukker, he focused on developing data-intensive building stock models that can simulate the building stock development as well as the associated material flows, energy demand and generation, and carbon emissions to support the formulation of policies relevant to the circular economy, energy transition and climate change mitigation.